Sensing Foreign DNA: The Role of DNA-PKcs in Human Anti-viral Innate Immunity

Dayana Bozhidarova Hristova

Department of Pathology
University of Cambridge
Newnham College

Supervisor: Brian Ferguson

This dissertation is submitted for the degree of Doctor of Philosophy

October 2021

DECLARATION

This dissertation is the result of my own work and includes nothing, which is the outcome of work done in collaboration except as declared here and specified in the appropriate figure legends or methods sections.

It is not substantially the same as any that I have submitted, or, is being concurrently submitted for a degree or diploma or other qualification at the University of Cambridge or any other University or similar institution except as declared in the Preface and specified in the text. I further state that no substantial part of my dissertation has already been submitted, or, is being concurrently submitted for any such degree, diploma or other qualification at the University of Cambridge or any other University or similar institution except as declared in the Preface and specified in the text.

The text in this dissertation does not exceed the 60,000-word limit (excluding references) set by the School of Biological Sciences.

ABSTRACT

Sensing Foreign DNA:
The Role of DNA-PKcs in Human Anti-viral Innate Immunity

Dayana Hristova

Host cell pattern recognition receptors (PRRs) are a first line of defence against pathogens and function to generate a productive innate immune response. PRRs sense pathogen-associated molecular patterns (PAMPs), such as viral genomic DNA, which is a major PAMP during DNA virus infection. Viral DNA sensing leads to the activation of the STING-TBK1-IRF3 signalling axis and the production of type I interferon. Previously, our work identified the non-homologous end-joining protein DNA-PKcs, part of the DNA-dependent protein kinase (DNA-PK) complex, as an intracellular PRR for cytoplasmic viral DNA in murine cells. After screening several human cell lines, we established a robust system to dissect the DNA sensing pathway in human fibroblasts. In these human cells DNA-PKcs was found to be essential for the production of type I interferon via the STING pathway in response to DNA and DNA virus infection and we found that the kinase activity of DNA-PKcs was not required for this response. Many DNA viruses evade the immune response by inhibiting the pathway. We make use of attenuated Herpes simplex virus 1 (HSV-1) and Vaccinia virus (VACV) that lack immunomodulatory proteins and drive type I interferon production. DNA-PKcs-/- cells have a defective immune response after infection with attenuated HSV and VACV. Furthermore, primary patient fibroblasts harbouring a mutation in DNA-PKcs showed a gain-of-function effect and an enhanced immune signaling to DNA and DNA virus infection. DNA-PKcs has also been linked to cell death during retrovirus integration although this has not been studied extensively. We carried out some preliminary work in this study, showing that DNA-PKcs-/- cells are more prone to cell death during HSV-1 infection and have reduced yields of virion production. This work demonstrates the role of DNA-PKcs as a viral DNA sensor in human cells and adds to the knowledge of the DNA sensing processes that are essential for anti-viral innate immunity.

ACKNOWLEDGEMENTS

First and foremost, I would like to thank my supervisor, Brian Ferguson, for giving me the incredible opportunity to undertake a PhD project in his lab. He has been a supportive and inspiring mentor who has helped me grow as a scientist and has given me a lot of opportunities. His infectious enthusiasm and positive and calm attitude have motivated me to keep going in the most stressful situations. Brian has guided me not only in my career but also in my personal development, for which I am extremely grateful.

Secondly, I would like to thank all current and past members of the Ferguson lab, as well as members of other labs in the Department of Pathology. I have made lifelong friendships and learned a lot from them. They have provided joy and happiness during the highs and have been great support during the lows throughout those years.

Last but not least, I would like to thank Ivan, my family (especially my mother) and my close friends. They have always believed in me and encouraged me to keep going. My special thanks go to Ivan, who has been my biggest support in this journey. He has been there at my worst helping me bounce back and has shared my joy at my best. Without the help and support of everyone mentioned above, I would not have been able to reach this far.

ABBREVIATIONS

PRR	pattern recognition receptors
PAMP	pathogen-associated molecular patterns
DAMP	damage-associated molecular patterns
TLR	Toll-like receptors
RIG-I	Retinoic acid-inducible gene
NOD	nucleotide-binding oligomerisation domain-containing protein
RLR	Retinoic acid-inducible gene (RIG-I)-like receptors
LRR	leucine-rich repeat
MyD88	myeloid differentiation primary response gene 88
NF-κB	nuclear factor kappa-light-chain-enhancer of activated B cells
TRIF	TIR-domain-containing adapter-inducing interferon-β
MDA5	melanoma differentiation-associated protein 5
CARD	caspase activation and recruitment domain
MAVS	mitochondrial antiviral signalling protein
TBK1	(TANK)-binding kinase 1
IKK	IκB-related kinase
LGP2	laboratory of genetics and physiology 2
TLR9	Toll-like receptor 9
ISD	interferon stimulatory DNA
cGAS	cyclic GMP-AMP synthase
IFI16	IFN inducible gene 16
AIM2	absent in melanoma 2
MRE11	meiotic recombination 11
LRRFIP1	leucine-rich repeat flightless-interacting protein 1
DDX60	DEAD/H box helicase 60
DDX41	DEAD/H-box helicase 41
STING	stimulator of interferon genes
Ntase	nucleotidyltransferase
ssDNA	single-stranded DNA
cGAMP	cyclic GMP-AMP
VACV	vaccinia virus
HSV	herpes simplex virus
CMV	cytomegalovirus
HIV	human immunodeficiency virus
VSV	vesicular stomatitis virus
PYHIN	pyrin and HIN200 domain-containing protein
ALR	AIM2-like receptor
PYD	pyrin domain
ASC	apoptosis-associated speck-like protein containing a

	CARD domain
DSB	double-strand break
NHEJ	non-homologous end-joining
SCID	severe combined immunodeficiency
MEF	mouse embryonic fibroblast
ER	endoplasmic reticulum
COPII	coat protein complex II
ARF	ADP-ribosylation factor
IKK	IκB-related kinases
IFNLR	IFN lambda receptor
IFNAR	IFN alpha receptor
IL10RB	IL-10 receptor subunit beta
JAK-STAT	Janus kinase-signal transducer and activator of transcription
ISG	interferon-stimulated gene
ATF2	activating transcription factor 2
CBP	CREB binding protein
TFIID	transcription factor II D
NK	natural killer cell
IκB	inhibitor of Kappa-B
COP	Copenhagen strain
WR	Western Reserve
MVA	Modified Vaccinia virus Ankara
CVA	Chorioallantois vaccinia virus Ankara
EEV	extracellular enveloped virus
IMV	intracellular mature virion
MLKL	mixed lineage kinase domain-like protein
RIPK3	receptor-interacting protein kinase 3
DAI	DNA-dependent activator of IRFs
KSHV	Kaposi's Sarcoma-associated herpesvirus
HTLV-1	Human T-lymphotropic virus 1
HBV	hepatitis B virus
HEAT	Huntingtin, elongation factor 3, protein phosphatase 2A, and the yeast kinase TOR1
FAT	FRAP, ATM and TRAP domain
DSBs	double-stranded breaks
Cas9	CRISPR-associated 9 protein
DMEM	Dulbecco's Modified Eagle Medium
FCS	fetal calf serum
Pen-Strep	penicillin/streptomycin
MEM	Minimum Essential Medium
NEAA	non-essential amino acids
RPMI	Roswell Park Memorial Institute
CRISPR	Clustered Regularly Interspaced Short Palindromic Repeats
sgRNA	single-guide RNA

NF-H2O	nuclease free water
PCR	polymerase chain reaction
ctDNA	calf thymus DNA
HSV-1	Herpes Simplex Virus-1
S17	strain 17
CPE	cytopathic effect
MOI	multiplicity of infection
CMC	carboxy-methyl cellulose
HRP	horseradish peroxidase
SeV	Sendai virus
DTT	dithiothreitol
dT	deoxythymine
qPCR	quantitative polymerase chain reaction
RT-qPCR	Quantitative real time-polymerase chain reaction
Ct	cycle threshold
RIPA	radioimmunoprecipitation assay
BCA	bicinchoninic assay
SDS-PAGE	Sodium dodecyl sulphate polyacrylamide gel electrophoresis
APS	ammonium persulphate
TEMED	tetramethylethylenediamine
TBS	Tris-buffered saline
TBST	Tris-buffered saline with 0.1% v/v tween-20
HEPES	4-(2-hydroxyethyl)-1-piperazineethanesulfonic
DAPI	6-diamidino-2-phenylindole
ELISA	Enzyme-linked immunosorbent assay
APC	allophycocyanin
7AAD	7-amino-actinomycin D
htDNA	herring testes DNA
ctDNA	calf thymus DNA
ISD	immunostimulatory DNA
HFF	human foreskin fibroblasts
RPE-1	retinal pigment epithelial cell 1
MMTV	mouse mammary tumour virus
RNAP II	ribonucleic acid polymerase II
SIDSP	STING-independent DNA sensing pathway
T-vec	Talimogene laherparepvec

Contents

1. Introduction

1.1 The innate immune system

1.1.1 Overview

The mammalian immune system protects the host from harmful pathogens and is broadly divided into two subsystems: innate and adaptive immunity. Innate immunity is present since birth and is the first line of defence against infections. It serves to detect invading pathogens and provide a bridge for the generation of adaptive immunity. The adaptive immune response, also known as acquired immunity, consists of highly specialised immune cells that are specific to the pathogen presented and can generate long-lasting immunological memory. In this work we will focus on the innate immune response.

1.1.2 Pathogen recognition receptors

The sensing of pathogens by the innate immune system is a crucial step in the generation of a productive immune response. There is a constant ongoing arms race between pathogen and host, where the host is equipped with germline-encoded pattern recognition receptors (PRRs) that recognise highly conserved pathogen-associated molecular patterns (PAMPs) or damage associated molecular patterns (DAMPs) originating from tissues. PAMPs comprise nucleic acids, lipids, proteins or carbohydrates from pathogens that can be recognised by a variety of PRRs. For a long time, it has been known that host cell surface receptors can identify PAMPs on intruding pathogens and alarm the innate immune system. However, more recently it has been appreciated that it is equally important to survey the host cell cytoplasm and protect it from intracellular invaders. The PRR family include Toll-like receptors (TLRs), Retinoic acid-inducible gene 1 (RIG-I) like receptors (RLRs), nucleotide-binding oligomerisation domain-containing protein (NOD)-like receptors (NLRs) and intracellular DNA sensors. PRRs will be discussed below in more detail with a particular focus on intracellular DNA sensors.

In cases when the innate immune system is not able to eliminate the infection, it can result in death of the cell and there is a fine balance between those processes to ensure minimal tissue damage and maintain homeostasis. The process of PAMP or DAMP detection must be tightly regulated in order to avoid unnecessary immune activation that can lead to the development of immune disease states. Cells express DNases, such as DNase II in endosomes and Three-prime repair exonuclease 1 (TREX1) in the cytoplasm, which degrade and prevent harmful accumulation of cytoplasmic DNA (Okabe *et al.*, 2005; Rice *et al.*, 2007; Yang, Lindahl and Barnes, 2007) and unwanted activation of the immune system. Sterile inflammation can occur when these pathways are dysregulated. For instance, TREX1 deficiency leads to the development of Aicardi-Goutieres syndrome (AGS) (Crow, 2013), which is a debilitating inflammatory disorder that affects the brain and the skin of children. Such conditions highlight the importance of the innate immunity and the necessity to study its processes.

1.2 Intracellular PRRs

1.2.1 Toll-like receptors

Toll-like receptors (TLRs) are a class of PRRs that can recognise PAMPs (DNA, RNA and microbial cell walls) from a number of species, such as viruses, bacteria, protozoa and fungi (Janeway and Medzhitov, 2002; Akira, Uematsu and Takeuchi, 2006). Toll proteins were first described in *Drosophila* and flies with a mutant *toll* gene were found to have a defective immune response to fungal infection (Lemaitre *et al.*, 1996). Up to date, 10 members of the TLR family have been described in humans and from these, five are responsible for sensing pathogen-associated nucleic acids (Kawai and Akira, 2011). TLRs are expressed on the cell surface or in endosomal compartments. TLR 3, 7, 8 and 9 reside in the phagosomes of macrophages and plasmacytoid dendritic cells (pDCs), which are highly specialised in the immune response to viruses (Asselin-Paturel *et al.*, 2001). TLR3, 7 and 8 recognise viral RNA. Polyinosinic:polycytidylic acid (PolyI:C) is an immunostimulant commonly used in research that is similar in structure to double-stranded RNA and

is detected by TLR3 (Fortier *et al.*, 2004; Li *et al.*, 2015). TLR9, on the other hand, senses unmethylated cytosine–phosphate–guanosine (CpG) motifs that are abundant in microbial DNA (Hemmi *et al.*, 2000; Yasuda *et al.*, 2009; Ohto and Shimizu, 2016) and not mammals, which methylate genomic CpG motifs at the cytosine base (Smith and Meissner, 2013). Upon ligand binding, TLR9 induces the production of IFNα, IFNλ and multiple inflammatory cytokines and the receptor was shown to sense the DNA of HSV and a number of other herpesviruses (Lund *et al.*, 2003; Hochrein *et al.*, 2004; Megjugorac *et al.*, 2004; Megjugorac, Gallagher and Gallagher, 2009).

TLRs are a large family of transmembrane receptors that have extracellular leucine-rich repeat (LRR) domain and an intracellular Toll/IL-1 receptor (TIR) domain that transmits signals to initiate a downstream signalling cascade. The LRR domain binds directly to specific ligands causing dimerisation and a conformational change that allows the cytoplasmic TIR domain to transduce the signal to myeloid differentiation primary response gene 88 (MyD88) adaptor protein, which leads to nuclear factor kappa-light-chain-enhancer of activated B cells (NF-κB) signalling (Hultmark, 1994). As well as signalling to NF-κB, TLR3 can also signal to interferon regulatory factor 3/7 (IRF 3/7) to stimulate the immune response via TIR-domain-containing adapter-inducing interferon-β (TRIF) (Bell *et al.*, 2003; Matsushima *et al.*, 2007; Fitzgerald and Kagan, 2020). NF-κB and IRF3 are transcription factors that drive IFN and inflammatory gene signatures by binding directly to the promoters of specific genes and they will be described in more detail in section 3.

1.2.2 Retinoic acid-inducible gene (RIG-I) like receptors

Apart from TLRs, exogenous RNA can also be sensed in the cell cytoplasm by the RLR family of cytosolic RNA sensors. There are three known RLR members: retinoic acid-inducible gene (RIG-I), melanoma differentiation-associated protein 5 (MDA5) and laboratory of genetics and physiology 2 (LGP2) (Andrejeva *et al.*, 2004; Yoneyama *et al.*, 2004; Rothenfusser *et al.*, 2005). RIG-I and MDA5 bind viral RNA via a DExD/H box helicase domain and a C-terminal domain, which results in a

conformational change that allows their caspase activation and recruitment domains (CARD) to interact with mitochondrial antiviral signalling protein (MAVS) (Seth *et al.*, 2005). RIG-I is able to discriminate self from non-self RNA by binding to 5' di- or tri-triphosphate modified ends of dsRNA, normally capped in mammalian cells. MDA5 recognises double-stranded RNAs, which are not typically present in large enough quantities in mammalian cells to be recognised as pathogenic. MAVS is an adaptor protein that resides in the membranes of mitochondria and peroxisomes. The CARD domains of RLRs bind to the CARD domains of MAVS to induce oligomerisation. This process results in the formation of a large signalling complex that culminates in the recruitment and activation of the (TANK)-binding kinase 1 (TBK1)/ Inhibitor of nuclear factor kappa-B kinase subunit epsilon (IKKε) kinases, which stimulates IFN-I antiviral immune response via the transcription factors IRF3/7 and NF-κB (Kawai *et al.*, 2005; Meylan *et al.*, 2005; Xu *et al.*, 2005). LGP2, on the other hand, is the only receptor that does not contain a CARD and has been shown to have a regulatory role for the other RLRs by titrating their activity in response to RNA ligation (Rothenfusser *et al.*, 2005; Satoh *et al.*, 2010).

1.2.3 Intracellular DNA sensors

The capacity of DNA to stimulate the immune system has been known for more than 50 years (Isaacs, 1963). Toll-like receptor 9 (TLR9) was the first described sensor of DNA in endosomes (Hemmi *et al.*, 2000). These receptors survey the endosomes and lysosomes of pDCs, macrophages and B cells for microbial DNA. More recently, a second category of intracellular DNA sensors was revealed, responsible for monitoring the cytoplasm of all cell types for the presence of harmful levels of DNA. Under normal physiological circumstances the cytoplasm has very low levels of DNA and as such, when significant amounts are present in this compartment, it is a clear signal of infection or cellular stress. The first studies that showed this applied dsDNA to the cytosol of cells or infected them with *Listeria monocytogenes*, which resulted in the generation of IRF3-mediated IFN-I antiviral immune response independently or TLR9 (Daniel B. Stetson and Medzhitov, 2006; Ishii *et al.*, 2006). This has also been shown to occur after DNA virus infection with retroviruses,

herpesviruses or poxviruses, among others (Ferguson *et al.*, 2012; Morchikh *et al.*, 2017; Wang *et al.*, 2017) or following artificial administration of various species of purified dsDNA. Intracellular DNA recognition is dependent on the length and the structure of the transfected DNA, where oligomers shorter than 25 bp and not in the B-form helix arrangement failed to stimulate IFN-I immunity (Daniel B. Stetson and Medzhitov, 2006; Ishii *et al.*, 2006). An example of synthetic dsDNA that can stimulate the intracellular immune response is 45 bp interferon stimulatory DNA (ISD), from the genome of *Listeria monocytogenes,* which lacks unmethylated CpG motifs (Stetson, 2006a).

A considerable amount of progress has been made into unravelling cytoplasmic DNA sensors and the downstream signalling pathways. Some of these include cyclic GMP-AMP synthase (cGAS) (Sun *et al.*, 2013), IFN inducible gene 16 (IFI16) (Unterholzner *et al.*, 2010), DNA-dependent protein kinase (Ferguson *et al.*, 2012), absent in melanoma 2 (AIM2) (Hornung *et al.*, 2009), RNA-polymerase III (RNA pol III) (Ablasser *et al.*, 2009; Chiu, MacMillan and Chen, 2009), DEAD/H-box helicase 41 (DDX41) (Z. Zhang *et al.*, 2011), meiotic recombination 11 (MRE11) (Kondo *et al.*, 2013), leucine-rich repeat flightless-interacting protein 1 (LRRFIP1), DHX9 and DHX36 (Kim *et al.*, 2010), DEAD box helicase 60 (DDX60) (Moeko *et al.*, 2011), etc. Some of these sensors are depicted in Figure 1 and will be described in more detail below.

The signalling of most DNA sensors converges at the activation of the stimulator of interferon genes (STING) adaptor protein (Ishikawa, Ma and Barber, 2009), which is a central mediator of the innate immune response to cytoplasmic dsDNA (Barber, 2015). STING facilitates the production of type I IFNs and inflammatory cytokines predominantly via the recruitment and phosphorylation of TBK1 and IRF3 (Ishii *et al.*, 2006, 2008; Tanaka and Chen, 2012) but also through the NF-κB signalling branch (Abe and Barber, 2014) (Figure 1,2). IFN-I is pivotal in the establishment of an antiviral state in the cell and is therefore a major signalling output of cytoplasmic DNA sensing. Some of the sensors have also been implicated in the induction of

inflammasome formation (Figure 1) or programmed cell death in response to virus infection.

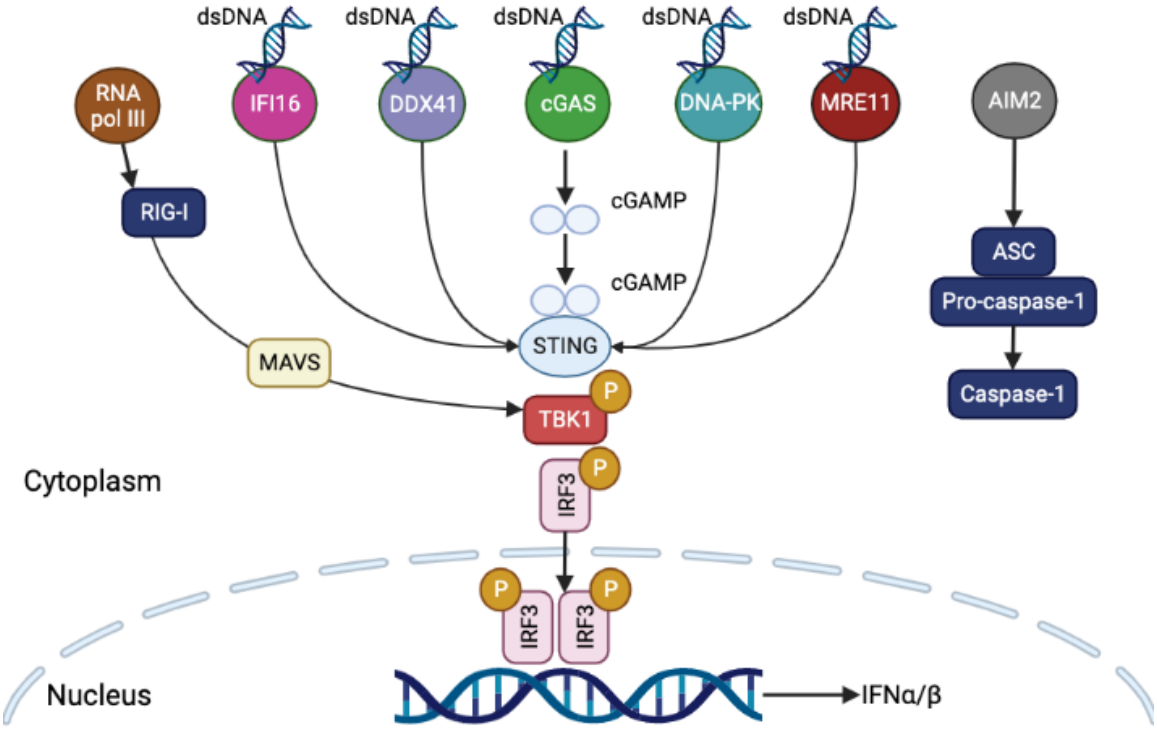

Figure 1. Intracellular DNA sensors.
IFI16, DDX41, cGAS, DNA-PK and MRE11 sensors all converge onto activating STING protein. Activated STING recruits TBK1 and IRF3 and phosphorylated IRF3 homodimers translocate to the nucleus to initiate the IFN transcriptional program. AIM2 mediates inflammasome formation upon DNA sensing in caspase-dependent manner. RNA pol III converts DNA into RNA, which is detected by RIG-I RNA sensor and signals via MAVS/TBK1/IRF3 to induce IFN-I response.

The presence of DNA in the cytoplasm is a clear danger signal for sensing by PRRs that survey this compartment, but it is less clear how foreign DNA is sensed in other subcellular compartments like the nucleus. The nucleus was initially considered as an "immune-privileged" environment for DNA detection since it comprises genomic self-DNA, although this concept has been challenged (Kerur *et al.*, 2011; Li *et al.*, 2012). IFI16 and cGAS have been shown to have nuclear roles in DNA sensing and novel nuclear DNA sensors, such as hnRNPA2B1, are emerging (Chan and Gack, 2016; Lahaye *et al.*, 2018; Zhang, Flavell and Li, 2019). The nature of the stimulus, the cell type and the subcellular compartmentalisation can impact the choice of DNA sensor that will confer antiviral immunity to the host cell (Okude, Ori and Kawai,

2021). Even though we have gained a lot of insight into the biology of DNA PRRs, there are still gaps in the understanding of the molecular mechanisms in their activation, localisation and how they cooperate with each other.

1.2.3.1 cGAS

cGAS is the most widely studied DNA sensor which was first identified by James Chen in 2013 (Lijun *et al.*, 2013). The protein belongs to the nucleotidyltransferase (NTase) family and contains an N-terminal DNA binding domain, through which it directly interacts with cytosolic DNA (Jiaxi *et al.*, 2013; Lijun *et al.*, 2013; Franz *et al.*, 2018). cGAS detects dsDNA with high affinity but it can also recognise single-stranded DNA (ssDNA) (Kranzusch *et al.*, 2013). It senses DNA in a sequence-independent but length-dependent manner. The structure of cGAS has been solved and it reveals that hydrogen bonds and electrostatic interactions mediate the interaction between the enzyme and the nucleic acid backbone (Civril *et al.*, 2013; D. Gao *et al.*, 2013). The binding induces dimerisation of cGAS and enables its active site to catalyse the synthesis of the second messenger cyclic GMP-AMP (2'3'-cGAMP) from ATP and GTP. Upon ligand binding, liquid droplets are created which increase the concentration of cGAS and cGAMP, accordingly (Jiaxi *et al.*, 2013; Mingjian and J., 2018). cGAMP can then activate STING, creating higher-order STING oligomers that stimulate the IFN-I response (Shang *et al.*, 2019). cGAMP can also be transferred to bystander resting cells via gap junctions. It stimulates neighbouring cells expressing STING to produce IFN-I in a more efficient way than cytokines, which are often blocked by viruses (Ablasser *et al.*, 2013; A. *et al.*, 2015).

Initially cGAS was thought to reside exclusively in the cytoplasm, but a number of studies have shown its localisation in the nucleus and one study has reported cGAS to be positioned in the plasma membrane (Barnett *et al.*, 2019). cGAS was shown to translocate to the nucleus during mitosis and nuclear membrane disintegration (M. *et al.*, 2016; Zhong *et al.*, 2020). The nuclear export signal of cGAS is essential for cGAS translocation to the cytoplasm during DNA stimulation and mutating it,

reduced the interferon response to DNA (Sun *et al.*, 2021). A nuclear role for cGAS in HIV DNA sensing was reported in a study by Lahaye *et* al, where cGAS cooperated with NONO viral capsid sensor to enable HIV-2 DNA sensing and activate STING (Lahaye *et al.*, 2018). Moreover, in the nucleus cGAS is involved in the DNA damage response, suppressing DNA repair and promoting tumorigenesis (Liu *et al.*, 2018). Structural studies have demonstrated that nuclear cGAS is associated with nucleosomal histones that prevent unwanted activation of the synthase by genomic self-DNA (Boyer *et al.*, 2020; Kujirai *et al.*, 2020; Michalski *et al.*, 2020; Pathare *et al.*, 2020; Tomoya *et al.*, 2020; Zhao *et al.*, 2020).

cGAS functions to sense a number of virus infections in multiple cell types, such as fibroblasts, keratinocytes, macrophages and instigates IFN-I signalling via STING (D. Gao *et al.*, 2013; Schoggins *et al.*, 2014). The enzyme is able to recognise DNA viruses, such as vaccinia virus (VACV), herpes simplex virus (HSV) type 1 and 2, cytomegalovirus (CMV), adenovirus, etc (Tan *et al.*, 2015). cGAS knockout mice are more susceptible to HSV-1 infection and have diminished immune response, as well as higher viral titres (Li *et al.*, 2013). cGAS DNA sensor is also able to detect the complementary DNA generated during infection with the retroviruses human immunodeficiency virus (HIV), Dengue virus, vesicular stomatitis virus (VSV), among others (D. Gao *et al.*, 2013; Sun *et al.*, 2013, 2017). Additionally, cGAS was shown to recognise bacteria, such as *M. tuberculosis* and elicit an interferon response (Wassermann *et al.*, 2015; Watson *et al.*, 2015).

1.2.3.2 IFI16

IFI16 belongs to pyrin and HIN200 domain-containing (PYHIN) family of proteins, as well as the AIM2-like receptor (ALR) family (Paludan and Bowie, 2013). IFI16 contains HIN domains that bind to DNA and a pyrin domain (PYD) that facilitates protein-protein interactions mediating downstream signalling. IFI16 is the first sensor shown to bind ss and dsDNA and activate an innate immune response (Jakobsen *et al.*, 2013). Similar to cGAS, IFI16 recognises DNA in a length-dependent

but sequence-independent manner. IFI16 associates with DNA via electrostatic interactions and the protein utilises its HIN domains to scan along the DNA strand (Stratmann *et al.*, 2015). Downstream of this event, IFI16 induces IFN-I antiviral immune response by activating STING. It has been reported that IFI16 can stabilize STING but the exact interaction between the PYD domain of the DNA sensor and STING is not fully understood (Almine *et al.*, 2017). Apart from IFN-I immunity, IFI16 can also instigate inflammasome formation or pyroptosis in response to virus infections. In the context of KSHV infection IFI16 has been shown to induce DNA-mediated inflammasome complex formation in the nucleus, which is translocated to the cytoplasm (Kerur *et al.*, 2011). Moreover, IFI16 has been documented to initiate the activation of caspase-1 leading to pyroptosis during HIV infection (Doitsh *et al.*, 2014).

IFI16 is expressed in most cell types and it can function as a DNA sensor in the nucleus and the cytoplasm (Unterholzner *et al.*, 2010; Conrady *et al.*, 2012; Horan *et al.*, 2013; Chiliveru *et al.*, 2014; Orzalli *et al.*, 2015). It has been extensively studied in relation to HSV-1 infection whose replication cycle is executed in the cell nucleus. Upon viral DNA sensing, IFI16 has been shown to undergo acetylation and translocation to the cytoplasm to facilitate downstream immune signalling (Ansari *et al.*, 2015). Moreover, the receptor has been shown to cooperate with cGAS and stabilise cGAMP for the generation of a productive immune response in response to DNA virus infection in macrophages and keratinocytes (Jønsson *et al.*, 2017). The ALR has also been demonstrated to colocalise with VACV viral replication compartments in the cell cytoplasm and induce the production of inflammatory cytokines (Almine *et al.*, 2017). Moreover, during HSV-1 infection, IFI16 can suppress viral replication by binding to viral transcription start sites (Johnson *et al.*, 2014). HSV, on the other hand, has developed ways to counteract the function of the DNA sensor by degrading IFI16 in ICP0-dependent manner (Orzalli, DeLuca and Knipe, 2012). Apart from the DNA sensing role of IFI16, the PYHIN protein has also been implicated in the DNA damage response suggesting that it can bind to free DNA ends and stimulate the innate immune response (Kerur *et al.*, 2011).

1.2.3.3 AIM2

AIM2 is another member of the PYHIN and ALR families of proteins. It is expressed in certain cell types, such as keratinocytes, cells of monocytic lineage and intestinal epithelium (Bürckstümmer *et al.*, 2009; Di Micco *et al.*, 2016). AIM2 binds different types of DNA, such as self-DNA, as well as DNA derived from multiple viruses and bacteria (Muruve *et al.*, 2008; Hornung *et al.*, 2009; Choubey and Panchanathan, 2017). The receptor interacts with the sugar-phosphate backbone of the nucleic acid in sequence-independent manner (Jin *et al.*, 2012). AIM2 differs from the other DNA sensors that stimulate the canonical STING/IRF3-dependent pathway. In contrast to IFI16, the N-terminal pyrin domain associates with the apoptosis-associated speck-like protein containing a CARD (ASC) (Bürckstümmer *et al.*, 2009). ASC in turn binds to the CARD domain of pro-caspase-1, which results in the formation of the inflammasome complex. As a result, IL-1β and IL-18 facilitate the induction of the inflammatory response or pyroptosis. Furthermore, the AIM2 inflammasome has been shown to initiate apoptosis (Gaidt *et al.*, 2017). AIM2 activation and inflammasome formation have been reported in response to DNA virus infections with VACV or mouse cytomegalovirus (Rathinam *et al.*, 2010).

1.2.3.4 DNA-PK

DNA-PK is a heterotrimeric complex that consists of the Ku70/80 heterodimer and the DNA-dependent protein kinase catalytic subunit (DNA-PKcs). DNA-PK has been mainly studied for its function in the non-homologous end-joining (NHEJ) process that repairs DNA double-strand breaks (DSBs) (Smith and Jackson, 1999; Mahaney, Meek and Lees-Miller, 2009). Moreover, loss of function of the DNA-PK complex *in vivo* causes severe combined immunodeficiency syndrome (SCID) due to defective V(D)J recombination in T- and B- cells (Kienker, Shin and Meek, 2000). Ku70/Ku80 detect and associate with the broken DNA ends in a sequence-independent manner (Mahaney, Meek and Lees-Miller, 2009), whereas DNA-PKcs complexes with Ku and DNA, and processes the broken ends through many phosphorylation events (Rivera-

Calzada *et al.*, 2007; Davis, Chen and Chen, 2014). DNA-PKcs affinity for DNA is greatly diminished in the absence of the Ku protein (Yaneva, Kowalewski and Lieber, 1997; Walker, Corpina and Goldberg, 2001).

The complex has been shown to have the propensity to sense viral DNA, which was first discovered in immunoprecipitation assays in HEK293T cells. In mouse embryonic fibroblasts (MEFs), DNA-PKcs drives STING/IRF3-dependent immunity in response to DNA. MEFs or mice deficient in the protein exhibited diminished IFN-I and inflammatory cytokine response during MVA and HSV-1 infection (Ferguson *et al.*, 2012). More recently, a study demonstrated a STING-independent DNA sensing role for DNA-PK in human monocytes (Burleigh *et al.*, 2020), which suggests that the cell type specificity influences the preference of PRR pathway mechanism. Furthermore, Ku70 has also been implicated in viral DNA sensing driving IFN-III but not IFN-I response mainly in HEK cells (X. Zhang *et al.*, 2011).

The kinase activity of DNA-PKcs is critical for the DNA repair process (Kurimasa *et al.*, 1999). However, the catalytic function has been shown to be dispensable for the innate immune response in murine cells (Ferguson *et al.*, 2012) although results from other studies are not in concordance with this notion (Burleigh *et al.*, 2020; Sun *et al.*, 2020; Justice *et al.*, 2021). DNA-PK is expressed in most cell types and it repairs damaged DNA in the nucleus, while during viral DNA sensing, it has been shown to co-localise with MVA viral factories in the cytoplasm (Ferguson *et al.*, 2012). DNA-PK may interact with other sensors, such as IFI16 or cGAS in the context of virus infection (Sun *et al.*, 2020; Justice *et al.*, 2021). The implications for the DNA-PK complex as a viral DNA sensor will be discussed in more detail in section 5 below.

1.2.3.5 MRE11

MRE11 is another DNA damage repair protein that has been proposed to act as a DNA sensor. MRE11 is part of the MRN complex that also comprises RAD50 and

NSB1. RAD50 and MRE11 cooperate for executing the NHEJ process (Yuan *et al.*, 2012). DNA transfection was shown to induce the phosphorylation of ATM and MRE11 was found to be partially responsible for IFNβ production in STING-dependent manner (Kondo *et al.*, 2013). MRE11 mutants lacking nuclease activity enhanced the immune signalling to DNA (Kondo *et al.*, 2013).

1.2.3.6 RNA pol III

RNA pol III is an unusual DNA sensor in that it converts viral DNA into RNA with 5'-triphosphate, which is a potent activator of RIG-I and the MAVS signalling pathway (Ablasser *et al.*, 2009; Chiu, MacMillan and Chen, 2009). This can be beneficial to the host as it allows the RNA sensing pathway to detect DNA virus infections. RNA pol III is unique in its ability to recognise DNA in a sequence-dependent manner and it has been shown to be activated by AT-rich DNA and specifically by the synthetic ligand polydA:dT (Ablasser *et al.*, 2009; Chiu, MacMillan and Chen, 2009). The sensor can function in both the nucleus and the cytoplasm of the cell. It was recently found that in humans mutant RNA pol III decreased IFN production during varicella zoster virus (VZV) infection (Ogunjimi *et al.*, 2017). RNA pol III has also been implicated in the sensing of adenovirus (C. and Erik, 2012) while its involvement in the immune response to HSV-1 infection has been controversial (Chiu, MacMillan and Chen, 2009; Jesper *et al.*, 2010; Unterholzner *et al.*, 2010).

1.2.3.7 DDX41

DDX41 is a member of the DEAD-box containing helicases that can sense viral DNA of adenovirus and HSV-1 in the cytosol of dendritic cells (Z. Zhang *et al.*, 2011). When the expression levels of IFI16 were reduced, DDX41 was responsible for the interferon response to DNA, illustrating that the choice of DNA sensor in a given system may be governed by the expression pattern. It uses its DEAD domain to interact with DNA and subsequently activates STING and IFN-I signalling (Omura *et al.*, 2016). However, several reports have published data that DDX41 appeared dispensable for the induction of DNA-driven IFN-I immune response (Abe *et al.*,

2013; Lijun *et al.*, 2013; Eric, Saskia and Erik, 2014) and thus, further work is necessary to elucidate the role of DDX41 in DNA sensing.

1.2.3.8 hnRNPA2B1

hnRNPA2B1 pertains to the hnRNP family and is a novel DNA sensor that detects DNA in the nucleus (Lei, Mingyue and Xuetao, 2019). Upon activation with a DNA ligand, the protein is dimerised and demethylated, followed by a translocation to the cell cytosol. In the cytoplasm hnRNPA2B1 mediates IFN production in STING-dependent manner (Zhang, Flavell and Li, 2019). The receptor has also been documented to enhance the translation of STING, IFI16 and cGAS mRNAs during virus infection (Lei, Mingyue and Xuetao, 2019). In contrast, hnRNPA2B1 has been implicated in the release of enveloped HSV-1 from infected cells (Xusha *et al.*, 2021) showing the multifaceted roles of the ribonucleoprotein during virus infection.

1.3 Intracellular DNA sensing signalling pathway

Many immune and non-immune cells, such as epithelial cells, macrophages, dendritic cells and fibroblasts, possess the DNA sensing machinery (Ishikawa, Ma and Barber, 2009; Takeuchi and Akira, 2010; Unterholzner *et al.*, 2010) and this machinery is essential for initiating an antiviral response to DNA virus infections (Luecke and Paludan, 2015). Downstream of PRR activation, the best-characterised signalling output of DNA sensing is the STING-TBK1-IRF3 signalling axis, which culminates in type I IFN transcription (Ishikawa and Barber, 2008; Jin *et al.*, 2008; Zhong *et al.*, 2008) (Figure 2). Apart from that, additional pathways can be activated, leading to NF-kB signalling, inflammasome activation, or cell death. IRF3 and NF-kB induce the expression of interferons (Figure 2), cytokines and chemokines, which can activate monocytes, lymphocytes and non-immune cells, as well as attract more leukocytes to the site of infection with the aim of eliminating the pathogen and restoring homeostasis (Paludan and Bowie, 2013; Gui *et al.*, 2019).

Some of the key components of the DNA sensing pathway downstream of PRR activation will be discussed in more detail below.

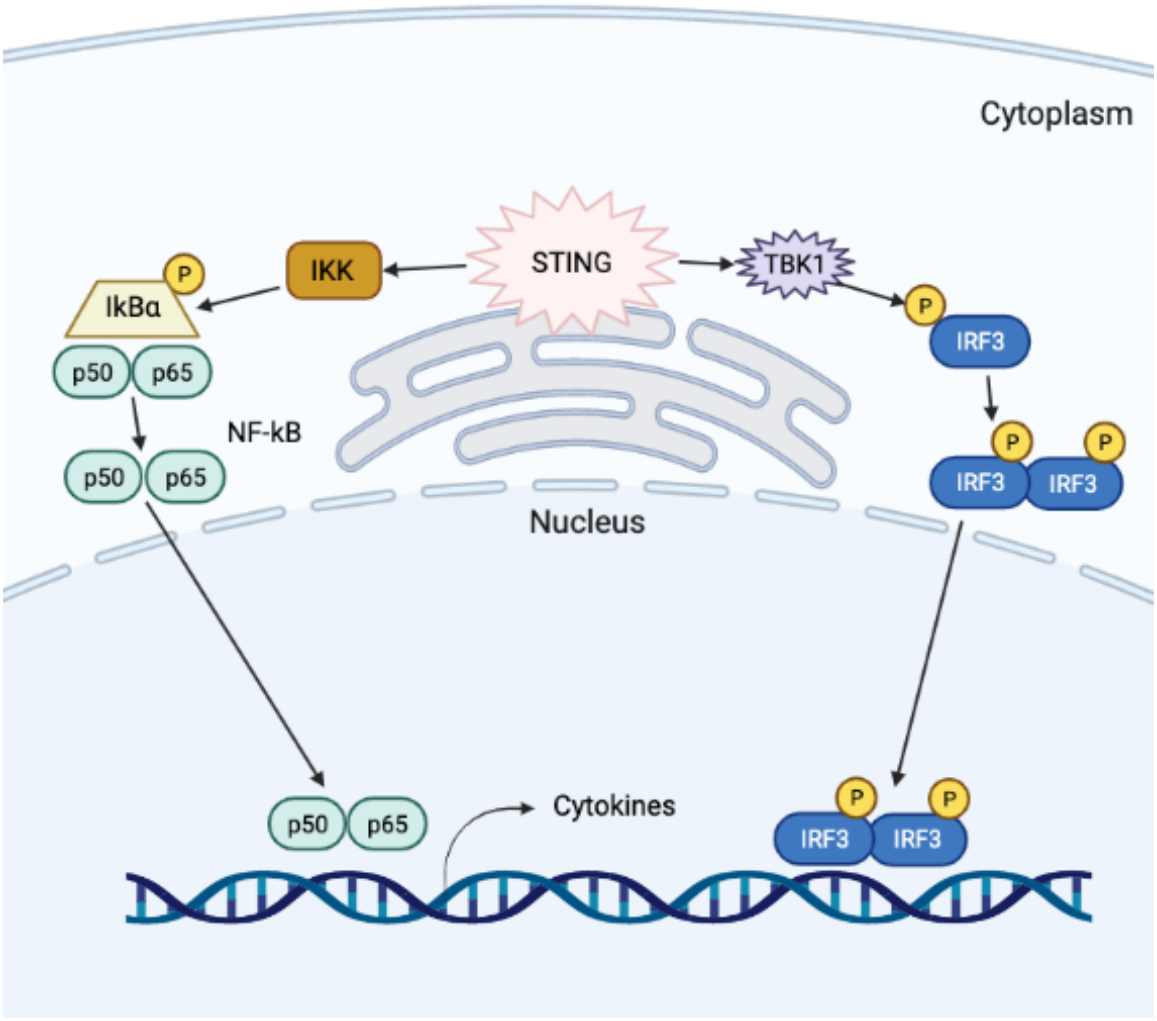

Figure 2. Intracellular DNA sensing pathway.
STING is central to the DNA sensing pathway. Activated STING can signal downstream to TBK1, which will promote the recruitment and phosphorylation of IRF3. Alternatively, STING can signal to the NF-kB pathway by activating the IKK family and inducing the degradation of IkBa, which results in the release of NF-kB. However, the mechanism for the stimulation of NF-kB by STING is unclear. Active IRF3 and NF-kB transcription factors translocate to the nucleus and initiate the inflammatory transcriptional program.

1.3.1 STING adaptor protein

Stimulator of interferon genes (STING), encoded by the transmembrane protein 173 (*TMEM173*) gene, plays a central role as a scaffolding protein in the immune response to DNA, downstream of PRRs (Ishikawa and Barber, 2008; Jin *et al.*, 2008; Zhong *et al.*, 2008; Ishikawa, Ma and Barber, 2009; Sun *et al.*, 2009). STING was first

discovered to sense cyclic dinucleotides (CDNs) produced by bacteria (Burdette *et al.*, 2011), but it was later shown that it could bind cGAS-derived 2'3'-cGAMP with higher affinity, which enabled STING activation and generation of the IFN response (Diner *et al.*, 2013; Jiaxi *et al.*, 2013). STING has been shown to induce IFN in response to transfected DNA and to a number of viruses, such as HSV-1, CMV, vesicular stomatitis virus (VSV), as well as to bacteria including *L. monocytogenes* and *M. tuberculosis* (Ishikawa and Barber, 2008; Ishikawa, Ma and Barber, 2009; Manzanillo *et al.*, 2012; Hansen *et al.*, 2014).

The human STING protein comprises four transmembrane helices and a large cytosolic domain that is involved in signal transduction and that binds to CDNs (Burdette *et al.*, 2011; Shang *et al.*, 2012). STING has been postulated to have co-evolved with cGAS in vertebrates (Wu *et al.*, 2014). Upon cGAMP binding, the adaptor protein encloses the second messenger deep in its binding pocket by bringing together two C-terminal wings of STING monomers (Shang *et al.*, 2012) and the binding site is topped by antiparallel β-sheets that further enclose the structure (P. Gao *et al.*, 2013; Zhang *et al.*, 2013). STING has also been reported to bind DNA without the involvement of other proteins (Abe *et al.*, 2013). However, this interaction failed to induce IFN expression in HEK293T cells dismissing the role of STING as a DNA sensor (Burdette *et al.*, 2011; Jiaxi *et al.*, 2013).

In a resting state, STING resides in the endoplasmic reticulum (ER), anchored by its N-terminal domain (Ishikawa and Barber, 2008; Saitoh *et al.*, 2009; Sun *et al.*, 2009). In the presence of cytosolic DNA, STING in a complex with cGAMP undergoes a conformational change and translocates to the ER-Golgi intermediate compartment (ERGIC), which allows it to activate its downstream partners (Ishikawa, Ma and Barber, 2009; Dobbs *et al.*, 2015). The trafficking process is facilitated by coat protein complex II (COPII) and ADP-ribosylation factor (ARF) (Gui *et al.*, 2019). In the Golgi apparatus, STING is palmitoylated, which is important for the activation of the protein (Mukai *et al.*, 2016). STING translocation event has also been linked to autophagy (Saitoh *et al.*, 2009), which keeps excessive immune activation in check.

After STING has translocated to the ERGIC, TBK1 kinase is recruited, which phosphorylates STING at several sites in the C-terminus. Phosphorylation at serine 366 has been reported to be pivotal to the DNA-induced STING-dependent immune response (Tanaka and Chen, 2012; Liu *et al.*, 2015). STING protein can be subjected to a number of posttranslational modifications for optimal signalling, such as ubiquitination by TRIM32 or TRIM56 to positively regulate the induction of IFN response to DNA (Tsuchida *et al.*, 2010; Zhang *et al.*, 2012). On the other hand, phosphorylation by ULK1 kinase on serine 366 or ubiquitination by RNF5 for degradation are negative regulators of the pathway and can prevent STING hyperactivation (Zhong *et al.*, 2009; Konno, Konno and Barber, 2013).

TBK1 phosphorylation of STING creates an overall negative surface charge that attracts interferon regulatory factor 3 (IRF3) to the complex (Liu *et al.*, 2015). IRF3 is also phosphorylated by TBK1, which results in its activation and dimerisation. Active phospho-IRF3 dimers traffic to the nucleus where they associate with the promoters of IRF-inducible genes in a sequence-dependent manner to drive the transcription of type 1 IFN genes (Fujii *et al.*, 1999). Fibroblasts, macrophages and DCs lacking STING fail to induce an inflammatory response and IRF3 translocation after DNA stimulation (Ishikawa and Barber, 2008; Ishikawa, Ma and Barber, 2009) and Poly(I:C), an RNA homologue, was shown to produce IFN independently of STING. STING can also induce the activation and nuclear translocation of the NF-κB transcription factor in response to DNA even though the exact mechanism is not clearly understood (Abe and Barber, 2014; Balka *et al.*, 2020). IRF3 and NF-κB signalling will be described in more detail in the next section.

1.3.2 IRF3 signalling

The IRF transcription factor family consists of 9 members, IRF 1-7 (Mamane *et al.*, 1999; Taniguchi *et al.*, 2001). They are stimulated downstream of multiple PRRs, such as TLRs, RLRs and a number of intracellular DNA sensors, and induce the expression of a vast plethora of antiviral and inflammatory genes. IRFs contain a

DNA-binding domain at the N-terminus and with it they recognise a specific sequence in the promoters of IRF-inducible genes, named the IRF response element (IRE) (Fujii *et al.*, 1999). Their C-terminus enables interactions with other transcription factors including STATs (Mamane *et al.*, 1999; Taniguchi *et al.*, 2001).. IRF1, IRF3, IRF5 and IRF7 are essential for the generation of IFN-I responses. IRF3 and IRF7 are the most homologous in structure and are central mediators of the IFN-I response downstream of PRR signalling (Honda, Takaoka and Taniguchi, 2006). IRF7 is mainly abundant in pDCs, whereas IRF3 is ubiquitously expressed in multiple cell types. IRF3 transcription factor is constitutively expressed in cells while IRF7 is involved in a positive feedback loop and its expression is reinforced by type I IFN (Marié, Durbin and Levy, 1998; Sato *et al.*, 1998; Honda *et al.*, 2005). In a resting state, IRF3 and IRF7 reside in the cytoplasm but upon viral infection, they undergo phosphorylation and translocation to the nucleus (Lin *et al.*, 1998; Sato *et al.*, 1998; Yoneyama *et al.*, 1998). The IκB-related kinases (IKK) TBK1 and IKKε have been shown to phosphorylate the transcriptional regulators (Fitzgerald *et al.*, 2003; Sonia *et al.*, 2003). IRF3 is phosphorylated at many residues, such as S385, S386, S396, etc. but S386 phosphorylation has been found to be essential for IRF3 activation (Mori *et al.*, 2004). Cells lacking IRF3 failed to induce IFN-I and were susceptible to infections with multiple viral and bacterial pathogens (Sato *et al.*, 2000). Apart from type I IFN, IRF3 can also stimulate the expression of other inflammatory cytokines, such as CXCL10, CCL5, etc (Sakaguchi *et al.*, 2003; Brownell *et al.*, 2014). However, it is currently unknown whether IRF3 can regulate their expression pattern depending on the cell type or PRR.

1.3.3 Interferons

IFNs are produced early during infection and are essential for the establishment of an antiviral state in the cell. They signal in autocrine and paracrine manners to the infected cell or other nearby cells. IFN was observed for the first time during influenza virus infection as a factor produced by infected cells that was able to prevent viral replication in other cells (Isaacs and Lindenmann, 1957). There are three known classes of IFNs (type I, II, III). These signal by binding to their

corresponding receptors. Type I associates with IFN alpha receptor 1 and 2 (IFNAR1/2), type II with IFN gamma receptor 1 and 2 (IFNGR1/2), type III with IFN lambda receptor 1 (IFNLR1) and IL-10 receptor subunit beta (IL10RB) (de Weerd and Nguyen, 2012). The receptors engage the Janus kinase-signal transducer and activator of transcription (JAK-STAT) signalling pathway and induce the expression of a wide range of interferon-stimulated genes (ISGs), which have antiviral and immunomodulatory functions (Daniel B Stetson and Medzhitov, 2006; Murray, 2007). They can restrict viral entry into cells, impede replication and hinder the release of virions from the infected cells. ISGs can also modulate the sensitivity of a cell to interferon by upregulating the expression of PRRs or downstream signalling components (Schneider, Chevillotte and Rice, 2014; Hoffmann, Schneider and Rice, 2015).

Type I IFNs are conserved among vertebrates and they comprise 13 *IFNA* genes in humans and 1 *IFNB1* gene, which are expressed ubiquitously, as well as *IFNW1, IFNE* and *IFNK* (Taniguchi *et al.*, 1980; Weissmann and Weber, 1986; Pestka, Krause and Walter, 2004). *IFNB1* is an essential cytokine contributing to the early innate immune response after virus infection. *IFNB1* expression is induced by the cooperative action of IRF3, NF-κB and AP-1 (a dimer of activating transcription factor 2 (ATF2) and c-Jun) transcription factors forming an enhanceosome on the promoter (Kim and Maniatis, 1997; Ford and Thanos, 2010). This is followed by CREB binding protein (CBP)-mediated acetylation of histones at the IFNB1 promoter region, recruitment of the transcription factor II D (TFIID) complex and initiation of transcription (Agalioti *et al.*, 2000; Honda, Takaoka and Taniguchi, 2006).

Type II IFN comprises only IFNγ, which is expressed by T cells and natural killer (NK) cells, and is stimulated by IL-18 and IL-12 instead of PRRs (Schroder *et al.*, 2004). Type III IFNs consist of 4 members, IFNλ1-4, which are expressed by multiple cell types upon viral infection (Kotenko *et al.*, 2003; Sheppard *et al.*, 2003; Hamming *et al.*, 2013; Prokunina-Olsson *et al.*, 2013). These cytokines are mostly

produced by type 2 myeloid dendritic cells (5-wiki). Their function is similar to type I interferons but less strong and mostly as a primary antiviral defence in epithelial cells as the expression of IFNLR1 is restricted to epithelial tissues (2, 3,11 – wiki).

1.3.4 NF-κB signalling

The NF-κB pathway is involved in a broad number of cellular processes and can be activated by multiple stimuli and receptors. NF-κB family transcription factors play important roles in the antiviral response by inducing the expression of inflammatory cytokines and chemokines. The NF-κB family includes 5 members: RelA (p65), RelB, c-Rel, p50/105 and p52/100, which can form dimers with each other, of which p50/65 is the most common (Huxford *et al.*, 1998; Napetschnig and Wu, 2013). NF-κB can be stimulated downstream of PRRs, such as RLRs, TLRs and some of the intracellular DNA sensors. In resting state, NF-κB activation is inhibited by inhibitors of KappaB (IκB) in the cytosol, which obscure the nuclear localisation signal of the transcription factor (Baeuerle *et al.*, 1988; Huxford *et al.*, 1998). Most ligands stimulate the canonical NF-κB pathway where IκB is phosphorylated by the IκB kinases (IKK) complex, which enables released NF-κB to translocate to the nucleus and stimulate gene expression (Régnier *et al.*, 1997; Zandi *et al.*, 1997).

Downstream of DNA sensors, NF-κB can be stimulated in STING/TBK1- or TRAF6-dependent manner (Abe and Barber, 2014). IKKε has been implicated in the STING/TBK1-dependent activation of NF-κB where TBK1 and IKKε kinases act redundantly in myeloid cells and require TAK and IKK complex for NF-κB activation (Balka *et al.*, 2020). Intracellular DNA is considered to be a weak activator of NF-κB as some papers have reported little NF-κB activation. Overall, the precise mechanisms by which STING drives NF-κB activation are not clearly understood.

1.4 Viral DNA sensing

1.4.1 VACV

Vaccinia virus belongs to the *Poxviridae* family of *Orthopoxviruses* and is the most extensively studied poxvirus. VACV is a large dsDNA virus whose linear genome consists of around 190 kbp coding for approximately 200 genes (Goebel *et al.*, 1990). VACV is highly immunogenic and is widely known for its use as the vaccine used to eradicate smallpox. There are a number of VACV strains, such as the Copenhagen (COP) and Western Reserve (WR) strains, which are widely used in research (Goebel *et al.*, 1990), as well as the Lister vaccine strain. Due to its high immunogenicity, VACV has significant side effects when used as a vaccine, which led to the development of safer attenuated strains. Modified Vaccinia virus Ankara (MVA), for example, was derived from the parental strain Chorioallantois vaccinia virus Ankara (CVA), by more than 570 passages in chicken embryo fibroblasts. MVA has lost its ability to replicate in human cells and has multiple immunomodulatory genes deleted. In VACV the most of the immunomodulatory genes are situated at the termini of the genome, while the central regions contain more highly conserved genes involved in virus replication (Volz and Sutter, 2017). Due to its attenuation, MVA is able to generate a productive innate immune response by the host, which has enabled researchers to gain insights on how VACV is sensed by PRRs.

VACV replicates exclusively in the cell cytosol where host nucleic acid sensing PRRs are abundant (Rathinam and Fitzgerald, 2011; Goubau, Deddouche and Reis e Sousa, 2013). Early viral genes are expressed in cytoplasmic cores before the genome is released for replication, which takes place in specialised regions called viral factories (Condit, Moussatche and Traktman, 2006; Moss, 2013). Immature virions traffic through the Golgi and progress into becoming extracellular enveloped viruses (EEVs), which infect more cells in the vicinity (Payne, 1980; Roberts and Smith, 2008). Meanwhile, intracellular mature virions (IMVs) accumulate in the cytoplasm and are secreted after lysis of the cell. Fibroblasts and keratinocytes in the skin are

the primary site of infection for VACV, which then transfers to monocytes at the site of infection (Hickman *et al.*, 2013; Parekh *et al.*, 2019).

The main PAMP during VACV infection is DNA, which is immediately recognised by sensors at the cytosolic viral factories. VACV and innate signalling have co-evolved together and almost one-half of the genes in VACV genome encode proteins that inhibit host innate immune response. Therefore, the attenuated strain MVA has been pivotal in understanding the interplay between the poxvirus and innate sensors. A number of studies have demonstrated that cGAS/STING are key mediators of the host immune response to MVA (Ferguson *et al.*, 2012; Dai *et al.*, 2014; Takahama *et al.*, 2017; Georgana *et al.*, 2018). MVA-infected human or mouse cells lacking these components revealed defective induction of type I IFNs and CXCL10. Moreover, IFI16 and DNA-PK have been shown to be important DNA sensors during MVA infection. DNA-PK complex components were shown to co-localise with viral factories in the cytosol and mediated the induction of IFN-I response to MVA but not to RNA virus in fibroblasts (Ferguson *et al.*, 2012). Similarly, IFI16 was found at MVA viral factories and mediated the induction of ISGs and CCL5 in keratinocytes (Almine *et al.*, 2017). In addition to this, the RNA sensing pathway has been implicated in the generation of the host immune response to MVA. MDA-5 detects RNA in the cytosol produced during VACV gene expression and stimulates IRF3-dependent IFN immunity (Delaloye *et al.*, 2009).

1.4.2 HSV-1

HSV-1 belongs to the *Herpesviridae* family. HSV-1, along with HSV-2 are alpha-herpesviruses that can establish life-long infection in the host by establishing latency in the trigeminal and dorsal root ganglia (Steiner and Benninger, 2013). In acute infection, HSV-1 is the cause of herpes labialis, genital herpes or keratitis and in more severe cases it can lead to encephalitis when the host is immunocompromised (Danastas, Miranda-Saksena and Cunningham, 2020). Approximately 70% of the global population carry the virus and nearly 100% of those above 65% have already been infected with HSV (Looker *et al.*, 2015).

HSV genome is linear dsDNA of around 150 kbp that codes for around 70 genes. The viral nucleic acid is enclosed by an icosahedral viral capsid, which is further enveloped in tegument. The tegument comprises many viral proteins important for establishing a favourable environment for virus replication within the host. The outermost layer of the HSV virion includes a number of glycoproteins that facilitate viral entry into the host cell (Kukhanova, Korovina and Kochetkov, 2014), such as fibroblasts, epithelial, neuronal or immune cells. Following fusion with the cell membrane, the virion is de-enveloped and the viral genome encaged in the capsid is transported to nuclear pores where it docks. The viral genome is injected through nuclear pores into the cell nucleus. The HSV genome can adopt a latent form in the nucleus of neuronal cells without any viral transcription until the virus is reactivated. The only active piece of viral DNA is the Latency Associated Transcript-DNA (LAT-DNA), which gives rise to LAT after splicing. LAT suppresses apoptosis of the infected cells and prevents the expression of lytic genes during latency (2,3 – wiki). HSV can also enter a lytic cycle when transcription is initiated and immediate early (IE) genes are expressed (Radtke *et al.*, 2010). Examples of the IE genes include infected cell polypeptide 0 (*ICP0*), *ICP4* and *ICP27*. This is followed by the transcription of early genes essential for viral replication, as well as late genes that encode virion structure proteins, such as VP24, VP25, etc. The final stage in the virus lifecycle is assembly of the viral capsid and egress of mature virions into the extracellular space (Alandijany, 2019).

PRRs have been shown to sense herpesviral DNA, as well as mitochondrial DNA that is released into the cytoplasm as a result of cytotoxic stress during HSV infection (Paludan *et al.*, 2011; Reinert *et al.*, 2016; Sun *et al.*, 2019). Endosomal HSV-1 DNA is recognised by TLR9, which stimulates NF-κB and IRF7 signalling and leads to the production of IFNα, mainly in pDCs (Lund *et al.*, 2003; Fiola *et al.*, 2010; Kawai and Akira, 2011). The cGAS/STING pathway is also critical for the innate immune response to herpesviruses. cGAS-/- mice are more susceptible to infection with HSV-1 (Li *et al.*, 2013; Christensen and Paludan, 2017) and in THP1 cells, HSV-1 induces

cGAS/STING-mediated IFN-I production (Reinert *et al.*, 2016). cGAS has been shown to reside both in the cytosol and the nucleus and in the cytosol of macrophages, cGAS senses herpesviral DNA that has leaked from proteasomally degraded viral capsids (Horan *et al.*, 2013). Another DNA sensor that senses HSV-1 dsDNA in macrophages is AIM2, which is counteracted by HSV VP22 viral inhibitor (Maruzuru *et al.*, 2018). Nuclear DNA sensors, such as hnRNPA2B1, can detect herpesviral DNA. hnRNPA2B1 interacts with the DNA and transports it from the nucleus to generate a type I interferon response in STING-dependent manner (Lei, Mingyue and Xuetao, 2019) IFI16 predominantly resides in the nucleus and has also been implicated in sensing herpesvirus DNA genome in this compartment to stimulate IFN in STING-dependent manner in human foreskin fibroblasts (HFFs), while cGAS stabilises IFI16 (Orzalli *et al.*, 2015). A number of studies have validated the findings that IFI16 and cGAS act in cooperation to generate a productive immune response to DNA (Orzalli *et al.*, 2015; Almine *et al.*, 2017; Jønsson *et al.*, 2017). Another way in which IFI16 can interfere with HSV-1 lifecycle is by associating with transcription sites and impeding viral transcription (Johnson *et al.*, 2014). Moreover, IFI16 acetylation promotes its translocation to the cytoplasm where it mediates the STING-dependent signalling to drive IFN production (Ansari *et al.*, 2015). IFI16 also has cytoplasmic sensing functions and has been observed to co-localise with HSV-1 DNA in the cytoplasm.

The DNA-PK complex is important for the host defense immunity to HSV-1, particularly in fibroblasts. *In vivo* and *in vitro* studies revealed that mice or murine fibroblasts lacking DNA-PKcs fail to generate a productive inflammatory cytokine response to HSV-1 (Ferguson *et al.*, 2012). Recently, DNA-PKcs was reported to localise at the nuclear periphery of HSV-infected human fibroblasts and interact with IFI16 for the induction of IFN immunity, suggesting for the cooperative activity of these sensors (Justice *et al.*, 2021). Similar to vaccinia virus, RNA sensors are also involved in the stimulation of host immunity against HSV-1. Viral DNA leaked from impaired capsid in the cytoplasm is converted to RNA by RNA Pol III and sensed by RIG-I to induce IFN in MAVS-dependent manner (Chiu, MacMillan and Chen, 2009).

Moreover, MDA-5 has been reported to recognise HSV-1 (Jesper *et al.*, 2010) but the source of the ligand for the receptor stimulation is unknown.

1.4.3 Viral antagonists of the DNA sensing pathway

If a certain cellular pathway is targeted for viral inhibition, this is good evidence that the pathway is involved in the immune response against the particular virus. Viruses have evolved to evade or inhibit immune mechanisms at different levels including inhibiting exposure of the viral nucleic acid to cytosolic sensors and inhibiting signalling from DNA sensors to IFN induction. An example is VACV protein C16, which associates with Ku70/80 from the DNA-PK complex and prevents its binding to the viral DNA (Peters *et al.*, 2013) (Figure 4). In addition to this, C4 is another viral protein that is able to bind Ku70 and impairs IRF3 activation and cytokine production in response to VACV infection (Scutts *et al.*, 2018) (Figure 4). It has been postulated that the poxvirus uses several strategies to inhibit DNA-PK due to its high expression levels in fibroblasts cells, which are the first site of infection. VACV also targets cGAS and cGAS-derived cGAMP to prevent viral recognition by the host immunity. For instance, VACV B2 protein, also called poxvirus immune nuclease (poxin), is an early viral gene that is able to cleave and degrade cGAMP (Eaglesham *et al.*, 2019). VACV mutants deficient in B2 display lower viral yields in mice (Eaglesham *et al.*, 2019). Downstream of DNA sensors, VACV has developed strategies to evade IRF3 and NF-κB signalling. C6 has been shown to inhibit the innate sensing pathway downstream by interfering with TBK1/IKKε signalling and restricting type I IFN signalling (Unterholzner *et al.*, 2011). VACV and viral mutants lacking C6 are more immunogenic *in vivo* (García-Arriaza *et al.*, 2013; Sumner, Ren and Smith, 2013; Q. Marín *et al.*, 2018). VACV has also developed several ways to suppress NF-κB signalling. One example is B14 protein, which interacts with IKKβ to inhibit its phosphorylation and the subsequent degradation of IκBα (Chen *et al.*, 2008; Tang, Chakraborty and Xu, 2018) that prevents NF-κB from translocating to the nucleus.

HSV-1 can also suppress the host innate immune signalling at various stages. At the level of the DNA sensors, the E3 ubiquitin ligase HSV-1 infected cell protein 0 (ICP0) can target IFI16 and DNA-PK for degradation via its RING finger domain (Figure 4). In the case of IFI16, the sensor is tagged for proteasomal degradation by ICP0 in the nucleus of HFF cells (Orzalli, DeLuca and Knipe, 2012; E., Leela and Bala, 2013). In contrast, ICP0 did not mediate IFI16 degradation in HepaRG or U20S cells (Delphine *et al.*, 2013). Another target of ICP0 is DNA-PKcs, whose protein levels are rapidly decreased during infection with WT HSV (Lees-Miller *et al.*, 1996). In cells deficient for DNA-PKcs, HSV-1 replicated more efficiently and produced higher viral yields. cGAS levels are also affected by HSV-1 infection through the action of UL41 viral protein, which degrades host mRNAs (Huang *et al.*, 2015). Furthermore, cGAS catalytic activity can be hindered by other herpesviral proteins, such as VP22 (Hew *et al.*, 2015; Zhang *et al.*, 2018) and UL37 has been shown to deamidate and inactivate cGAS. VP22 has also been implicated in preventing AIM2 inflammasome formation (Maruzuru *et al.*, 2018).

Downstream of DNA sensors, HSV-1 has employed an arsenal of strategies for viral immune evasion. Some examples are the herpesviral proteins ICP27 and UL46, which abrogate the interaction between STING and TBK1. While ICP27 prevents TBK1 phosphorylation of IRF3 by associating with STING/TBK1 complex (Christensen *et al.*, 2016), UL46 interacts with STING and TBK1 and prevents TBK1 dimerisation (Thibaut, Maria and M., 2021). Interestingly, in certain cancer cell types ICP0 was shown to stabilise STING, which promoted HSV-1 propagation in the infected cells (Kalamvoki and Roizman, 2014). Downstream of STING signalling, ICP0 has been reported to block IRF3- and IRF7- dependent induction of ISGs (Lin *et al.*, 2004).

1.4.4 Virus-induced cell death

Virus infection can often lead to death of the infected cell either by direct viral lysis or programmed cell death. Cell death is a host defence mechanism to prevent virus propagation and dissemination within cells and can be triggered by PRR signalling

pathways. Viruses on the other hand have evolved various tactics to combat these events.

In the case of HSV-1, the virus has been implicated in the induction of different forms of regulated cell death, both apoptosis and necroptosis, in infected cells. Interestingly, depending on the cell type, HSV can either induce, or inhibit apoptosis. In immune cells, such as dendritic cells and macrophages, it is beneficial for the virus to promote cell death pathway activation as these cells are involved in the efficient generation of immunity, while enabling the virus to amplify in non-immune cells (FLECK *et al.*, 1999; Kruse *et al.*, 2000; Mikloska, Bosnjak and Cunningham, 2001; Müller *et al.*, 2004; Bosnjak *et al.*, 2005). In epithelial cells and fibroblasts, cell death is likely to be inhibited by HSV to allow the successful generation of virion progeny and viral spread. HSV-1 instigates apoptosis in transformed but not primary cells (Martine, Jennifer and A., 1999) and it is well established now that the herpesvirus induces the apoptotic pathway early on but delays and inhibits it later from actual killing of the infected cells (Leopardi and Roizman, 1996; Koyama and Adachi, 1997; Galvan and Roizman, 1998; Martine, Jennifer and A., 1999). HSV-1 expresses a number of viral proteins with anti-apoptotic activities, such as ICP4, ICP24 and ICP27 (Martine and A., 1999; Aubert and Blaho, 2003; Nguyen, Kraft and Blaho, 2005). However, one of the immediate-early genes involved in triggering apoptosis and caspase activation is ICP0 (Sanfilippo and Blaho, 2006). Deletion of ICP0 renders HSV-1 incapable of triggering apoptosis after cycloheximide treatment, which is not observed when ICP4 or ICP22 viral genes are deleted (Sanfilippo and Blaho, 2006). HSV-1 must therefore benefit from the early induction of apoptosis in infected cells, which is only to be prevented later. However, the benefit from this mechanism is not clearly understood yet.

Apoptosis signalling can be divided into extrinsic and intrinsic pathways depending on the origin of the cell death stimulus (Figure 3). Extrinsic apoptosis refers to signalling from apoptotic ligands that come from cell death receptors, while intrinsic refers to ligands originating from the mitochondria, such as cytochrome c.

Downstream, those pathways converge onto activation of executioner caspase 3 and cleavage of the DNA repair protein Poly (ADP-ribose) polymerase-1 (PARP-1) to trigger apoptosis. The cleavage produces an 89 kDa by-poduct from 116 kDa protein (Martine, Jennifer and A., 1999).

When the apoptosis pathway is inactivated, an alternative form of regulated cell death, necroptosis can be triggered (Figure 3). Necroptosis is initiated by multiple stimuli, all of which lead to the activation of receptor-interacting protein kinase 3 (RIPK3). A downstream target that is phosphorylated by RIPK3 is mixed lineage kinase domain-like protein (MLKL). MLKL oligomerises and translocates to the cell plasma membrane initiating necroptosis. DNA-dependent activator of IRFs (DAI/ZBP1), which has been initially considered as a cytosolic DNA sensor, has been implicated in the necroptosis pathway. In the context of HSV-1 infection, DAI senses viral DNA and signals to RIPK3 for cell death pathway activation (Pham *et al.*, 2013; Guo *et al.*, 2018). However, HSV-1 ICP6 viral protein combats this by blocking the formation of the DAI/RIP3/MLKL signalosome during herpesviral infection (Wang *et al.*, 2014) (Figure 3). This was found to be true for human cell systems, which are natural hosts for HSV-1 infection. In mouse cells on the other hand, ICP6 appears to have a pro-necroptotic role independent of DAI (Wang *et al.*, 2014; Huang *et al.*, 2015). Thus, HSV-1 has evolved ways to restrict cell death in human cells, while in non-natural hosts like murine cells, necroptosis is efficiently initiated, which restricts viral replication (Yu *et al.*, 2016).

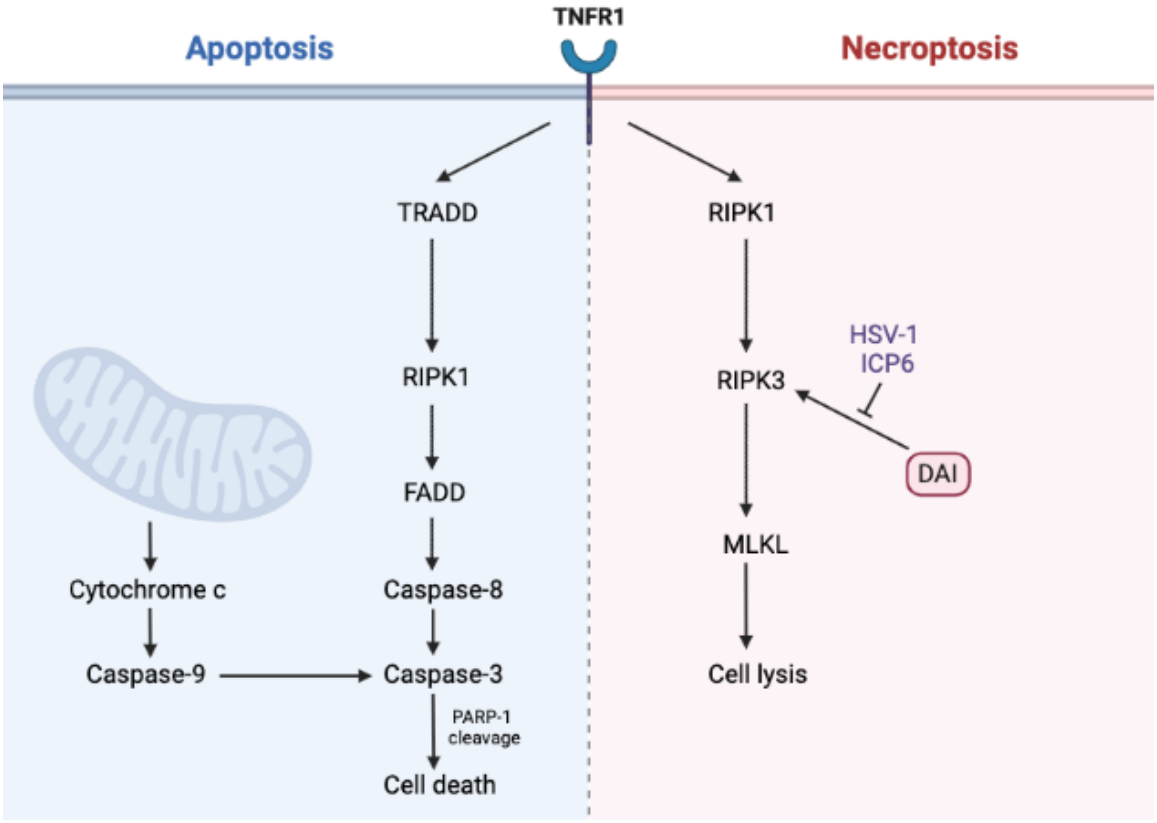

Figure 3. Programmed cell death pathways.

The intrinsic apoptosis pathway is associated with cytochrome c release from mitochondria, which activates caspases 3 and 9, PARP-1 cleavage and cell death. On the other hand, the extrinsic pathway originates from external stimulate that activate receptors, such as TNFR1. Subsequently, RIPK1, FADD and caspases 3 and 8 are activated. Resulting in the death of the cell. Necroptosis signalling engages RIPK1, RIPK3 and MLKL kinases that drive cell lysis. DAI sensor can signal to RIPK3 for necroptosis activation, which is blocked by HSV ICP6 viral protein in human cells.

1.5 The DNA-PK complex

1.5.1 DNA-PK and the innate immune response to DNA

DNA-PK was established as a viral DNA sensor driving IFN-I responses in primary mouse embryonic fibroblasts (Ferguson *et al.*, 2012) (Figure 4). DNA-PKcs-/- MEFs were defective in the expression of inflammatory genes, such as *CXCL10, IFNB1, IL-6* after 6 hours of stimulation with 10 μg/ml concatenated ISD DNA, compared to their

WT counterpart. The same phenotype was observed in the context of MVA and HSV-1 infections at MOI 5. Fractionation experiments showed that a fraction of DNA-PK resides in the cytoplasm and Ku70 was reported to bind STING in the cytoplasm, as well as to localise to cytosolic MVA viral factories. Downstream of STING, IRF3 was shown to translocate to the nucleus after DNA stimulation of WT cells and this event was abrogated in MEFs lacking DNA-PKcs, suggesting that DNA-PKcs is required for the IRF-3-dependent immune response to DNA. Finally, the authors demonstrated that the kinase activity of DNA-PKcs was not essential for its DNA function. Kinase dead mutant *scid* mice and cells treated with NU7026 inhibitor produced comparable levels of inflammatory chemokines and cytokines compared to Balb/c mice and WT cells, respectively. A later study by Morchikh *et al* looked at the role of DNA-PK as a DNA sensor in human cells (Morchikh *et al.*, 2017). DNA-PK was shown to form a ribonucleoprotein complex with HEXIM1, long non-coding RNA NEAT1 and paraspeckle components, called the HDP-RNP complex. The complex was found to be required for the upregulation of *IFNB1* and *IFNA* mRNAs and for the phosphorylation of IRF3 in response to stimulation with 10 µg/ml ISD for 6 hours in HeLa cells. It was also shown to be essential for mediating the IFN-I immunity to Kaposi's Sarcoma-associated herpesvirus (KSHV) in HUVEC cells. The authors detailed the mechanism for this process to rely on the interaction of the HDP-RNP complex with cGAS upon DNA detection. This event was followed by remodelling of the complex and activation of the STING-TBK1-IRF3 signalling axis. More recently, a study by Burleigh *et al* identified a non-canonical STING-independent DNA sensing pathway (Burleigh *et al.*, 2020) (Figure 4). They showed this in HEK293T cells, which lacked cGAS and STING but still managed to induce phosphorylation of IRF3 and upregulate *IFNB1* after 16 hours of stimulation with 8 µg/ml calf thymus DNA. DNA-PK was identified to be essential for driving this non-canonical pathway in U937 and THP1 cells and the kinase activity was found to be important for this process, shown by the use of NU7441 DNA-PKcs kinase inhibitor. A downstream target of DNA-PKcs kinase activity was found to be the heat-shock protein HSPA8, which was specific to the DNA sensing pathway and distinguished it from the role of DNA-PK in DNA damage repair. DNA-PK induced the expression of a broad range of

interferons in response to DNA stimulation in U937 cells. Furthermore, DNA-PK was shown to become active in a secondary wave of innate immune signalling peaking at around 16 hours after stimulation. In the same year as this study, another report demonstrated the role of DNA-PKcs in antiviral immunity in human fibroblast and monocyte cells (Sun *et al.*, 2020). Replication of VSV and HSV-1 was suppressed in HFF and THP1 cells when DNA-PKcs kinase activity was inhibited by NU7441 during infection at low MOI 0.01. In addition, phosphorylation of IRF3 and expression of *IFNB1* and *CXCL10* genes were increased in the cells treated with NU7441 during viral infection or DNA stimulation with 1 μg/ml herring testes DNA. The authors found that DNA-PK was able to phosphorylate cGAS at T68 and S213 residues and this resulted in the loss of cGAS catalytic activity to drive the activation of the STING-dependent signalling pathway. Higher levels of inflammatory markers were also observed during infection in mice *in vivo* in the presence of NU7441 inhibitor. Moreover, cells isolated from *scid* mice and from patients harbouring DNA-PKcs mutation displayed enhanced immune signalling to DNA and DNA virus infection. The authors of this study postulated that DNA-PK blocks cGAS signalling in STING-proficient cells while it acts as a DNA sensor in cells deficient in STING. Cooperation between IFI16 and DNA-PK has also been reported in the generation of a productive immune response to HSV in human fibroblast cells (Justice *et al.*, 2021). DNA-PK was recruited by IFI16 at viral DNA deposition sites at the nuclear periphery during the first hours of HSV-1 infection in HFF cells. DNA-PKcs kinase activity was shown to be important as it phosphorylated IFI16 on T149, which facilitated the induction of the inflammatory cytokine response. Inhibition of DNA-PKcs by NU7441 resulted in a decrease of IFNβ, CXCL10 and GM-CSF expression in response to virus infection while TNF-α and IL-6 levels were increased. In contrast to the former study by Sun *et al*, HFF cells whose DNA-PKcs activity was impaired by NU7441 produced higher titres of HSV virion production by 24 hours, validating the antiviral role of DNA-PK in this system. Similarly to IFI16, DNA-PK was also found to impede viral transcription. It was reported that both viral and DNA damage ligands induced IFI16 phosphorylation by DNA-PK and initiated innate signalling, suggesting for a link between DDR and DNA-PK/IFI16-mediated immune responses.

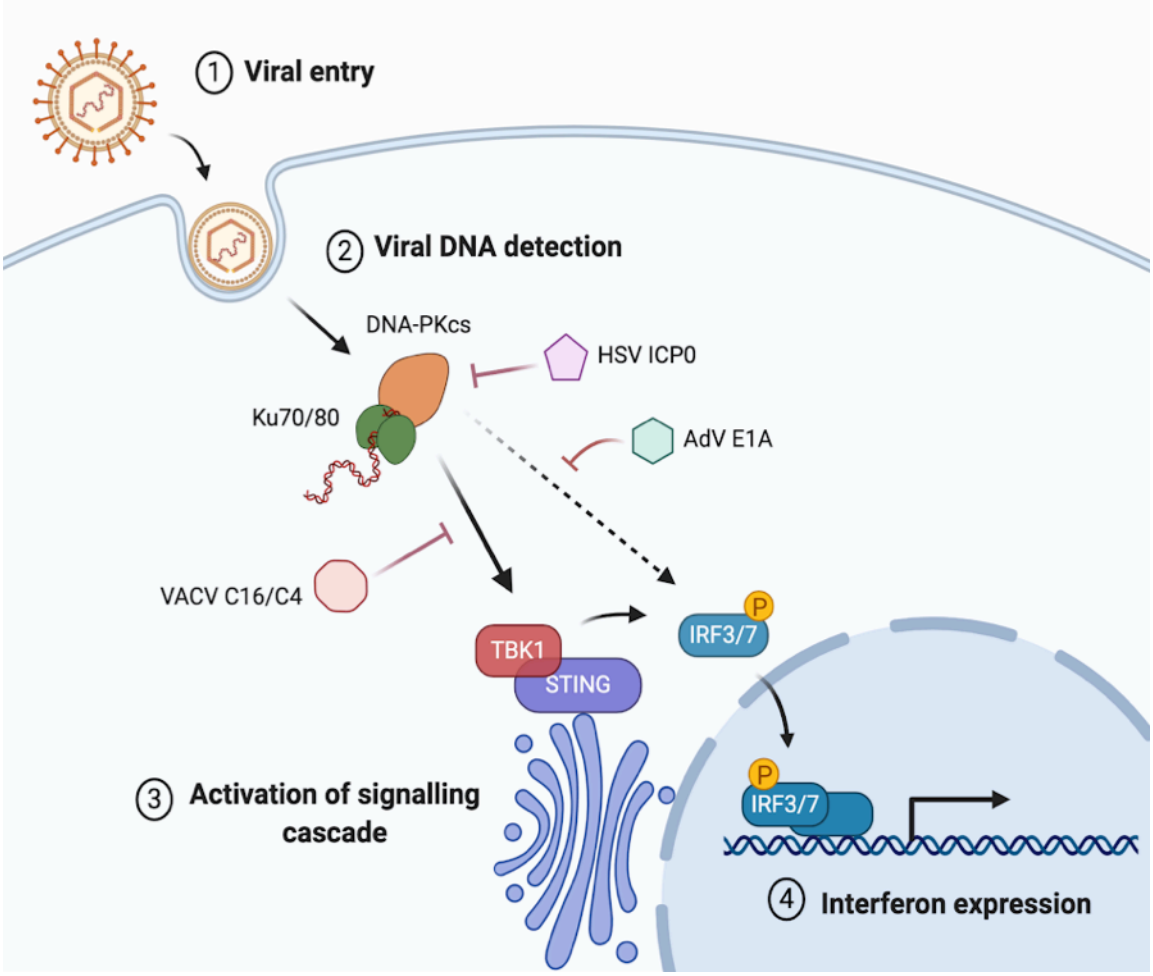

Figure 4. DNA-PK and antiviral innate immunity.

DNA-PK complex recognises intracellular viral DNA and activates the IFN innate immune response through activation of the STING adaptor protein or via the direct phosphorylation of the IRF3 transcription factor. The indicated viral proteins (HSV ICP0, VACV C16/C4, AdV E1A) suppress the innate immune response by blocking the signalling pathway at various stages.

Ku components of the DNA-PK complex have also been implicated in the human antiviral immune response to DNA. Ku70 was shown to induce *IFNL1* and *CCL5* expression in response to stimulation with linearised or HSV-2G DNA in HEK293 and mouse spleen cells (X. Zhang *et al.*, 2011). Pulldown assays revealed the cytosolic DNA sensing function of Ku70. The induction of the type III IFN response in this system depended on the activity of IRF1/7 transcription factors. Later on, the same group discovered that downstream of viral DNA detection, Ku70 translocated

from the nucleus to the cytoplasm, which depended on the cellular acetylation levels (Sui, Chen and Imamichi, 2021) and STING was found to be responsible for the activation of IRF and induction of IFNλ downstream of Ku70 activation (Sui *et al.*, 2017). Ku70/80 heterodimer was shown to detect viral DNA from hepatitis B virus (HBV) in liver-derived cells (Li *et al.*, 2016). This prompted the translocation of Ku70/80 to the cytoplasm and drove the expression of CCL3, CCL5, IFNβ, IL-1β and IL-6. DNA-PKcs and cytosolic PARP-1 were reported to be involved in chemokine expression in IRF1-dependent manner. Human T-lymphotropic virus 1 (HTLV-1) is another DNA virus that is sensed by Ku70 in HeLa and THP1 cells (Wang *et al.*, 2017). HTLV ssDNA90 was able to induce the expression of Ku70 and Ku was found to recognise the viral DNA in the cytoplasm after 8 hours of transfection and to associate with STING driving the phosphorylation of IRF3. Knockdown of Ku70 in human monocyte-derived macrophages revealed that Ku70 mediated the upregulation of IFNβ, IFNλ, CCL5, IL-6 and TNF-α after 24 hours of co-culture with MT2 cells that secrete HTLV particles.

1.5.2 DNA-PK in disease

DNA-PKcs is a key mediator of the NHEJ DNA damage repair pathway, which is essential for V(D)J recombination in T- and B-cells (Kulesza and Lieber, 1998). As such, any defects in the NHEJ pathway lead to depleted levels of lymphocytes, which clinically manifests in the development of a severe combined immunodeficiency (SCID) phenotype. SCID patients are susceptible to all kinds of infections, many of which could be life threatening. Currently, the only available treatment is haematopoietic stem cell transplantation while there is ongoing work focusing on gene therapy (Santilli *et al.*, 2008). Several genetic mutations have been found to be associated with the development of SCID and they involve the different steps in V(D)J recombination. Most of the genetic defects are found in the *RAG1, RAG2* or *Artemis* genes (Klaus *et al.*, 1996; Moshous *et al.*, 2001). In 2009, Van der Burg *et al* described a DNA-PKcs mutation in SCID patients (van der Burg *et al.*, 2009). Typical of the SCID phenotype, patients displayed low levels of T- and B-cells and were

sensitive to ionizing radiation due to a defect in NHEJ. Analysis of the DNA-PKcs locus revealed 2 genetic variations: a glycine deletion and a missense p.L3062R mutation, which was shown to be disease-causing.

DNA-PKcs is a highly conserved protein of around 4000 amino acids and several domains. At the N-terminus are situated Huntingtin, elongation factor 3, protein phosphatase 2A, and the yeast kinase TOR1 (HEAT) repeats followed by an LRR domain that has a DNA binding capacity (Brewerton *et al.*, 2004; Gupta and Meek, 2005). The protein has multiple autophosphorylation sites concentrated in clusters, such as ABCDE and PQR clusters. The C-terminal part is involved in binding to Ku80 and contains FRAP, ATM and TRAP (FAT), PI3 kinase and FATC domains (Falck, Coates and Jackson, 2005). The p.L3062R mutation is found in the FAT domain and does not affect the kinase activity or the expression levels of the protein. The structure of DNA-PKcs is depicted in Figure 5. Other spontaneous mutations have been identified in mice, dogs and horses (McGuire and Poppie, 1973; Bosma and Carroll, 1991; Peterson *et al.*, 1995; Meek *et al.*, 2001) and in these models the DNA-PKcs kinase activity is abolished, suggesting some species-specific differences in the mutation sites that can lead to the SCID phenotype.

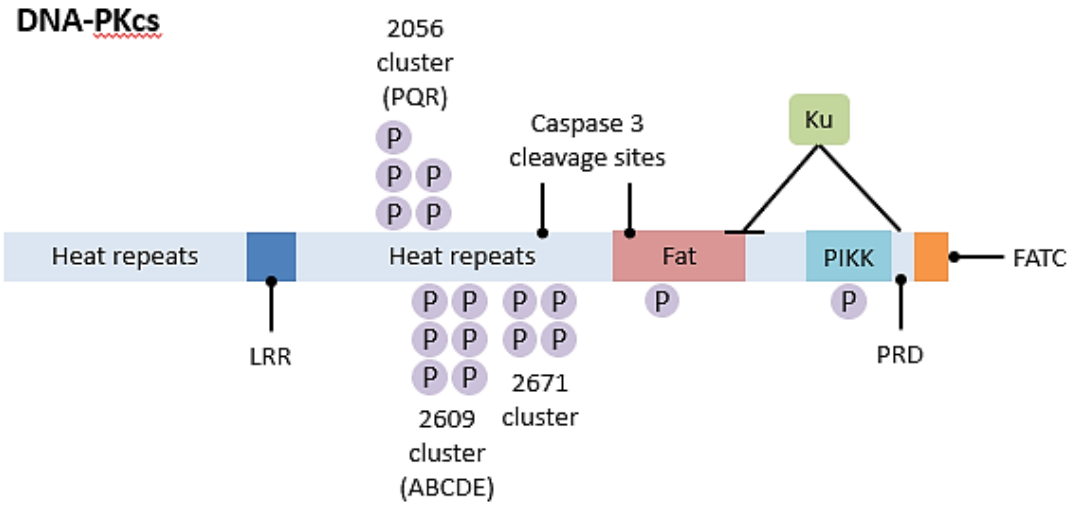

Figure 5. Domain structure of DNA-PKcs.
At the N-terminus are situated HEAT repeats followed by the leucine-rich region (LRR). DNA-PKcs has several autophosphorylation clusters, such as ABCDE and PQR cluster. The DNA-PKcs mutation

p.L3062R is situated in the FAT domain. The C-terminal part is the kinase catalytic domain of the protein and is also responsible for binding to Ku.

During NHEJ, Ku70/80 detect and bind to free DNA ends at double-stranded breaks (DSBs). Following this, DNA-PKcs is recruited and phosphorylates itself and a number of downstream target proteins that facilitate the end processing and subsequent DNA ligation (Figure 6). Artemis is a protein involved in DNA processing and V(D)J recombination, whose activity depends on DNA-PKcs phosphorylation (Niewolik *et al.*, 2006). L3062R mutant DNA-PKcs can recruit Artemis at DSBs (Figure 6), however, the mutated protein might influence the positioning or activation of Artemis as higher number of palindromic nucleotides after irradiation were observed in patient cells. As already mentioned, a recent study analysed the viral DNA sensing response in fibroblasts isolated from patients with DNA-PKcs L3062R mutation (Sun *et al.*, 2020). The authors reported that some of the patients presented with autoimmune diseases, such as granuloma, and the levels of inflammatory cytokines and ISGs were elevated in their whole-blood cells and fibroblasts. Taken together, these observations imply that *PRKDC* mutations can potentiate the innate immune response to DNA.

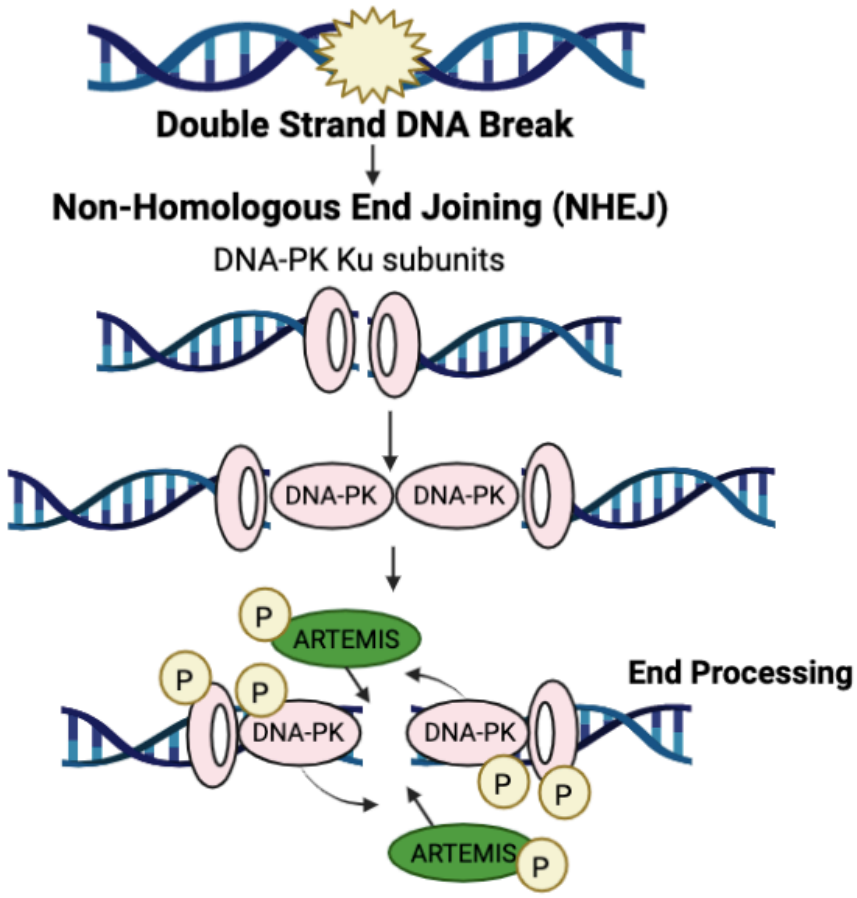

Figure 6. Association of the DNA-PK complex with DNA.
Following DNA damage, the DNA-PK complex mediates the NHEJ process. Ku subunits recognise and associate with free DNA ends. DNA-PKcs is then recruited to the complex, which phosphorylates downstream targets and facilitates end processing of the DNA. Artemis is part of this process and is recruited and phosphorylated by DNA-PKcs.

1.6 Project aims

The main aim of this study is to understand the contribution of DNA-PKcs to intracellular DNA sensing in human cells. The current literature around this topic illustrates that different cell types employ distinct signalling mechanisms to sense DNA and mount an immune response. Given the cell type specificity, we set out to dissect the DNA-PKcs-mediated DNA sensing pathway in a human single cell line.

The aims of this project are therefore:

- To understand if DNA-PKcs is required for the immune response to DNA and DNA virus infection in human cells
- To examine what is the signalling mechanism downstream of DNA-PKcs activation
- To determine whether the kinase activity is essential in the immune response to DNA
- To identify whether DNA-PKcs contributes to virus-induced cell death

2. Materials and Methods

2.1 Cell culture

2.1.1 Types of cell lines

WT and edited cell lines used for experiments in this study are shown in Table 2.1.1. Tert-immortalised HFF cells expressing CRISPR-associated 9 (Cas9) protein were kindly gifted from Dr. Michael Weekes and control and L3062R fibroblasts were a gift from Dr. Alexandre Belot. All knockout cell lines were developed in this study with the exception of RPE DNA-PKcs-/- cells, which were created by Dr. Ben Trigg.

Cell line	Cell type
HFF WT	Tert-immortalised human foreskin fibroblasts stably expressing Cas9
HFF DNA-PKcs-/-	Human foreskin fibroblasts derived from HFF WT
HFF STING-/-	Human foreskin fibroblasts derived from HFF WT
HFF cGAS-/-	Human foreskin fibroblasts derived from HFF WT
Control fibroblasts	Primary fibroblasts isolated from the skin of healthy patients
L3062R fibroblasts	Primary fibroblasts isolated from the skin of patients harbouring a mutation in the PRKDC gene (L3062R)
HeLa WT	Epithelial adenocarcinoma cell line
HeLa DNA-PKcs-/-	Epithelial adenocarcinoma cell line
RPE-1 WT	hTert-immortalised retinal pigment epithelial cells
RPE-1 DNA-PKcs-/-	hTert-immortalised retinal pigment epithelial cells
A549	Lung carcinoma epithelial cells
HaCaT	Transformed aneuploid immortal skin keratinocytes
MRC5T	Diploid lung fibroblast with T antigen
Hap-1	Near haploid chronic myeloid leukemia cell line
CEF	Chicken embryonic fibroblasts
BHK-21	Baby hamster kidney cells
U20S	Human bone osteosarcoma epithelial cells
Vero	Monkey kidney epithelial cells

Table 2.1.1: Cell lines used in this study

2.1.2 Cell culture conditions

All cell lines were incubated at 37°C, 5% CO_2 and 3% O_2. RPE-1 cells were cultured in Dulbecco's Modified Eagle Medium: Nutrient mixture F-12 (DMEM-F12; Gibco) with GlutaMAX, supplemented with 10% volume per volume (v/v) heat-inactivated fetal calf serum (FCS; Seralab), 0.2% weight per volume (w/v) sodium hydrogen carbonate and 50 μg/mL penicillin/streptomycin (Pen-Strep; Gibco). HeLa cells were cultured in Minimum Essential Medium (MEM; Gibco) with the addition of 10% v/v FCS, 50 μg/mL Pen-strep, 1% v/v non-essential amino acids (NEAA; Gibco) – glycine, L-alanine, L-asparagine, L-aspartic acid, L-glutamic acid, L-proline, L-serine, all at 100 nM. HFF, primary skin fibroblasts, HaCaTs, A549 and MRC5T cell lines were cultured in DMEM with 10% v/v FCS and 50 μg/mL Pen-strep. Hap-1 cells were cultured in Roswell Park Memorial Institute medium (RPMI; Gibco) with 10% v/v FCS and 50 μg/mL Pen-strep.

2.1.3 Passaging cells

Cells were passaged when they reached approximately 95% confluence. Monolayers were washed twice with sterile PBS (Sigma) and incubated with Trypsin/EDTA (Lonza) until they began to detach from the bottom of the flask. Detached cells were resuspended in DMEM 10% FCS and either counted and seeded for experiments, or approximately 10% were transferred to a new flask for further passaging. New frozen batches of cells were subjected to mycoplasma contamination test using MycoAlert detection kit (Lonza).

2.1.4 Seeding cells

Cells were trypsinised as described above (2.1.3), 10 μL cell suspension was mixed 1:10 with Trypan Blue (Sigma). Live cells that had not taken up Trypan blue dye were counted using a haemocytometer and the number of cells per 1 mL media was calculated. For qPCR, cells were seeded in 6-well plates, at 70% confluence for transfection of dsDNA ($4x10^5$ cells per well and $2x10^5$ for primary fibroblasts). For phosphoblotting, cells were seeded in 10 cm dishes at 80% confluence ($3x10^6$ cells per dish). For immunofluorescence and ELISA, cells were seeded in 24-well plates at

$1x10^5$ cells per well ($5x10^4$ for primary fibroblasts). For qPCR and ELISA, either duplicate or triplicate wells were seeded for each experimental condition (n=2 or 3) and for phosphoblotting, one dish was seeded per condition (n=1).

2.2 Generation of knockout cell lines by CRISPR/Cas9

Clustered Regularly Interspaced Short Palindromic Repeats (CRISPR)/Cas9 technology was used to generate DNA-PKcs-/-, cGAS-/- and STING-/- cells as part of this study.

2.2.1 Design of CRISPR/Cas9 sgRNAs

The human genomic PRKDC sequence was derived from Ensembl (ENSG00000253729, www.ensembl.org). The correct start codons were identified by translation of the exon DNA sequence using Expasy (www.web.expasy.org/translate/) and comparing it to the protein sequence on Uniprot (www.uniprot.org/). The Broad Institute single-guide RNA (sgRNA) Designer (www.broadinstitute.org/rnai/public/analysis-tools/sgrna-design) was used to design sgRNAs binding to the exons of interest (predicting the on-target efficiency and chance of off-target effects). The tool provided top five hits, out of which two were selected (PAM or repetitive sequences were avoided in the sgRNA sequence and a minimum of 0.25 on-target efficiency). Respective overhangs for Bbs1 high fidelity restriction enzyme were added to the forward and reverse primer of each pair and the whole sequence was commercially synthesized by Integrated DNA technologies, as complementary DNA oligonucleotides. Using this approach, Dr. Ben Trigg, a previous PhD student in the lab, created the *PRKDC* kinase sgRNAs. The single-guide RNAs (sgRNAs) targeting the 83^{rd} exon of the gene (11766^{th} and 11795^{th} base-pair nucleotides in the coding sequence), predicted to create a truncation in the C-terminal kinase domain of DNA-PKcs. *TMEM173* gRNA sequence was kindly provided by Prof. Jan Rehwinkel. Guide sequences are outlined in table 2.2.1 below.

Plasmid name	sgRNA sequence	Exon	Source
PRKDC kinase sgRNA 1	GATCACGCCGCCAGTCTCCA	83	Dr. Ben Trigg
PRKDC kinase sgRNA 2	CAGACATCTGAACAACTTTA	83	Dr. Ben Trigg
TMEM173 (STING)	GGTGCCTGATAACCTGAGTA	6	Prof. Jan Rehwinkel
MB21D1 (cGAS) sgRNA 1	CGGCCCCCATTCTCGTACGG	1	This study
MB21D1 (cGAS) sgRNA 2	CGATGATATCTCCACGGCGG	1	This study

Table 2.2.1 sgRNAs for the generation of CRISPR/Cas9 knockout cell lines
Target gene, exon and guide sequence used for successful generation of HFF, RPE and HeLa knockout cells

2.2.2 Cloning of DNA constructs

Guides were cloned into the pKLV-U6gRNA-EF(BbsI)-PGKpuro2ABFP lentivirus plasmid, kindly provided by Dr. James Edgar. sgRNA DNA oligos were diluted to 10 µM in nuclease free water (NF-H_2O) and 5 µL of each forward and reverse guide was combined in a polymerase chain reaction (PCR) tube (Starlab) and heated to 75 °C for 15 minutes using a Veriti thermocycler (Applied Biosystems). The thermocycler was then switched off and allowed to cool to room temperature to allow annealing. Annealed primers were diluted to 20 nM in NF-H_2O.

3 µg of the lentiviral vector were digested with BbsI-HF (NEB), run on a 1% agarose gel at 120 V, visualised using a UV light box and excised using a scalpel. DNA was extracted from the agarose gel using a QIAquick Gel Extraction Kit (Qiagen) and eluted in 10 µL NF-H_2O. The DNA concentration and purity was measured using a NanoDrop 2000 spectrophotometer.

sgRNAs were ligated into the digested plasmid at a 3:1 (insert:plasmid) molar ratio using T4 DNA ligase (Promega). The ligated plasmid was transformed into Stbl3 *E. Coli* by heat-shocking and allowed to grow for 1 hour at 37 °C. Following this, the transformed bacteria were spread onto LB agar with Carbenicillin (50 µg/mL) and incubated at 37 °C for 16 hours. Colonies were picked and grown in 5 mL LB

Carbenicillin at 37 °C for 16 hours for a Miniprep. DNA was purified using a QIAprep Spin Miniprep (Qiagen) and DNA concentration was measured using a NanoDrop 2000 spectrophotometer. Successful cloning was confirmed by Sanger sequencing.

2.2.3 Lentiviral transduction

On day 1, HEK293T cells were seeded in a 6-well plate so that they would be around 80% confluent at the point of transfection. On day 2, the media of the cells was replaced with antibiotic-free media and the lentivirus transfection plasmid mix (1μg pKLV-lenti vector + 0.7 μg gag/pol/rev/tat packaging proteins + 0.3 μg VSV-G envelope protein) was prepared in 50 μL Optimem and left to incubate for 5 minutes. In parallel 8 μL of Transit-LT1 was mixed with 200 μL Optimem and incubated for 5 minutes. The DNA and transfection mixes were combined together and incubated for 20 minutes before being applied to the HEK cells. On day 3, the media of the cells was replaced with fresh complete medium. In 24 hours, the viral cell supernatant was collected, spun at 336 x g for 10 minutes and filtered through 0.45 μm filter. The supernatant containing the CRISPR lentivirus was then added to HFF cells. On day 4, the culture medium was replaced by fresh complete media and 48 hours later, 0.5 μg/mL puromycin was added for selection of successfully transduced cells. A schematic representation of the different steps in the lentiviral transduction process is shown in figure 2.2.3. A puromycin kill curve test in HFFs determined that 0.5 μg/mL of the antibiotic was enough to kill the cells within seven days. Successfully transduced HFF cells that would survive antibiotic selection and were expanded and screened by western blot and immunofluorescence.

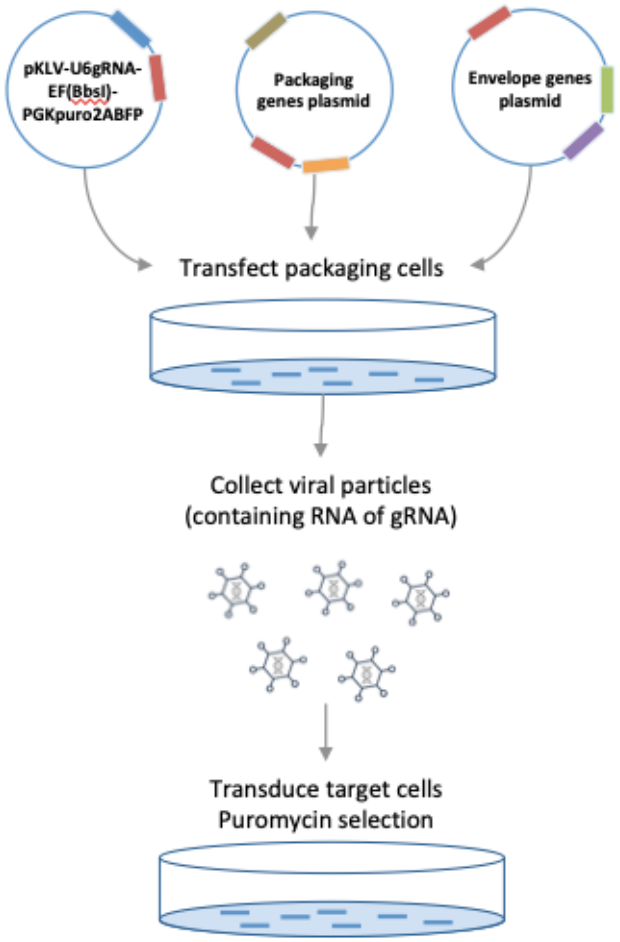

Figure 2.2.3 Steps in the generation of CRISPR/Cas9 knockout cells by lentiviral transduction.
Figure adapted from *Synthego.com*

2.2.4 CRISPR plasmid transfection

The *PRKDC* guide RNAs were also cloned into the mammalian expression vector pD1301-AD by Horizon Biotechnology. The plasmids comprised the sgRNAs under the U6 promoter and Cas9 expression was under the control of the CMV IE1 promoter and enhancer. DasherGFP and kanamycin resistance genes were encoded as selection markers. These plasmid vectors were used for the generation of HeLa DNA-PKcs-/- cells using an alternative approach to lentivirus transduction, as described below.

HeLa cells were seeded in a 6-well plate with nutrient-rich medium (~2x10^5 cells). On the next day, 2 µg of each pD1301-AD plasmid (PRKDC kinase sgRNA 1 and 2; in total 4 µg/well) were added to 200 µL of OptiMEM and 8 µL of Transit LT1 transfection reagent. The mix was vortexed and incubated for 20 minutes. The medium was aspirated from cells (~50% confluent) and 2.5 mL of fresh MEM with 2% v/v FCS, 1% v/v NEAA, 1% v/v Pen-strep were added to each well. The transfection mix was added drop-wise and cells were incubated overnight. On the following day, the transfection efficiency was checked by microscopy to check for the number of GFP^+ HeLa cells.

2.2.5 Single-cell FACS sorting

On day 4, transfected HeLa cells were washed in PBS and detached with 1 mL of 1x trypsin. Trypsin was diluted in MEM and cells were pelleted (181 g, 5 minutes). The pellet was resuspended in 500 µL of 2% FCS medium (less than 1x10^6 cells in suspension). GFP^+ cells were sorted as single-cell clones into a 96-well plate using a MoFlo cell sorter (Beckman Coulter).

2.2.6 Clonal selection and screening for knockout cells

Surviving clones were expanded into a 24-well plate once they reached confluency, followed by a 6-well plate and a T25 tissue flask. At this point, HeLa clones were left to reach confluency and whole cell protein lysate was harvested for immunoblotting or cells were seeded onto coverslips for immunofluorescence to screen for the loss of DNA-PKcs.

2.3 DNA manipulation

2.3.1 ISD

Immunostimulatory DNA (ISD) is a 180-bp double-stranded oligonucleotide DNA that had a sense strand sequence of 4 copies of the following DNA sequence: TACAGATCTACTAGTGATCTATGACTGATCTGTACATGATCTACA (Daniel B. Stetson and Medzhitov, 2006). To generate ISD synthetic, sense and antisense

oligonucleotides were mixed at a molar ratio of 1:1, heated to 95 °C for 5 min, then annealed at 60 °C for 15 min and cooled to room temperature.

2.3.2 Resolution and isolation of DNA by agarose gel electrophoresis

Agarose gel electrophoresis was used to analyse DNA samples. Samples were mixed with 6 x Gel Loading Dye (NEB) prior to loading onto a 1 % (w/v) agarose (Invitrogen) gel, supplemented with 10,000 x SYBR® Safe (Thermo Scientific), in TAE buffer (40 mM Tris, 1 mM EDTA and 20 mM acetic acid). HyperLadder 1 kbp DNA ladder was also electrophoresed in a separate well to allow size comparison. Gels were run at 80 V for 1 h and DNA was visualised by ultraviolet illumination using Gel Doc XR+ imaging system (Bio- Rad) and Image Lab 5.2 software.

2.4 Stimulation of cells with dsDNA

Cells were seeded in a 6-well plate in order to be 60-80% confluent on the following day. TransIT-LT1 (Mirus) was added to OptiMEM (200 µL/well; Gibco) and the mixture was incubated for 5 minutes at room temperature (RT). Herring testes DNA (htDNA) or calf thymus DNA (ctDNA) (Sigma-Aldrich) were added to the mix at a ratio of 1:3 (1 µg/mL of DNA and 3 µL of the lipid transfection reagent) and everything was incubated for 30 minutes at RT. Culture medium was replaced with fresh medium supplemented with 10% v/v FCS (~800 µL/well) and the transfection mix was added drop-wise to the wells. PolyI:C stimulation was used as a positive control (2 µg/mL). Cells were incubated for indicated times at 37°C and harvested for RNA extraction.

2.5 Drug treatment of cells

NU7441 DNA-PKcs kinase inhibitor (Cayman chemical) was dissolved in DMSO and 1 µM, 2 µM or 3 µM of the inhibitor were applied to cells 1 before stimulation or infection. AZD7648 DNA-PKcs kinase inhibitor (Sellekchem) was dissolved in DMSO and 2 µM of the inhibitor were applied to cells 1 before stimulation or infection. BX795 TBK1/IKKε kinase inhibitor (Invivogen) was dissolved in DMSO and 1 µM was applied to cells 1 before stimulation. MG132 proteasome inhibitor (Promega)

was was applied to cells at 10 μM at the time of virus infection. Etoposide (Abcam) was dissolved in DMSO and was added directly to the media of plated cells at a concentration of 30 μM for 2 hours.

2.6 Virus work

2.6.1 HSV-1

2.6.1.1 Preparation of HSV virus stocks

Herpes Simplex Virus-1 (HSV-1) strain 17 (S17) was grown on Vero cells. An S17 virus lacking ICP0 (also referred as dl1403) was a kind gift from Professor Gill Elliot (Stow and Stow, 1986). dl1403 contains a 2 kb deletion within *Vmw110* (ICP0) and it has been published that, in addition to the loss of ICP0, dl1403 also lacks functional gC expression (Cunha *et al.*, 2015). For simplicity, dl1403 will be termed ΔICP0 HSV-1. HSV ΔICP0 was grown on U20S cells as these cells were permissive to the attenuated virus strain. Vero or U20S cells were infected with HSV at multiplicity of infection (MOI) of 0.01 in reduced-serum medium (2.5% v/v FCS). Infected cells were left at 37°C for 3-5 days until they showed high levels of cytopathic effect (CPE). At that point, cells were scraped in the media and pelleted (2898 g, 10 minutes, 4°C). The pellet was resuspended in sterile PBS and freeze-thawed three times before centrifuging again to remove the cell debris. The supernatant was stored at -80°C.

2.6.1.2 Plaque assay titration

Vero cells were seeded in a 6-well plate in order to be ~90% confluent at the time of infection. The virus stock (section 2.6.1.1) was subjected to a ten-fold serial dilution in serum-reduced DMEM. Cell medium was aspirated, cells were infected with 1 mL of each dilution in duplicate and incubated at 37°C for 90 minutes with constant rocking. Following incubation, infection medium was discarded and cells were covered with 2 mL of semi-solid overlay medium (MEM supplemented with 1.5% w/v carboxy-methyl cellulose (CMC), 2.5% v/v FBS, 50 μg/mL Pen-Strep). The plate was left for 3 to 5 days at 37°C until plaques start forming. After that the overlay

was removed followed by 2 washes in PBS and plaques were stained with 2 mL per well of Touluidene blue (complemented with 4% PFA and PBS) for one hour at RT. The cell monolayer was then washed with PBS, rinsed with tap water and plaques were counted to calculate the plaque forming units per mL (PFU/mL).

2.6.1.3 Single-step growth curve analysis

Cells were seeded in a 6-well plate so that they would be confluent on the following day. Cells were counted and infected with HSV S17 at an MOI of 5. The mock wells were scraped into the infection medium immediately after and freeze-thawed 3 times. The remaining wells were left to incubate at 37°C for indicated times, such as 12, 24 and 48 hours and were harvested in the same way as the mock samples. After the freeze-thaw cycles, the cell debris were pelleted and the supernatant was used for a plaque assay titration on Vero cells (section 2.6.1.2) to quantify the number of infectious virions in each sample. Alternatively, cell supernatant from infected cells and cells could be collected separately. Scraped cells into PBS were freeze-thawed several times and the released in the supernatant and cell-associated virus were quantified by a plaque assay.

2.6.2 MVA

2.6.2.1 Growing MVA stocks

Modified Vaccinia Ankara (MVA) was kindly provided from Prof. Geoffrey Smith. MVA was grown on BHK-21, which are permissive to replication of this attenuated virus strain. 18-20 T175 flasks of confluent BHK-21 cells were infected with MVA at MOI 0.05 and left to incubate for 2 to 4 days at 37°C. Infected cells were harvested when wide-spread cytopathic effect was visible. Cells were scraped in the culture media and pooled together. The cell suspension was centrifuged at 4116 x g for 10 minutes at 4°C. The supernatant was decanted and the pellet was resuspended in PBS (500 µL per flask). Following this, the resuspension was freeze-thawed 3 times and sonicated 2 x 30 seconds at 2.5.

2.6.2.2 MVA immunotitration

On day 1, primary chicken embryonic fibroblasts (CEF; supplied by the Pirbright institute) were seeded in 6-well plates at $8x10^5$ cells/well, so that they would be confluent on the next day. On day 2, the virus stock was defrosted, sonicated once for 30 seconds and subjected to a 10-fold serial dilution in serum-reduced DMEM (2.5% FCS). Cell medium was aspirated, cells were infected with 1 mL of each dilution in duplicate and incubated at 37°C for 90 minutes with constant rocking. Following incubation, infection medium was discarded and cells were covered with 2 mL of semi-solid overlay medium (MEM supplemented with 1.5% w/v carboxy-methyl cellulose (CMC), 2.5% v/v FBS, 50 μg/mL Pen-Strep). The plate was left for 48 hours at 37°C. After 2 days, the overlay was removed and the cells were washed with PBS. Cells were then fixed with 2mL of ice-cold acetone:methanol at 1:1 ratio for 5 minutes at RT. Next, blocking buffer (3% FCS in PBS) was added to the cells overnight at 4°C. On the next day, the blocking buffer was replaced by primary anti-VACV Lister cocktail antibody (RayBiotech, MD-14-1041) at 1:2,000 in blocking buffer and was incubated for 1 hour at RT with gentle rocking. After the incubation, the primary antibody was washed 3 times with blocking buffer before secondary anti-rabbit horseradish peroxidase (HRP)-conjugated antibody (Sigma, A6154) was applied at 1:3,000 dilution for 45 minutes at RT in the dark. Finally, the cells were washed 3 times with blocking buffer before 0.5 mL of True-blue substrate (KPL) was applied to the cells for 15 minutes until plaques were visible. At this point the substrate was replaced by distilled water and stained plaques were counted and the titre of the MVA stock was calculated.

2.6.3 Virus infection of cells

Cells were seeded with a spare well or dish, which 16 hours later was trypsinised and counted. Total cell number was calculated and cells were infected at an MOI of 5 in serum-reduced media. The amount of virus added to the cells was calculated by the following formula: (cell number x MOI)/PFU. Before cell infection, MVA was sonicated once for 30 seconds at 2.5.

2.6.4 Sendai virus

The Cantell strain of Sendai virus (SeV), a kind gift from Steve Goodbourne (St. Georges University) was used as a positive control in virus infection assays. Cells were infected at 1:300 dilution in DMEM 2.5% FCS 1% P/S.

2.7 RT-qPCR

2.7.1 RNA extraction

Cells were washed with PBS and lysed in situ using 250 µL of lysis buffer (4M guanidine thiocyanate, 25 mM Tris pH7, and 143mM 2-ME) and 250 µL of 70% ethanol. The solution was centrifuged at 18, 000 g for 2 minutes at 4°C in silica columns (Epoch) as in all other subsequent centrifugation steps. The flow-through liquid was discarded and 500 µL of wash buffer 1 (1M guanidine thiocyanate, 25mM Tris pH7, 10% ethanol) was added to the columns and centrifuged. The same centrifugation steps were repeated twice with 500 µL wash buffer 2 (25mM Tris pH7, 70% ethanol). Finally, the RNA was eluted with 50 µL of NF-H_20 and centrifuged. For higher RNA yields, the eluent was passed back through the column and centrifuged one more time. The RNA concentration was measured by NanoDrop 2000 Spectrophotometer.

2.7.2 Complementary DNA (cDNA) synthesis

500 ng of RNA was mixed with 1 µL of deoxynucleoside triphosphate (10mM; Thermo Scientific) and 1 µL of oligo deoxythymine (dT) (500ng; Thermo Scientific). The mix was topped up with NF-H_20 to a total volume of 13 µL and heated up to 65°C for 5 minutes. After that, the following components were added to the mix: 4 µL of 5x first strand buffer (250 mM Tris-HCl pH8.3, 375mM KCl, 15mM $MgCl_2$; Invitrogen), 1 µL of 0.1M dithiothreitol (DTT) (Invitrogen), 0.25 µL of RNaseOUT recombinant RNase inhibitor (40U; Invitrogen) and 0.25 µL of Superscript III Reverse Transcriptase (50U; Invitrogen). The total volume was made up to 20 µL and incubated at 50°C for 60 minutes and at 72°C for 15 minutes.

2.7.3 Quantitative real time-polymerase chain reaction (RT-qPCR)

2.7.3.1 Targets

cDNA samples were analysed by quantitative polymerase chain reaction (qPCR) using primers to amplify specific regions of the genes of interest, ordered as DNA oligos (IDT). Target genes and primer sequences for human cells can be found in Table 2.7.3.1.

Gene	Forward primer	Reverse primer
GAPDH	ACC CAG AAG ACT GTG GAT GG	TTC TAG ACG GCA GGT CAG GT
CXCL10	GTG GCA TTC AAG GAG TAC CTC	GCC TTC GAT TCT GGA TTC AGA CA
IFNB1	ACA TCC CTG AGG AGA TTA AGC A	GCC AGG AGG TTC TCA ACA ATA G
IFNL1	CGC CTT GGA AGA GTC ACT CA	GAA GCC TCA GGT CCC AAT TC
IFNA2	AGT CAA GCT GCT CTG TGG GC	GTG AGC TGG CAT ACG AAT CA
ISG54	CTG AAG AGT GCA GCT GCC TG	CAC TTT AAC CGT GTC CAC CC
ISG15	AGC ATC TTC ACC GTC AGG TC	GAG GCA GCG AAC TCA TCT TT
NFKBIA	CTC CGA GAC TTT CGA GGA AAT	GCC ATT GTA GTT GGT AGC CTT

Table 2.7.3.1: Primers used to detect mRNA transcription in human cell lines

2.7.3.2 qPCR protocol

Master mixes were made containing 5 µL per reaction of qPCRBIO SyGreen Mix Hi-ROX (PCRBiosystems), as well as 1 µL per sample of the respective forward and reverse primers at 10mM **(**table 2.7.3.1). 2 µL of cDNA was added in duplicate to the wells of a 384-well reaction plate (Applied Biosystems) and 7 µL of the respective master mix was added on top (total 9 µL for a reaction). MicroAmp optical adhesive film (Thermo Scientific) was applied on top of the plate and it was centrifuged at 181 g for 1 minute prior to analysis with Viia7 Real-time PCR system (Applied Biosystems). The amplification program included an initial denaturation step of 30 seconds followed by 40 cycles of 3 seconds at 95°C for primer annealing and 30

seconds at 60°C for extension. The CT values were analysed as fold changes relative to the *GAPDH* housekeeping gene and the mock sample.

2.7.3.3 *Δ Δ Ct calculations*

Melt curves generated by qPCR were checked for presence of a single symmetrical peak, indicative of a single specific dsDNA amplicon generated during amplification of each gene with the specific primers. The raw cycle threshold (Ct) value for each amplicon was collected. Mean Ct values were calculated for technical duplicates, excluding those that appeared to be outliers compared to their technical and experimental replicates. ΔCt was calculated by subtracting the Ct value for the gene of interest from the Ct value of the reference gene: *GAPDH* in human cells. ΔΔCt was calculated by subtracting the ΔCt from each treated sample (e.g., each infection time point or stimulation condition) from the ΔCt of its relevant untreated sample. Once calculated, ΔΔCt values were used to generate a fold change value, using the calculation $2^{\Delta\Delta Ct}$, as an increase of one in Ct value results in a doubling of the amount of DNA in the PCR reaction. The mean fold change values calculated from experimental replicates were plotted as a bar chart, with standard deviation indicated by error bars.

2.8 Western blot

2.8.1 Harvesting whole cell protein lysates

Cells were scraped into PBS and pelleted (724 g, 5 minutes, 4°C). The pellets were resuspended in 100 µL per $3x10^6$ cells of radioimmunoprecipitation assay (RIPA) lysis buffer (50 mM Tris-HCL pH8, 150mM NaCl, 1% NP-40, 0.1% SDS, 0.5% Na Deoxycholate) and incubated on ice for 20-30 minutes. For phosphoblotting, all reagents used during lysis were ice-cold and the whole procedure was done on ice. At the indicated time point, cells were washed once in 5 mL PBS, then scraped into 5 mL of PBS and transferred to a falcon tube. Cells were pelleted by centrifugation (724 x g, 4 minutes, 4 °C) and resuspended in 80 µL RIPA buffer containing also

cOmplete Mini EDTA-free protease inhibitors (Roche), as well as PhosSTOP phosphatase inhibitor cocktail (Roche). Cells were lysed for 30 minutes on ice and 10 minutes on a rotating wheel at 4°C. After cell lysis, suspensions were centrifuged at 18, 000 g for 10 minutes at 4°C to pellet genomic DNA. Small amount of the supernatant (~15 µL) was taken for a bicinchoninic (BCA) assay (Thermo Scientific) to measure the protein concentration. The remaining supernatant (~100 µL) was transferred to a fresh eppendorf tube and mixed with 20 µL of 6x loading dye (1x final concentration; 300 mM Tris-HCl (pH6.8), 12 % w/v SDS, 60 % v/v glycerol, 0.6 % w/v bromophenol blue, and 600 µM 2-mercaptoethanol). Protein lysates were stored at -20°C and lysates for phosphoblotting were snap-frozen in a dry ice-ethanol bath and stored at -80 °C until use.

2.8.2 Sodium dodecyl sulphate polyacrylamide gel electrophoresis (SDS-PAGE)

Protein samples were run on 10-12% SDS polyacrylamide gels. SDS-PAGE gels were made using a Bio-Rad Protean III system. The running gel was prepared using 10-12% v/v polyacrylamide (Protogel), 0.39 M Tris pH 8.8, 0.1% w/v SDS, 0.1% w/v ammonium persulphate (APS) and 0.04% w/v tetramethylethylenediamine (TEMED) (Bio-Rad). The stacking gel consisted of 5% v/v polyacrylamide, 0.13 M Tris pH 6.8, 0.1% w/v SDS, 0.1% w/v APS and 0.1% w/v TEMED. Protein samples were defrosted on ice then boiled at 98 °C for 5 minutes. Insoluble material was pelleted by centrifugation at 18000 x g for 30 seconds. For western blotting of whole cell lysates and phosphoblotting, 50 µg of protein was loaded per well. PageRuler Plus prestained protein ladder (Thermo Scientific) was used as a molecular weight marker. Samples were run in a Mini-PROTEAN Tetra Vertical Electrophoresis Cell (BioRad) at 90 V for 15 minutes followed by 120 V for 120 minutes using a Tris-Glycine running buffer (25 mM Tris, 192 mM glycine, 0.1 % SDS).

2.8.3 Immunoblotting for DNA-PKcs

High molecular weight proteins, such as DNA-PKcs (460 kDa), were blotted using Precast 4-12% bis-Tris gradient Nu-PAGE gels (Invitrogen). 20-50 µg of protein

samples were loaded and run in the Novex Mini-Cell system (Invitrogen) with MES-SDS 1x running buffer at 190 V for 135 minutes.

2.8.4 Semi-dry transfer

Prior to stacking the transfer "sandwich", filter blotting paper (Bio-Rad), 0.2 µm nitrocellulose membrane (Amersham) and the gel were equilibrated in transfer buffer containing 20% v/v methanol, 2.5 mM Tris Base, and 19.2 mM glycine. Transfer was carried out at 25 V for 30 minutes using a Trans-Blot Turbo (Bio-Rad) for precast gels or Pierce Power Blotter semi-dry transfer machine (Thermo Scientific) for home-made gels.

2.8.5 Immunoblotting and imaging

The nitrocellulose membrane with the transferred proteins was blocked in 5% w/v milk in TBST for 60 minutes at RT, followed by three washes in Tris-buffered saline (TBS) with 0.1% v/v tween-20 (TBST). The membrane was incubated overnight on a rolling platform at 4°C with primary antibody (table 2.8.5) diluted in TBST. Following incubation, the protein membrane was washed three times at RT in TBST for 5 minutes and it was incubated with secondary antibody diluted in TBST (table 2.8.5) at RT in the dark for 2 hours. Lastly, the membrane was washed three times at RT in TBST for 10 minutes. Membranes were dried and stored in the dark at room temperature before imaging. Blots were imaged by a Li-Cor Odyssey CLx, and images were processed using the programme Image Studio. Densitometry analysis was performed by Fiji.

Antibody target	**Source and species**	**DF (WB)**	**DF (IF)**
cGAS	Santa Cruz (sc-515777); mouse	1:1,000	
DNA-PKcs (cocktail)	Thermo Scientific (ms-423-p1); mouse	1:750	1:250
IFI16	Santa Cruz (sc-8023); mouse	1:1,000	1:250
IkBa	Santa Cruz (sc-1648); mouse	1:1,000	

IRF3	Abcam (ab68481); rabbit	1:1,000	
Ku70	Abcam (ab3114); mouse	1:1,000	
MLKL	Santa Cruz (sc-293201); mouse	1:1,000	
TBK1	Abcam (ab40676); rabbit	1:1,000	
PARP-1	Abcam (ab6079-1); rabbit	1:1,000	
RIPK	Santa Cruz (sc-133102); mouse	1:1,000	
STING/TMEM173	Cell Signalling (13647); rabbit	1:1,000	
TREX-1	Santa Cruz (sc-271870); mouse	1:5,000	
Tubulin	Millipore (05-829); mouse	1:1,000	
HSV-1 ICP0	Santa Cruz (sc-53070); mouse	1:1,000	
VACV Lister	RayBiotech (MD-14-1041); rabbit	1:1,000	
p-IRF3 (Ser386)	Abcam (ab76493); rabbit	1:1,000	
p-MLKL (Ser358)	Cell Signalling (91689); rabbit	1:1,000	
p-TBK1 (Ser172)	Cell Signalling (5483S); rabbit	1:1,000	
p-RIPK (Ser166)	Cell Signalling (65746); rabbit	1:1,000	
p-STING (Ser366)	Cell Signalling (85735); rabbit	1:1,000	
p-DNA-PKcs	Abcam (ab18192); rabbit		1:250
γH2AX	Millipore (05-636); mouse		1:500
Anti-mouse secondary antibody (800)	Li-Cor (926-32210); goat	1:10,000	
Anti-rabbit secondary antibody (680)	Li-Cor (926-68071); goat	1:10,000	
Anti-mouse secondary	Alexa Fluor 488 (A21202); donkey		1:1,000
Anti-mouse secondary	Alexa Fluor 546 (A10036); donkey		1:1,000
Anti-rabbit secondary	Alexa Fluor 546 (A10040); donkey		1:1,000

Table 2. Primary and secondary antibodies used for immunoblotting (WB) and immunofluorescence (IF). DF = dilution factor.

2.9 Immunofluorescence

Cells were seeded in a 24-well plate on sterile 13 mm coverslips in order to be 60-

70% confluent on the following day. On day 2, the cells were fixed for 10 minutes with cold 4% w/v formaldehyde (Fisher Scientific) diluted in 250mM pH 7.4 4-(2-hydroxyethyl)-1-piperazineethanesulfonic acid (HEPES), followed by a second fixation step with cold 8% w/v formaldehyde in HEPES buffer. After two washes with PBS, the cells were permeabilised for 5-10 minutes with 0.25% v/v Triton X-100 in PBS, which was followed by two more washes in PBS. Non-specific binding sites were blocked with 5% w/v milk (Premier Food Groups) in PBS at RT for one hour. The cells were then incubated overnight at 4°C with primary antibody (table 2.8.5) at the indicated dilution in 1% w/v milk in PBS. Following this, the cells were washed with PBS three times and were incubated at RT for 30 minutes in the dark with secondary antibody (table 2.8.5) diluted 1:1000 in 1% w/v milk in PBS. The coverslips were washed twice with PBS and once with distilled water. Lastly, the glass coverslips were mounted onto slides with 10 µL of mounting solution (25 % glycerol v/v, 0.1 M Tris pH 8.5, 10 % Mowiol 4-88 w/v containing 4', 6-diamidino-2-phenylindole (DAPI) and were left to set at RT in the dark overnight. Zeiss Pascal Confocal microscope was used to visualise the samples (63x magnification) and the images were collected with Zeiss LSM Image Browser.

2.10 Enzyme-linked immunosorbent assay (ELISA)

A DuoSetELISA assay (R&D) was used to detect the presence of human CXCL10/IP-10 in the supernatants of infected or stimulated primary fibroblast cells.

2.10.1 Sample preparation

Cells were seeded in 24-well plates with biological duplicates per condition and were either stimulated or infected as previously described. At the stated time point, 1 mL of the supernatant was collected and stored at -80 °C.

2.10.2 ELISA

Initial optimisation assays were carried out to determine the dilution factor of samples to enable CXCL10 levels to fall within the standard curve, with samples diluted in PBS 1% PBS. Samples were diluted as appropriate and the assay

procedure was performed as described in the kit protocol, with technical duplicates done for each experimental sample, using TMB (Abcam) used as the substrate solution and 0.3 M H_2SO_4 as the stop solution.

2.10.3 Analysis

The optical density of each sample was measured using a LUMIstar Omega. The blank-corrected optical density at 450 nm was subtracted from that at 540 nm. A 4-parameter fit standard curve was applied to the standards of known concentration and used to calculate the amount of CXCL10 in experimental samples. Dilutions were accounted for, and mean values generated from technical and experimental replicates were plotted as a bar chart, with standard deviation indicated by error bars.

2.11 Flow cytometric quantification of cell death

Cells were seeded in a 10-cm dish (~$2x10^6$) to be ~80% confluent on the following day, infected with the HSV S17 virus and harvested at specific time points. Infected cells were trypsinised, centrifuged and washed twice in sterile PBS. The cell pellet was resuspended in 1 mL (for 0.25-1.0$x10^7$ cells) of 5x Annexin V binding buffer (50mM HEPES, 700mM NaCl, 12.5 mM CaCl2, pH7.4; BioLegend). An aliquot of 100 µL of the cell suspension was taken and incubated for 5 minutes at RT in the dark with 5 µL of allophycocyanin (APC) Annexin V, to detect early apoptosis and 5 µL of 7-amino-actinomycin D (7AAD) viability staining solution (50 µg/mL; provided with BioLegend detection kit), to detect late apoptosis. Cells were analysed by flow cytometry (MoFlo Astrios) along with the appropriate controls (Apoptotic cells generated by heat shock at 55°C for 20 minutes were mixed with live cells at a ratio 1:3).

2.12 Statistical analysis

Statistical analyses and graphs were produced using GraphPad Prism 9.0. Data was deemed significant if the p value was <0.05 and significance is represented on graphs by P <0.05 = *, P<0.01 = ** and P<0.001.

CHAPTER 3

3. Finding suitable cell lines for the study of the DNA sensing pathway

The main goal of this study is to define the role of DNA-PKcs in the antiviral immune response to DNA in the human system. Current literature indicates that the DNA-PKcs-mediated DNA sensing pathway is cell type-specific where distinct pathways are active in different contexts (Burleigh *et al.*, 2020; Sun *et al.*, 2020). However, the majority of published reports on this topic fail to characterise the pathway consistently in a single model, which is crucial given the cell type specificity. Therefore, we set out to find a robust human cell-based system in which we can investigate in depth the DNA-PKcs-driven PRR signalling pathway. We focused on finding a suitable immortalised cell line, which can be genetically manipulated for loss-of-function studies. In this chapter we present our findings on our choice of model after screening various cell lines and provide evidence as to why the chosen system is suitable for addressing the specific aims of our study.

3.1 Characterisation of a number of cell lines for an active PRR signalling pathway to DNA

In order to identify a suitable cell line to study the antiviral immune response to intracellular DNA, we screened a number of transformed cell lines of different origins that are physiologically relevant to DNA virus infection, such as human fibroblasts, epithelial cells or keratinocytes. Initially we determined which of these cell lines were capable of mounting a transcriptional response to intracellular DNA stimulation. In this study we use herring testes (htDNA), calf thymus DNA (ctDNA) or immunostimulatory DNA (ISD), which are ligands in activating the immune system. Ht and ctDNA are purified from mammalian cells and they lack the unmethylated CpG motif prevalent in many pathogenic genomes that is normally sensed by TLR9 in endosomes (Hemmi *et al.*, 2000; Yasuda *et al.*, 2009; Ohto and

Shimizu, 2016). ISD DNA was designed not to contain CpG so that it can be synthesized and still not activate TLR9. On the other hand, Poly(I:C), used as a positive control in activating the IRF3-dependent IFN-I response, is a synthetic analogue of double-stranded RNA present in many viruses and a potent activator of the TLR3 receptor (Fortier *et al.*, 2004; Li *et al.*, 2015). Cells were transfected with increasing concentrations of herring testes DNA or immunostimulatory DNA and probed for the transcriptional upregulation of *IFNB* (type-I interferon) and *CXCL10* mRNAs, which have antiviral activity and play an essential role in the STING/IRF3-dependent innate immune response. The transcriptional response was measured after 6 hours to monitor the immediate signalling response to DNA PRR stimulation and avoid secondary signalling. Cervical epithelial (HeLa) cells and keratinocytes (HaCaTs) showed approximately 100-fold increase in *CXCL10* mRNA levels with 1 μg of htDNA, compared to mock untransfected cells. Lung epithelial (A549) cells had more than 10-fold higher *CXCL10* mRNA levels with both DNA concentrations even though this did not reach statistical significance. HeLa cells did not induce *IFNB* expression, whereas HaCaTs and A549 showed, in a dose-response fashion, around 5-fold induction of *IFNB* levels with 5 μg of DNA, compared to the negative control. However, human fibroblasts (MRC5T) and leukemia (Hap-1) cells did not exhibit significant upregulation in the mRNA levels of both inflammatory markers in the majority of the stimulation conditions (Figure 3.1 A), which suggested that these two cell lines were not useful for further study. Tert-immortalised human foreskin fibroblasts expressing Cas9 protein (HFF) were also tested for their ability to respond to transfected DNA. Lower dose of htDNA induced up to 14-fold change mRNA expression of both innate immune markers compared to mock untransfected cells (Figure 3.1 B). HFFs were the only cell type that significantly increased *IFNB* and *CXCL10* mRNA levels in the DNA stimulation conditions, displaying properties of a suitable intracellular DNA sensing cell model.

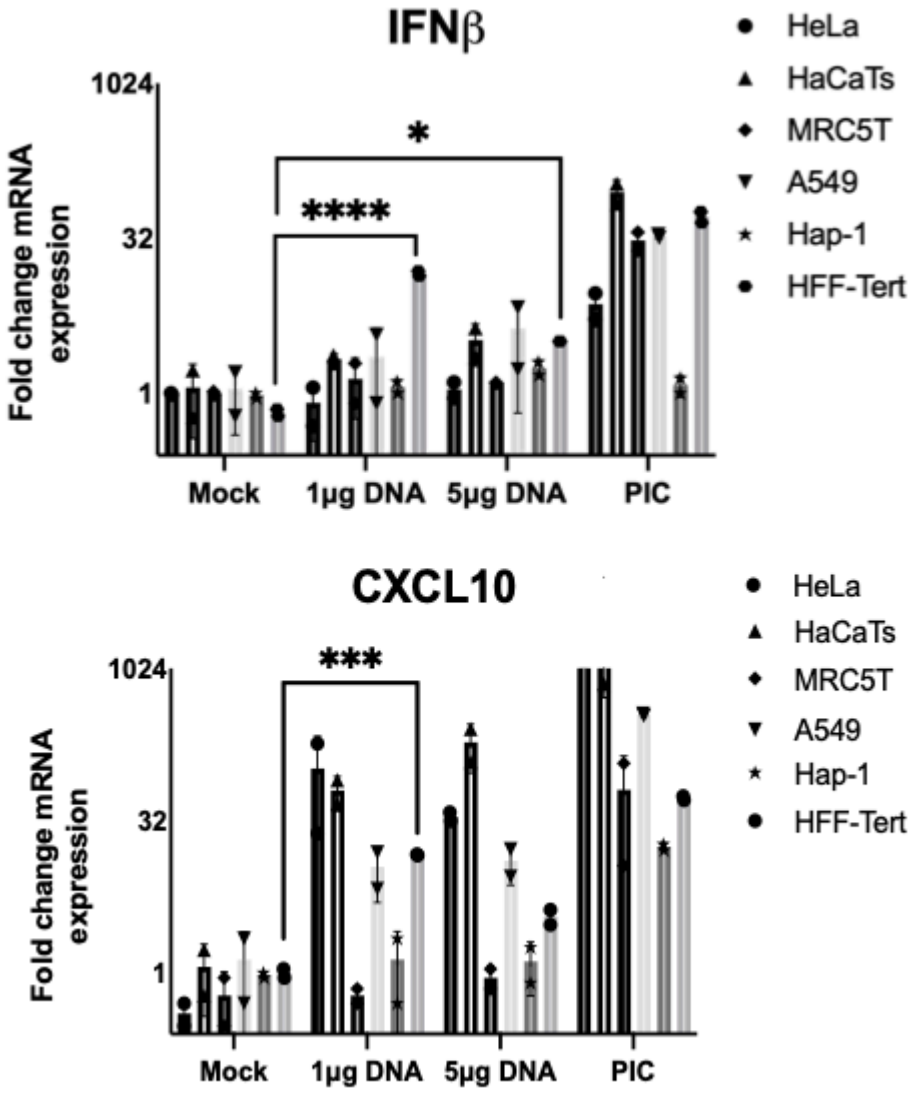

Figure 3.1 Many cell lines lack the capacity to mount an antiviral immune response to DNA.
Cells were transfected with 1 µg or 5 µg of htDNA in duplicates. 2 µg of Poly(I:C) was used as a positive control and mock untransfected cells were used as a negative control. At 6 hours post transfection, RNA was extracted and analysed by RT-qPCR for IFNβ and CXCL10. Data are presented as relative fold change in mRNA expression and normalised to GAPDH. Data are presented as mean +/- SD. Graphs are representative of at least 4 experiments. Statistical significance was calculated using ANOVA test; *P<0.05, **P<0.01, ***P<0.001. The comparisons were made between stimulated cells and their respective mock controls.

3.2 Examining cells for their protein expression profile of DNA sensing pathway components

The next step in the characterisation of suitable human cell lines was to identify which cells expressed our protein of interest (DNA-PKcs), as well as other key molecules of the intracellular DNA PRR signalling pathway. This was performed by taking whole cell lysates from the various cell lines and immunoblotting for DNA-PKcs, Ku70 and IFI-16, and the downstream components of the pathway, TBK1, STING and IRF3, as well as the negative regulator TREX-1 (Figure 3.2 A, B). We attempted to blot for cGAS also but discovered later that the antibody we used for this experiment was binding an antigen at the correct molecular mass, but that was also present in cGAS KO cells, so it was not suitable for this analysis.

HaCaTs, HeLa, A549 and HFF express most of the DNA sensing pathway components. DNA-PKcs expression in A549 cells was not detectable by WB, however immunofluorescence data (along with with HeLa and HFF cells) demonstrated good expression levels in the cell nucleus (Figure 3.2 C)**.** Immunoblot data showed that MRC5T fibroblasts likely do not express DNA-PKcs and that Hap-1 and MRC5T cells had no detectable levels of STING, which might be the reason why they did not respond to intracellular DNA stimulation (Figure 3.1 A). Therefore, we decided not to pursue the use of these cell lines in our study.

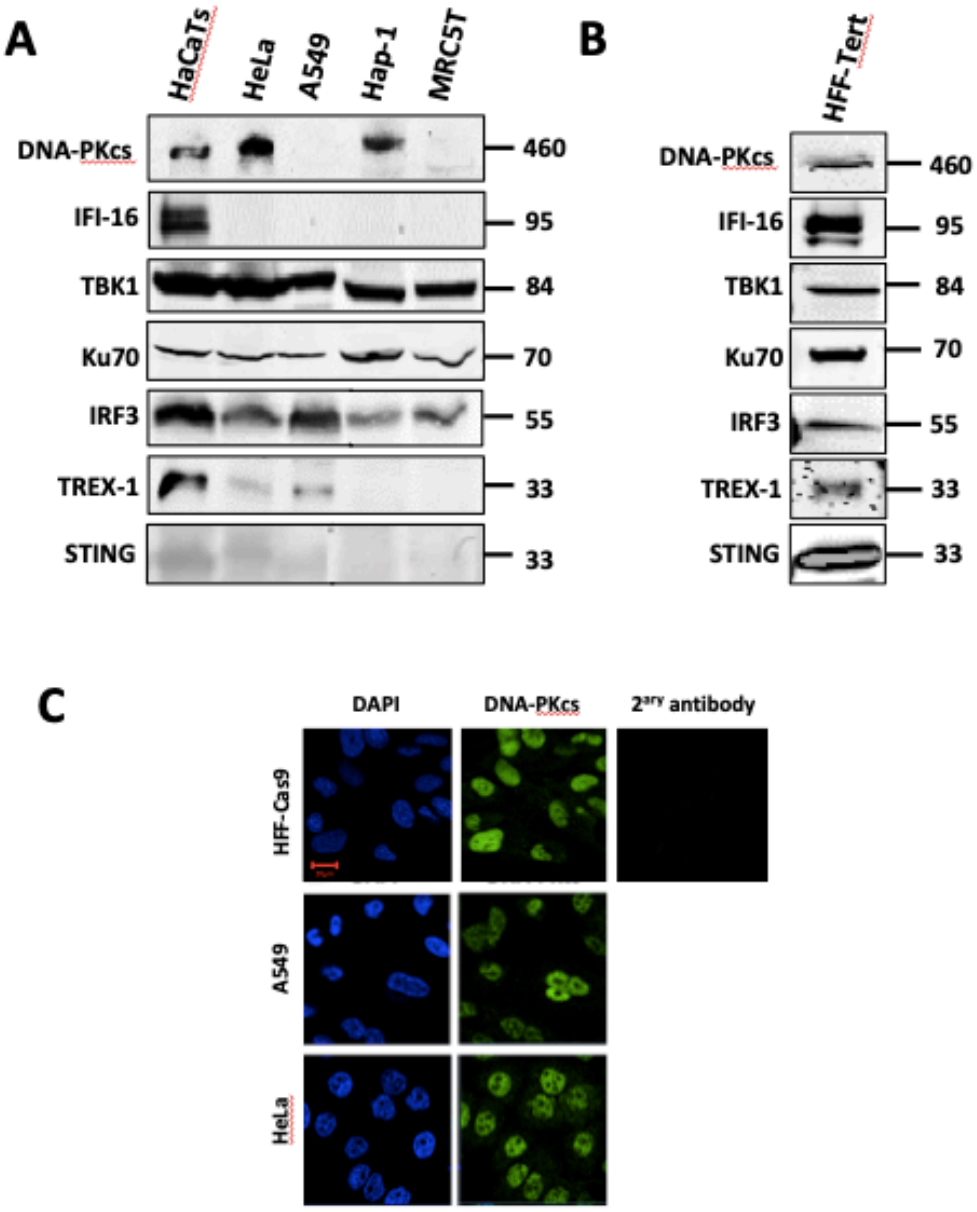

Figure 3.2 HFF cells express all key proteins in the DNA sensing pathway, among other cell lines. A), B) Whole cell protein lysates were collected from the indicated cell lines and immunoblotted for the proteins shown above. The predicted molecular mass of each protein in kDa is designated on the right. C) A549, HeLa and HFF cells were immunostained for DNA-PKcs in green. DAPI stains the nuclei in blue. The image in the right top-hand corner depicts cells only stained with green secondary anti-mouse antibody, used as a negative control. Scale bar: 20 μm.

HeLa, HaCaTs and A549 cells display dysregulated signalling in response to intracellular DNA

Next we validated whether the outcomes seen by qPCR analysis, i.e. the elevated expression of the innate immune markers, were due to phosphorylation and activation of known components in the DNA sensing pathway. Since these events are upstream of the changes in mRNA expression, we tested early signalling events in HeLa, A549 and HaCaTs after DNA stimulation. Cells were transfected with 1 µg of htDNA for 2, 4 and 6 hours (Figure 3.3 A). HeLa cells only showed around 14-fold upregulation of *CXCL10* in response to transfected DNA after 6 hours. HaCaTs demonstrated around 5-fold upregulation of *IFNB* at 4 hours and *CXCL10* at 6 hours, compared to the mock control. On the other hand, A549 showed a small upregulation (around 3-fold) of both transcripts 6 hours after stimulation.

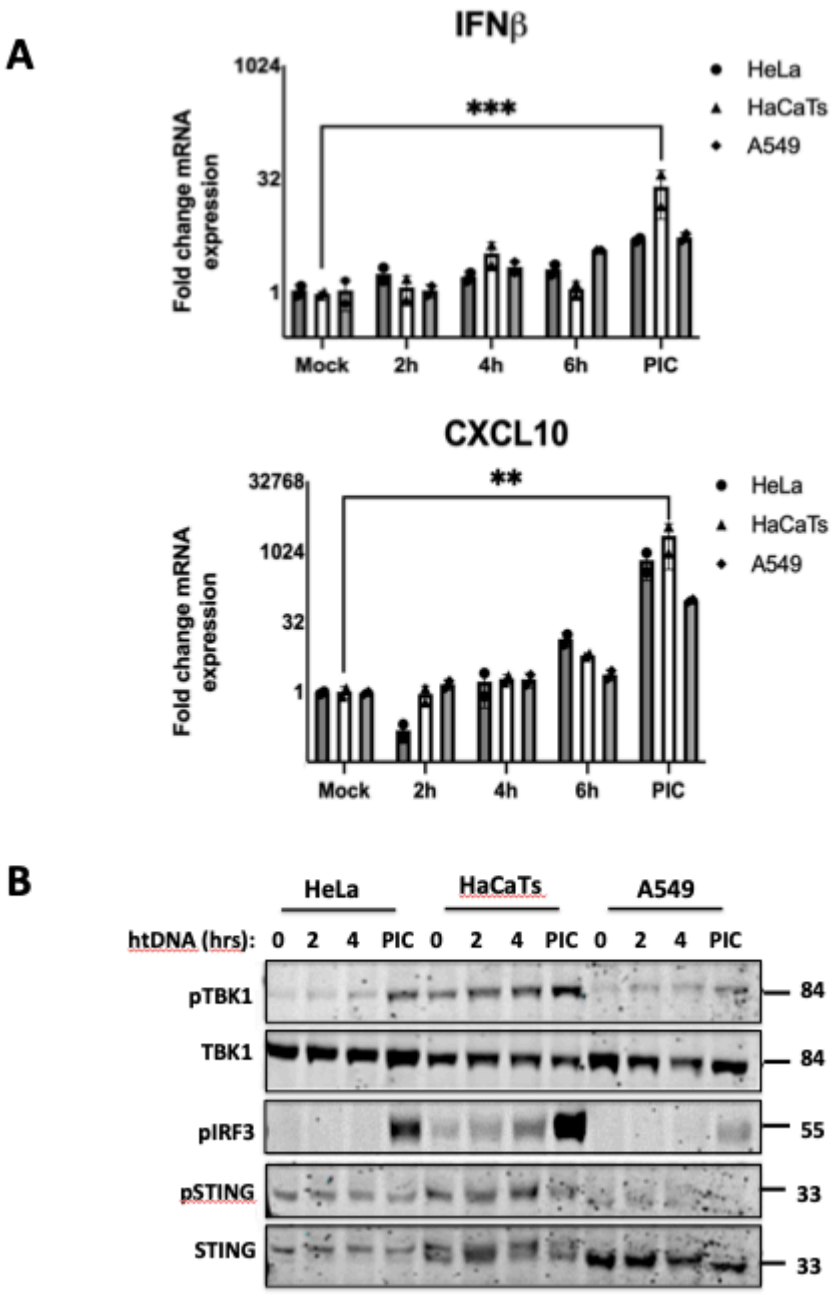

Figure 3.3. HeLa, HaCaTs and A549 cells display dysregulated responses to intracellular DNA.
A) Cells were transfected with 1 μg of htDNA in duplicate and incubated for 2, 4 and 6 hours. 2 μg of Poly(I:C) was used as a positive control and mock untransfected cells were used as a negative control. At the indicated time points, RNA was extracted and analysed by RT-qPCR for IFNβ and CXCL10. Data are presented as fold change in mRNA expression and normalised to GAPDH. Data are presented as mean +/- SD. Graphs are representative of 2 experiments. Statistical significance was calculated using ANOVA test; *P<0.05, **P<0.01, ***P<0.001. The comparisons were made between stimulated cells and their respective mock controls. B) Cells were stimulated with 5 μg htDNA for 2 and 4 hours, and with Poly(I:C) for 4 hours. At the indicated time points, whole cell lysates were immunoblotted for phosphorylated TBK1 at serine 172 and total TBK1, phosphorylated IRF3 at

serine 386, phosphorylated STING at serine 366 and total STING. Data are representative of 2 experimental repeats.

Following that, the three cell lines were stimulated with 5 μg of transfected htDNA for 2 and 4 hours. The samples were immunoblotted for the phosphorylated form of IRF3 at serine 386, phospho-TBK1 at serine 172 and phospho-STING at serine 366 (Figure 3.3 B). In the active DNA sensing pathway, TBK1 is recruited to STING and phosphorylates IRF3, which results in IRF3 dimerisation and translocation to the nucleus where it directly activates *IFNB* transcription. HaCaTs showed IRF3 and TBK1 phosphorylation at all time points, including in the untransfected cells, indicating that the human keratinocyte cell line has a pre-activated basal signalling state, which would be a confounding factor in our studies. A549 and Hela only showed faint bands for the active form of TBK1 at 4 hours and demonstrated no detectable levels of STING or IRF3 phosphorylation upon stimulation with this high dose of DNA, suggesting that this pathway is not active at detectable levels in these cells. For the reasons described above, we concluded that the three cell lines were not suitable human cell models for the study of the innate immune response signalling to intracellular DNA.

3.3 Human foreskin fibroblasts are a suitable model for DNA sensing

3.3.1 HFF cells expressing Cas9 are proficient for intracellular DNA sensing

Since the three cell lines described in the previous section displayed dysregulated innate signalling to DNA, we decided to further analyse the HFF candidate cell line as a potential cell model for our study. HFF cells have been lentivirally transduced to stably express Cas9. In order to test that the clonal selection process has not introduced an artefact that can affect the DNA sensing capacity of the cells, we compared them to a WT HFF cell line. The results showed clearly that both cell lines were able to respond to intracellular DNA by upregulating both *IFNB* and *CXCL10* expression compared to mock sample (Figure 3.4). HFF-Cas9 showed around 70-

fold induction of *CXCL10* transcription after 6 hours of htDNA transfection compared to HFF-Tert cells.

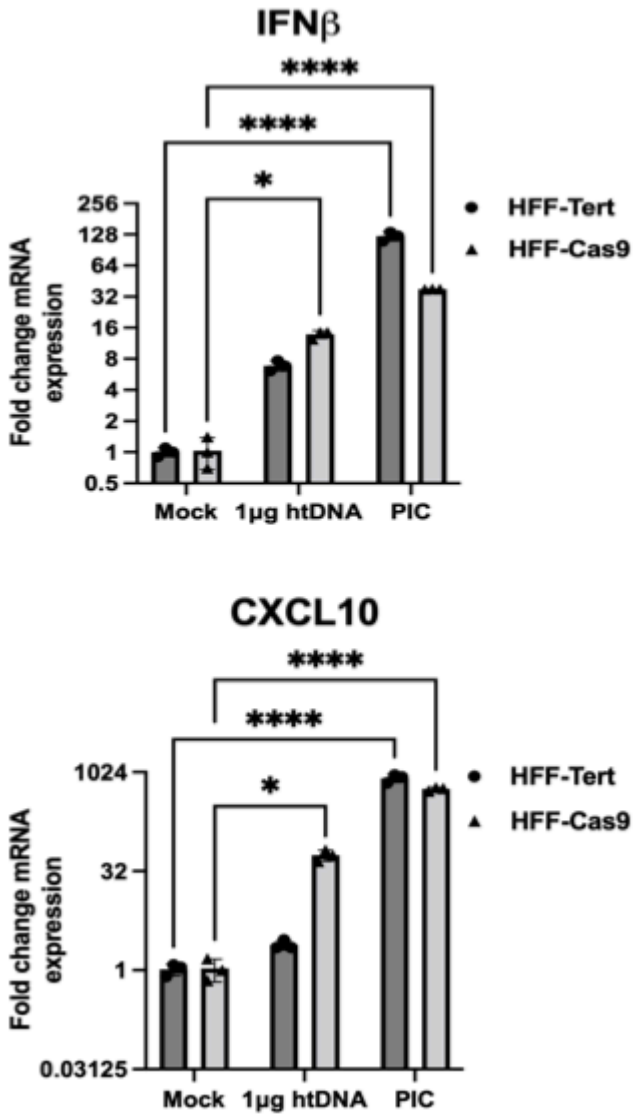

Figure 3.4. HFF cells expressing Cas9 are proficient in intracellular DNA sensing.
Cells were transfected with 1, 2 µg of htDNA in triplicate. 2 µg of Poly(I:C) was used as a positive control and mock untransfected cells were used as a negative control. At 6 hours post transfection, RNA was extracted and analysed by RT-qPCR for *IFNB* and *CXCL10*. Data are presented as fold change in mRNA expression and normalised to GAPDH. Data are presented as mean +/- SD. This experiment was performed once. Statistical significance was calculated using ANOVA test; *P<0.05, **P<0.01, ***P<0.001. The comparisons were made between stimulated cells and their respective mock controls.

3.3.2 HFF cells generate a productive STING-dependent IFN-I immune response to DNA

So far, our screening data demonstrated that HFF cells are a well-suited human cell line for analysis of DNA sensing mechanisms. These cells have the capacity to mount a robust antiviral immune response to intracellular DNA stimulation and express all components of the DNA sensing pathway. Apart from *IFNB* and *CXCL10,* we also measured the transcription levels of *IFNA4* and *IFNL1*. HFFs did not upregulate *IFNA4* or *IFNL1* transcript levels following DNA or RNA stimulation, pointing to cell type-specific activation of IFN responses to intracellular nucleic acid sensing (Figure 3.5 A).

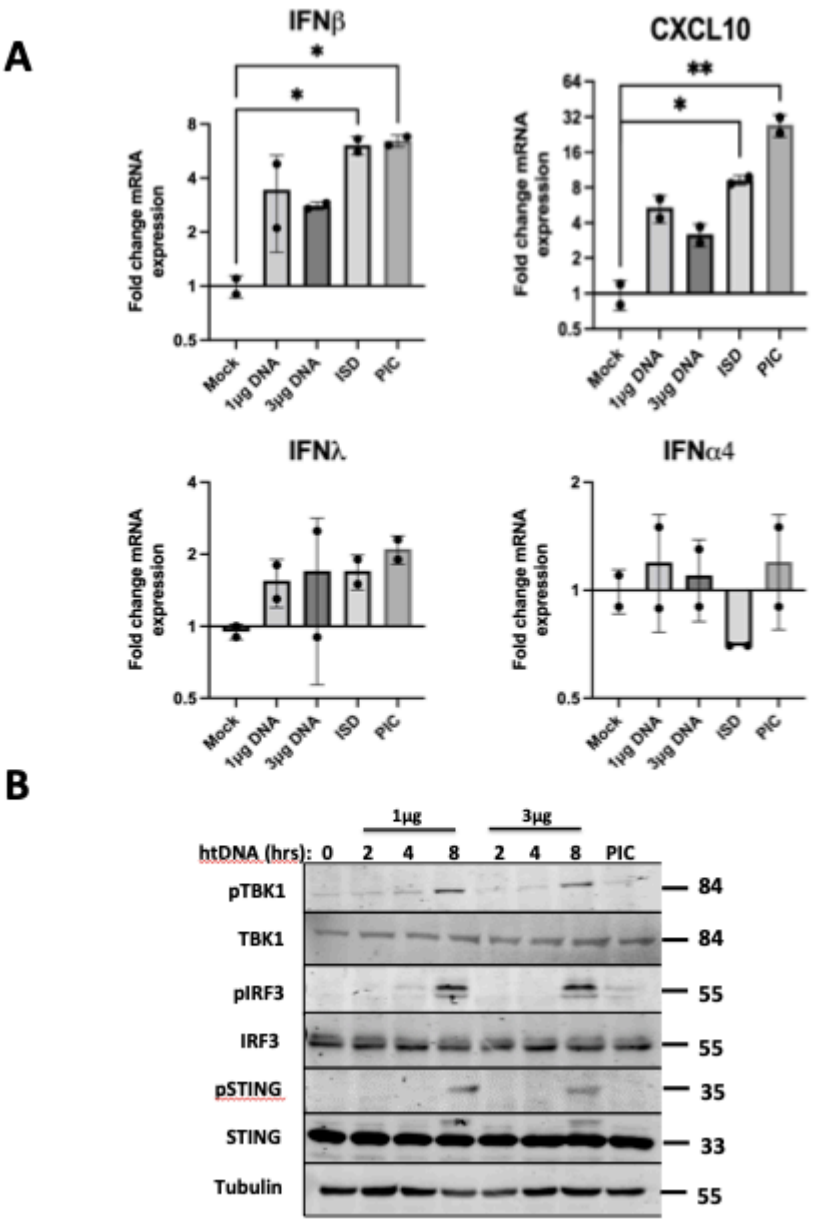

Figure 3.5. HFF cells generate a productive STING-dependent IFN-I immune response to DNA.
A) Cells were transfected with 1, 3 µg of htDNA or 7.5 µg of ISD in duplicate. 2 µg of Poly(I:C) was used as a positive control and mock untransfected cells were used as a negative control. At 6 hours post transfection, RNA was extracted and analysed by RT-qPCR for human IFNβ/α/λ and CXCL10 expression. The graph bars represent relative fold change in mRNA expression and are normalised to GAPDH. Data are presented as mean +/- SD. The upper 2 graphs were performed at least 3 times and the lower 2 once. Statistical significance was calculated using ANOVA test; *P<0.05, **P<0.01, ***P<0.001. B) Cells were transfected with 1, 3 µg of htDNA for 2, 4 and 8 hours and with Poly(I:C) for 8 hours. Whole cell lysates were immunoblotted for phosphorylated TBK1 at serine 172 and total TBK1, phosphorylated IRF3 at serine 386 and total IRF3, phosphorylated STING at serine 366 and total STING. Tubulin was used as a loading control. The experiment was repeated at least 3 times.

Moreover, HFFs stimulated with 1 or 3 μg of htDNA showed activated TBK1, STING and IRF3 at 8 hours post transfection (Figure 3.5 B) demonstrating that the intracellular DNA sensing pathway is functional in this cell line.

We next examined whether different types of DNA would elicit similar phosphorylation events in HFFs. We compared sizes of different DNA species on an agarose gel. HtDNA and ctDNA appeared as smears as they contain a mixture of different DNA strand lengths (Figure 3.6 A). HtDNA was on average larger in size than calf thymus DNA, while we could not detect the size of ISD. Stimulating fibroblast cells with htDNA or ctDNA induced phosphorylation of TBK1 and IRF3 while PRR activation with a low dose ISD did not activate the pathway (Figure 3.6 B). Collectively, the HFF characterisation set of data described in this section confirms that these cells manifest all DNA sensing features that make it an ideally suited system for our study.

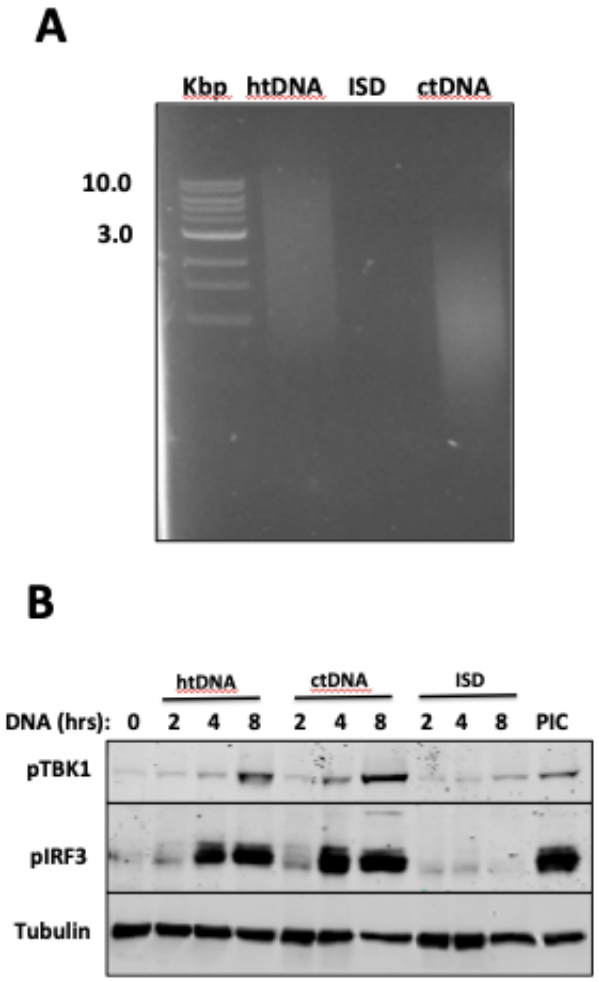

Figure 3.6 HFF cells produce a stronger immune response to purified rather than synthetic DNA. A) 500 ng of htDNA, ctDNA and ISD were run on 1% TAE agarose gel. The kilobase pair size is depicted on the left. B) HFF Cells were transfected with 1 µg of ctDNA, htDNA and 2 µg of ISD for 2, 4 and 8 hours and with Poly(I:C) for 8 hours. Whole cell lysates were immunoblotted for phosphorylated TBK1 at serine 172, phosphorylated IRF3 at serine 386, phosphorylated STING at serine 366. Tubulin was used as a loading control. The experiment was performed twice.

3.3.3 DNA-PKcs is rapidly activated in response to intracellular DNA in HFF cells

We identified that HFF have the capacity to mount IFN-I response and activate the STING/IRF3-dependent pathway to intracellular DNA. Our next focus was to examine the earliest events that happen in PRR activation during DNA sensing and understand whether DNA-PKcs plays a part in this process. When active, DNA-PKcs

kinase autophosphorylates on several residues, including serine 2056 (highlighted in Fig. 3.7 A), and phosphorylates a number of downstream targets that initiate signalling cascades. We observed a specific signal for the active phosphorylated form of DNA-PKcs on S2056 by immunofluorescence after htDNA transfection for 2 hours (Fig. 3.7 B). Etoposide was used as a positive control in this assay as a DNA damage-inducing agent that potently activates DNA-PKcs. In addition to this, we also tried performing this experiment by phosphoblotting, however this assay was not sensitive enough to pick up the phospho-DNA-PKcs signal and needs further optimisation. Overall, the immunofluorescence data points to the conclusion that early exposure of fibroblast cells to DNA ligand gets recognised by DNA-PKcs and induces its kinase activity.

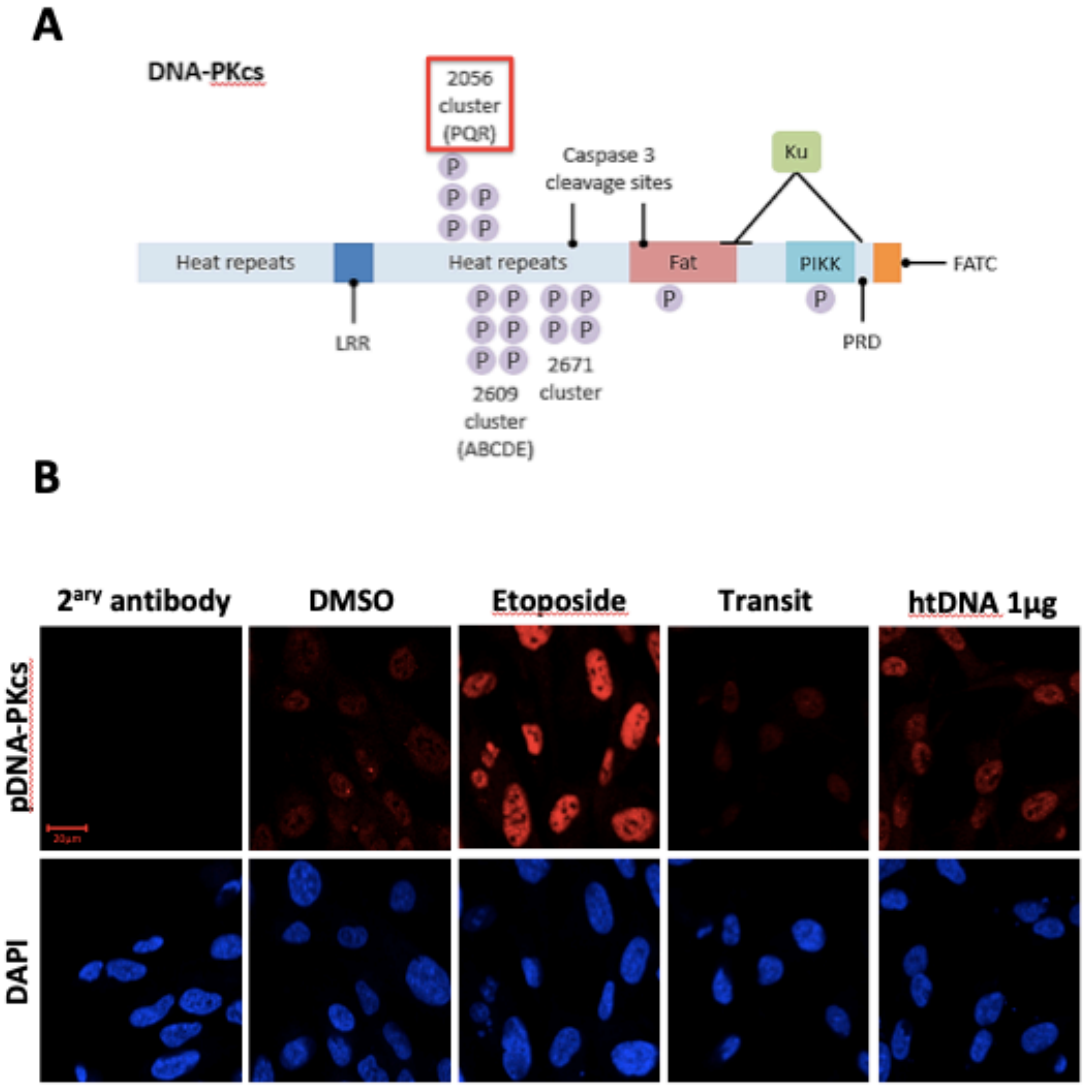

Figure 3.7 DNA-PKcs is rapidly activated in response to intracellular DNA in HFF cells.
A) Schematic representation of DNA-PKcs domain structure and phosphorylation sites. B) HFF cells were transfected with 1 µg of htDNA and fixed after 2 hours for immunofluorescence analysis. Cells treated with 30µM of etoposide for 1 hour were used as a positive control. Samples treated only with DMSO/Transit-LT1 were used as a negative control. Phospho-DNA-PKcs protein is stained in red and DAPI stains the nuclei in blue. The 2^{ary} antibody was used as negative control and to offset the background non-specific signal. Scale bar: 20 µm.

3.4 HFF cells induce IFN-I antiviral immune response to DNA virus infection

3.4.1 HSV-1 ICP0 targets DNA-PKcs for degradation

HFF cells can mount an innate immune response to a naked PAMP such as DNA, so we next assessed their ability to mount an anti-viral response to a viral pathogen and more specifically to a DNA virus. The genomes of large dsDNA viruses, such as VACV and HSV-1, trigger intracellular DNA PRRs but these viruses have in turn evolved various potent evasion mechanisms to block IFN-I production by inhibiting DNA-PK or downstream components of the DNA sensing pathway. Therefore, we made use of an attenuated HSV-1 and VACV that lack immunomodulatory proteins and are able to drive type I interferon production, and were shown to be sensed by DNA-PKcs in murine fibroblasts (Ferguson *et al,* 2012).

First we used an attenuated strain of HSV-1, HSV-1 ΔICP0, which lacks the early viral protein ICP0. ICP0 is a E3-ubiquitin protein ligase that interferes with the IRF3 signalling pathway and has also been shown to promote the degradation of DNA-PKcs rapidly after infection (Lees-Miller *et al,* 1996). We made a direct comparison in our system by infecting HFF cells with WT HSV S17 and HSV ΔICP0 at multiplicity of infection (MOI) of 5 (Figure 3.8 A). We observed a rapid decrease in total protein levels as early as 4 hours post infection while the protein levels in infected cells with the attenuated viral strain remained relatively constant. This is consistent with what has been shown before in HeLa cells infected with HSV-1 KOS strain where the DNA-PKcs levels were decreased by half 4 hours post infection (Lees-Miller, 1996).

We analysed the phosphorylation levels of IRF3, which correlated with the level of DNA-PKcs depletion during infection as we could only detect signal in HSV ΔICP0-infected fibroblasts between 4 and 6 hours post infection, at which time DNA-PKcs is depleted in WT HSV S17 infection. We detected phosphorylated IRF3 in HSV S17-infected cells only when we used MG132 to inhibit the activity of the proteasome; as

such, IRF3 signalling is restored when DNA-PKcs protein is not degraded (Fig. 3.8 B).

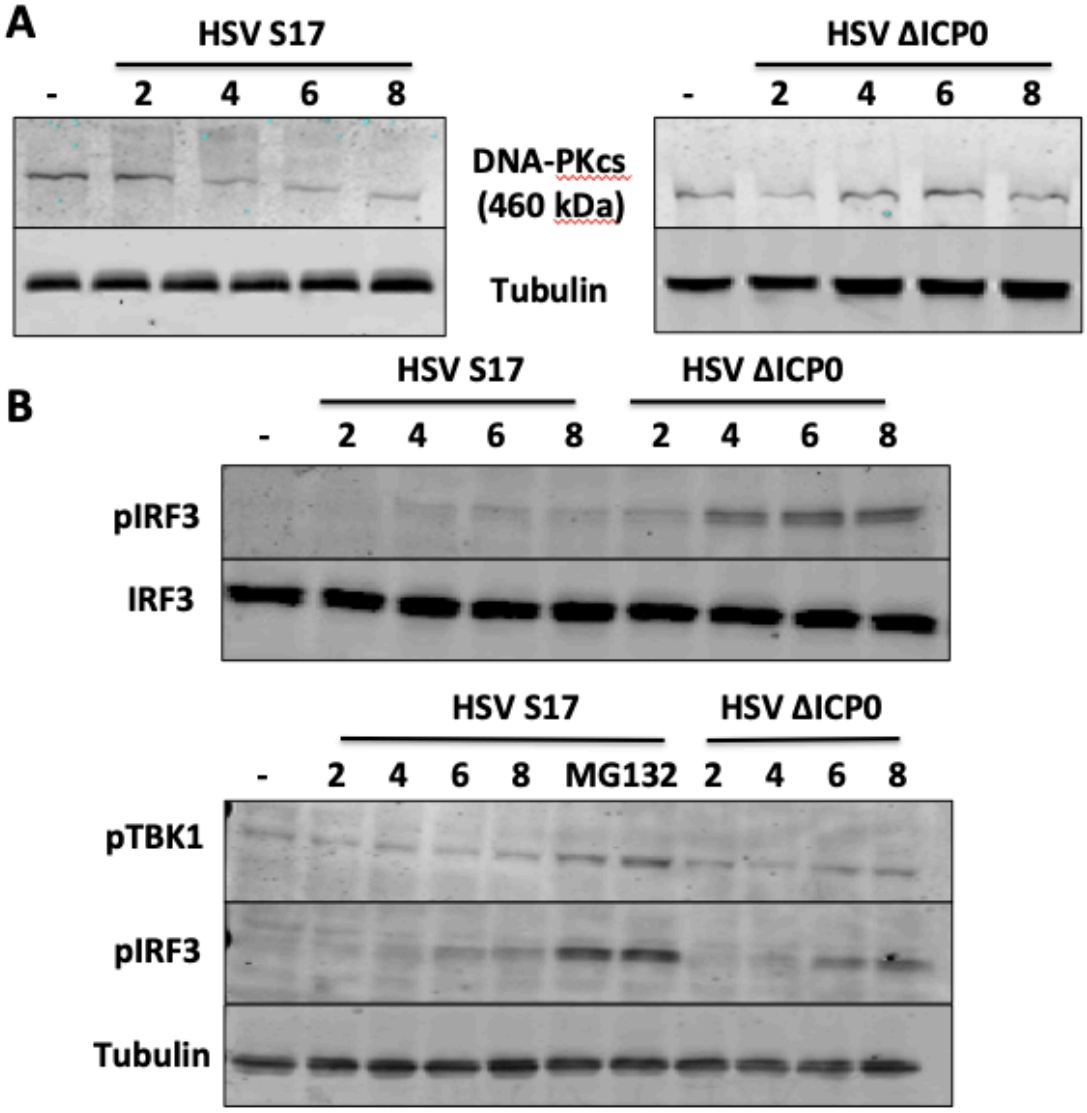

3.8 HSV-1 ICP0 targets DNA-PKcs for degradation.
HFF WT cells were infected with HSV S17 or HSV ΔICP0 at MOI5 and harvested at 2, 4, 6, 8 hours after infection. Mock uninfected cells were used as a negative control, B) HSV S17-infected cells were also treated with 10 μM MG132 proteasome inhibitor and harvested at 8 hours. Whole cell lysates were immunoblotted for A) total DNA-PKcs protein, B) phospho-IRF3 at serine 386, total IRF3 and phospho-TBK1 at serine 172. Tubulin was used as a loading control. Data are representative (n=2).

3.4.2 HFF cells mount IFN-I antiviral immune response to HSV-1 infection

Having established that HSV ΔICP0 activates IRF3 in HFF cells, we further characterised the innate immune response to this infection in the cells. HFFs were infected at MOI of 5 to ensure all cells were simultaneously infected (Fig. 3.9 A). Similarly to DNA PRR stimulation, the transcriptional response was measured after 6 hours to monitor the immediate response and avoid secondary waves of autocrine and paracrine signalling. Detection of HSV ICP27 mRNA levels confirmed that the cells were successfully infected and that HFF cells are permissive to an infection with HSV ΔICP0 virus (data not shown). Sendai virus (SeV), an RNA virus that potently stimulates the intracellular RNA sensor RIG-I, was used as a positive control (Kato, Takahasi and Fujita, 2011). *IFNB* and *CXCL10* mRNA levels were upregulated after 6 hours of HSV-1 ΔICP0 infection. Some low level *IFNL1* and *IFNA4* transcription was also detected in these cells. Time-course phosphoblotting demonstrated detectable phosphorylation of TBK1, IRF3 and STING as early as 4 hours after HSV-1 ΔICP0 infection and, as expected, SeV induced phosphorylation of IRF3 and TBK1 but not STING, since the adaptor protein STING is not involved in the RNA sensing pathway. To sum up, this panel of data supports the conclusion that HSV-1 ΔICP0 is able to infect and generate a productive immune response in HFF cells and is thus a useful tool for further analysis of intracellular DNA sensing mechanisms (Figure 3.9 B).

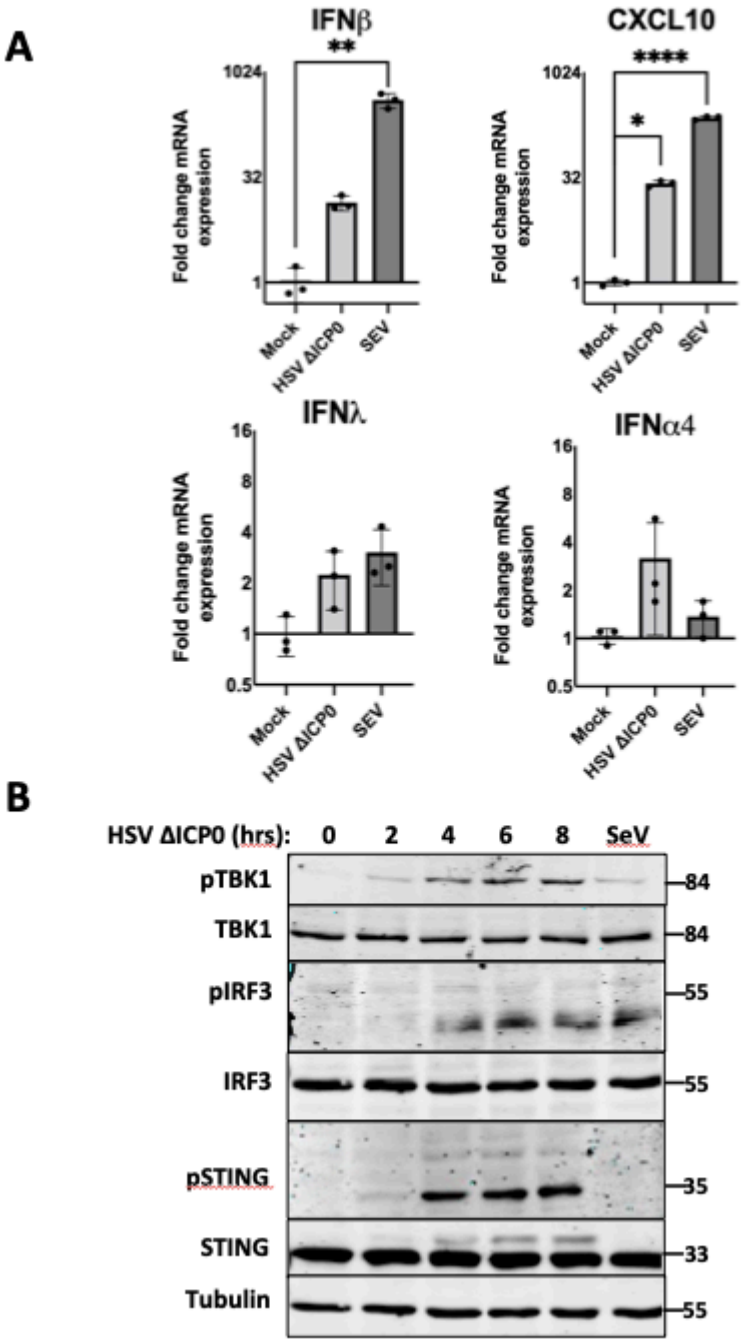

Figure 3.9 HFF cells mount IFN-I antiviral immune response to HSV-1 infection.
A) Cells were infected with HSV ΔICP0 at MOI of 5 and SeV (1:300) for 6 hours in triplicate. Mock uninfected cells were used as a negative control. RNA was extracted and analysed by RT-qPCR for IFNβ, IFNλ, IFNα, CXCL10 expression. The graph bars represent relative fold change in mRNA expression and are normalised to GAPDH. Data are presented as mean +/- SD. The upper 2 graphs were performed at least 3 times and the lower 2 once. Statistical significance was calculated using ANOVA test; *P<0.05, **P<0.01, ***P<0.001. B) Cells were infected with HSV ΔICP0 at MOI of 5 for 2, 4, 6, 8 hours and SeV (1:300) for 6 hours. Whole cell lysates were immunoblotted for phosphorylated TBK1 at serine 172 and total TBK1, phosphorylated IRF3 at serine 386 and total IRF3,

phosphorylated STING at serine 366 and total STING. Tubulin was used as a loading control. Data are representative of at least 3 experimental repeats.

3.4.3 HFF cells mount IFN-I antiviral immune response to MVA infection

DNA-PKcs was first described as a viral DNA sensor in murine fibroblasts using VACV as an infection model (Ferguson *et al*, 2012; Peters *et al,* 2013). VACV has developed ways to prevent the DNA-PK complex from binding to viral DNA and thus, suppressing the antiviral immune response (Scutts *et al,* 2018). For this reason, we used the Modified Vaccinia Ankara (MVA) strain of VACV, which is used as a poxvirus vaccine vector and has large regions deleted from its genome that encode multiple immunomodulatory proteins. MVA has also been shown to generate a productive IFN-I response in mouse fibroblasts (Ferguson *et al,* 2012). To test it in our system, we performed a time-course experiment where cells were infected with MVA at MOI 5 (Figure 3.10 A). The mRNA levels of *IFNB* and *CXCL10* were increased in a time-dependent manner. The longer the infection lasted, the higher the mRNA expression levels were, reaching a maximum of 19-fold change in CXCL10 and 10-fold change in *IFNB* levels at 8 hours post infection. Similarly to what we observed during HSV infection, MVA did not induce upregulation of *IFNA4* or *IFNL1* in HFF cells. However, no positive controls were included in this assay, meaning that these cells might not express the cytokines. Analysis of the intracellular signalling pathway during infection was also carried out by phosphoblotting for the activation of IRF3 (Figure 3.10 B). IRF3 activation peaked at 6 hours post infection with MVA. We noticed a non-specific band above phospho-IRF3 signal in MVA- and SeV-infected samples (shown by red arrow), which has also been reported during DNA stimulation in another study as a downstream target of DNA-PKcs during innate sensing (Burleigh *et al,* 2020). Overall, this panel of data confirms that MVA is a suitable infection model for the study of DNA virus-driven DNA sensing pathways in human fibroblasts.

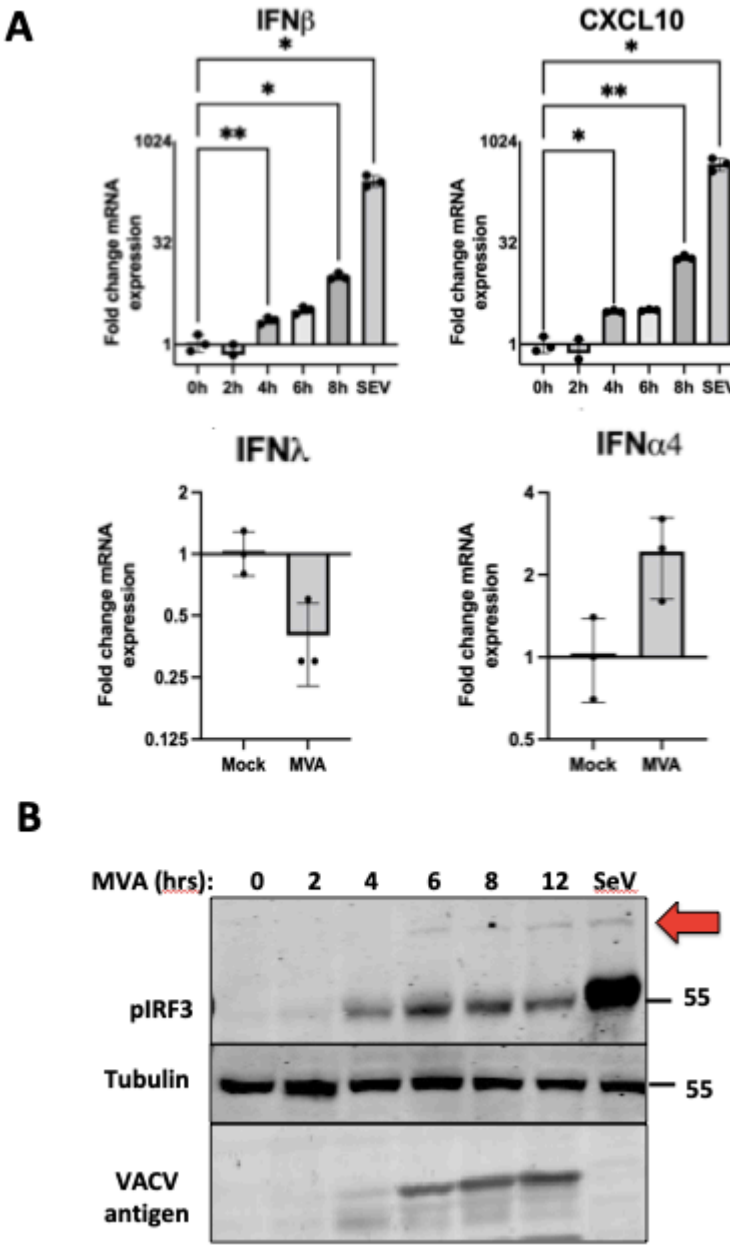

Figure 3.10 HFF cells mount IFN-I antiviral immune response to MVA infection.
A) Cells were infected with MVA at MOI of 5 for 2, 4, 6, 8 hours in triplicate. Mock uninfected cells were used as a negative control and SeV (1:300) was used as a positive control. RNA was extracted and analysed by RT-qPCR for IFNβ, CXCL10, IFNα and IFNλ expression. The graph bars represent relative fold change in mRNA expression and are normalised to GAPDH. Data are presented as mean +/- SD. Graphs are representative of at least 2 repeats. Statistical significance was calculated using ANOVA (upper graphs) and paired Student's t test (lower graphs); *P<0.05, **P<0.01, ***P<0.001. B) Cells were infected for 2, 4, 6, 8, 12 hours and harvested and immunoblotted for the phosphorylation of IRF3 at serine 386 and for VACV antigen. Tubulin was used as a loading control. Data are representative of at least 3 repeats.

3.5 Primary human fibroblasts phenocopy HFF cells in their immune response to intracellular DNA

3.5.1 Primary fibroblasts mount an immune response to intracellular DNA

To understand if immortalisation of fibroblasts altered their response to intracellular DNA, we also characterised primary cells for their ability to sense and respond to DNA. Human fibroblasts isolated from the arm skin of healthy donors express known components of the DNA PRR activation pathway, such as TBK1, IRF3 and STING (Fig. 3.11 A), as well as DNA-PKcs protein (Fig. 3.11 B). Primary fibroblasts significantly upregulated *IFNB* and *CXCL10* mRNA levels after DNA transfection (Fig. 3.11 C). Moreover, ELISA immunoassay showed that *CXCL10* protein levels were significantly higher at 24 hours after htDNA, ctDNA and Poly(I:C) transfection compared to mock untreated cells (Fig. 3.11 D). Chemokine levels were much more elevated at 24 hours in comparison to 6 hours. CtDNA in particular induced much higher levels of CXCL10 secretion compared to htDNA, suggesting for some level of DNA specificity in the immune response to DNA. Additionally, primary skin cells activated the PRR signalling pathway in response to intracellular htDNA and the phosphorylation levels of TBK1, IRF3 and STING signalling components were sustained until at least 18 hours post transfection (Fig. 3.11 E).

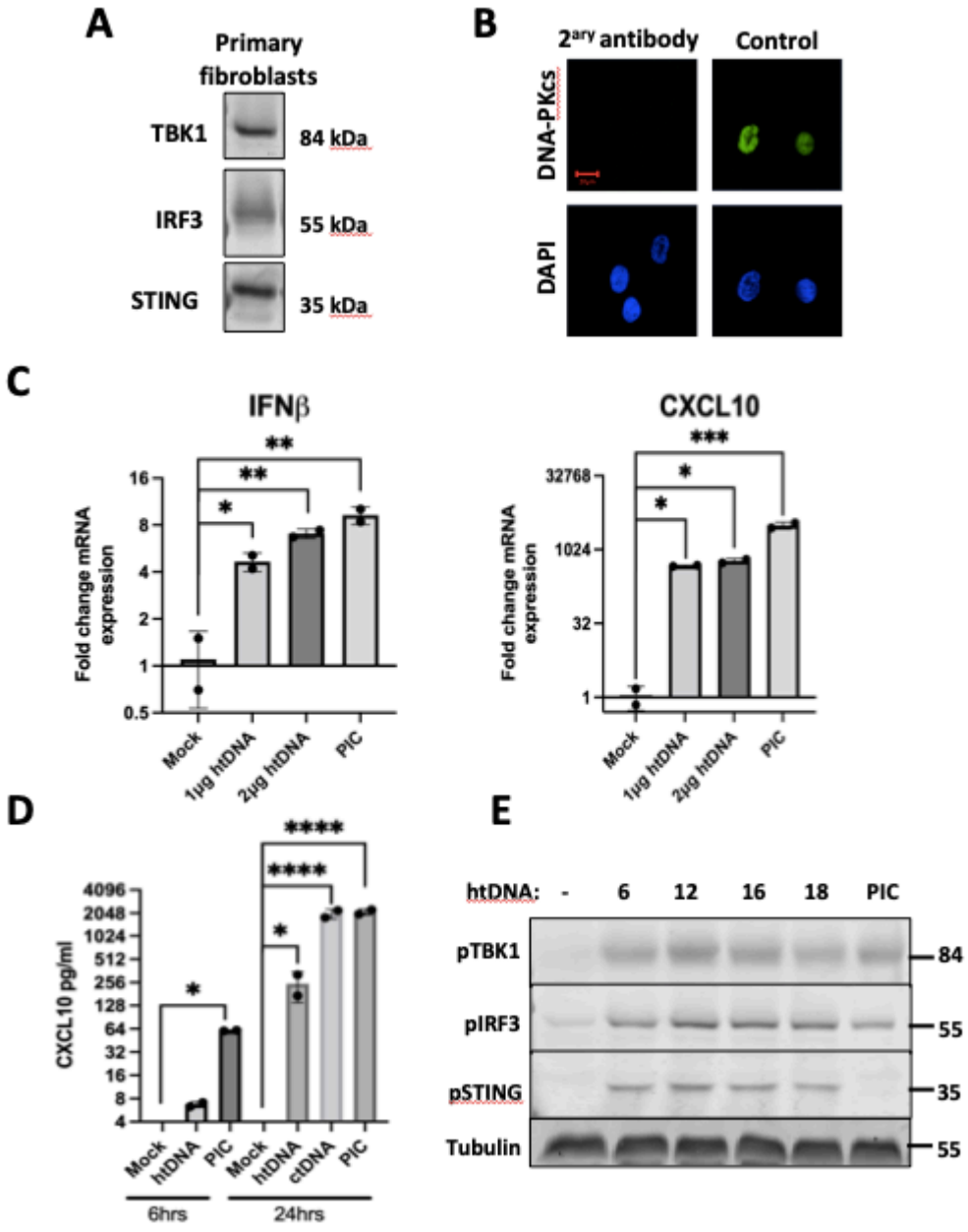

Figure 3.11 Primary human fibroblasts phenocopy HFF cells in their immune response to intracellular DNA.

A) Whole cell lysates obtained from primary fibroblasts were immunoblotted for total TBK1, IRF3 and STING. The molecular weight of each protein in kDa is designated on the right. B) Primary cells were immunostained for DNA-PKcs in green. DAPI stains the nuclei in blue. Scale bar: 20 μm. C) Cells were transfected with 1, 2 μg of htDNA and 0.5 μg Poly(I:C) for 6 hours in duplicate. Mock untreated cells were used as a negative control. RNA was extracted and analysed by RT-qPCR for IFNβ and CXCL10 expression. The graph bars represent relative fold change in mRNA expression and are normalised to GAPDH. Data are presented as mean +/- SD. Graphs are representative of 2 repeats. Statistical significance was calculated using ANOVA test; *P<0.05, **P<0.01, ***P<0.001. D) Cells were transfected with 2 μg of htDNA, ctDNA and 0.5 μg Poly(I:C) for 6 and 24 hours in duplicate. Mock untreated cells were used as a negative control. Cell supernatants were harvested and analysed by

ELISA for the concentration of CXCL10 protein. The experiment was repeated 3 times. E) Cells were transfected with 2 μg of htDNA for 6, 12, 16, 18 hours. Poly(I:C) was used as a positive control and mock untreated cells were used as a negative control. Whole cell lysates harvested at the indicated time points were immunoblotted for the phosphorylation of IRF3 at serine 386, TBK1 at serine 172 and STING at serine 366. Tubulin was used as a loading control. Images are representative of 3 experimental repeats.

3.5.2 Primary fibroblasts activate the DNA sensing pathway in response to DNA virus infection

Next, we set out to define the innate immune response of primary fibroblasts to DNA virus infection. Similar to HFF cells, primary cells were also permissive to HSV-1 ΔICP0 and MVA infection and we observed increased levels of *IFNB* and *CXCL10* transcripts at 6 hours post HSV infection (Fig. 3.12 A). In an ELISA assay the skin cells secrete up to 3 ng/ml *CXCL10* at 24 hours post HSV ΔICP0 infection (Fig. 3.12 B). Surprisingly, there was very low to no level of detection of CXCL10 protein in the supernatant of MVA-infected samples. Both the transcriptional RT-qPCR and protein ELISA assays showed that primary cells produced much more *CXCL10* in response to HSV ΔICP0 compared to MVA infection, which could be attributed to the fact that MVA induces little CXCL10 transcription. To sum up, the primary cells characterisation data provided us with enough evidence that these cells present similar DNA sensing features to the transformed HFF cell line and are a useful tool for our study.

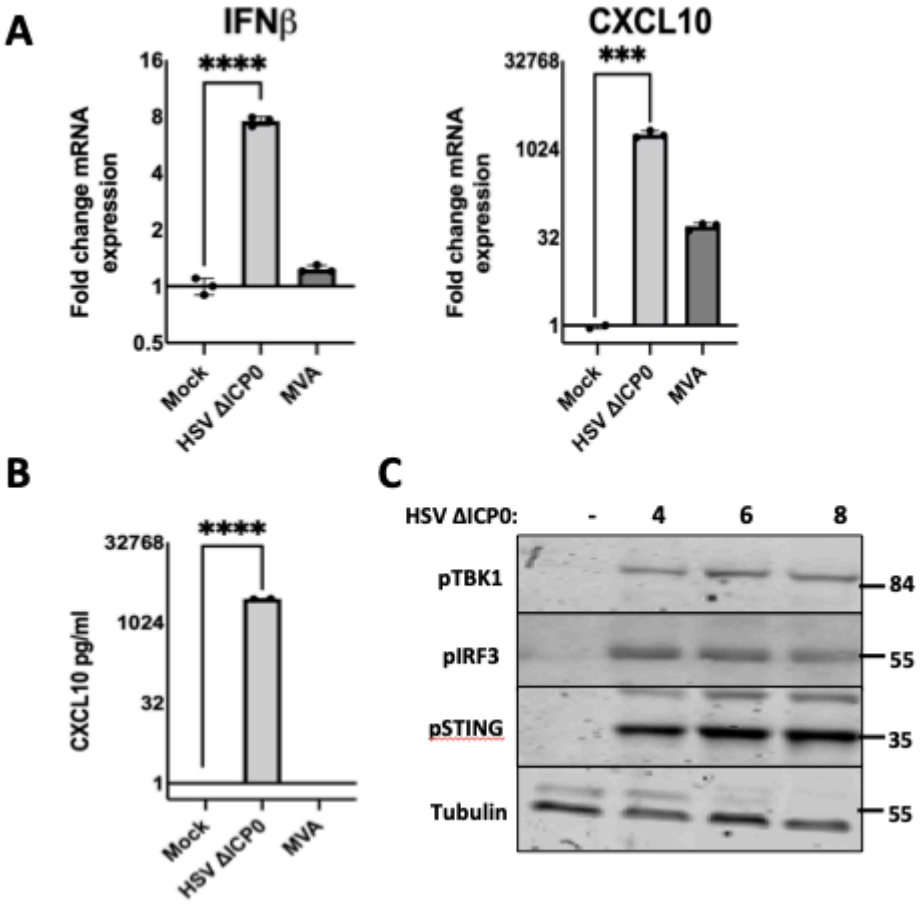

Figure 3.12 Primary fibroblasts activate the DNA sensing pathway in response to DNA virus infection.

A) Cells were infected with HSV ΔICP0 and MVA at MOI 5 for 6 hours in triplicate. RNA was extracted and analysed by RT-qPCR for IFNβ and CXCL10 expression. The graph bars represent relative fold change in mRNA expression and are normalised to GAPDH. Data are presented as mean +/- SD. Graphs are representative of 2 repeats. Statistical significance was calculated using ANOVA test; *P<0.05, **P<0.01, ***P<0.001. B) Cells were infected with HSV ΔICP0 and MVA at MOI 5 for 24 hours in duplicate. Mock uninfected cells were used as a negative control. Cell supernatants were harvested and analysed by ELISA for the concentration of CXCL10 protein. The graph is representative of 3 repeats. Statistical significance was calculated using one-way ANOVA test; *P<0.05, **P<0.01, ***P<0.001. C) Cells were infected with HSV ΔICP0 at MOI 5 for 4, 6, 8 hours. Mock uninfected cells were used as a negative control. Whole cell lysates harvested at the indicated time points were immunoblotted for the phosphorylation of IRF3 at serine 386, TBK1 at serine 172 and STING at serine 366. Tubulin was used as a loading control. Images are representative of 2 experimental repeats.

Summary

In this chapter we focused on developing a robust model and tools for our study on the role of DNA-PKcs in human antiviral immunity. We demonstrated that not all human cell lines had a functional DNA sensing pathway or expressed the DNA-PKcs protein. Transformed HFFs and primary human fibroblasts however demonstrated all desired qualities for a well-suited model to study DNA-PKcs-mediated PRR activation, which is similar to what was found in murine fibroblasts (Ferguson *et al,* 2012). However, this cannot be applied in general to all fibroblast cell lines as another transformed fibroblast cell type, MRC5T, did not have the capacity to produce an immune response to DNA. Given the cell type specificity of this process, it is critical to study it in depth in a single human cell model, which currently lacks in the literature concerning DNA-PKcs-dependent DNA sensing. Therefore, we concentrated our efforts on characterising the pathway solely in HFF cells and the next chapter addresses the question of whether DNA-PKcs, and other known DNA sensing components are required for the antiviral immune response in this system.

CHAPTER 4

4. The role of DNA-PKcs in DNA sensing in human fibroblasts

The role of DNA-PKcs as a DNA sensor that activates the IRF3-mediated innate immune response was initially defined in mice, and specifically in murine fibroblasts (Ferguson *et al,* 2012). However, the defined role of DNA-PKcs in the human innate immune system has remained controversial. The literature so far indicates that the DNA-PKcs-driven immune response can vary across cell types and the majority of the published reports fail to characterise it consistently in one model. In 2017, Morchikh *et al.* showed that DNA-PK is part of a ribonuclear complex that detects viral DNA and induced IFN-I response in STING/IRF3-dependent manner in HeLa and HEK cells (Morchikh *et al,* 2017). More recently, a report by Burleigh *et al* demonstrated that DNA-PK mediates a non-canonical STING-independent IFN response to DNA in human monocytes (Burleigh *et al*, 2020). Moreover, a third study suggested that DNA-PK utilises this non-canonical pathway to drive the immune response in cells that lack STING while it inhibits cGAS signalling in cells proficient for STING, such as human fibroblasts (Sun *et al*, 2020). Given the cell type-specific nature of this pathway, we focused our efforts on understanding what part DNA-PKcs plays solely in the human fibroblast cell system. Our main approach to study this was by generating cells that lack the NHEJ protein using the CRISPR/Cas9 system. In this chapter, we present data generated from loss-of-function studies that examine whether DNA-PKcs and other DNA sensing components contribute to the generation of the immune response to DNA and DNA virus infection in HFF cells.

4.1 Generation of tools for studying the DNA sensing pathway

Having characterised human foreskin fibroblasts (HFF) cells as a suitable model for studying intracellular DNA sensing in Chapter 3, we set out to define the contribution of DNA-PKcs in this process. To do that, we first generated

CRISPR/Cas9-edited DNA-PKcs knockout cell lines in HFF cells stably expressing Cas9. The *PRKDC* gene, which encodes DNA-PKcs, consists of 86 exons and we designed two different single guide RNAs targeting exon number 83 in the C-terminal kinase domain (Fig 4.1 A). This region was chosen for targeting as previous attempts using guides targeting exons at the N-terminus were unsuccessful, showing residual protein by immunoblotting (data not shown). The knockouts were created by lentiviral transduction and antibiotic selection. Both gRNAs worked to cut the *PRKDC* gene and allowed sucessful generation of cells lines where the DNA-PKcs protein level was reduced by % as measured by western blotting and immunofluorescence using an antibody that recognises the N-terminal part of the protein (amino acids 1-2713) (Fig 4.1 B, C). It was not feasible to generate single-cell clonal populations using this line, but the level of protein reduction was good enough to use for functional characterisations. The level of DNA-PKcs protein knockout was also found to be stable over multiple passages (not shown).

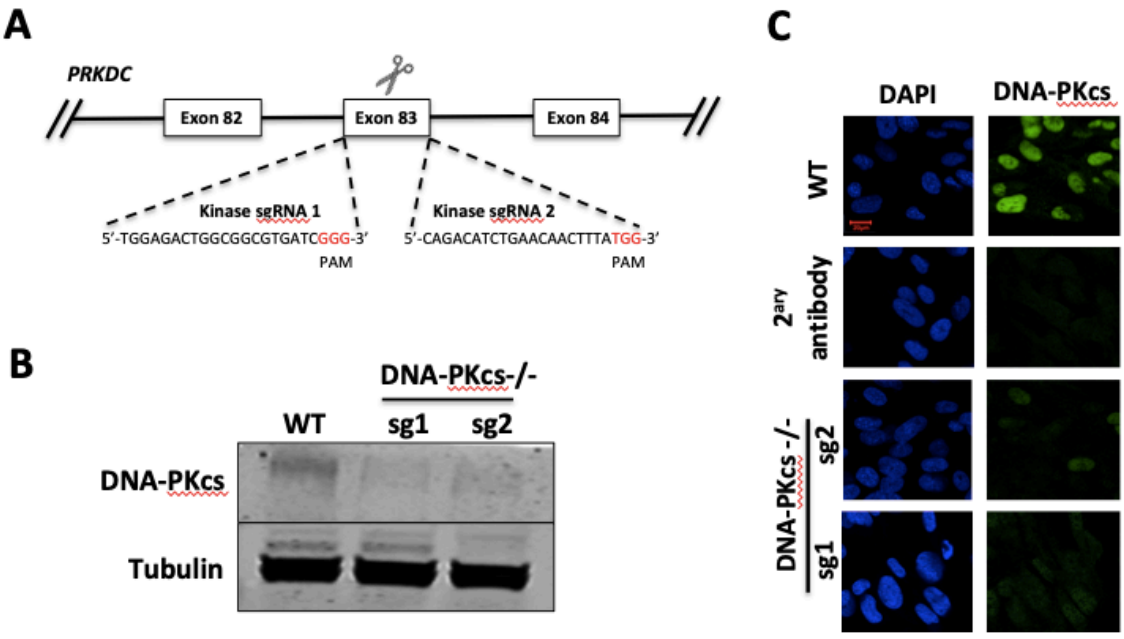

Figure 4.1 Generation of HFF DNA-PKcs-/- cell lines by CRISPR-Cas9.
A) Two single guide RNAs were designed to target exon 83 at the C terminus of the *PRKDC* gene. B) Whole cell lysates were obtained from the WT and lentivirally transduced HFF cells and immunoblotted for DNA-PKcs. Lentiviral transduction was performed by a current postdoc in the lab, Dr Marisa Oliveira and the DNA-PKcs blot was performed by a current PhD student in the lab, Emma Wagner. Tubulin was used as a loading control; C) HFF WT and DNA-PKcs-/- cells were stained for

DNA-PKcs in green and DAPI stained the nuclei in blue. The 2^{ary} antibody only was used as a negative control. Scale bar: 20 µm. Data are representative (n=3).

Using the same methodology, we created STING and cGAS knockouts in the HFF cells with sgRNAs that target the human *TMEM173* and *MB21D1* genes, respectively (Fig. 4.2 A). Both cGAS and STING were successfully knocked out (Fig 4.2 B). We also attempted to knock out IFI16, however, there was no indication of successful gene editing with the guide that we tried and we did not pursue further guide designs (Fig 4.2 C).

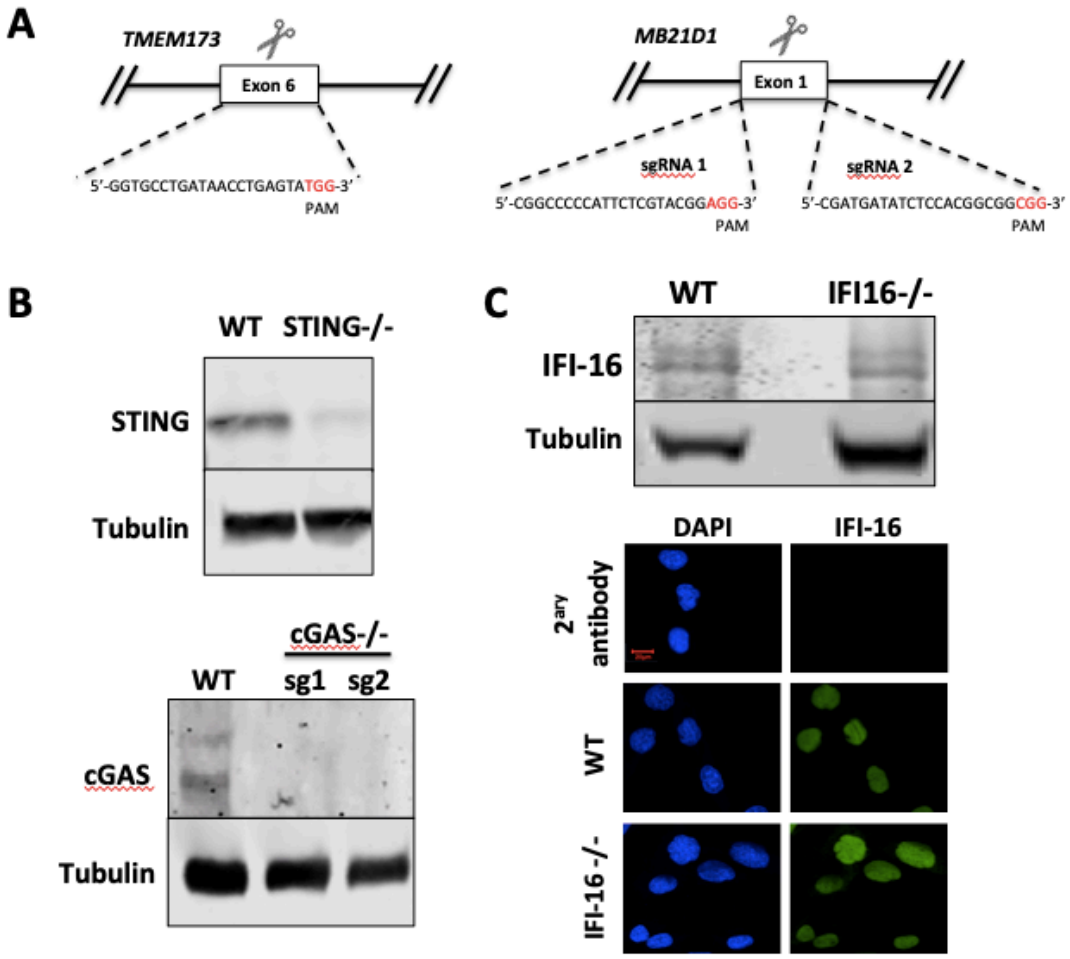

Figure 4.2 Generation of HFF STING-/- and cGAS-/- cell lines by CRISPR-Cas9.
A) HFF cells were lentivirally transduced with CRISPR plasmids expressing a single gRNA that targets STING at exon 6 or two gRNAs that target cGAS in different parts of exon 1. STING and IFI-16 sgRNA sequences were kindly provided by Jan Rehwinkel and cGAS sgRNAs were designed by Marisa Oliveira. The lentiviral transduction was performed by Marisa Oliveira. B) Whole cell lysates were

obtained from HFF STING-/- and cGAS-/- cells and immunoblotted for STING and cGAS, respectively. Tubulin was used as a loading control. The cGAS blot was performed by Emma Wagner; C) Whole cell lysates from HFF IFI-16-/- were tested for their expression of IFI-16 by Western blot; HFF IFI-16-/- were stained for IFI-16 in green and cell nuclei were stained by DAPI in blue. The 2^{ary} antibody only was used as a negative control. Scale bar: 20 μm. STING and cGAS blots were performed at least 2 times. IFI-16 immunoblot and immunofluorescence were performed once.

4.2 Characterisation of phenotype of STING/cGAS KO cell lines during DNA stimulation

Following the successful creation of the KO cell lines, our next goal was to characterise them for their ability to respond to DNA. Cells that lack STING or cGAS failed to mount IFN-I response after 6 hours of htDNA stimulation. HFF STING-/- cells demonstrated 7 times lower *IFNB* mRNA expression, whereas *CXCL10* expression was decreased around 20 times compared to WT cells (Fig 4.3 A). HFF cGAS-/- cells showed 3-fold lower *IFNB* mRNA expression compared to DNA-stimulated WT cells (Fig 4.3 B). This data indicate that the canonical cGAS/STING intracellular DNA sensing pathway functions in human fibroblasts to generate IFN-I response to exogenous DNA.

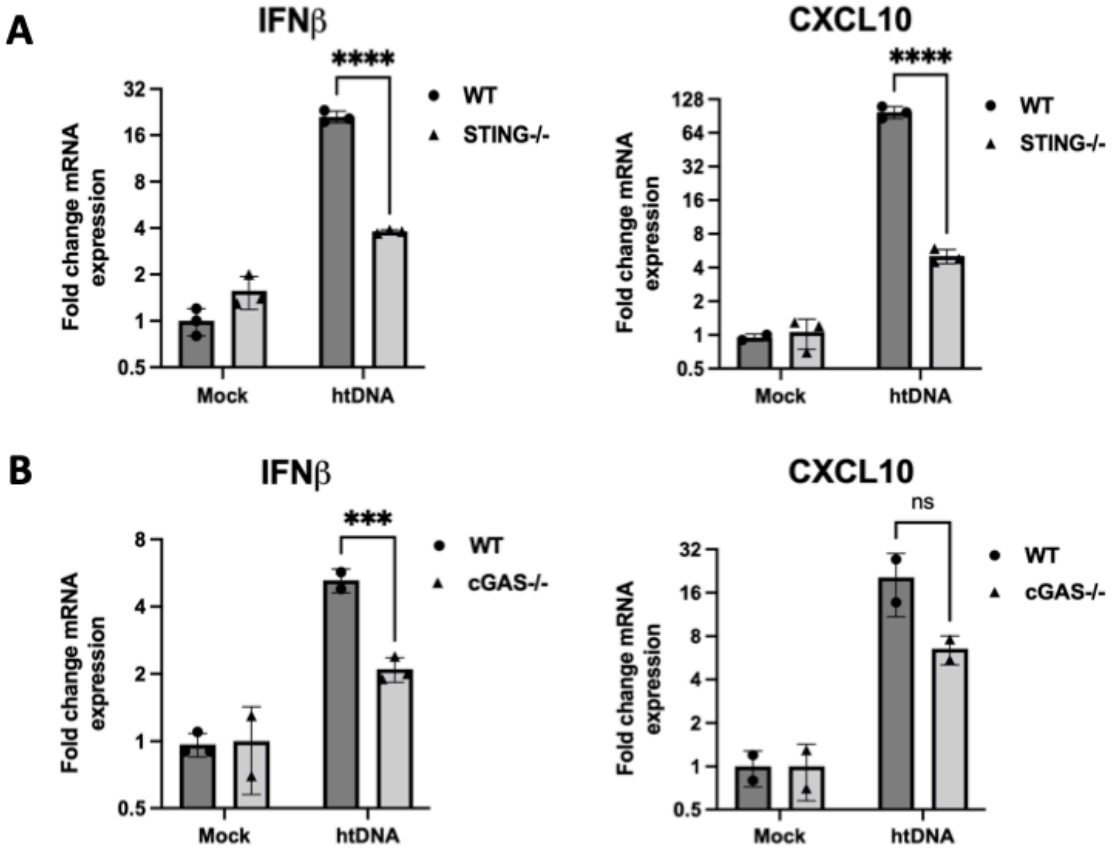

4.3 cGAS and STING are required for the IFN response to DNA in human fibroblast cells.
A) HFF WT and STING-/- and B) HFF WT and cGAS-/- sg1 cells were transfected with 1 μg htDNA in triplicate and mock untransfected cells were used as a negative control. 6 hours post transfection, RNA was extracted and analysed by RT-qPCR for IFNβ and CXCL10. Data are presented as relative fold change in mRNA expression relative to mock untreated cells and normalised to GAPDH. Data are presented as mean +/- SD. Data are representative of at least 2 experiments. Statistical significance was calculated using ANOVA test; *P<0.05, **P<0.01, ***P<0.001, ****P<0.0001.

To further define the signalling downstream of intracellular DNA, we analysed the role of TBK1/IKKε in the immune response to DNA. For this we treated HFF cells with the TBK1/IKKε kinase inhibitor BX795 prior to htDNA transfection and observed that the IFN response was abolished in the inhibitor-treated cells compared to untreated control cells (Fig 4.4). This data indicates that the intracellular DNA sensing pathway in human fibroblasts depends on TBK1/IKKε.

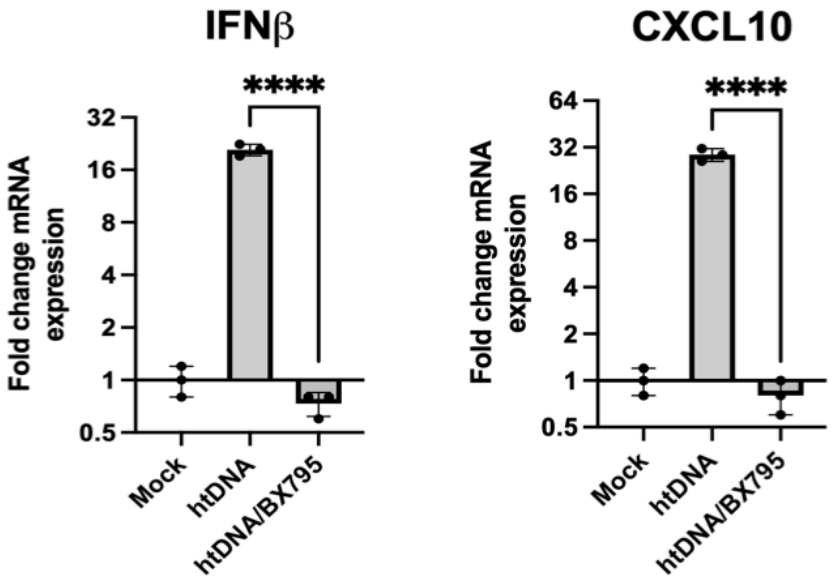

4.4 TBK1/IKKε are required for the IFN response to DNA in human fibroblast cells.
HFF WT cells were pre-treated with 1 μM of BX795 TBK1/IKKε kinase inhibitor before being transfected with 1 μg htDNA in triplicate. Untransfected cells were used as a negative control. At 6 hours post transfection, RNA was extracted and analysed by RT-qPCR for IFNβ and CXCL10. Data are presented as relative fold change in mRNA expression relative to mock untreated cells and normalised to GAPDH. Data are presented as mean +/- SD. Data are from a single experiment that was performed with Marisa Oliveira. Statistical significance was calculated using ANOVA test; *P<0.05, **P<0.01, ***P<0.001, ****P<0.0001.

To understand in more detail how loss of cGAS and STING impacts the mechanisms of intracellular DNA sensing, we analysed known phosphorylation events in the activation of the DNA sensing pathway. Human fibroblast cells deficient in STING or cGAS showed a strong reduction in the phosphorylation of the transcription factor IRF3 as early as 6 hours after DNA transfection (Fig. 4.5 A, B), indicating that both components act in the same pathway. Densitometry analyses confirmed that p-IRF3 levels were reduced by 70% in STING-/- cells at 6 hours of ctDNA stimulation and by 96% in cGAS-/- at 6 hours of htDNA stimulation. IRF3 phosphorylation in response to transfected RNA mimic Poly(I:C) was unaffected by either cGAS or STING knockout confirming the specificity of this pathway for DNA.

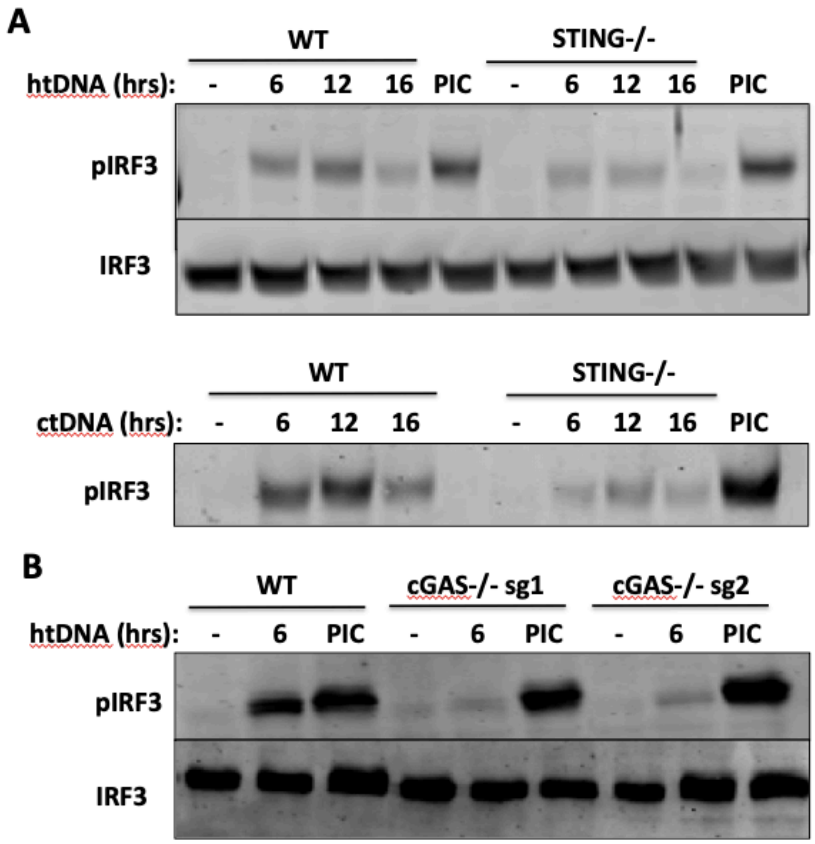

4.5 cGAS and STING are required for intracellular DNA-driven IRF3 phosphorylation in human fibroblast cells.
A) HFF WT and STING-/- cells were stimulated with 1 µg htDNA or ctDNA and harvested at 6, 12, 16 hours after transfection. B) HFF WT and cGAS-/- (sg1 and sg2 lines) were stimulated with 1 µg htDNA for 6 hours. Mock untransfected cells were used as a negative control and cells stimulated with Poly(I:C) were used as a positive control. Whole cell lysates were immunoblotted for phospho-IRF3 at serine 386 and total IRF3.

4.3 Functional characterisation of DNA-PKcs-/- cell lines

4.3.1 Intracellular DNA stimulation

The role of cGAS and STING in DNA sensing has been documented in the fibroblast cell system. In mouse embryonic fibroblasts STING has been shown to induce IFN-I response to ISD and HSV-1 DNA (Ishikawa *et al,* 2009). Furthermore, fibroblasts isolated from cGAS-/- mice failed to induce *IFNB* during HSV-1 infection (Li *et al,* 2013) and cGAS has been shown to cooperate with IFI16 in the generation of STING-mediated IFN-I immune response to plasmid DNA in human foreskin fibroblasts

(Orzalli *et al,* 2015). The cGAS/STING-TBK1-IRF3 axis that leads to the generation of type I IFN response to intracellular DNA is considered as the classical/canonical pathway in mammalian cells and our results confirm that this pathway is active in human foreskin fibroblasts. However, whether and how DNA-PKcs contributes to this signalling pathway in human fibroblasts is unknown. To investigate this, we performed several stimulation assays using HFF WT and DNA-PKcs-/- cells. Following stimulation with either htDNA or ctDNA, DNA-PKcs-/- cells were deficient in *IFNB* transcription. Similarly, cells that lack DNA-PKcs showed significant reduction in *CXCL10* mRNA transcription after stimulation with both types of DNA, compared to WT (Fig 4.6 A). This data was also reproduced at a later time point (16 hrs post stimulation) (Fig 4.6 B). In addition, in DNA-stimulated DNA-PKcs-/- cells we observed almost 90% reduction in the expression of interferon-stimulated gene 54 (*ISG54*), which is a direct target of IRF3 transcriptional activity (Fig. 4.6 C). In contrast, *NFKBIA* induced downstream of NF-κB signalling was not expressed in our system following DNA stimulation. Overall, this data indicate that human fibroblasts require DNA-PKcs to mount IFN-I response to intracellular DNA and this is predominantly dependent on IRF3 activation.

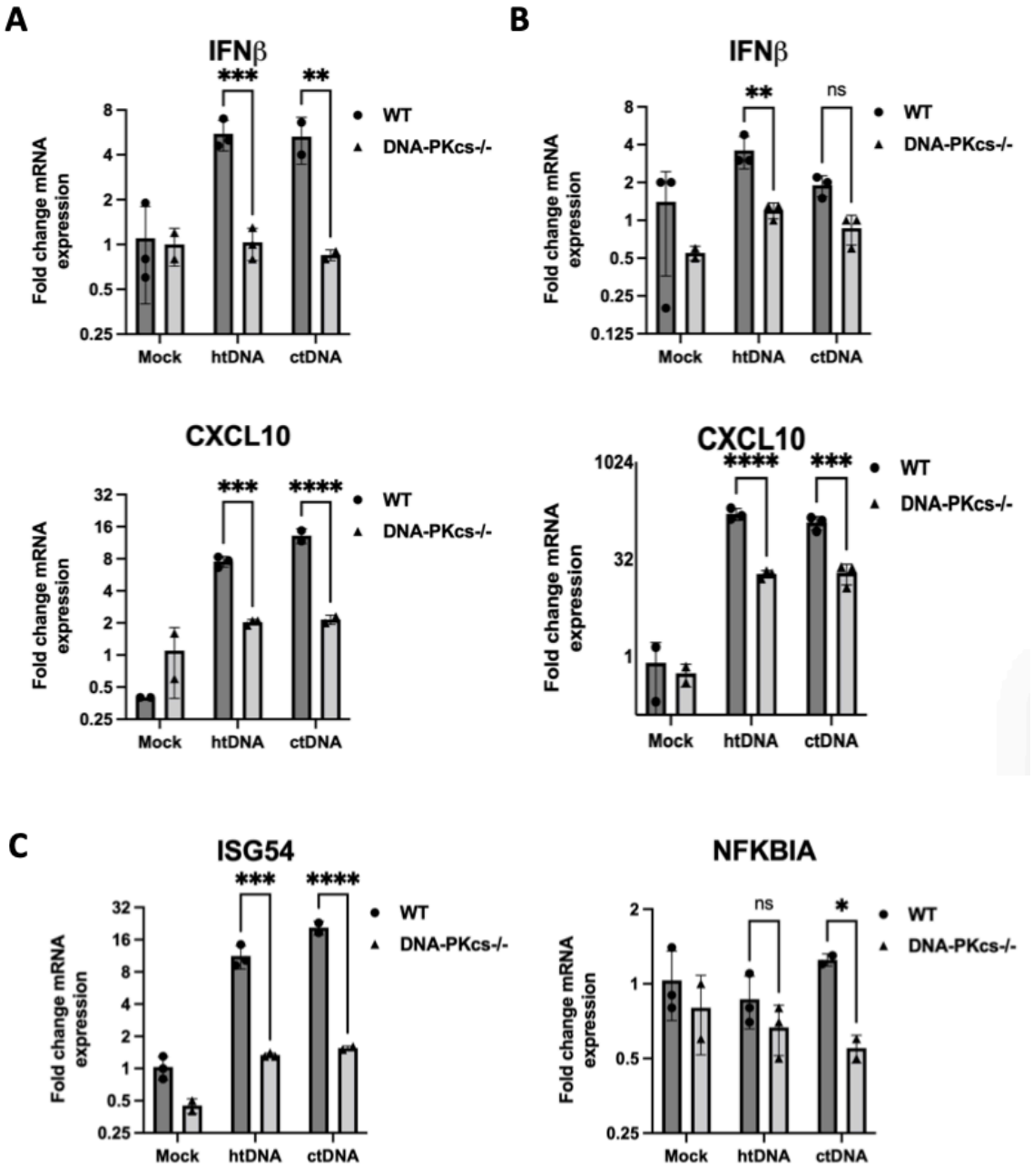

4.6 Human fibroblast cells deficient in DNA-PKcs are defective in mounting type I IFN response to DNA.

HFF WT and DNA-PKcs-/- sg1 cells were transfected with 1 μg htDNA or ctDNA in triplicate and mock untransfected cells were used as a negative control. At A, C) 6 hours or B) 16 hours after transfection, cells were harvested and analysed by RT-qPCR for IFNβ, CXCL10, ISG54 and NFKBIA. Data are presented as relative fold change in mRNA expression relative to mock untreated cells and normalised to PPIA/GAPDH housekeeping gene. Data are presented as mean +/- SD. Graphs are representative of three experimental repeats; Panel C was performed by Marisa Oliveira once. Statistical significance was calculated using ANOVA test; *P<0.05, **P<0.01, ***P<0.001, ****P<0.0001.

Next, we used phosphoblotting to understand the impact of DNA-PKcs on the intracellular signalling events that lead to the generation of the IFN-I immune response. We specifically assayed the phosphorylation of core DNA sensing components, STING and IRF3, upstream of IFN transcription. STING phosphorylation in response to ctDNA or htDNA transfection was clearly identified at all time-points tested in WT DNA-stimulated cells, but almost abrogated at early and late time points in DNA-PKcs-/- cells. These results were reproducible between both sg1 and sg2 KO cell populations (Fig 4.7). Densitometry analysis confirmed that p-STING levels were reduced by 90% in DNA-PKcs-/- cells at 6 hours post htDNA stimulation. Similarly, the phosphorylation of IRF3 on serine 386 was clearly observed in WT DNA-stimulated cells but strongly reduced in the DNA-treated DNA-PKcs-/- cells and a similar observation was made for the phosphorylation of TBK1 on serine 172 (Fig. 4.7 A). We also attempted to check for the phosphorylation of IRF3 on residue S396 (not shown), which gave data consistent with our observations of S386 phosphorylation in DNA-stimulated WT and KO cells. IRF3 S386 phosphorylation gave consistently better signal in our immunoblot assays, so we present only this one in our western blot results.

There was no STING phosphorylation in WT or KO cells transfected with Poly(I:C) as expected, and importantly no loss of pIRF3 signal in DNA-PKcs-/- cells following Poly(I:C) stimulation, indicating the specificity of DNA-PKcs function in the intracellular DNA sensing pathway. DNA-PKcs is therefore required for the activation of the STING-dependent DNA sensing pathway and acts upstream of STING.

Interestingly, we observed a non-specific band above total STING protein in WT stimulated cells (shown by yellow arrow), which might be attributed to the fact that the antibody picked up the phospho-STING signal, or it might be as a result of posttranslational modification of the protein following its activation, such as palmitoylation or ubiquitination.

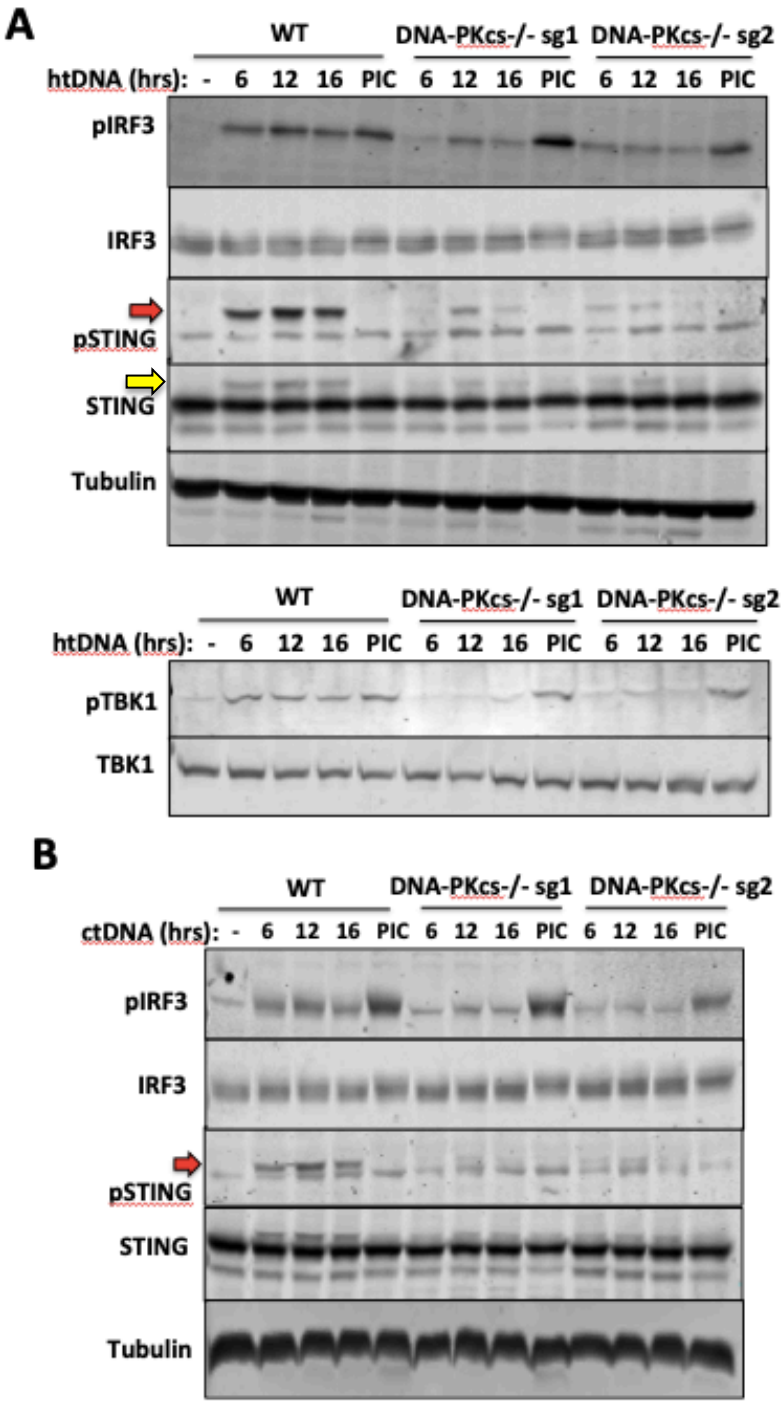

4.7 DNA-PKcs is required for the activation of the STING-dependent DNA sensing pathway to DNA in human fibroblasts.

HFF WT and DNA-PKcs-/- sg1, sg2 cells were stimulated with A) 1 μg htDNA or B) 1 μg ctDNA and harvested at 6, 12, 16 hours after transfection. Mock untransfected cells were used as a negative control and cells stimulated with Poly(I:C) were used as a positive control for IRF3 phosphorylation.

Whole cell lysates were immunoblotted for phospho-IRF3 at serine 386, total IRF3, phospho-STING at serine 366 (red arrow points to specific band) and total STING, phospho-TBK1 at serine 172 and total TBK1. Tubulin was used as a loading control. Data shown are representative (n=2+).

In case there was a dose-dependency of signalling through DNA-PKcs, we also tested a stimulation with a high dose (5 µg) of htDNA. This stimulation reproduced the same phenotype in the KO cell lines as with the lower DNA concentration (Fig. 4.8). In this instance, HFF cells deficient in DNA-PKcs failed to phosphorylate STING at all time points, confirming that the phenotype we see does not depend on the ligand dose.

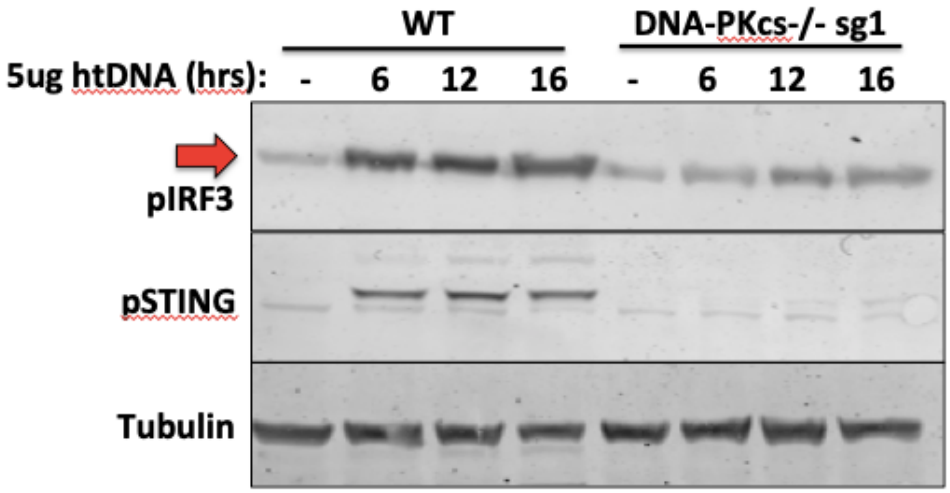

4.8 The role of DNA-PKcs in the DNA-mediated STING signaling pathway does not depend on the dose of DNA.
HFF WT and DNA-PKcs-/- sg1 cells were stimulated with 5 µg htDNA and harvested at 6, 12, 16 hours after transfection. Mock untransfected cells were used as a negative control. Whole cell lysates were immunoblotted for phospho-IRF3 at serine 386 and phospho-STING at serine 366 (red arrow points to specific band). Tubulin was used as a loading control. Data shown are representative (n=2).

Considering DNA-PKcs KOs mostly abrogated STING activation and that cGAS acts in this pathway (Fig 4.3 B), we set out to measure the effect of DNA-PKcs on cGAS activity. We attempted to quantify cGAMP concentrations in DNA-PKcs KO cells following DNA stimulation to understand whether DNA-PKcs and cGAS cooperate together to sense DNA and induce the production of IFN-I. cGAMP positive controls proved that the assay was technically working, but we were unable to detect any

measurable levels of cGAMP in the cell lysates, possibly due to the very low levels of cGAS expression in those cells (data not shown).

4.3.2 DNA virus infection

Having established that DNA-PKcs is required for sensing exogenous DNA in human fibroblasts, our next aim was to define its role in sensing DNA viruses. We infected wild type and sg1 and sg2 DNA-PKcs KO populations with HSV ΔICP0 or MVA at an MOI of 5 (Fig 4.9). Both KO lines were impaired in their ability to upregulate *IFNB* and *CXCL10* transcription during infection with the DNA viruses.

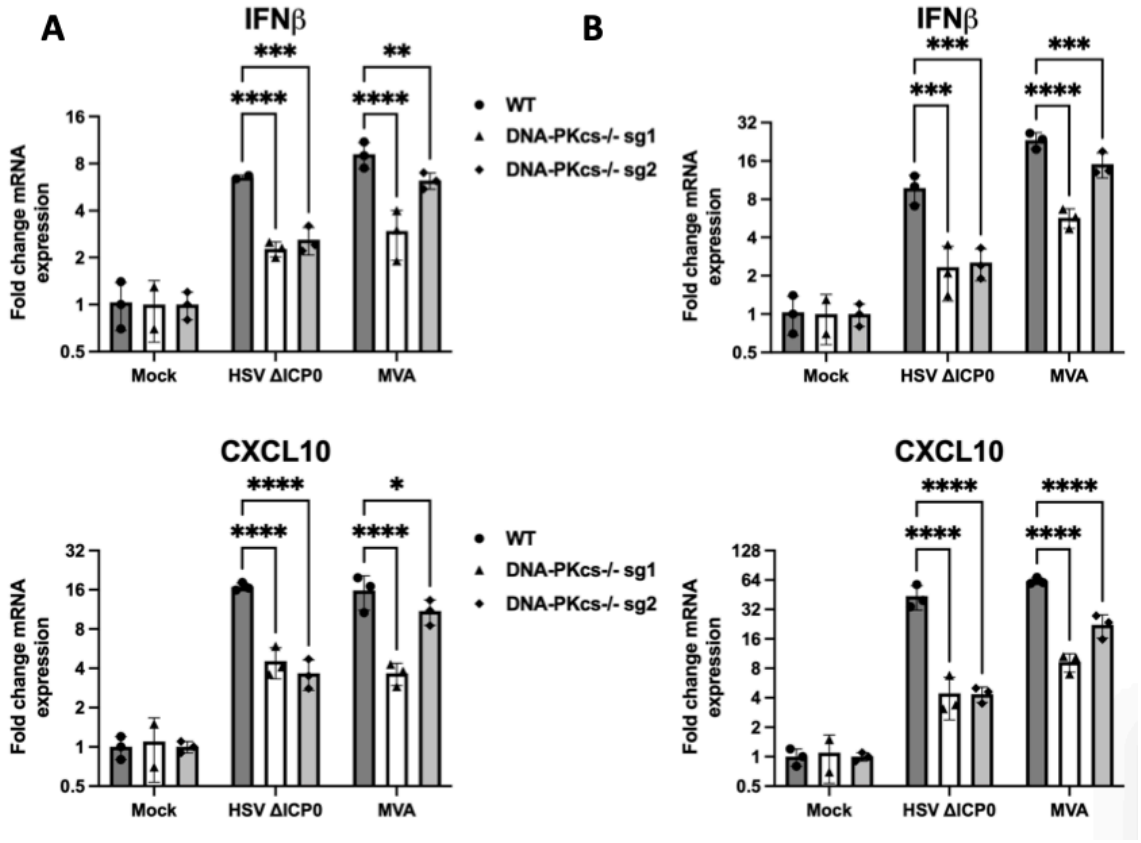

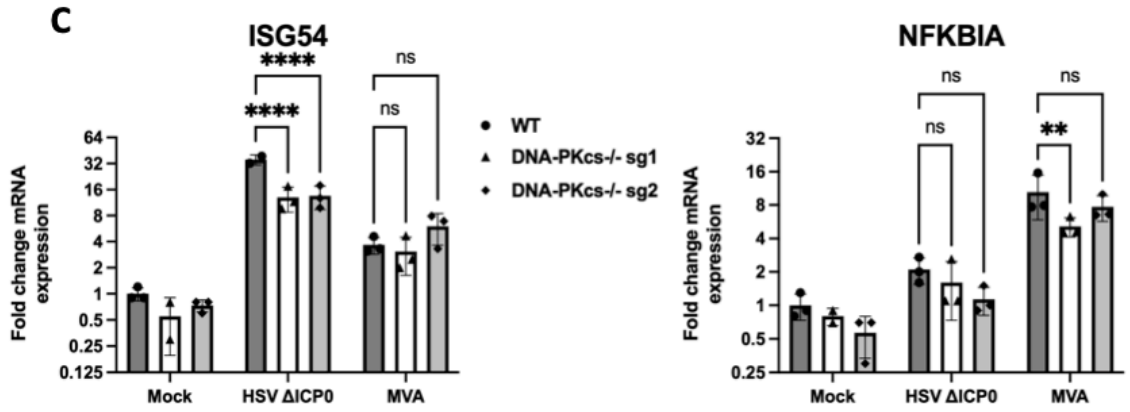

4.9 Human fibroblast cells deficient in DNA-PKcs are defective in mounting type I IFN response to DNA virus infection.

HFF WT and DNA-PKcs-/- sg1, sg2 cells were infected with HSV ΔICP0 or MVA at high MOI 5 in triplicate and mock uninfected cells were used as a negative control. At A) 6 hours or B) 16 hours after infection, RNA was extracted and analysed by RT-qPCR for A, B) IFNβ and CXCL10; C) ISG54 and NFKBIA. Data are presented as relative fold change in mRNA expression relative to mock untreated cells and normalised to GAPDH. Data are presented as mean +/- SD. Graphs are representative of two independent experiments; panel C was performed by Marisa Oliveira. Statistical significance was calculated using ANOVA test; *P<0.05, **P<0.01, ***P<0.001.

DNA-PKcs-/- cells demonstrated an impaired ability to upregulate *ISG54* in response to HSV infection while *NFKBIA* levels were unaffected, suggesting that the HSV-driven immune response in HFF cells is mainly dependent on IRF3 activity (Fig 4.9C). MVA induced expression of *NFKBIA* independently of DNA-PKcs, showing that the NF-κB pathway is active in HFFs and DNA-PK is not required for its activation by MVA infection.

We then analysed the activation of the intracellular DNA-driven signalling pathway during DNA virus infections in cells that lack DNA-PKcs. In these experiments, both HSV ΔICP0 and MVA infection at MOI 5 and 10 resulted in IRF3 and STING phosphorylation as early as 2-4 hours post infection. DNA-PKcs-/- cells, however, showed little or no STING phosporylation and displayed reduced phosphorylation of IRF3 at all time points and with both MOIs (Fig 4.10 A, B). This data illustrates that DNA-PKcs is required for the STING-dependent innate immune response to DNA virus infection in human fibroblast cells.

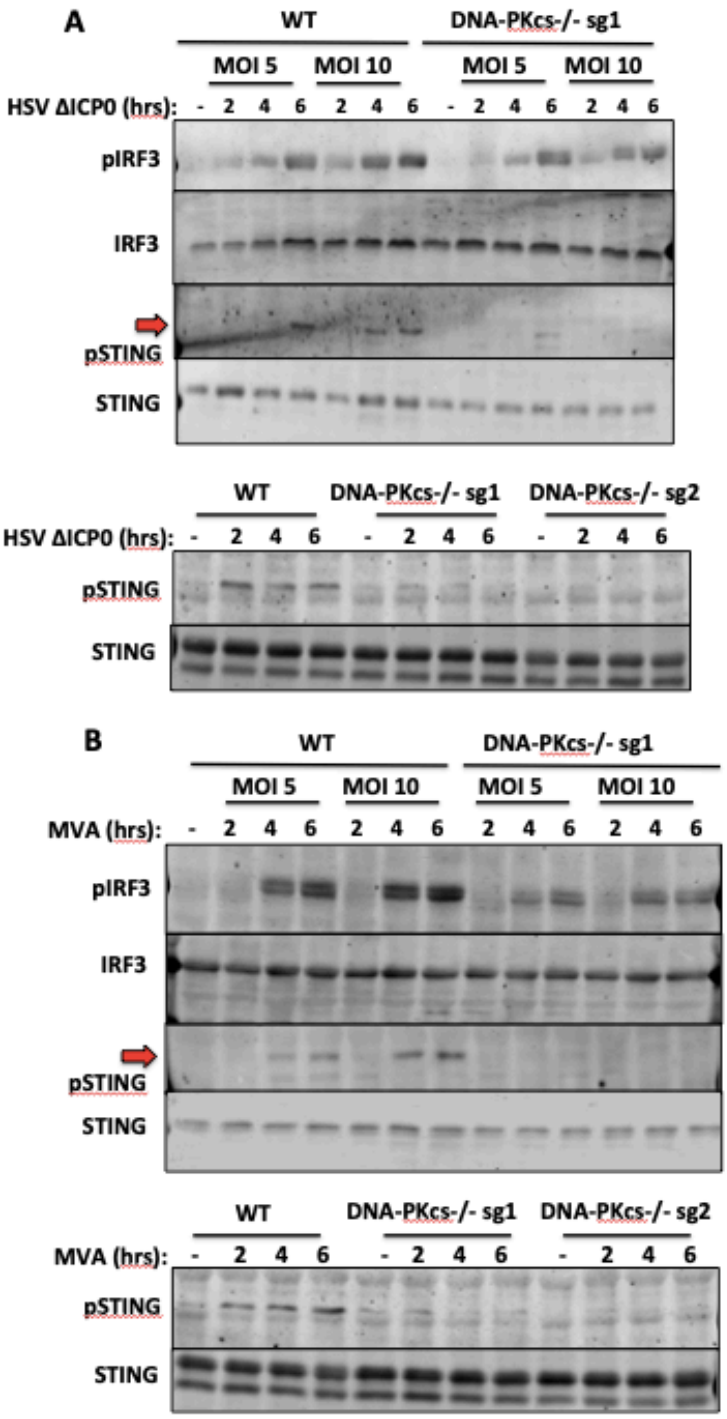

4.10 DNA-PKcs is required for the activation of the STING-dependent DNA sensing pathway to DNA virus infection in human fibroblast cells.

A, B top panels) HFF WT and DNA-PKcs-/- sg1 cells were infected with HSV ΔICP0 or MVA at MOI 5, MOI 10; A, B bottom panels) WT and DNA-PKcs-/- sg1, sg2 cells were infected with HSV ΔICP0 or MVA at MOI 5 and harvested at 2, 4, 6 hours after infection. Mock uninfected cells were used as a negative control. Whole cell lysates were immunoblotted for phospho-IRF3 at serine 386, total IRF3, phospho-STING at serine 366 (red arrow points to specific band in A) and total STING. Data shown are representative (n=2).

4.4 Functional characterisation of DNA-PKcs mutant primary fibroblasts

Although the data generated in DNA-PKcs-/- HFFs was clear, we aimed to investigate the same question with a second model system. For this we used a physiologically similar model; primary human skin fibroblasts isolated from the skin of healthy donors (control fibroblasts) or from patients that harbor a missense L3062R mutation in the *PRKDC* gene (L3062R fibroblasts). L3062 is located in the FAT domain of the protein close to the kinase domain. Patients with this mutation develop a SCID phenotype due to impaired V(D)J recombination, and the mutation causes defective recruitment of Artemis to sites of DNA damage (van der Burg *et al.*, 2009). However, it is not clear whether this mutation can affect the role of DNA-PKcs in DNA sensing and anti-viral immunity.

4.4.1 Primary fibroblasts harbouring a mutation in DNA-PKcs show enhanced immune signalling to intracellular DNA

DNA-PKcs mutant L3062R fibroblasts do not have a defect in DNA-PKcs expression and, similar to control fibroblasts, express the protein mainly in the nucleus (Fig. 4.11 A). We set out to perform a functional characterisation of the immune signalling response to DNA in these cells. When we looked into the upstream phosphorylation events in response to DNA, the phenotype in the mutant cells was different from what we observed with the KO cell lines. DNA-stimulated L3062R mutant fibroblasts demonstrated increased phosphorylation of TBK1, IRF3 and STING at early and late time points compared to control fibroblasts that showed lower levels of phosphorylation in response to DNA (Fig. 4.11 B, D). Furthermore, densitometry analysis showed that p-STING levels were increased by 50% in L3062R cells at 6 hours post htDNA stimulation. Importantly, in Fig. 4.11 D, the phosphorylation levels of pTBK1 during Poly(I:C) treatment were not different between mutant and control cells, indicating that the elevated phosphorylation events in L3062R compared to control fibroblasts were specific to DNA stimulation.

Enhanced phosphorylation of IRF3 was also observed during HSV ΔICP0 infection (Fig. 4.11 C) demonstrating an enhanced immune response to DNA virus in the mutant cells. Densitometry analysis showed that p-IRF3 levels were increased by 30% in L3062R cells at 6 hours post HSV infection.

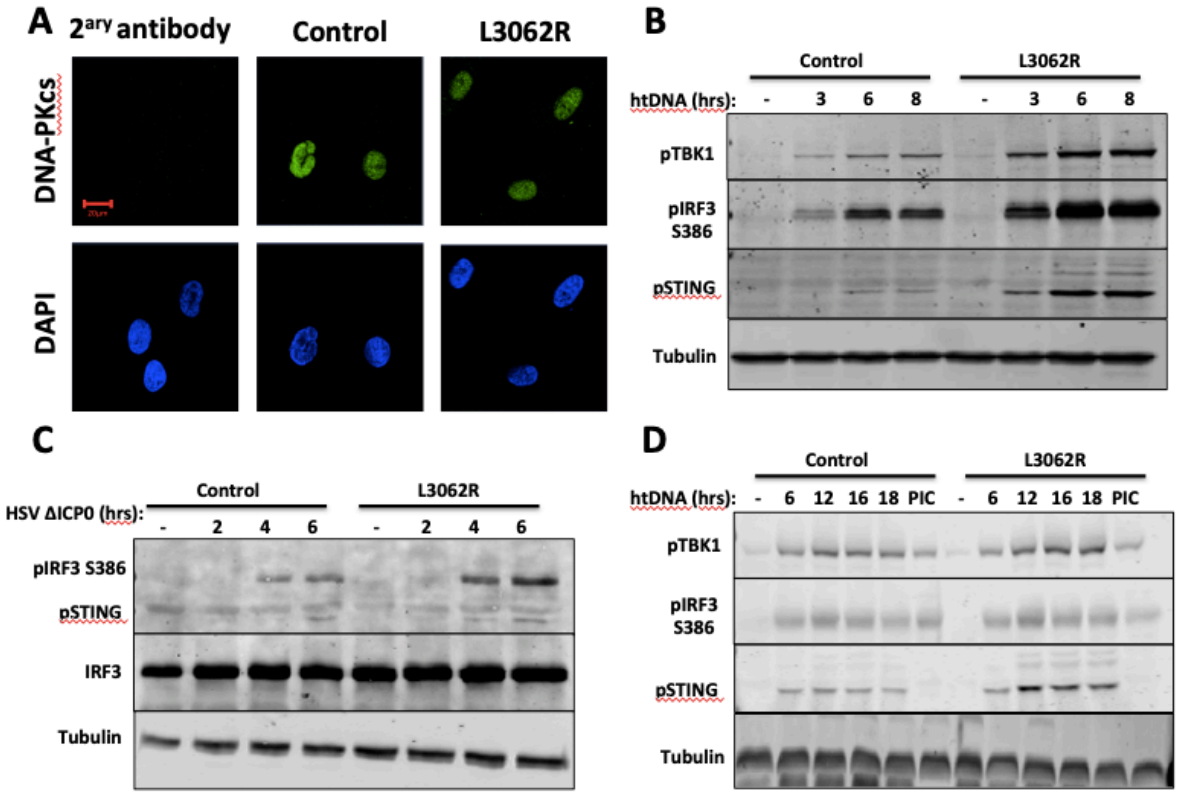

4.11 Human primary fibroblasts harbouring a mutation in DNA-PKcs show an enhanced STING signalling to DNA and DNA virus infection.

A) Healthy control and L3062R mutant primary fibroblast cells were immunostained for DNA-PKcs and counterstained with DAPI. Secondary antibody only was used as a positive control. Scale bars: 20 μm. B) Control and L3062R primary fibroblast cells were stimulated with 1 μg of htDNA and harvested at B) 3, 6, 8 hours and D) 6, 12, 16, 18 hours. C) Healthy control and L3062R mutant primary fibroblast cells were infected with HSV ΔICP0 MOI 5 and harvested at 2, 4, 6 hours after infection. Mock unstimulated/uninfected cells were used as a negative control and in D) Poly(I:C) was used as a positive control for IRF3 phosphorylation. Whole cell lysates were immunoblotted for phospho-TBK1 at serine 172, phospho-IRF3 at serine 386, phospho-STING at serine 366. Tubulin was used as a loading control. Data shown are representative (n=2).

4.4.2 Primary fibroblasts harbouring a mutation in DNA-PKcs have an increased transcriptional response to intracellular DNA

Preliminary data looking at the transcriptional output from immune signalling to DNA in mutant fibroblasts validated our observations that L3062R cells are more sensitive to DNA stimulation or virus infection and generate a stronger immune response compared to wild type cells. Mutant fibroblasts showed significantly higher levels of *IFNB* and *CXCL10* transcription after DNA stimulation and HSV DNA virus infection compared to the healthy control cells (Fig. 4.12 A, B). Interestingly, we observed that the resting mutant cells displayed around 22-fold upregulation in *CXCL10* levels without any treatment suggesting that these cells already have an active immune signalling pathway and produce a boosted response after stimulation.

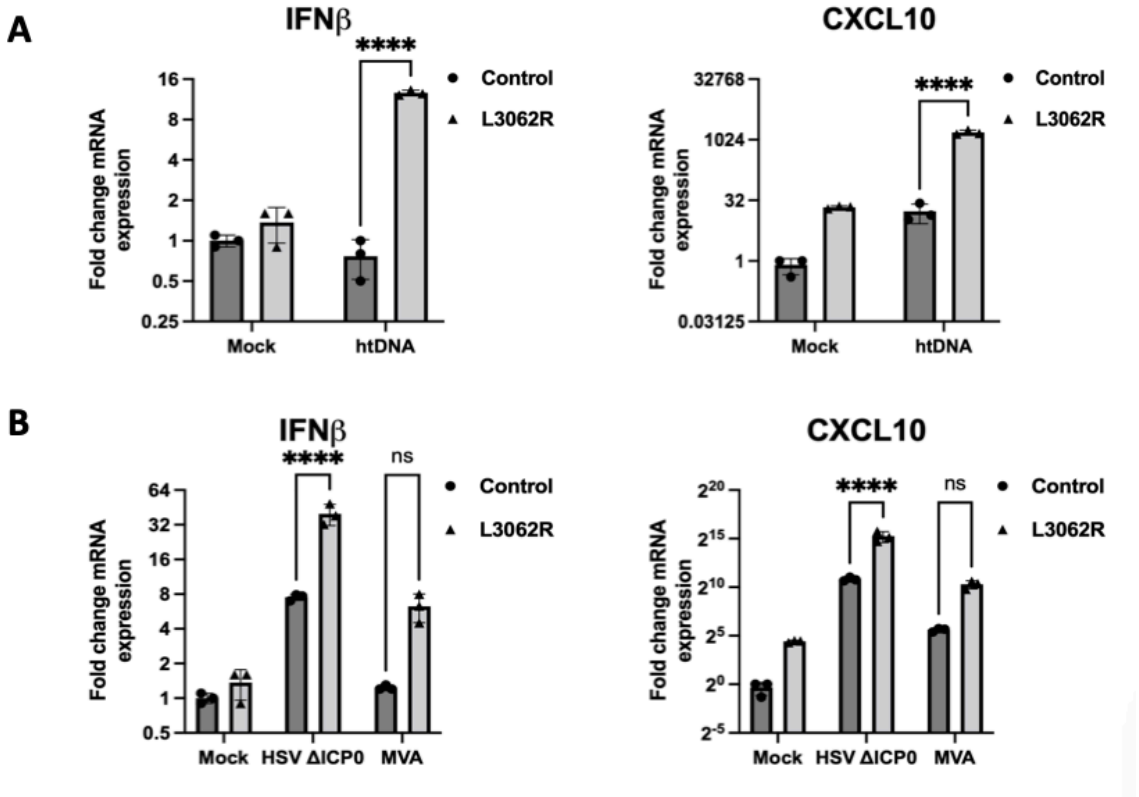

4.12 Primary fibroblasts harbouring a mutation in DNA-PKcs have an increased immune transcriptional response to DNA
A) Control and mutant primary cells were stimulated with 1 µg htDNA or B) infected with HSV ΔICP0 or MVA at MOI 5 in triplicate and mock unstimulated/uninfected cells were used as a negative control. At 6 hours hours after infection, RNA was extracted and analysed by RT-qPCR for IFNβ and CXCL10. Data are presented as relative fold change in mRNA expression relative to mock untreated cells and normalised to GAPDH. Data are presented as mean +/- SD. The experiment was performed once. Statistical significance was calculated using ANOVA test; *P<0.05, **P<0.01, ***P<0.001.

4.4.3 Primary fibroblasts harbouring a mutation in DNA-PKcs show a defective CXCL10 protein secretion in response to DNA

We also analysed secretion of CXCL10, which is a late event downstream of transcription. In contrast to our findings in the previous section, L3062R mutant fibroblasts were found to secrete less CXCL10 protein than wild type control cells after DNA stimulation or virus infection (Fig. 4.13 A, B). An ELISA assay showed that DNA-PKcs mutant cells had an impaired ability to secrete CXCL10 chemokine after 12 and 24 hours of stimulation with htDNA and ctDNA stimulation or infection with HSV ΔICP0.

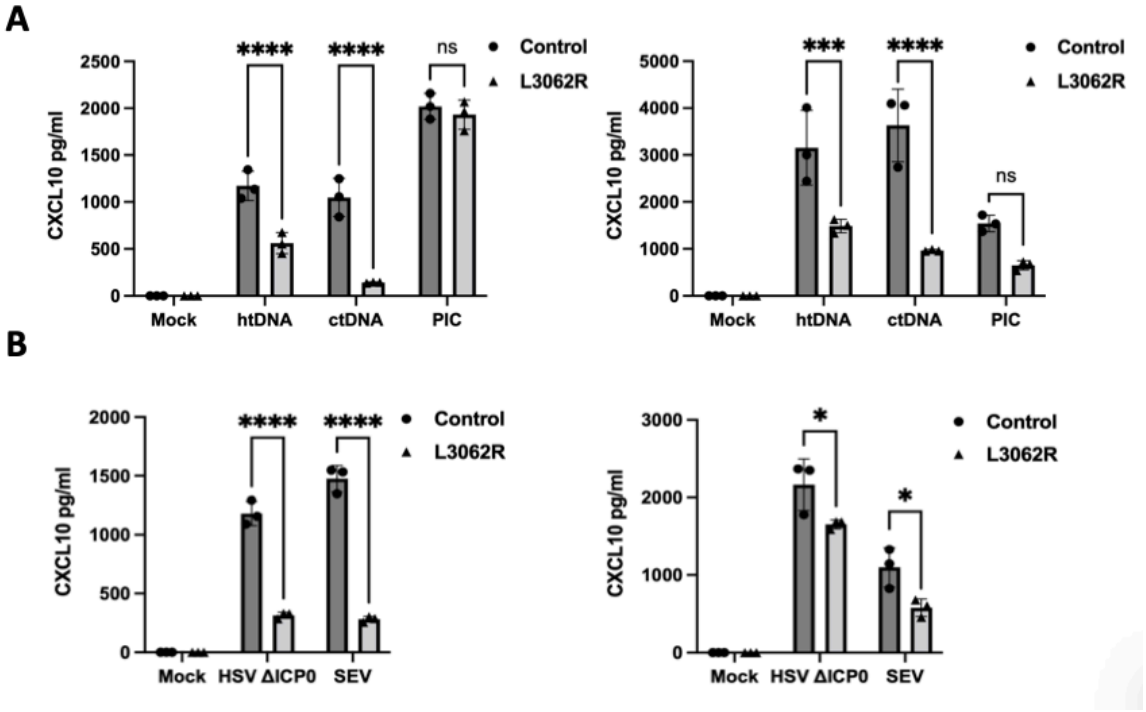

4.13 Human primary fibroblasts harbouring a mutation in DNA-PKcs show a defective CXCL10 immune response to DNA and DNA virus infection.
A) Healthy control and mutant L3062R primary skin fibroblasts were stimulated with 2 µg of htDNA and ctDNA or B) infected with HSV ΔICP0 at MOI 5 for 24 hours (left side) and 12 hours (right side)

in triplicate. 0.5 μg Poly(I:C) and SeV (1:300 DF) were used as a positive control and mock unstimulated/uninfected cells were used as a negative control. Cell supernatant was harvested at the indicated time points and analysed for the concentration of secreted CXCL10 by an ELISA assay. Data are presented as mean +/- SD. Graphs are representative of 2 experiments. Statistical significance was calculated using ANOVA test; *P<0.05, **P<0.01, ***P<0.001, ****P<0.0001.

Taken together, the primary cell characterisation data suggests that L3062R mutation in the *PRKDC* gene exerts a gain-of-function effect on the intracellular DNA sensing pathway. The primary cell data does not recapitulate the conclusions of cultured cells, which could be attributed not only to the difference in the nature of the DNA-PKcs mutation, but also to the origin of the cells. Primary fibroblasts were isolated from the arm skin of teenagers, while HFF cells are foreskin adult fibroblasts. In addition to this, we observed basal differences in CXCL10 transcription between healthy and mutant primary fibroblasts, which could be the result of donor-to-donor variation. Further assays with multiple individuals would need to be performed to assess how abnormal the variation of transcription is. However, L3062R mutant fibroblasts appear to have an overactivated innate immunity, which is consistent with previous observations. Patients with missense *PRKDC* mutations have been reported to develop autoimmune diseases (Esenboga *et al.*, 2018). A recent study revealed that whole-blood cells from patients with the mutation had elevated levels of ISGs and that HSV-1 infection of fibroblasts isolated from these patients produced much higher amounts of *IFNB*, *CXCL10* and *ISG54* compared to control cells (Sun *et al*, 2020). Although the CXCL10 ELISA data is unclear, the signalling data indicate that DNA-PKcs L3062R is a gain-of-function mutation in the STING-dependent DNA sensing pathway, whilst being a loss-of-function allele in the context of self-DNA repair and V(D)J recombination. Further analysis of this mutation to both processes will help to uncover how DNA-PKcs functions in self-DNA repair and STING-dependent innate immunity.

Summary

To summarise, our data illustrates that DNA-PKcs is required for the activation of the STING/IRF3-dependent innate immune response to exogenous cytosolic DNA and DNA virus in human fibroblast cells, consistent with findings in murine fibroblasts (Ferguson *et al,* 2012). The phenotype we observe does not depend on the concentration of DNA and is consistent at early and late time points after stimulation or infection, contrary to a recent report outlining 2 waves of DNA-driven immune gene transcription in human monocytes (Burleigh *et al,* 2020). Furthermore, we show that the DNA sensor cGAS acts in the pathway and contributes to the DNA-driven type I IFN production, which is consistent with other findings in literature demonstrating cooperation between DNA-PKcs and cGAS in human cells (Morchikh *et al*, 2017; Sun *et al*, 2020). A pertinent question remaining in the field is whether the kinase activity of the DNA-PKcs protein is necessary for DNA sensing. We sought to understand this using a pharmacological approach, which will be discussed in the next chapter.

CHAPTER 5

5. The role of DNA-PKcs kinase activity in DNA sensing in human fibroblasts

We have shown that DNA-PKcs is required for the intracellular DNA-mediated immune response in human fibroblasts. Since the DNA-PKcs protein has both DNA-binding and kinase activities, either or both of these might be required for its function in anti-viral immunity. Our CRISPR/Cas9 gene editing approach lead to reduction of DNA-PKcs protein, so we could not use these cell lines to distinguish between the two possibilities. As such, we next set out to use pharmacological inhibition to understand whether the catalytic kinase activity of the protein is required for the function of DNA-PKcs in DNA sensing. In murine fibroblasts, Ferguson *et al* reported that the enzymatic activity was not necessary for the generation of the IRF3-dependent immune response to DNA (Ferguson *et al,* 2012). In that study, the small molecule inhibitor, NU7026 was used to block the kinase function of DNA-PKcs. This inhibitor however demonstrated poorer selectivity for DNA-PKcs over other PIKK enzymes (Leahy *et al.*, 2004). In order to gain more insights into what happens in human cells, we tested two inhibitors (NU7441 and AZD7648) proven to selectively and potently block DNA-PKcs kinase activity. Recent reports using the NU7441 inhibitor have shown that the kinase activity of the protein is essential for generating a productive immune response to intracellular DNA. Burleigh *et al* showed that DNA-PKcs phosphorylates downstream targets such as HSPA8 to mediate the immune response to DNA in STING-independent manner (Burleigh *et al*, 2020). On the other hand, Sun et al proposed in their study that DNA-PKcs phosphorylates and inhibits the enzymatic activity of cGAS and as such, prevents the activation of the cGAS/STING-dependent antiviral immune response (Sun *et al*, 2020). In this chapter, we will discuss our findings on the inhibition of DNA-PKcs kinase activity during DNA sensing in HFF cells.

5.1 Generating tools for DNA-PKcs kinase inhibition

We took a pharmacological approach using small molecule kinase inhibitors in order to identify whether the catalytic activity of DNA-PKcs is important for the innate immune response to DNA. For this we used the DNA-PKcs kinase inhibitor NU7441 that is a highly potent inhibitor of DNA-PKcs with reported specificity over other PIKK family enzymes (Leahy *et al,* 2004). First we tested the efficacy of the NU7441 inhibitor in our HFFs by treating them with etoposide, a DNA damage-inducing agent that inhibits the activity of topoisomerase II and induces double-stranded DNA breaks (Fig 5.1 A). Free double-stranded DNA ends are recognised by the DNA-PK complex and DNA-PKcs becomes activated and autophosphorylates itself, as well as phosphorylates multiple downstream targets including p53 and the histone H2AX (Durocher and Jackson, 2001; Kinner *et al.*, 2008). Following etoposide treatment, we could detect phosphorylated H2AX in nuclear foci by immunofluorescence (Fig 5.1 B). However, in the presence of the kinase inhibitor this signal was strongly diminished, indicating that NU7441 can potently block the enzymatic activity of DNA-PKcs.

DNA-PKcs is rapidly activated following DNA stimulation, which results in autophosphorylation of the protein as detected by an antibody that recognises phospho-S2056 (Fig. 3.7). We analysed the impact of kinase inhibition on DNA-PKcs autophosphorylation after DNA stimulation and found that cells treated with DNA and NU7441 showed strong reduction in DNA-PKcs autophosphorylation (red fluorescent signal) compared to DNA treatment alone (Fig. 5.1 C). This data indicates that NU7441 can inhibit DNA-PKcs autophosphorylation and phosphorylation of downstream targets in the presence of exogenous DNA or following DNA damage.

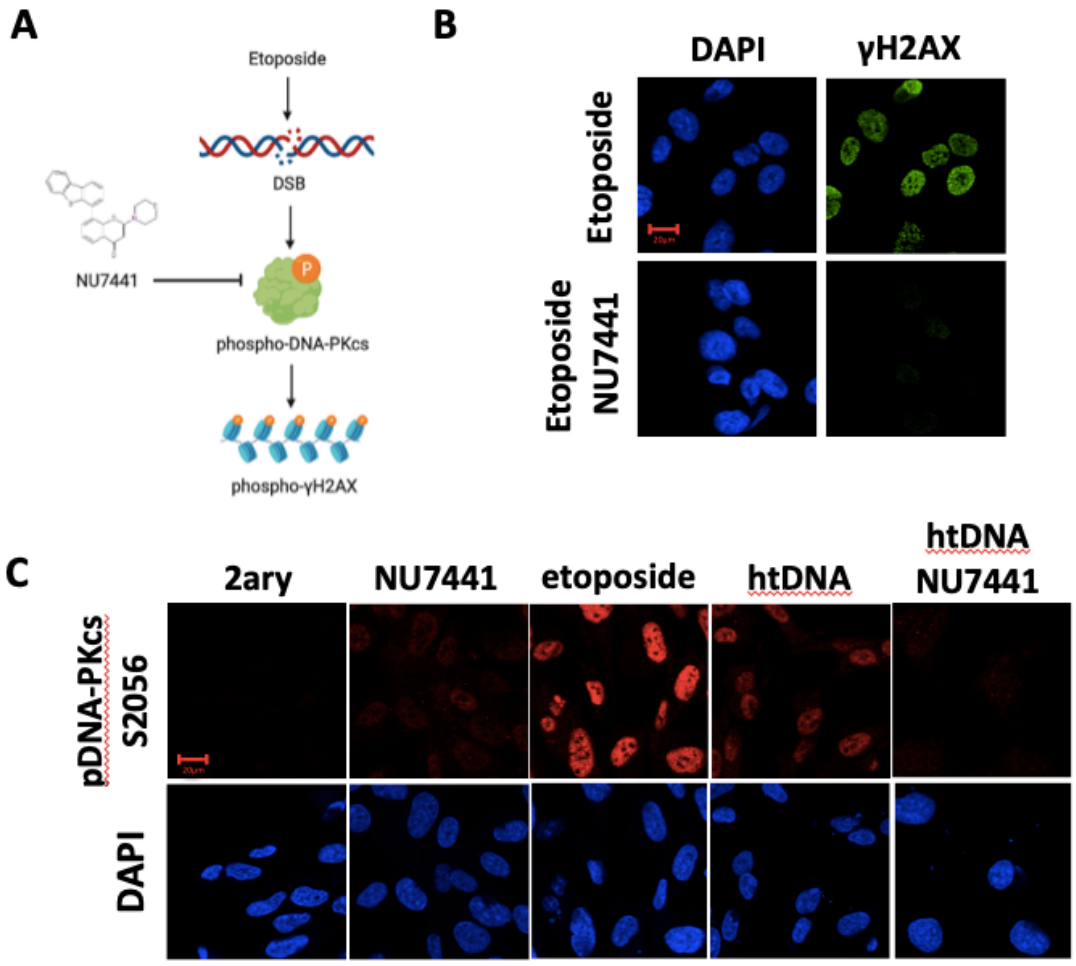

5.1 NU7441 inhibitor can block the kinase activity of DNA-PKcs.
A) A schematic illustrating the activation of the DNA-PKcs kinase activity and its inhibition by NU7441. Etoposide induces double-stranded breaks in the DNA and as a result, DNA-PKcs autophosphorylates and phosphorylates downstream target proteins such as the histone H2AX. NU7441 blocks the catalytic function of DNA-PKcs. B) HFF WT cells were pre-treated for one hour with 3 μM of NU7441. Then 30 μM of etoposide was added to the cells for 2 hours or C) cells were stimulated with 1 μg htDNA for 2 hours in the presence or absence of 3 μM NU7441. Cells were fixed and immunostained for the presence of B) phosphorylated H2AX, γH2AX (in green), C) phosphorylated DNA-PKcs at serine 2056 (in red). DAPI stained the nuclei in blue. Secondary antibody was used as a negative control. Scale bars: 20 μm. The data are representative (n=2). Panel B) was performed by Dr Brian Ferguson.

5.2 NU7441 enhances DNA-mediated immune signalling

To analyse the effect of Nu7441 on signalling downstream of intracellular DNA sensing, HFF cells were treated with 3 μM of inhibitor and transfected with DNA or

Poly(I:C). This treatment exhibited increased and prolonged TBK1, IRF3 and STING activation after stimulation with 1 μg of htDNA (increase by 60% in p-TBK1 levels at 8 hours) or ctDNA (increase by 96% in p-TBK1 levels at 8 hours) (Fig. 5.2 A, B). Signals were increased during inhibitor treatment as early as 6 hours and sustained the stronger signal until 12 and 16 hours compared to cells treated with DNA alone, whose signal peaked at around 8 hours.

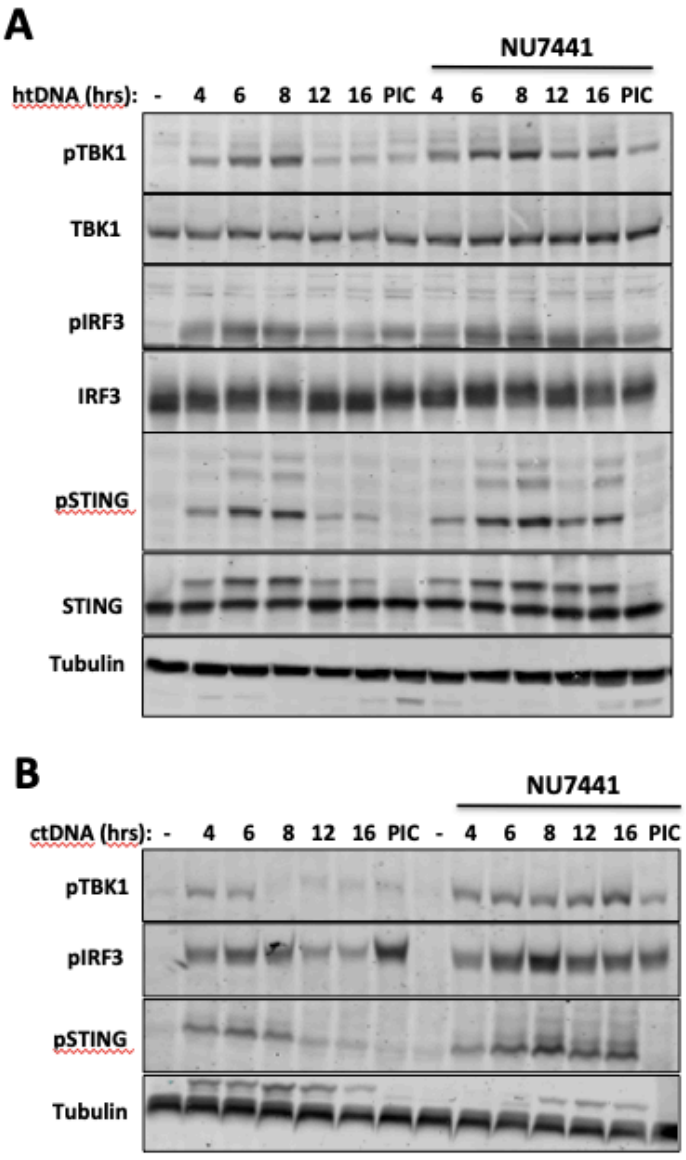

5.2 NU7441 enhances DNA-mediated immune signalling.
WT HFF cells were stimulated with 1 μg A) htDNA or B) ctDNA for 4, 6, 8, 12 hours in the presence or absence of 1 hour pre-treatment with 3 μM NU7441. Mock unstimulated cells were used as a negative control and Poly(I:C)-treated fibroblast cells were used as a positive control. Whole cell lysates were immunoblotted for phosphorylated TBK1 at serine 172 and total TBK1, phosphorylated

IRF3 at serine 386 and total IRF3, phosphorylated STING at serine 366 and total STING. Tubulin was used as a loading control. Data shown are representative of >2 experiments.

5.3 The effect of NU7441 on STING activation is DNA dose-dependent

Having identified that NU7441 enhanced the DNA-mediated immune signalling, we wanted to characterise further this effect with different DNA doses. HFF WT cells were transfected with increasing doses of htDNA or ctDNA with or without NU7441 treatment and harvested at 6 hours. In these experiments the phosphorylation of TBK1 was increased in all conditions in the presence of inhibitor. On the other hand, phospho-STING and phospho-IRF3 signals were higher in the presence of NU7441 at the lowest dose of DNA (1μg), but reduced compared to WT cells transfected with higher doses of DNA (5μg, 8μg and 10μg) (Fig. 5.3 A). We delved further into this and performed a direct comparison of cells stimulated with high (5μg) and low (1μg) dose of htDNA or ctDNA in the presence or absence of NU7441 and harvested the cells at different time points. The same outcome was observed where the phosphorylation signals for STING and IRF3 were almost absent in inhibitor-treated cells exposed to high dose of DNA at 6 and 8 hours. Interestingly, this effect appeared to be mostly specific to the DNA-driven immune response as any differences in the phosphorylation signals after stimulation with transfected Poly(I:C) were not as pronounced (Fig. 5.3 B).

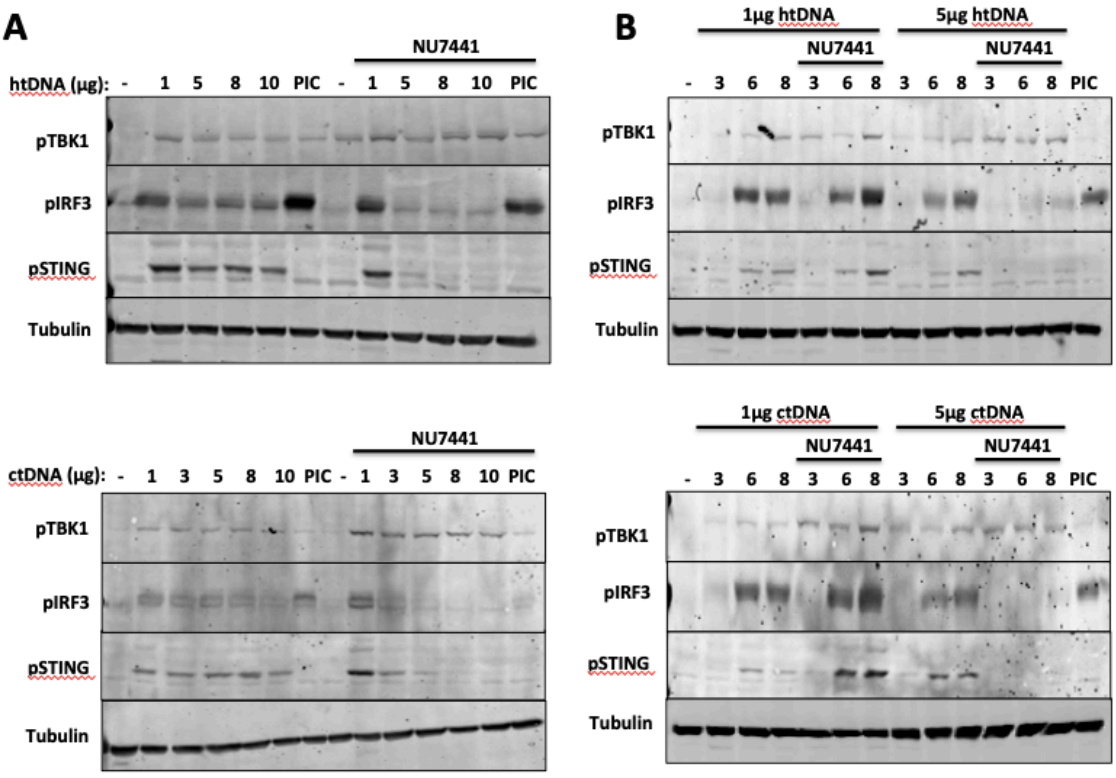

5.3 The effect of NU7441 on STING activation depends on the dose of DNA.
A) HFF WT cells were stimulated with 1 µg, 5 µg, 8 µg, 10 µg htDNA or 1 µg, 3 µg, 5 µg, 8 µg, 10 µg ctDNA for 8 hours in the presence or absence of 1 hour pre-treatment with 3 µM NU7441 kinase inhibitor. B) HFF WT cells were stimulated with 1 µg and 5 µg htDNA or ctDNA for 3, 6 and 8 hours in the presence or absence of 1 hour pre-treatment with 3 µM NU7441 kinase inhibitor. Mock unstimulated cells were used as a negative control and Poly(I:C)-treated fibroblast cells were used as a positive control. Whole cell lysates were immunoblotted for phosphorylated TBK1 on serine 172, phosphorylated IRF3 on serine 386 and phosphorylated STING on serine 366. Tubulin was used as a loading control.

5.4 Impact of NU7441 on the anti-viral response to DNA virus infection

In addition to the observed NU7441 phenotype during transfection of exogenous DNAs, we wanted to investigate the outcome during DNA virus infection in HFF cells. We pre-treated cells with increasing concentrations of the DNA-PKcs kinase inhibitor before infecting the cells with HSV-1 ΔICP0 or MVA viruses for 8 hours (Fig. 5.4). SeV was used as a positive control to activate IRF3. The effect of the

inhibitor was comparable with what was observed when cells were transfected with low doses of DNA. The phosphorylation of TBK1 and IRF3 were elevated with the varying concentrations of the small molecule drug compared to a virus infection alone. STING activation was not affected by the presence of Nu7441. Similar to what we showed in Fig. 3.10 B, a non-specific band was observed above the phosphorylated IRF3 signal in all MVA-infected samples and in SeV-infected fibroblasts cells without the presence of NU7441.

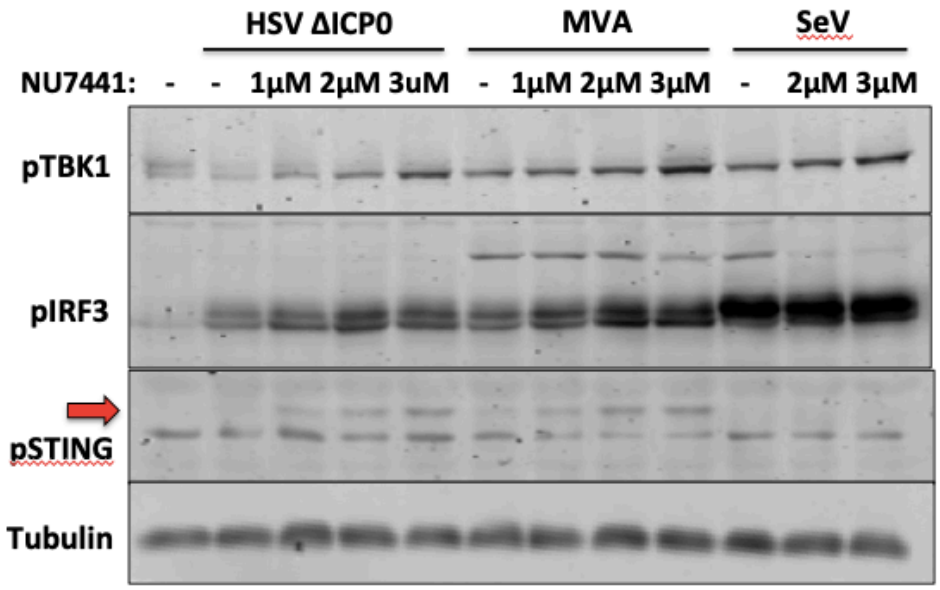

5.4 NU7441 enhances the immune signalling response to DNA virus infection.
HFF-Tert WT cells were infected with HSV ΔICP0 and MVA at MOI 5 for 8 hours in the presence or absence of one hour pre-treatment with NU7441 inhibitor (1 μM, 2 μM or 3 μM). Mock uninfected cells were used as a negative control and cells infected with SeV (1:300 DF) in the presence or absence of NU7441 (2 μM and 3 μM) were used as a positive control. Whole cell lysates were immunoblotted for phosphorylated TBK1 on serine 172, phosphorylated IRF3 on serine 386 and phosphorylated STING on serine 366 (specific band shown by red arrow). Tubulin was used as a loading control. Data shown are representative (n= 3).

Next we tested whether the MOI of the viruses made a difference in the outcome when the kinase activity of DNA-PKcs is blocked, as we had seen previously with higher doses of DNA. We infected HFF WT cells with virus at MOI 5 and MOI 10, and harvested the cells at 4-12 hours later (Fig. 5.5). In this experiment the MOI of infection did not alter the phenotypic outcome of intracellular signalling. Consistent with data in Fig 5.4, phosphorylation of TBK1 on serine 172 was increased when the

inhibitor was applied to HSV ΔICP0- or MVA-infected fibroblasts. In addition to this, the non-specific band above phospho-IRF3 (shown by red arrow) was apparent again during MVA virus infection (Fig. 5.5 B). The infection set of data confirms the enhancement of TBK1/IRF3 activation in the presence of NU7441.

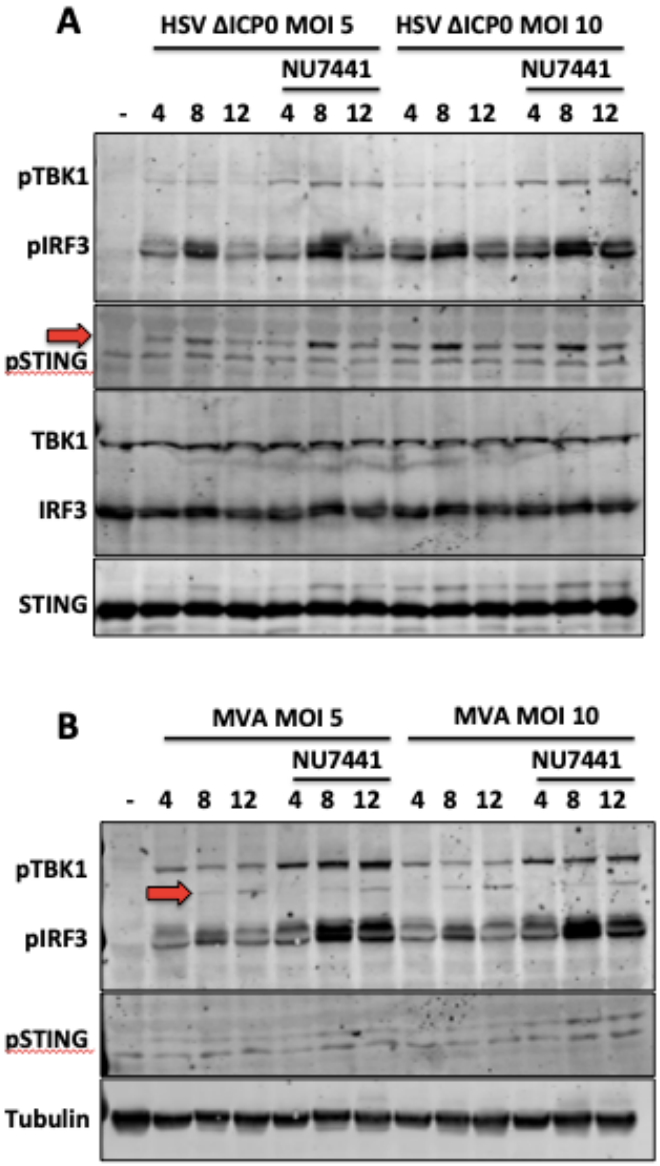

5.5 NU7441 enhancement effect on the immune signalling response to DNA virus infection does not depend on the amount of virus.
HFF WT cells were infected with A) HSV ΔICP0 and B) MVA at MOI 5 and MOI 10 for 4, 8, 12 hours in the presence or absence of one hour pre-treatment with 3 μM NU7441. Mock uninfected cells were used as a negative control. Whole cell lysates were immunoblotted for phosphorylated TBK1 on serine 172 and total TBK1, phosphorylated IRF3 on serine 386 and total IRF3, phosphorylated STING

on serine 366 (specific band shown by red arrow) and total STING. Tubulin was used as a loading control. Data shown are representative (n= 2).

5.5 NU7441 enhances the DNA-mediated TBK1 signalling in primary fibroblast cells

Finally, we obtained preliminary data from a second cell model, primary fibroblasts isolated from the skin of healthy donors. Primary cells stimulated with low and high dose of DNA gave similar results to immortalised fibroblasts. pTBK1 was increased in cells treated with Nu7441 and stimulated with 1 or 5 ug DNA, although pIRF3 on serine 386, was not affected (Figure 5.6).

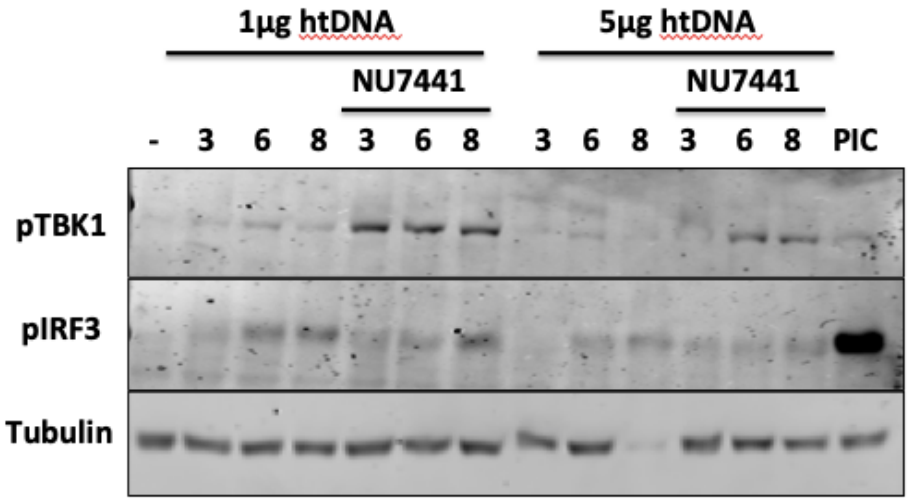

5.6 NU7441 enhances the DNA-mediated TBK1 signalling in primary fibroblast cells.
Primary skin fibroblast cells were stimulated with 1 µg and 5 µg htDNA for 3, 6 and 8 hours in the presence or absence of 1 hour pre-treatment with 3 µM NU7441 kinase inhibitor. Mock unstimulated cells were used as a negative control and Poly(I:C)-treated fibroblast cells were used as a positive control. Whole cell lysates were immunoblotted for phosphorylated TBK1 on serine 172 and phosphorylated IRF3 on serine 386. Tubulin was used as a loading control. This experiment was performed only once.

5.6 NU7441 has an off-target effect on the DNA sensing pathway that activates TBK1

Given the inconsistent data from Nu7441, we explored the possibility that Nu7441 has off-target effects. As already described above, we observed increased TBK1 activation during DNA stimulation (Fig 5.7 A). To understand if the Nu7441-dependent enhancement of TBK1 activation was dependent on its interaction with DNA-PKcs, we used HFF DNA-PKcs-/- cells as a comparison in the same experimental setup. Surprisingly, there was increased TBK1 phosphorylation in DNA-PKcs-/- cells treated with the DNA-PKcs kinase inhibitor (Fig 5.7 A). Furthermore, we applied increasing concentrations of NU7441 on unstimulated cells or cells stimulated with two doses of htDNA or Poly(I:C). Consistent with the previous data, elevated phospho-TBK1 signal is observed when cells were treated with any of the inhibitor concentrations during DNA stimulation (Fig. 5.7 C). This result was not observed with the Poly(I:C) control however, implying that this effect is specific to DNA. This set of data indicates that the NU7441 DNA-PKcs kinase inhibitor exhibits an off-target effect on the DNA sensing pathway that activates TBK1 even in the absence of DNA-PKcs and as such, it cannot be used to inform on the contribution of DNA-PKcs kinase activity on intracellular DNA sensing.

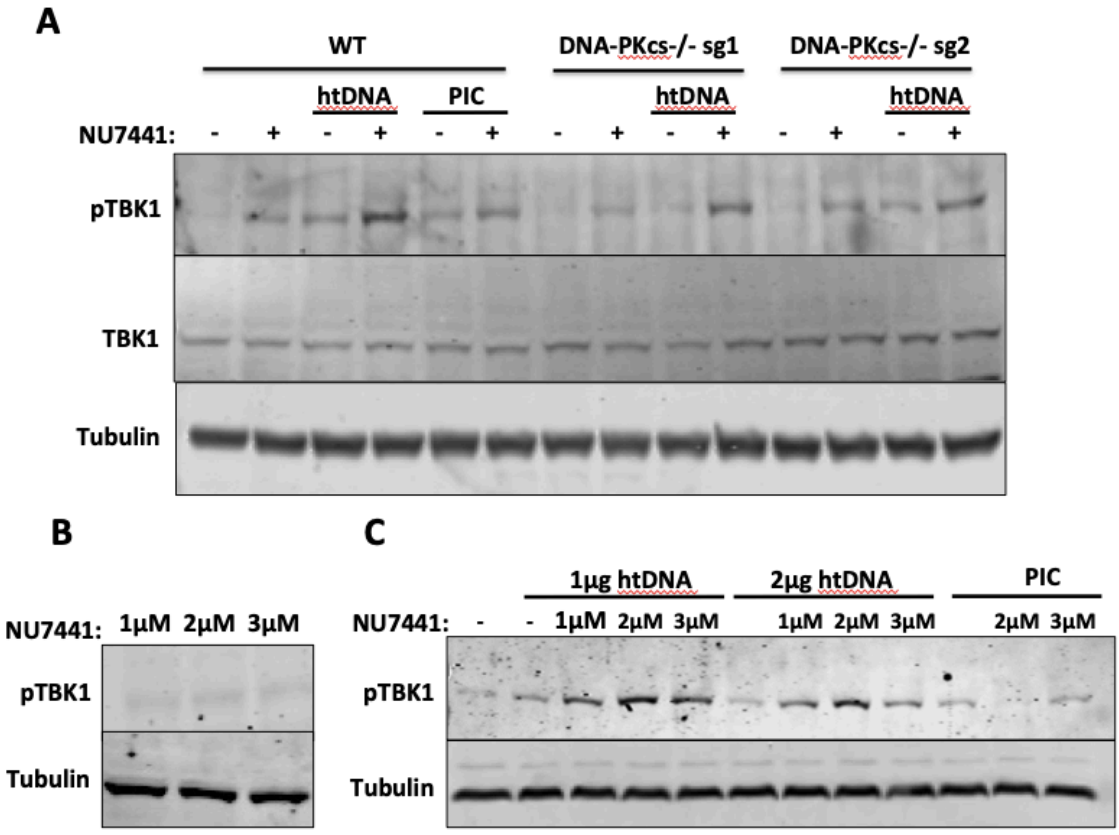

5.7 NU7441 has an off-target effect on the DNA sensing pathway that activates TBK1
A) HFF WT and DNA-PKcs-/- sg1, sg2 cells were stimulated with 1 μg htDNA for 8 hours with or without 3 μM NU7441 pre-treatment. Mock untreated cells were used as a negative control and Poly(I:C) +/- NU7441 was a positive control. Whole cell lysates were immunoblotted for phosphorylated TBK1 on serine 172 and total TBK1. B) HFF WT cells were treated with 1 μM, 2 μM and 3 μM NU7441. Whole cell lysates were immunoblotted for phosphorylated TBK1 on serine 172. C) HFF WT fibroblasts were stimulated with 1 μg or 2 μg htDNA in the absence or presence of increasing concentrations of NU7441 (1 μM, 2 μM and 3 μM). Mock untreated cells were used as a negative control and Poly(I:C) +/- 2 μM or 3 μM NU7441 were used as a positive control. Whole cell lysates were immunoblotted for phosphorylated TBK1 on serine 172. Tubulin was used as a loading control. Data shown are representative (n=2).

5.7 AZD7648 can potently inhibit DNA-PKcs activity without any off-target effects on the DNA sensing pathway

Since we identified that the NU7441 inhibitor produced an off-target effect in the DNA sensing pathway and was not suitable for our study, we tested a second DNA-PKcs kinase inhibitor. AZD7648 is a recently discovered small molecule that is very potent at inhibiting DNA-PKcs activity (IC_{50} = 0.6 nM) and shows greater selectivity

for the protein compared to NU7441 over different PIKKs (Fok *et al.*, 2019). It is an ATP-competitive inhibitor that binds to DNA-PK selectively and inhibits its kinase activity. Initially, we tested the capacity of the inhibitor to block the kinase activity of DNA-PKcs in HFFs. Cells were treated with etoposide in the presence or absence of AZD7648 (Fig. 5.8 A). We found that 2 μM of AZD7648 was able to potently block DNA-PKcs kinase action confirmed by reduction of H2AX phosphorylation. Next, we assessed the effect of AZD7648 on intracellular DNA-driven innate immnue signalling. Phosphoblotting data demonstrated no difference in TBK1 or IRF3 between the DNA-transfected cells in the presence or absence of the inhibitor. Importantly, even though there was reduced IRF3 and TBK1 activation in DNA-stimulated DNA-PKcs-/- cells compared to WT cells, treatment with AZD7648 made no difference to the levels of phosphorylation (Figure 5.8 B). Altogether, this data indicate that AZD7648 can potently and selectively block DNA-PKcs without off-target effects in the DNA sensing pathway and that DNA-PKcs kinase inhibition has little or no effect on TBK1/IRF3 signalling following DNA stimulation.

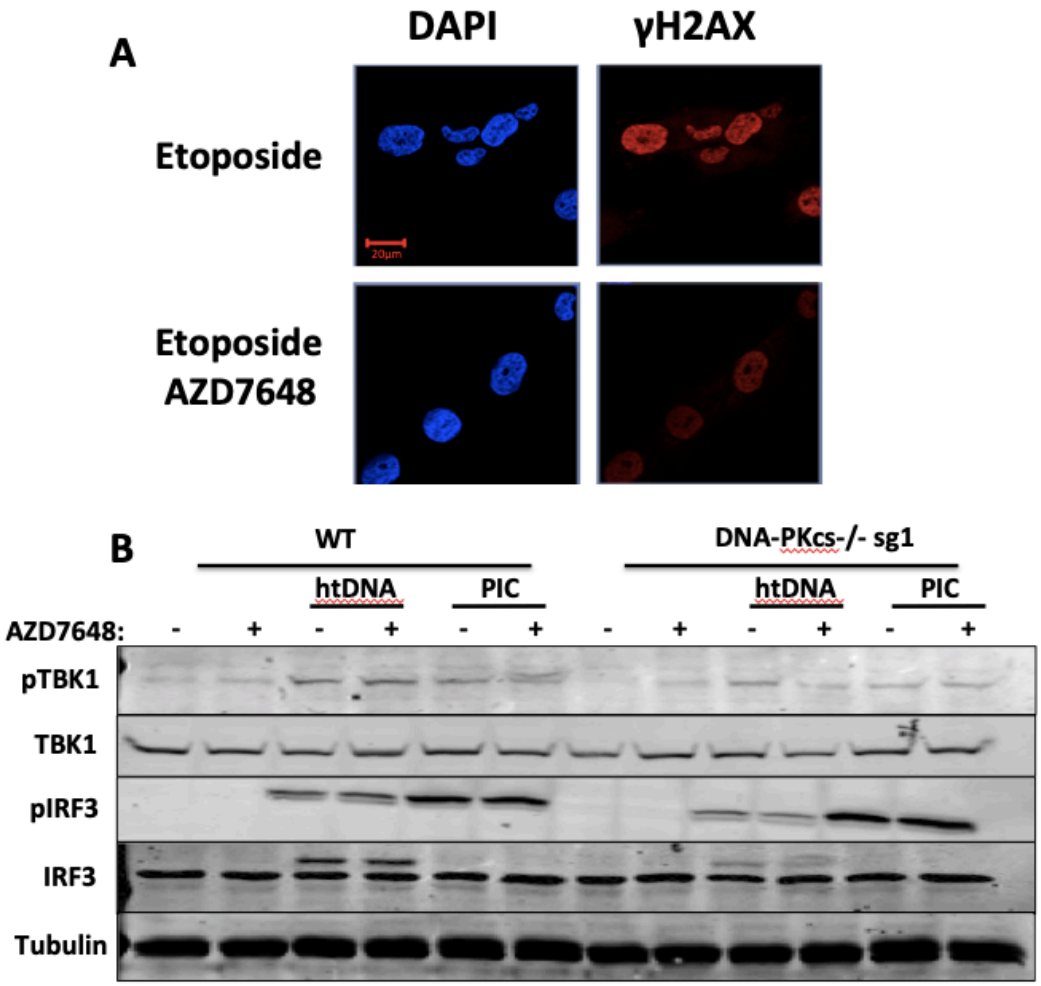

5.8 AZD7648 can potently inhibit DNA-PKcs activity without any off-target effects on the DNA sensing pathway.
A) HFF WT cells were pre-treated for one hour with 2 μM of AZD7648. Then 30 μM of etoposide was added to the cells for 2 hours presence or absence of the inhibitor. Cells were fixed and immunostained for the presence of phosphorylated H2AX, γH2AX (in red). DAPI stained the nuclei in blue. Scale bars: 20 μm. The assay was performed by Brian Ferguson. B) HFF WT and DNA-PKcs-/- sg1 cells were stimulated with 1 μg htDNA for 8 hours with or without 2 μM AZD7648 pre-treatment. Mock untreated cells were used as a negative control and Poly(I:C) +/- NU7441 was a positive control. Whole cell lysates were immunoblotted for phosphorylated TBK1 on serine 172 and total TBK1, phosphorylated IRF3 on serine 386 and total IRF3. Tubulin was used as a loading control. This experiment was performed twice.

5.8 DNA-PKcs kinase activity is dispensable for DNA sensing

Having identified that AZD7648 is effective in blocking the kinase activity of DNA-PKcs and that inhibition does not have an effect on the immune signalling to intracellular DNA, we set out to examine the effect of the inhibitor on the

transcriptional output during DNA stimulation in HFF cells. For this, we stimulated human fibroblasts with htDNA in the presence or absence of AZD7648 and observed that the drug treatment caused no changes in the mRNA expression levels of *IFNB* or *CXCL10* (Fig. 5.9). This data is consistent with our phosphoblotting data (Fig. 5.8 B) and indicates that the kinase activity of DNA-PKcs is dispensable for its DNA sensing functions.

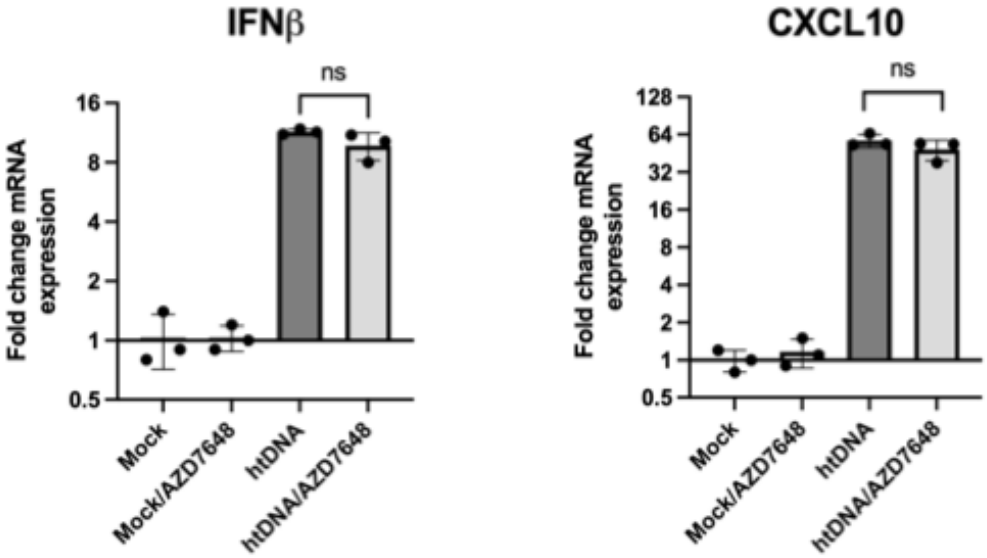

5.9 DNA-PKcs kinase activity is dispensable for DNA sensing
HFF WT cells were transfected with 1 μg htDNA in triplicate in the presence or absence of 2 μM AZD7648 and mock untransfected/AZD7648-treated cells were used as a negative control. 6 hours post transfection, RNA was extracted and analysed by RT-qPCR for IFNβ and CXCL10. Data are presented as relative fold change in mRNA expression relative to mock untreated cells and normalised to GAPDH. Data are presented as mean +/- SD. Data are representative of at least 2 experiments and this experiment was performed by Marisa Oliveira.

Summary

In summary, we showed that the widely used NU7441 DNA-PK inhibitor can potently block DNA-PKcs kinase activity but exhibits an off-target effect in the DNA sensing pathway that activates TBK1, which makes it an inappropriate tool for this study. We showed that AZD7648 blocks the enzymatic activity of DNA-PKcs without introducing any off-target effects in the DNA PRR activation pathway. The kinase

inhibition of DNA-stimulated fibroblasts made no difference to the expression of inflammatory genes or the upstream intracellular phosphorylation events. Our findings demonstrate that the catalytic function of DNA-PKcs is non-essential for its sensing functions in antiviral immunity. In the future, a more direct way to confirm this conclusion will be with the generation of knock-in kinase-dead DNA-PKcs mutant cells. So far, our findings are consistent with data from murine fibroblasts (Ferguson *et al,* 2012). Both MEFs from *scid* mice expressing a kinase-dead mutant of DNA-PKcs, and WT MEFs treated with NU7026 DNA-PKcs inhibitor still expressed *IFNB* and *CXCL10* genes in response to DNA. Although these findings are in contradiction with the published studies in monocytes (Burleigh *et al*, 2020) and fibroblasts (Sun *et al*, 2020), which concluded that DNA-PKcs kinase activity is essential for DNA sensing, both studies used the NU7441 inhibitor, which we show here can activate TBK1 independently of DNA-PKcs. We propose that the conclusions of these studies need to be revisited with the updated information about NU7441's effect on the innate sensing pathway and that AZD7648 provides a more suitable small molecule inhibitor of DNA-PKcs kinase activity.

6. Role of DNA-PKcs in virus-induced cell death

In the previous chapters we identified a role for DNA-PKcs as a DNA sensor in human fibroblasts, which mediates STING-dependent signalling in response to intracellular DNA stimulation and DNA virus infection. In the case when PRR activation is not able to eliminate a virus, infection can result in death of the cell by programmed cell death or direct lysis. There is a fine balance regulating these cellular events, which helps to ensure minimal tissue damage but at the same time activates cellular immunity. Preliminary unpublished observations by Dr Ben Trigg in the lab previously showed that cells deficient in DNA-PKcs were quicker to exhibit cytopathic effect post herpesvirus infection. Other published reports have also demonstrated DNA-PKcs to play a part in virus-induced cell death during retroviral integration (Cooper *et al,* 2013; Skalka *et al,* 1999). However, the mechanism for this is not well understood or whether it has a link with viral DNA recognition. In this chapter, we investigate the contribution of DNA-PKcs to virus-induced cell death and its relation to DNA sensing.

6.1 Generation of DNA-PKcs CRISPR knockout cell lines

Previous observations in the lab regarding the involvement of DNA-PKcs in virus-induced cell death were made in Tert-immortalised retinal pigment epithelial (RPE-1) cells. RPE cells were genetically modified to knock out the expression of DNA-PKcs protein using the CRISPR/Cas9 single guide RNAs described in chapter 4 (Figure 6.1 A), which target exon 83 located in the kinase domain of the protein (Fujimori *et al.*, 1997). Cells were transiently transfected with a CRISPR plasmid containing the two guides and single cell-sorted by flow cytometry (Chapter 2.2). Clonal populations were screened for the expression of DNA-PKcs by western blotting, which showed the successful generation of RPE DNA-PKcs-/- cell line (Fig 6.1 B). We checked for the expression of other DNA sensing components (Fig 6.1 B). RPE cells expressed most of the key constituents of the DNA sensing pathway and their expression levels were not altered in the knockout cell line.

We used the same methodology to create knockouts in HeLa cells. Generation of DNA-PKcs KOs in HeLa was successful and we obtained two DNA-PKcs-/- cell populations from single-cell clones as shown in Fig 6.1 C. The knockout populations were deficient in DNA-PKcs but expressed IRF3 and STING similarly to the parental HeLa WT cell line.

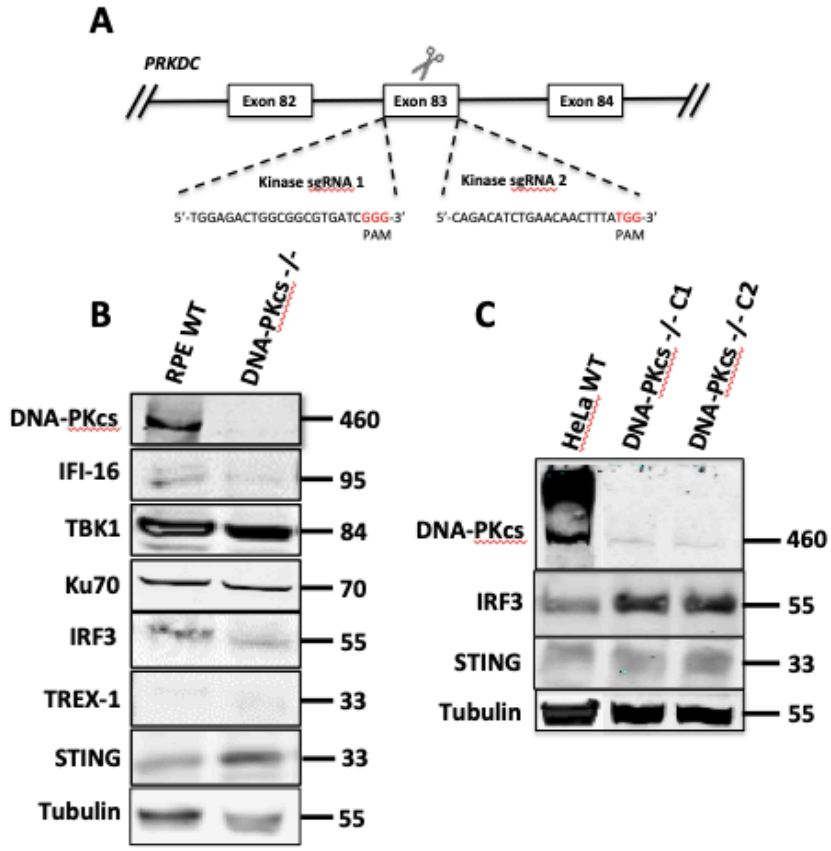

6.1 Generation of HeLa and RPE DNA-PKcs-/- cell lines via CRISPR/Cas9.
A) sgRNA design targeting exon 83 of the *PRKDC* gene in the kinase domain of the protein. B) Whole cell lysates were obtained from RPE WT and DNA-PKcs-/- clonal cell population and immunoblotted for DNA-PKcs, IFI-16, TBK1, Ku70, IRF3, TREX-1 and STING. C) Whole cell lysates were obtained from HeLa WT and two DNA-PKcs-/- clonal cell populations (C1 and C2) and immunoblotted for DNA-PKcs, IRF3 and STING. Tubulin was used as a loading control. DNA-PKcs, TBK1, IRF3 and STING blots were performed twice.

6.2 RPE and HeLa cells fail to mount an immune response to DNA

Initially, we investigated whether RPE and HeLa cell lines were responsive to intracellular DNA stimulation or DNA virus infection. Consistent with previous

findings in the lab, we observed that RPE-1 cells did not drive the transcription of *IFNB* or *CXCL10* in response to htDNA or ISD stimulation (Fig 6.2 A). Similarly, infecting the cells with HSV ΔICP0 did not elicit IFN-I transcription response in RPE-1 cells (Fig 6.2 B). Nevertheless, Poly(I:C) and SeV could potently activate the upregulation of *IFNB* or *CXCL10* immune genes. With regards to immune signalling, we could not detect any phosphorylation events of TBK1, IRF3 or STING at early or late time points post HSV ΔICP0 infection (Fig 6.2 C). Taken together, this data indicates that RPE-1 cells do not trigger STING/IRF3-driven IFN-I immune response to intracellular or viral DNA ligands specifically, despite the fact that they express key proteins of the DNA sensing pathway.

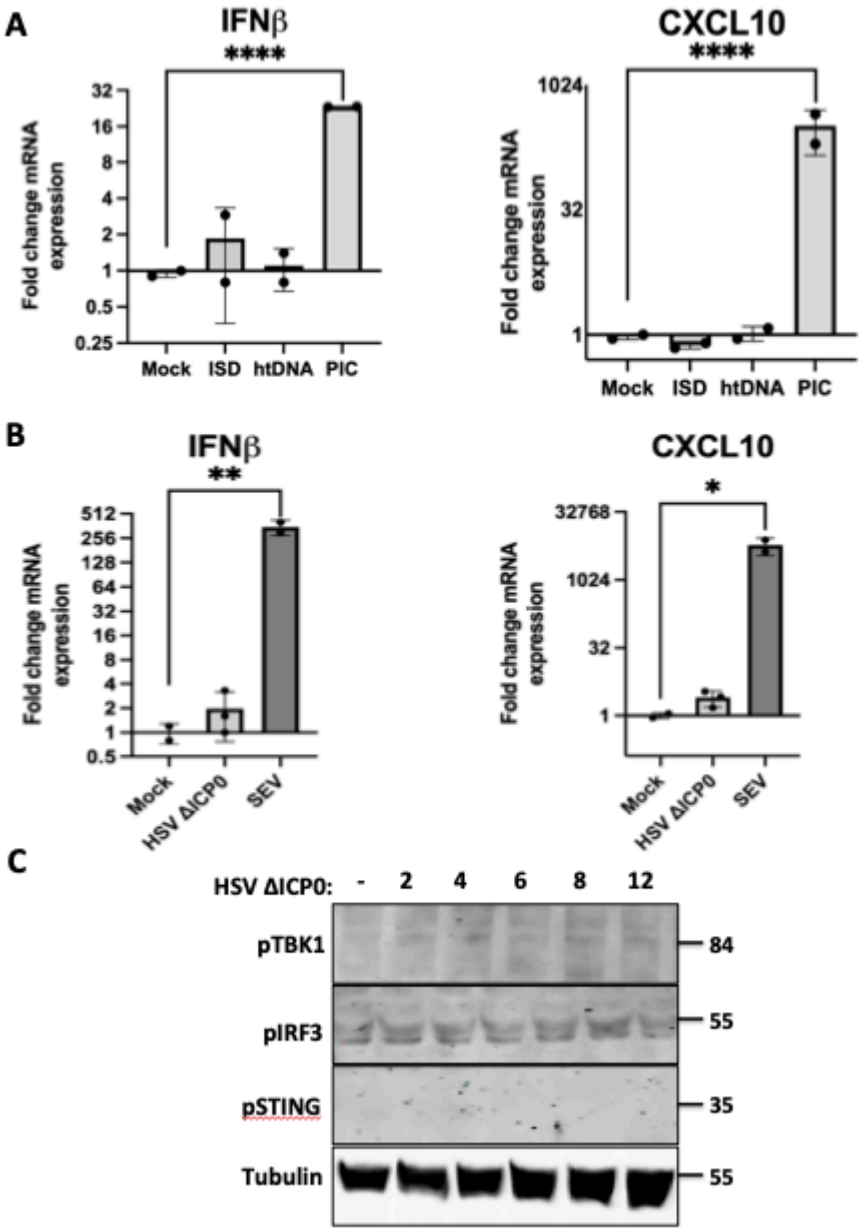

6.2 RPE cells do not have a functional DNA sensing pathway.

RPE WT cells were A) transfected with 1 µg htDNA or 7.5 µg ISD in duplicate, or B) infected with HSV ΔICP0 at MOI 5 in triplicate and mock untransfected/uninfected cells were used as a negative control. 1 µg Poly(I:C) and SeV (1:300 DF) were used as positive controls. 6 hours post transfection/infection, RNA was extracted and analysed by RT-qPCR for IFNβ and CXCL10. Data are presented as relative fold change in mRNA expression relative to mock untreated cells and normalised to GAPDH. Data are presented as mean +/- SD. Data are representative of at least 2 experimental repeats. Statistical significance was calculated using ANOVA test; *P<0.05, **P<0.01, ***P<0.001 C) RPE WT cells were infected with HSV ΔICP0 at MOI 5 and harvested at 2, 4, 6, 8, 12 hours post infection. Mock uninfected cells were used as a negative control. Whole cell lysates were immunoblotted for phospho-TBK1 at serine 172, phospho-IRF3 at serine 386, phospho-STING at serine 366. Tubulin was used as a loading control. This experiment was performed once.

As described in chapter 3, DNA failed to potently stimulate the IFN-I transcriptional response, as well as the intracellular DNA-driven signalling pathway in HeLa cells (Fig 3.1, 3.3). Further attempts exposing the cells to transfected htDNA or ISD did not trigger any upregulation of immune genes even though the cervical cancer cells were responsive to transfection with Poly(I:C) (Fig. 6.3 A).

We observed that HeLa had lost their expression of STING, which might be the explanation for the lack of DNA-mediated immune response in these cells (Fig. 6.3 B). We speculate that the protein expression levels were downregulated with the passage number as we observed loss of STING in HeLa cells at late passages and the HeLa DNA-PKcs KO cell lines we generated had lost expression of STING protein (not shown). Overall, the lack of a consistent functional DNA sensing machinery in RPE-1 and HeLa cells confirm that they are not suitable models to study intracellular DNA-driven innate immunity. However, these DNA-PKcs knockout cell lines allow analysis of other functions of this kinase in host-pathogen interplay.

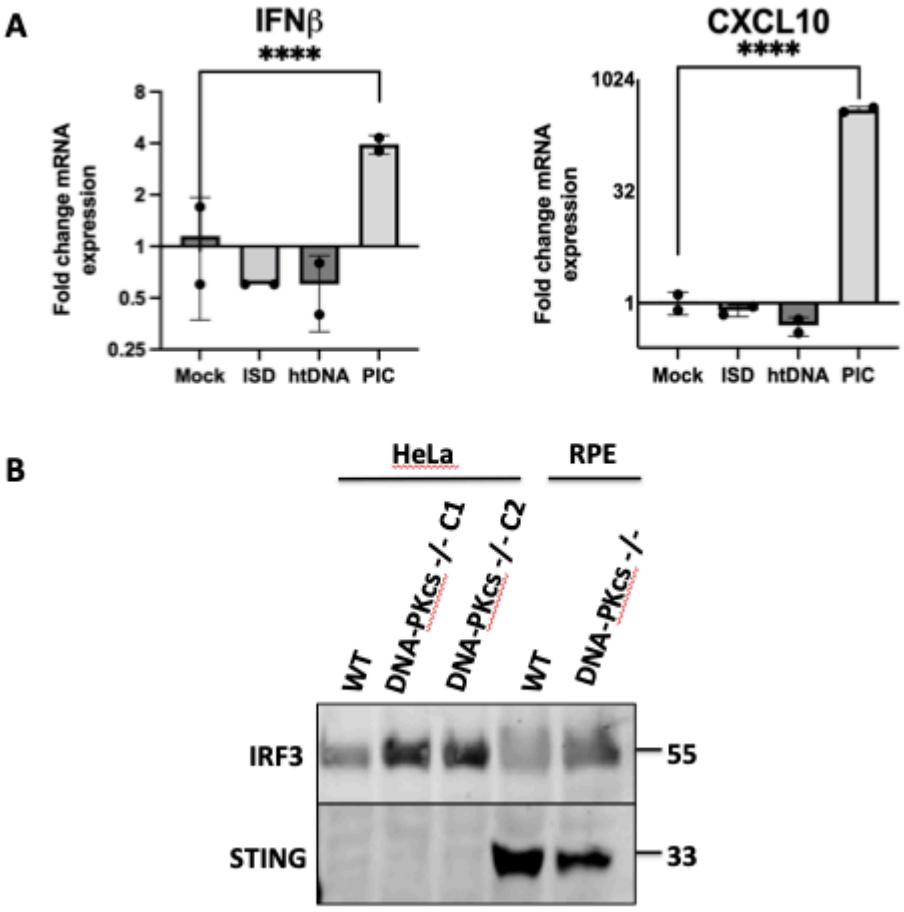

6.3 HeLa cells lost their capacity to mount DNA-mediated IFN-I transcription.
A) HeLa WT cells were transfected with 1 µg htDNA, 7.5 µg ISD in duplicate and mock untransfected cells were used as a negative control. 1 µg Poly(I:C) was used as a positive control. 6 hours post transfection, RNA was extracted and analysed by RT-qPCR for IFNβ and CXCL10. Data are presented as relative fold change in mRNA expression relative to mock untreated cells and normalised to GAPDH. Data are presented as mean +/- SD. Data are representative of at least 2 experimental repeats. Statistical significance was calculated using ANOVA test; *P<0.05, **P<0.01, ***P<0.001. B) Whole cell lysates were obtained from HeLa and RPE WT, DNA-PKcs-/- cells and immunoblotted for total IRF3 and STING.

6.3 HSV-infected RPE DNAPKcs-/- cells show advanced cytopathic effect

Previous findings in the lab demonstrated that RPE cells deficient in DNA-PKcs were more susceptible to herpesvirus-induced cytopathic effect (CPE), which involves structural changes in host cells caused by the virus and can result in lysis and cell

death. We repeated those assays by infecting RPE WT and DNA-PKcs-/- cells with the wild type herpesvirus strain, HSV S17 at MOI of 0.01 or 4. RPE DNA-PKcs-/- cells showed advanced CPE at 48 hours post HSV S17 infection with low and high MOI (Fig. 6.4 A). The advanced CPE in the knockout cells was also observed at 24 hours post HSV S17 infection with MOI of 4. To assess whether this advanced CPE was caused by alteration in cell death pathways in DNA-PKcs KO cells, we first quantified apoptotic cell death by flow cytometry using Annexin V/ 7-AAD staining. Annexin V binds to phosphatidylserine in the outer leaflet of the plasma membrane of cells undergoing early apoptosis (Meers and Mealy, 1994). 7-aminoactinomycin (AAD) discriminates between living and dead cells/cells in late apoptosis, has strong affinity for the GC regions in double-stranded DNA and is excluded from viable cells with intact impermeable cell membrane. At 24 hours post infection with high MOI of HSV, RPE *PRKDC*-/- cells showed 50% more cells in early and late apoptosis compared to RPE-1 WT cells (Figure 6.4 B), suggesting that DNA-PKcs might have a protective role against HSV-1 induced cell death in retinal epithelium cells. However, this data is only preliminary and needs to be repeated.

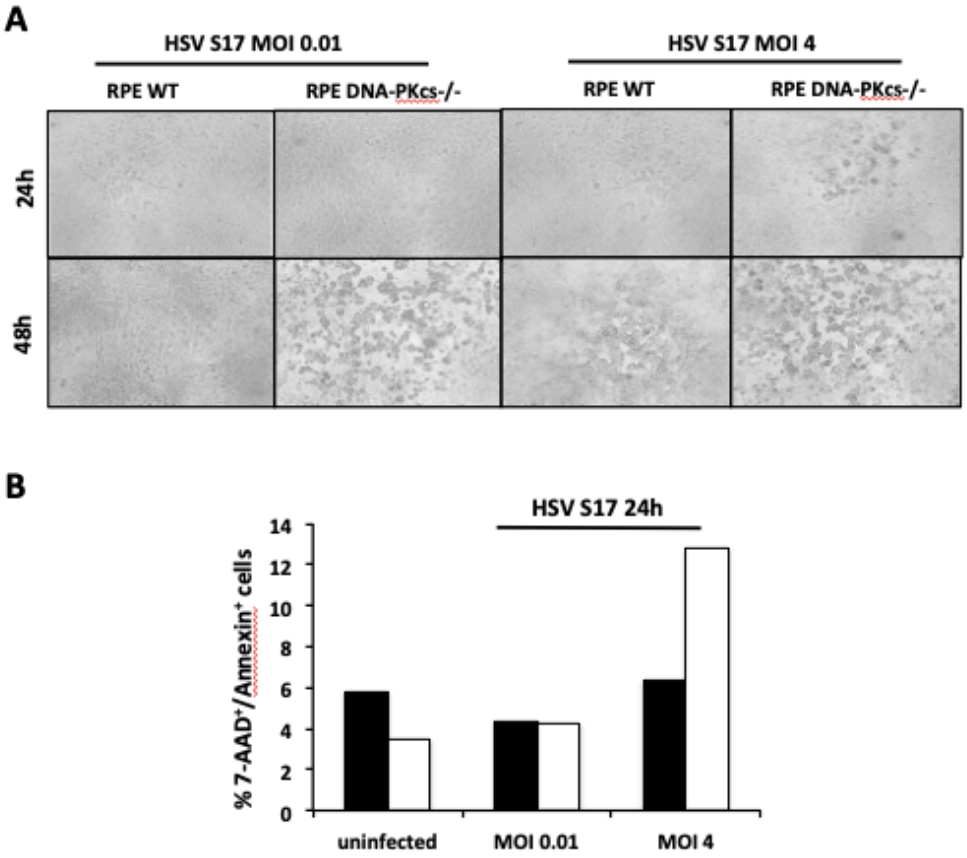

6.4 HSV-infected RPE DNA-PKcs-/- cells show advanced cytopathic effect.
A) RPE-1 WT and PRKDC-/- cells were infected with HSV-1 S17 (MOI 0.01 and 4) for 24 and 48 hours. The panel shows representative phase-contrast images; 10x magnification. B) RPE-1 WT (black bars) and *PRKDC*-/- cells (white bars) were infected with HSV-1 S17 (MOI 0.01 and 4) for 24 hours and labelled with 7AAD and Annexin for flow cytometry analysis. Mock uninfected cells were used as a negative control. The bars represent the percentage of $7AAD^+/Annexin^+$ cells (n=1).

6.4 HSV-infected RPE and HeLa DNAPKcs-/- cells show greater PARP cleavage

After identifying that cells deficient in DNA-PKcs are more prone to virus-induced cell death, we wanted to explore in more detail the mechanism behind this process. Therefore, we analysed specific programmed cell death pathway activation in our knockout cell lines. The analysis was performed by immunoblotting HSV S17-infected RPE WT and *PRKDC*-/- cell lysates for phosphorylation of MLKL at serine 358 and phosphorylation of RIPK3 at serine 166, as well as for cleaved PARP-1.

MLKL and RIP kinases are both activated and phosphorylated in TNF-induced necroptosis (Dhuriya and Sharma, 2018) and thus, we used them as markers of necroptotic cell death. On the other hand, PARP-1 cleavage by caspases is considered as a hallmark of apoptosis. PARP-1 was cleaved 6 hours post infection and there was more cleavage in RPE cells lacking DNA-PKcs. However, no phosphorylation of MLKL or RIPK was observed (Fig. 6.5 A).

In these assays, HSV-1 antigen indicated that RPE-1 cells were successfully infected and permissive to HSV-1 infection. Wild type herpesvirus induced host protein synthesis shutoff in RPE cells, evident by the decrease in the host protein signals. Protein production was shut off in WT cells as early as 4 hours, whereas it was not evident until 12 hours in DNA-PKcs-/- cells. This effect was not replicated when retinal cells were infected with HSV-1 ΔICP0 (Fig. 6.5 B). Tubulin levels remained constant throughout all time points in both cell lines infected with HSV-1 ΔICP0, and there appeared to be some PARP cleavage in DNA-PKcs-/- cells compared to WT cells.

In HeLa cells we again observed more pronounced PARP cleavage during WT HSV-1 infection in DNA-PKcs KO cells, and this was consistent between two knockout clonal populations while we did not observe the host protein shut-off effect evident in RPE cells and tubulin levels remained constant throughout the time points of infection (Fig. 6.5 C). Of note is that the HSV antigen band intensities were stronger in HeLa KO cells compared to WT, suggesting that a productive viral infection might be more efficient in the absence of DNA-PKcs and this in turn, could lead to enhanced cytopathic effect and PARP cleavage in the KO cell lines. Overall, this set of data implies that DNA-PKcs protects against virus-mediated apoptosis and that ICP0 E3 ligase might be interacting with DNA-PKcs to promote host protein shutoff in the retinal epithelium.

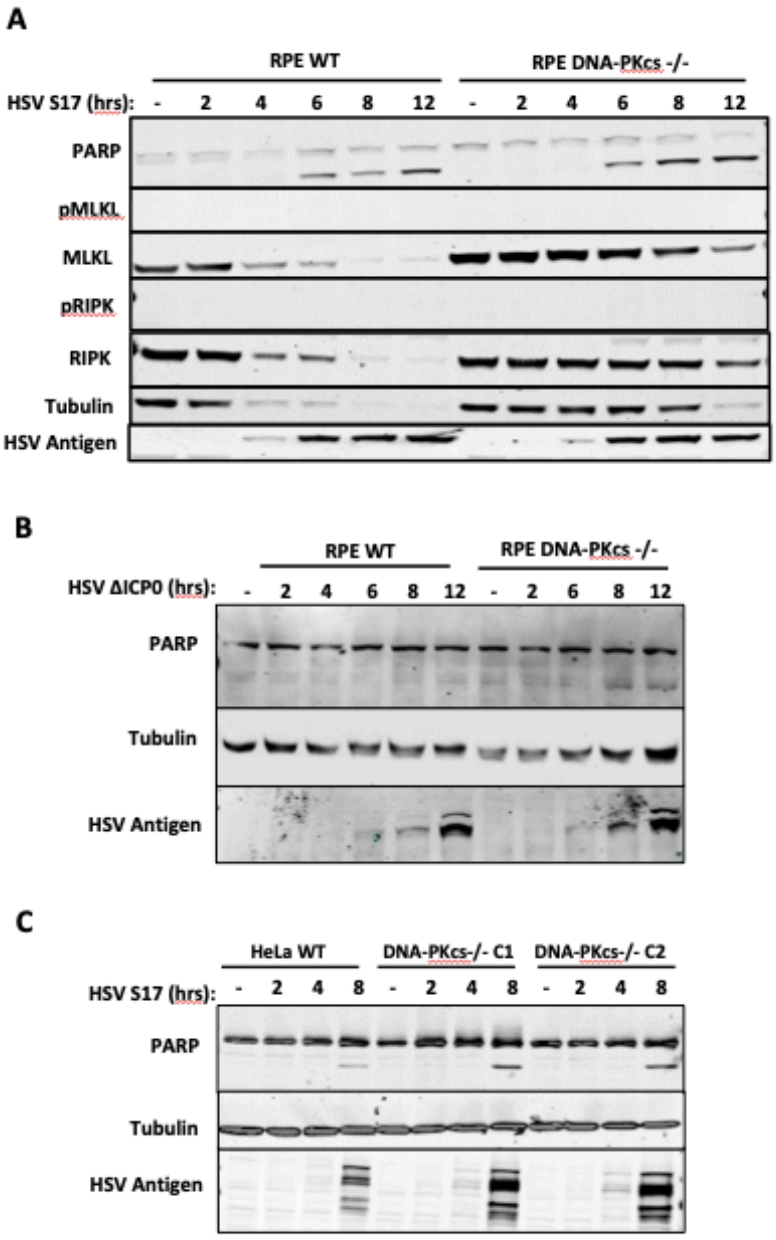

6.5 HSV S17-infected RPE and HeLa DNA-PKcs-/- show signs of programmed cell death pathway activation.

A) RPE WT and DNA-PKcs-/- cells were infected with HSV S17 at MOI 5 and harvested at indicated hours post infection. Mock uninfected cells were used as a negative control. Whole cell lysates were immunoblotted for PARP-1, phospho-MLKL at serine 358 and total MLKL, phospho-RIPK at serine 166 and total RIPK and HSV-1 antigen. Tubulin was used as a loading control. The experiment was performed twice. B) RPE WT and DNA-PKcs-/- cells were infected with HSV ΔICP0 at MOI 5 and harvested at 2, (4), 6, 8, 12 hours post infection. Mock uninfected cells were used as a negative control. Whole cell lysates were immunoblotted for PARP-1 and HSV-1 antigen. Tubulin was used as a loading control. The experiment was performed twice. C) HeLa WT and DNA-PKcs-/- C1, C2 cells were infected with HSV S17 at MOI 5 and harvested at 2, 4, 8 hours post infection. Mock uninfected cells were used as a negative control. Whole cell lysates were immunoblotted for PARP-1 and HSV-1 antigen. Tubulin was used as a loading control. The experiment was performed once.

6.5 HSV-infected RPE DNA-PKcs-/- cells produce fewer infectious virions

We showed evidence that cells lacking DNA-PKcs are more prone to virus-induced apoptosis. Another question we asked was how the absence or presence of DNA-PKcs affects the virus replication. To answer this, we carried out a single-step growth curve to quantify the amount of virus produced by RPE WT and DNA-PKcs-/- cells infected with HSV S17 (Fig. 6.6). At 24 hours post infection the WT cells had produced around 3 times more infectious virus particles compared to the knockout cell line, quantified by virus plaque formation assay (Fig. 6.6 A). Meanwhile, the amount of virions released in the cell supernatant was not significantly altered between both cell types (Fig. 6.6 B). These results implied that DNA-PKcs might be involved in altering the kinetics of virion production. Furthermore, we also performed a growth curve assay in which we collected cell-associated and released virus together and quantified the total amount of virus by plaque formation assay (Fig. 6.6 C). The assay demonstrated that RPE-1 PRKDC$^{-/-}$ cells produced nearly 30 times fewer HSV-1 infectious virions at 24 and 48 hours compared to RPE-1 WT cells. These findings suggest that HSV-infected KO cells might be producing fewer virions as a result of the increased cell death. Alternatively, more efficient viral replication in DNA-PKcs-/- cells might be promoting cell lysis and leading to reduced viral output.

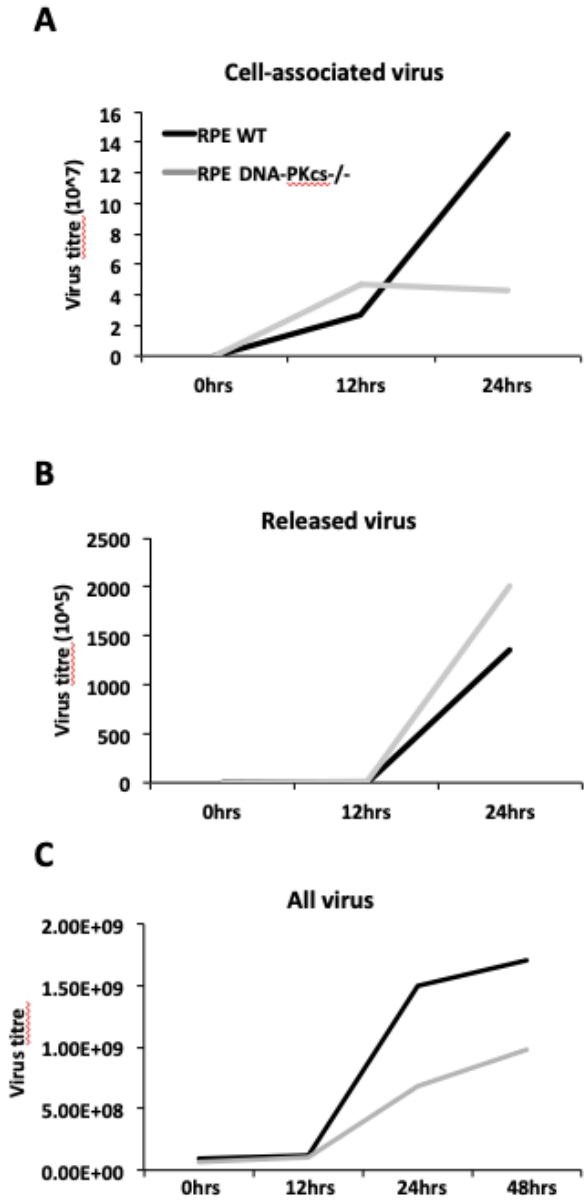

6.6 HSV-infected RPE DNA-PKcs-/- cells produce fewer infectious virions.
RPE-1 WT and PRKDC-/- cells were infected with HSV-1 S17 at MOI 5 for 12, 24, 48 hours and A) cell lysates, B) cell supernatants or C) lysates and supernatant pooled together were harvested for titration by plaque assay. Mock uninfected samples (0hrs) were used as a negative control. The Y-axis shows the virus titre (n=1). The experiments were performed once.

Summary

As outlined in chapter 3, many cell lines lack the capacity to respond to DNA or DNA virus by activating IFN-I innate immunity. However, these systems could allow us to study other roles of the protein and discriminate from its DNA sensing function. We found another role for DNA-PKcs in virus-induced cell death where cells deficient in this protein were more susceptible to cytopathic effect and showed greater PARP-1 cleavage, a hallmark of apoptotic death. Published data using murine *Prkdc* mutant *scid* cells reported similar findings, demonstrating that DNA-PKcs-/- cells were unable to integrate HIV DNA and died by apoptosis (Skalka *et al*, 1999). On the other hand, another study presented contradictory data in CD4 T-cells during HIV infection where inhibiting DNA-PK prevented cell death (Cooper *et al,* 2013). More specifically, they showed that DNA-PK phosphorylated p53 and H2AX during viral integration and promoted cell death. The literature points to the conclusion that the role of DNA-PKcs in cell death might be cell type- and pathogen-specific, similarly to what we have described regarding its DNA sensing function. Finally, we observed less HSV-1 virion production in DNA-PKcs-/- RPE cells, which could have resulted from the higher cell death rate in the knockout cells. Alternatively, DNA-PKcs might be beneficial for more efficient viral replication, which however would not explain why HSV-1 targets DNA-PKcs for degradation.

7. Discussion

HFF cells are a suitable model for the study of the DNA sensing pathway

We identified Tert-immortalised human foreskin fibroblasts (HFF) as a suitable model to study the antiviral DNA sensing pathway (Chapter 3). These cells were able to efficiently activate the STING/TBK1/IRF3 signalling pathway and mount a type-I interferon response to intracellular DNA and DNA virus infection. This is consistent with murine cells as the discovery of DNA-PKcs as a novel DNA sensor was performed in mouse embryonic fibroblasts (MEFs) (Ferguson *et al*, 2012). Fibroblasts are a primary cell target of virus infection in multiple tissues (Boyd *et al.*, 2020; Krausgruber *et al.*, 2020) and they express high levels of DNA-PK protein. We showed that HFF cells have an active STING/IRF3-dependent DNA sensing pathway that culminates in the activation of IFN-I immune response. HFFs are therefore an ideal model for the study of the DNA-PK-mediated antiviral immunity. However, we observed that not all fibroblast cell lines have a functional DNA sensing pathway as MRC5T immortalised cells lacked the ability to generate a productive immune response to DNA (Fig. 3.1). We speculate that many cell lines switch off this pathway during the transformation process (Sokolowska and Nowis, 2018), indicating that careful selection of a suitable cell type is crucial for studying this pathway. Other cell types suitable for DNA virus infection are keratinocytes and epithelial cells. Therefore, we tested HeLa and HaCaT cell lines. HaCaTs have been used in studies investigating the DNA sensing function of IFI16 (Almine *et al.*, 2017). We observed that these cells were firing the DNA sensing pathway even in steady-state conditions without treatment (Fig. 3.2). On the other hand, HeLa cells have been used in DNA-PK studies in the context of DNA sensing (Morchikh *et al*, 2017) but in our hands, the cervical cancer cells failed to stimulate the STING/IRF3 phosphorylation and activation downstream of DNA stimulation.

Given the main aim of this project to understand the contribution of DNA-PK to intracellular DNA sensing in human cells, we took the approach of analysing the

signalling in a single cell line, a feature lacking in other studies on the role of human DNA-PKcs in DNA sensing. Reports in other cell lines, such as monocytes, HEK, HeLa or fibroblasts point to the idea that there are distinct and cell type-specific DNA PRR activation pathways. In 2017, Morckikh *et al* reported that DNA-PK cooperates with cGAS to drive type I IFN gene expression in a STING-dependent manner (Morckikh *et al,* 2017). Their conclusions come from assays performed in HeLa, HEK and HUVEC cells. A recent study carried out in U937, HEK and THP1 cells on the other hand reported that DNA-PK acted independently of cGAS and STING to drive the IFN immune program to DNA (Burleigh *et al,* 2020). A third study performed in HFF and THP1 cells proposed that DNA-PK restricts cGAS signalling activity in response to DNA or DNA virus (Sun *et al,* 2020). These data highlight that the DNA-PK-mediated DNA sensing pathway may be cell type-specific and thus, it requires careful examination in a single system, before being applied to other model systems. For this reason, we concentrated our efforts on dissecting the pathway and gaining insights into the DNA-PKcs-mediated antiviral immunity in HFFs .

DNA-PKcs is activated upon exposure to intracellular DNA in HFF cells

We showed that DNA-PKcs was rapidly activated after DNA transfection as the protein became autophosphorylated on serine 2056 (Fig. 3.7 A). We observed by immunofluorescence that this phospho-signal was mostly nuclear. This questions from where DNA-PKcs exerts its DNA sensing function, which is not yet well understood. In murine fibroblasts, DNA-PKcs was identified as a cytoplasmic viral DNA sensor and DNA-PK was shown to colocalise with MVA viral factories in the cytoplasm (Ferguson *et al*, 2012). Further to this, nuclear and cytoplasmic fractionation assays demonstrated that DNA-PKcs is localised in the cell cytosol as well as the nucleus. Apart from that, studies have identified additional cytosolic roles for DNA-PK in phosphorylating cytoskeletal proteins in the cytoplasm during virus infection (Kotula *et al.*, 2013). DNA-PK is mostly known for its function as a DNA damage repair protein in the nucleus. The protein is highly concentrated in the nuclear cell compartment, which is the reason why we observe such a strong signal

in the nucleus in our immunofluorescence analysis (Fig. 3.7 A). There is a more diluted pool of DNA-PKcs protein in the cell cytosol of fibroblast cells from where the protein could be detecting, for example, poxviral DNA.

Recently, Ku70, part of the trimeric DNA-PK complex, was shown to rapidly translocate from the nucleus to the cytoplasm after DNA transfection or HSV-1 infection to drive *IFNL1* expression and type III IFN response in HEK and HeLa cells and this process was regulated by the cellular acetylation status (Sui *et al,* 2021). In another study, cytoplasm-translocated Ku70/80 detected Hepatitis B virus (HBV) DNA and stimulated CCL3/5 chemokine transcription (Li *et al,* 2016). In these studies the localisation of DNA-PKcs was not analysed so it is unclear whether or how DNA-PKcs moves between sub-cellular localisations during its sensing of viral DNA. With regards to evidence from other DNA sensors, nuclear IFI16 was also found to translocate to the cytoplasm upon the detection of viral DNA in the nucleus to induce IFN-I transcriptional program (Ishikawa *et al,* 2008; Unterholzner *et al*, 2010; Almine *et al,* 2017). In the case of HSV-1 infection, IFI16 can detect the viral genome in the nucleus, resulting in acetylation of the protein and translocation to the cytoplasm (Ansari *et al,* 2015). Interestingly, in a recent study IFI16 was reported to recruit DNA-PK to viral DNA at the nuclear periphery. This event was followed by phosphorylation of IFI16 by DNA-PKcs during HSV-1 infection and the stimulation of antiviral cytokine expression in HFF cells (Justice *et al,* 2021).

The localisation of cGAS is also controversial. cGAS is reported to reside in the cytoplasm, nucleus and plasma membrane in resting cells (M. *et al.*, 2016; Barnett *et al.*, 2019; Volkman *et al.*, 2019; Zhong *et al.*, 2020; Sun *et al.*, 2021) and has even been shown to localise predominantly in the nucleus where its activity against self-DNA is regulated by chromatin tethering (Tomoya *et al.*, 2020; Zhao *et al.*, 2020). In a couple of studies DNA-PK has been proposed to cooperate with cGAS in regulating the innate immune response to DNA (Morckikh *et al,* 2017; Sun et al, 2020). Overall, we hypothesise that in the fibroblast system DNA is detected by the fraction of DNA-PKcs residing in the cytosol, or in the case of nuclear viral DNA sensing, DNA-PKcs

likely acts in cooperation with other sensors/co-regulatory molecules to translocate and transmit the signal to the cytoplasm.

Another pertinant question is what type of DNA is recognised by DNA-PKcs to initiate the innate immune responses. We found that a mixture of different DNA lengths were able to stimulate immune signalling (Fig. 3.6). In its response to double -stranded DNA breaks in the nucleus, Ku binds with strong affinity to free DNA ends and recruits DNA-PKcs kinase for further end processing and downstream signalling (Mari *et al.*, 2006; Meek, Dang and Lees-Miller, 2008). Burleigh *et al* showed that sonicated but not circular plasmid DNA was able to induce *IFNB* transcription and phosphorylation of IRF3 in human cells, indicating that DNA-PK recognises the nucleic acid ends to drive the immune response (Burleigh *et al,* 2020). We also know that DNA-PK recognises DNA in a sequence-independent manner (Mari *et al.*, 2006), with the exception of one publication, which showed that DNA-PK can specifically recognise the NRE1 DNA sequence element with high affinity to repress mouse mammary tumour virus (MMTV) transcription (Giffin *et al.*, 1996). Sequence-independent DNA recognition however raises the question how DNA-PK might discriminate self from non-self DNA. Several other factors apart from the ones mentioned above can determine whether DNA is recognised as a sign of danger: 1) methylation status; 2) subcellular compartmentalisation and abundance; 3) chromatinisation/accessibility of DNA. As already mentioned, we use DNA purified from herring or calf cells that lacks unmethylated CpG motifs abundant in microbial genomes and are specifically detected by TLR9 PRRs in endosomes (Hemmi *et al.*, 2000; Yasuda *et al.*, 2009; Ohto and Shimizu, 2016). This allows us to study only the immune outcomes mediated by cytosolic DNA sensors. The cytosol is generally considered as DNA-free environment and DNA misplaced in the cytoplasm is potent at triggering the immune response, as well as naked DNA not associated with histones or chromatin-binding proteins inside the nucleus. We assume that DNA-PK detects free DNA ends during DNA sensing. The question then is how DNA-PKcs can distinguish between self-DNA damage and foreign DNA to initiate the DNA damage response or to signal to STING and induce the immune response. One explanation

could be inferred from a recent study in human monocytes where DNA-PK was reported to phosphorylate HSPA8 downstream target that was not activated during DNA damage but helped to delineate the innate immune response from the role of DNA-PK in the DNA repair pathway (Burleigh et al, 2020). It is likely that DNA-PK cooperates with other signalling mediators to shape the appropriate responses downstream of self or non-self DNA recognition.

HFF cells mount IFN-I but not IFN-III immune response to DNA

Interferons are central to establishing an antiviral response in an infected cell. Their expression is driven by the IRF transcription factors. IRF1, IRF3, IRF5 and IRF7 are essential for the generation of IFN-I responses downstream of PRR activation. IRF7 is mainly abundant in pDCs and IRF5 is predominantly expressed in B cells, monocytes, macrophages, whereas IRF3 is ubiquitously expressed in multiple cell types (Au *et al.*, 1998; Lopez-Pelaez *et al.*, 2014). Once phosphorylated, they translocate to the nucleus and promote the expression of IFNs. Similarly, PRR activation can induce the phosphorylation and degradation of IκB, which releases the inhibition on NF-κB (Régnier *et al.*, 1997; Zandi *et al.*, 1997). IRF and NF-κB transcription factors bind to ISRE or NF-κB promoter regions in the nucleus to induce the expression of innate immune genes, such as different classes of *IFNs, CXCL10, CCL5, ISG56,* etc.

When we stimulated HFF cells with DNA or infected them with DNA virus, we demonstrated an increase in *IFNB*, a type I IFN (Fig. 3.9). In our assays, we did not observe large fold change differences in *IFNB* mRNA expression. This might be the case for several reasons. *IFNB* is already expressed at low basal levels in cells and it needs the synergistic association of several transcription factors with promoter regions (ISRE, NF-kB and AP-1) to form the interferon enhanceosome and drive expression (Honda, Takaoka and Taniguchi, 2006; Wang *et al.*, 2010). *CXCL10* expression on the other hand can be initiated when only one of the promoter regions (ISRE or NF-kB) are engaged (Brownell *et al.*, 2014), meaning that it could

be stimulated downstream of the IRF or NF-kB signalling pathways. Moreover, during virus infection *IFNB* was shown not to be expressed by all cells simultaneously (Zhao *et al,* 2012). This stochastic expression was found to be the result of cell-to-cell variability at different stages of the virus infection process, which could be another factor why we quantify lower *IFNB* mRNA levels in our assays. It is noteworthy that in our HFF DNA stimulation experiments we did not see upregulation of *IFNA4*, type I IFN, or *IFNL1*, type III IFN (Fig. 3.9) *IFNA4* is another type I interferon that is generally expressed in plasmacytoid dendritic cells by IRF7 (Au *et al.*, 1998; Yeow *et al.*, 2000). Further to this, the IFN was also shown to be transcribed following DNA stimulation in human monocytes (Burleigh *et al,* 2020). We were surprised not to observe type III IFN transcription in our system upon DNA treatment. *IFNL1* is produced in large amounts in epithelial cells in response to RNA virus infection (Hemann, Gale Jr and Savan, 2017). In 2011, Zhang *et al* documented a role for Ku in mediating type III IFN response to DNA. The group revealed in their study that Ku70 activated IRF1/7 and induced the expression of *IFNL1* in response to DNA and HSV-2 (Zhang *et al,* 2011) and they later reported that these events were STING-dependent (Sui *et al,* 2017). Their study was performed in HEK 293 and primary mouse spleen cells implying that these might be cell type-specific responses.

Knockout of Ku in human but not murine cells is lethal and we did not test in our system whether Ku components are necessary for the DNA-PKcs-induced immunity in human cells. However, there is increasing evidence in the literature highlighting the role of Ku in DNA sensing and that the different components of the trimeric complex might be cooperating together in the generation of a productive immune response. For instance, knockdown studies in liver-derived cells demonstrated that Ku70/80 in cooperation with DNA-PKcs and PARP-1 recognised HBV DNA and induced chemokine secretion in IRF-1-dependent manner (Li *et al*, 2016). Similarly, knockdown studies in human monocytes implicated Ku70 in the sensing of HTLV-1 and the induction of IFN-I response (Wang *et al,* 2017). The pathogen and cell type-specific response seem to determine what class of IRFs and interferons are

activated. In the future it would be interesting to explore whether other IRFs, apart from IRF3, are active in HFFs. IRF3/7 are the targets of TBK1/IKKε activity and IRF3 is ubiquitously expressed in most cell types suggesting that the IRF3-dependent pathway in our cell system could be applied to more models rather than it being fibroblast-specific. The expression level of different IRFs in cell types might skew the DNA immune response as to which class of IFNs are stimulated. Furthermore, IFNλ has been shown to be activated by NF-κB only (Swider *et al.*, 2014) and we see very little NF-κB activity in immortalised HFFs in response to DNA pointing to another explanation as to why type III IFN response is not induced in this cell model.

HSV-1 ICP0 viral protein targets DNA-PKcs for degradation

ICP0 E3 ligase is an early expressed HSV protein that targets DNA-PKcs for degradation, while the levels of other DNA damage proteins, like Ku, are not targeted by this protein (Lees-Miller *et al.*, 1996). ICP0 also contributes to HSV-1 evasion of the host immune response by blocking the IRF3 signalling pathway and interferon production (Lin *et al.*, 2004). In our experimental system, we illustrated DNA-PKcs levels were reduced early after infection and there was no phosphorylation of IRF3 in cells infected with WT HSV-1, whereas DNA-PKcs levels were stable and IRF-3 phosphorylation was observed in cells infected with HSV-1 ΔICP0 (Fig. 3.8). We propose that ICP0 targets DNA-PKcs for degradation due to its role in sensing viral DNA and that IRF3 signalling is restricted in HFF cells during infection with WT HSV due to the depleted levels of DNA-PKcs. In a study by Lees-Miller *et al*, the authors suggest that ICP0 degrades DNA-PKcs to alleviate its inhibition on ribonucleic acid polymerase II (RNAP II) and thus, allowing other proteins, such as HSV ICP27, to interact with RNAP II and promote viral transcription (Dai-Ju *et al.*, 2006). Both explanations are possible if DNA-PK has multiple functions in restricting a productive infection in the cells, thereby HSV-1 has evolved a strategy to combat DNA-PKcs antiviral effects.

HSV ICP0 has been extensively studied with respect to its interplay with IFI16. ICP0 was reported to target IFI16 for proteasomal degradation in HFFs and oral keratinocytes (Orzalli, DeLuca and Knipe, 2012). However, this has been challenged by other studies claiming that IFI16 is not directly targeted for degradation (Delphine *et al.*, 2013). In human foreskin fibroblasts, IFI16 was shown to detect HSV-1 DNA in the nucleus and low levels of cGAMP produced by nuclear cGAS stabilised IFI16 to drive IFN expression in STING-dependent manner (Orzalli *et al.*, 2015). Further to this, IFI16 was also found to suppress viral replication by binding to transcription start sites (Roy *et al.*, 2019), similarly to what was proposed about DNA-PK. We could not check for the role of IFI16 in our HFF system in relation to DNA-PK, as we were unsuccessful in creating IFI16-/- cell lines (Fig. 4.2). As already mentioned, a recent publication revealed that in HSV-infected HFF cells DNA-PK phosphorylated and was recruited to the nuclear envelope by IFI16 (Justice *et al*, 2021). We know that cGAS contributes to the generation of IRF3-dependent IFN-I response in our model. In the future it would be interesting to assess whether IFI16 contributes to the antiviral immunity in human fibroblasts and how DNA-PK, cGAS and IFI16 might be coordinating the immune response to viral DNA.

The first stage of a productive HSV-1 infection is the fusion of the viral envelope with the cell plasma membrane, which is cell type-specific. In fibroblasts, this happens through the nectin-1 receptor (Philipp *et al.*, 2021). Following fusion, the virion is de-enveloped and the nucleocapsid is transported to the cell nucleus via microtubules. The capsid docks onto nuclear pores and the herpesviral DNA is injected inside. This raises the question how cytosolic DNA sensors would be able to detect HSV-1 genomic DNA? While the virions are transported from the periphery of the cell towards the nucleus, defective virion particles may leak DNA into the cytoplasm, which would be detected by cytosolic PRRs. Alternatively, a study carried out in macrophages indicated that cGAS sensed HSV-1 DNA in the cytosol due to viral capsid degradation by the proteasome (Horan *et al.*, 2013). Apart from viral DNA, HSV-infection causes cellular stress that leads to the release of mitochondrial DNA, which is detected in the cell cytoplasm. Furthermore, as already mentioned

above, DNA sensors can also detect viral DNA in the nucleus, which is the case for IFI16 and cGAS. DNA-PK was reported in a recent study in fibroblasts to unite with IFI16 at the nuclear periphery where HSV DNA is deposited and to cooperatively initiate immune signalling (Justice *et al*, 2021), which suggests for a nuclear role of DNA-PK in HSV-1 DNA sensing. The authors propose in their study that this event happens before ICP0 degrades DNA-PKcs at around 6 hours post infection. Moreover, in a study by Smith *et al* the unusual structure of HSV genome containing nicks and gaps was shown to induce the antiviral activities of DNA-PK and the addition of 5' flaps to the viral DNA boosted DNA-PK activation (Smith *et al.*, 2014). Overall, it is possible that DNA-PK can detect HSV DNA inside the nucleus and transduce the signal to the cytoplasm while any leaked DNA into the cytosol to be surveilled by the pool of DNA-PK in this subcellular compartment to initiate STING signalling and the antiviral immune response.

DNA-PK is involved in a complex interplay with a number of viruses that inhibit the activity of the NHEJ complex or utilise it for their own benefit (reviewed in (Hristova, Lauer and Ferguson, 2020). One prominent example is adenovirus that has been shown to deploy an array of ways, such as protein mislocalisation or degradation to inactivate the DNA damage response while also interacting with DDR proteins at replication sites that promote the viral life cycle. Adenovirus E4orf6 viral protein can suppress DNA-PKcs autophosphorylation (Turnell and Grand, 2012). Furthermore, adenovirus E1A was recently found to block IRF3 phosphorylation in the DNA sensing pathway in human monocytes where DNA-PK was shown to activate IFN-I in STING-independent manner (Burleigh, 2020). It is highly likely that the strategies adenovirus uses to inhibit DNA-PK are linked to the antiviral immune functions of the complex. Such interactions with adenovirus and a number of other viruses remain to be explored.

MVA induces IFN-I innate immune response in HFF cells

We found that HFF cells infected with MVA mounted antiviral IFN-I immune response (Fig. 3.10), in line with what was observed in murine fibroblasts (Ferguson, 2012). MVA has been imperative in understanding the innate immunity to VACV. The virus strain is able to induce the immune response in most cell types due to large deletions and mutations in immunomodulatory regions. Contrary to HSV-1, where a single deletion of ICP0 restores interferon signalling, VACV employs an arsenal of viral proteins to block the DNA sensing pathway at different stages. Two viral proteins expressed by VACV, C16 and C4, were reported to bind to the Ku heterodimer and prevent its interaction with the poxvirus DNA (Scutts *et al.*, 2018), validating the importance of DNA-PK in generating immunity to VACV. Moreover, it was proposed that this was as a result of the high expression levels of the DNA-PK complex in fibroblasts, which are a primary target of VACV infection. Other examples are Poxvirus immune nuclease (poxin), also called protein B2, which cleaves cGAMP, E5 that binds and inhibits cGAS, and multiple proteins that target IRF3 and NF-κB signalling downstream of PRRs (Eaglesham *et al.*, 2019; Unterholzner *et al.*, 2011; Chen *et al.*, 2008). The reason why VACV has developed numerous ways to modulate the STING pathway in particular can be linked to the fact that its viral life cycle is largely restricted to the cytoplasm where it replicates its dsDNA genome. DNA-PK and IFI16 were documented to localise at MVA viral factories in the cytoplasm of mouse embryonic fibroblasts and keratinocytes (Almine *et al.*, 2017; Ferguson *et al*, 2012), which illustrates their functions as cytosolic DNA sensors in the context of VACV infection.

Non-transformed primary fibroblasts display similar DNA sensing features as HFF cells

We wanted to test a second cell model in our study that has not gone through the transformation or immortalisation process and thus, would be more physiologically relevant. For this we chose primary fibroblasts isolated from the skin of healthy

donors. These cells nicely phenocopied HFF cells in the capacity to mount IFN-I immune response to intracellular DNA and DNA virus infection (Section 3.5). A paper published by the group of Michael Weekes demonstrated that the proteome profile of HFFF-Tert cells matched the one of primary HFFF cells in the context of HCMV DNA virus infection, which supports our conclusions (Nightingale *et al.*, 2018). Primary fibroblasts can be passaged for a limited number of times, which limited options for genetic manipulation of these cells and amount of assays that can be performed. Nonetheless, a primary cell model helps to validate some of the data we obtained in HFFs and for checking that the immortalisation does not make a difference to our conclusions.

Limitations and advantages of CRISPR KO cell lines

The use of CRISPR KO cell lines is the cleanest way to study the role of a protein in a given pathway over other approaches, such as siRNA knockdown techniques. Genetic manipulation of DNA-PK is challenging, as cells lacking some of the complex components are not viable or can exhibit poor growth rates. For instance, knocking out Ku is lethal for human but not mouse cells. Nevertheless, we managed to create DNA-PKcs-/- HFF cell lines and use them for our study without noticing any major growth defects in the KO cell lines. We created CRISPR KO cell lines using lentiviral transduction of sgRNAs into cas9-expressing cells and subsequent antibiotic selection and thereby we ended up with a mixed pool of heterozygous and homozygous knockout cells. This pool may provide more representative data than single-cell clonal populations. Some of the cells in these populations, however, displayed low-level expression of the DNA-PKcs protein (Fig. 4.1). This might be the reason why in some stimulation and infection studies residual immune gene expression or phosphorylation signal was produced by the knockout cells. However, since we did not perform our assays with a clonal knockout cell population, we cannot rule out the fact that there might be additional active pathways in our system and that the residual signals could be attributed to them.

The gold standard to check for CRISPR off-target effects are complementation studies, where the gene of interest is inserted back into the knockout cell line to check whether the phenotype can be rescued. DNA-PKcs is a very large protein (around 460 kDa), which makes it technically challenging to be cloned into an expression vector and re-introduced into cells. Nonetheless, we used two single guide RNAs targeting different PAM sequences in the *PRKDC* gene to create separate DNA-PKcs-/- cell lines. The phenotypes we observed were found to be reproducible between both lines, independent of the stimulation or infection model. In addition to this, these findings are compatible with what was shown in the murine fibroblast system, providing good evidence that the phenotype we observe is not as a result of CRISPR off-target effects.

The cGAS-STING/ IRF3 signalling axis is required for the IFN-I immune response in HFF cells

Using CRISPR/Cas9 KO cGAS and STING lines, we confirmed that these proteins are essential components for the generation of IFN-I response to DNA in HFFs (Fig. 4.3). Furthermore, inhibition of TBK1/IKKε abrogated the DNA-mediated IFN-I response, confirming TBK1/IKKε are essential for the signalling pathway (Fig. 4.4). These outcomes were expected, as previous studies have identified the components to be important for the DNA-induced innate immunity in fibroblasts (Ishikawa, Ma and Barber, 2009; Schoggins *et al.*, 2014; Chen, Sun and Chen, 2016). STING is known for its ability to induce *IFNB* in response to ISD and HSV-1 in mouse embryonic fibroblasts (Ishikawa *et al,* 2009). DNA-PK was demonstrated to act upstream of the STING/TBK1/IRF3-signalling axis (Ferguson, 2012). TBK1-/- and IRF3-/- MEFs were deficient in upregulating the expression of *IFNB, CXCL10, ISG54* immune genes to DNA and MVA, and Ku70 was shown to interact with STING by immunoprecipitation. During HSV-1 infection, fibroblasts from cGAS-/- mice were deficient in inducing *IFNB* demonstrating a role for cGAS in herpesviral immunity in this model (Li *et al,* 2013). Furthermore, Orzalli *et al* demonstrated that cGAS and IFI16 are necessary for the generation of STING-mediated IFN-I immune response to

plasmid DNA in human foreskin fibroblasts (Orzalli *et al,* 2015). Overall, this evidence supports our findings for the requirement of cGAS and STING in the generation of IFN immune response to intracellular DNA and DNA virus infection in fibroblasts.

DNA-PKcs is required for the STING-dependent IFN-I immune response to DNA and DNA virus infection in HFF cells

We showed in HFFs that DNA-PKcs is required for the STING activation and the signalling response to intracellular DNA and DNA virus infection (Fig. 4.7, 4.10). These findings are consistent with another report in HeLa, HEK and HUVEC cells which identified that STING was activated downstream of DNA-PK and cGAS (Morchikh *et al*, 2017). Furthermore, a study by Sui *et al* focusing on the role of Ku documented that STING is an essential mediator of the Ku70-mediated immune response to DNA mainly in HEK cells (Sui *et al*, 2021). In contrast, a recent paper described a non-canonical DNA sensing pathway in human monocytes downstream of DNA-PK that acts independently of cGAS and STING and the authors called the STING-independent DNA sensing pathway (SIDSP) (Burleigh *et al*, 2020). In addition, another study showed that DNA-PK was able to directly phosphorylate IRF3 in the nucleus even though this finding has not been reproduced by other groups (Karpova *et al.*, 2002).

After the delivery of DNA to cells, two main pathways downstream of STING can be activated, the IRF3 and NF-κB pathways (Balka *et al.*, 2020). We checked for the activation of NF-κB pathway by immunoblotting for the phosphorylated version of IκBα (data not shown). We could not detect any signal in stimulated HFF cells suggesting that the DNA-induced STING/TBK1/IRF3 pathway is predominantly active in this cell model. We also checked for the induction of *NFKBIA* gene downstream of NF-κB signalling in DNA-stimulated or infected HFF cells (Fig. 4.6, 4.9). We observed only little upregulation in the context of MVA infection, which was not mediated by DNA-PK (Fig. 4.9 C). Intracellular DNA is known to be a weak

activator of NF-κB *in vitro* and the mechanism by which STING activates NF-κB is somewhat unclear. In murine fibroblasts it was shown that NF-κB was not involved in the immune response to DNA, which is in line with our findings (Ferguson, 2012). DNA-PKcs-/- MEFs completely abrogate the translocation of IRF3 to the nucleus in response to DNA while this was not the case for p65 translocation. Our data showed that there was NF-κB activity, but we do not fully understand how and whether it contributes to the antiviral immune response in HFF cells.

In human fibroblasts, we show that DNA-PKcs is required for the activation and phosphorylation of STING in response to exogenous DNA. It remains to be explored how DNA-PKcs activates STING in the DNA-induced innate immune signalling. We can envision several potential scenarios based on evidence from the literature. cGAS produces cGAMP cyclic di-nucleotide, which is a central activator of the STING scaffolding protein. We speculate that DNA-PKcs might cooperate with cGAS during DNA sensing. In fact, a recent paper showed that cGAS interacted with all components of the DNA-PK complex in DNA-stimulated and HSV-infected THP1 cells and that DNA-PKcs was able to phosphorylate cGAS at T68 and S213 (Sun *et al*, 2020). DNA-PK was also shown to form a ribonucleoprotein complex with cGAS and paraspeckles components to drive STING signalling in the context of ISD stimulation and KSHV infection (Morchikh *et al*, 2017). We attempted to check in our system whether DNA-PK drives the innate immunity to DNA in cooperation with cGAS. We used an ELISA assay to quantify the levels of cGAMP in DNA-stimulated WT and DNA-PKcs-/- HFF cells; however, we could not detect any measurable levels of cGAMP in our sample, consistent with evidence in the literature that fibroblasts express low levels of cGAS and that infected fibroblasts produced cGAMP at levels below the limit of detection (Orzalli *et al*, 2015). A potential future experiment to address this question would be an enzymatic assay to check for cGAS activity in stimulated WT and DNA-PKcs-/- cells.

Another explanation on the mechanism of STING activation could be inferred from studies revealing direct interaction of DNA-PK complex with STING. Several reports

demonstrated that Ku was able to form a complex with STING upon DNA transfection or HTLV infection (Ferguson *et al.*, 2012; Sui *et al.*, 2017; Wang *et al.*, 2017). In one of the studies the authors showed that the DNA binding domain of Ku70 was necessary for the protein-protein interaction ((Ferguson *et al.*, 2012; Sui *et al.*, 2017; Wang *et al.*, 2017). In addition to this, STING was also reported to bind DNA directly but the physiological relevance of this is not fully understood. A third theory on STING activation downstream of DNA-PKcs might implicate the role of IFI16 in DNA sensing. Recently, it was shown that DNA-PK interacts with IFI16 at HSV DNA deposition in the nuclear periphery of HFF cells (Justice *et al*, 2021). IFI16 was also shown to interact with STING in response to DNA and that its pyrin domain, in cooperation with cGAMP, is required for STING activation in HaCaT cells (Almine *et al*, 2017). Overall, we lack mechanistic insights on the link between DNA-PK detection of DNA and STING activation. While some studies show that DNA-PK can drive the interferon response independently of STING, the immune adaptor is clearly activated downstream of DNA-PKcs in the human fibroblast system. DNA-PKcs has not been identified to directly interact with STING and other receptor proteins, such as Ku or cGAS likely mediate the interaction and STING activation.

NU7741 DNA-PKcs kinase inhibitor exerts an off-target effect on TBK1 activation during DNA sensing

In our attempts to determine the dependence of the kinase activity of DNA-PKcs on its role in DNA sensing, we showed that DNA-stimulated HFF and primary fibroblasts treated with the DNA-PKcs kinase inhibitor NU7441 displayed enhanced STING/IRF3 activation and increased TBK1 phosphorylation (Fig. 5.2, 5.6). NU7441 does inhibit DNA-PKcs kinase activity (Fig. 5.1), but we hypothesised there may also be off-target effect of this inhibitor. The NU7441-dependent TBK1 phosphorylation was present in cells lacking DNA-PKcs (Fig. 5.7), which confirmed that NU7441 has DNA-PKcs-independent effect on TBK1 activation. This effect however, appeared to be independent of STING or IRF3 as the increased activation of these components was variable during virus infection and was only consistently observed when cells

were stimulated with 1 μg DNA (Fig). This effect may be via direct activation of TBK1 that leads to its autophosphorylation on S172, or by an indirect effect on other kinases, such as IKKβ, which was shown to phosphorylate TBK1 (Clark *et al.*, 2011). This result shows that NU7441 DNA-PKcs kinase inhibitor interferes with the DNA sensing pathway downstream of STING and independently of DNA-PKcs. The data has implications for studies that have used NU7441 in defining the role of DNA-PKcs in PRR activation and therefore, the use of the inhibitor and conclusions of studies using it in the context of DNA sensing will need to be re-evaluated. A study by Sun *et al* reported the same observations in NU7441-treated HFF cells in the context of DNA stimulation or VSV and HSV-1 infection (Sun, 2020). They presented higher levels of phosphorylation of TBK1 and IRF3 and increased *IFNB* and *CXCL10* expression in the presence of the DNA-PKcs inhibitor. The authors concluded that in STING-proficient cells DNA-PKcs restricts cGAS signalling highlighting a pro-viral role for DNA-PK. Furthermore, in the paper describing SIDSP in monocytes, specific conclusions about DNA-PKcs are based on the use of the NU7441 throughout the study (Burleigh, 2020). The authors presented data from NU7441-inhibitor treated primary fibroblasts, which showed enhanced expression of *IFNB* upon DNA stimulation, proposing that there is an alternative DNA sensing pathway. The conclusions from such studies will need to be revised with the updated information about NU7441 activating TBK1 signalling.

Interestingly, we observed that the effect of NU7441 was dependent on the dose of the DNA ligand for STING and IRF3 phosphorylation (Fig. 5.3). In chapter 3 Fig, we observed that transfection of cells with higher concentration of DNA induced lower expression levels of immune gene transcripts. We think that this result might be due to reduced transfection efficiency, i.e. transfection with higher ligand concentration is less efficient and leads to lower amount of DNA delivered to the cytoplasm. We speculate that there might be a threshold of DNA concentration that can be added to the cells and less ligand is able to overcome the enhanced activation effect on STING. Importantly, we did not see a change in the phenotype when DNA-PKcs-/- cells were stimulated with lower and higher doses of DNA (Fig. 4.8), illustrating that the

requirement of DNA-PKcs for DNA sensing does not depend on the concentration of the stimulus.

DNA-PKcs contributes to HSV-induced cell death in cells with non-functional DNA sensing pathway

We found that many cell types display a non-functional DNA sensing pathway, as discussed in chapter 3. Among these, RPE cells expressed known components of the pathway but failed to respond to intracellular DNA stimulation (Fig. 6.2). However, we have not been able to check for cGAS expression in these cells, which might be one explanation for the lack of immune response to DNA. Alternatively, we think that cells might lose their ability to detect DNA during the immortalisation process, which could hold true for Tert-immortalised RPE cells. A previous member of the lab, Dr Christian Ku, on the other hand, showed that HeLa cells do phosphorylate innate immune signalling proteins downstream of DNA sensing. However, we could not repeat this observation and saw no phosphorylation of STING or IRF3 in response to DNA (Fig. 3.3 B). We noticed that the levels of total STING protein declined with the passage number and HeLa cells were no longer able to mount IFN-I innate immune response to DNA (Fig. 6.3). Nonetheless, this enabled us to use the DNA-PKcs-/- RPE and HeLa cells to examine the contribution of DNA-PKcs to other aspects of virus biology independent of STING activation. We discovered that HSV-infected RPE and HeLa cells deficient in DNA-PKcs were more prone to virus-induced cell death (Fig. 6.5). Apoptosis is an established antiviral host defense mechanism that cells deploy to prevent virus replication and dissemination. In the context of HSV infection, HSV has been reported to induce or inhibit apoptosis in different cell types. The virus promotes programmed cell death in immune cells, such as T-cells, dendritic cells or macrophages to suppress the activation of the immune response, while it inhibits apoptosis in epithelial cells (Leopardi and Roizman, 1996; Koyama and Adachi, 1997; Galvan and Roizman, 1998; Martine, Jennifer and A., 1999). ICP0 HSV protein has also been shown to induce apoptosis (Sanfilippo and Blaho, 2006). We observed that in retinal epithelial cells HSV S17,

but not HSV ΔICP0, was able to induce PARP-1 cleavage (considered as a hallmark of apoptosis). PARP is inactivated and cleaved by executioner caspases during regulated cell death and the size of the cleavage fragments can define the enzymes that digested the protein and hence the type of cell death. The 89kDa fragment suggests apoptotic cell death (Martine, Jennifer and A., 1999), which is consistent with what we observed in our immunoblot assays (Fig. 6.5). DNA-PKcs also has caspase-3 cleavage sites in its structure, which were implicated in negative regulation of inflammation by apoptosis (Bharti *et al.*, 1998). Interestingly, DNA-PKcs appeared to have a protective role against apoptosis as DNA-PKcs-/- cells demonstrated greater PARP cleavage at around 8 hours post infection with HSV (Fig. 6.5). DNA-PKcs has been implicated in virus-induced cell death in several studies, albeit its role is controversial. One report that supported our findings used a different virus model and showed that murine *PRKDC* mutant *scid* cells were unable to integrate retroviral HIV DNA and as a result, died by apoptosis (Skalka *et al*, 1999). More recently, a study showed that inhibition of DNA-PKcs kinase activity by NU7441 or DNA-PK knockdown induced more double-stranded breaks mediated by M1 virus and promoted apoptosis (Xiao *et al.*, 2018). In addition, the authors discovered that DNA-PK blockade was also able to reduce IFN signalling and promote more virion production in M1-infected cells. Contrary to these findings, another study presented data in CD4 T-cells during HIV infection where inhibiting DNA-PK prevented cell death (Cooper *et al,* 2013). More specifically, they showed that DNA-PK phosphorylated p53 and H2AX during viral integration and promoted cell death. It appears that the phenotype we observe is cell type-specific and there can be implications for HSV-1 ICP0 and DNA-PKcs depending on the cell model. In the epithelial cells we tested it appears that DNA-PKcs takes on an anti-apoptotic role protecting from virus-induced cell death. HSV has also been implicated in inducing necroptosis (Yu and He, 2016). We attempted to check for necroptotic pathway activation in our cell models, however we could not observe any phosphorylation signal of RIPK3 or MLKL (Fig 6.5). The evidence we have is not enough to state whether this pathway is inactive in our cell lines or it is not induced

by HSV since we have not included necroptosis-inducing positive controls in our assays.

We managed to discriminate the DNA sensing function of DNA-PKcs from its role in cell death as we found that RPE and HeLa cells lacked the ability to respond to DNA. In addition, previous findings by Dr Ben Trigg showed that HFFF cells did not induce PARP cleavage after infection with HSV-1. It would be interesting to investigate whether DNA-PKcs initiates a DDR response upon HSV infection that stalls the infected cells from going into apoptosis. It is noteworthy that we observed less severe HSV-induced host protein shut-off in RPE cells lacking DNA-PKcs (Fig. 6.5). Virus-induced host protein synthesis shutdown is a common strategy for viruses to redistribute the cell resources for the benefit of the virus. Several herpesviral proteins were identified to mediate this process, such as virus host shutoff (vhs) protein and ICP27 (He *et al.*, 2020). We found that infection of RPE cells with attenuated strains of HSV-1, such as HSV ΔICP0, did not exhibit the same protein shutoff effect (Fig 6.5). The same was observed during infection with oncolytic HSV1716, which has a mutation in ICP34.5 (data not shown). Our data suggests that DNA-PKcs might play a part in coordinating the HSV-induced protein shutdown response in RPE cells. We did not observe the same effect in HeLa cells though (Fig. 6.5), suggesting for a cell type-specific event.

HSV-infected RPE DNAPKcs-/- cells produce fewer infectious virions

Analysis of the virus growth kinetics showed that retinal epithelial cells deficient in DNA-PKcs produced fewer infectious virions than their WT counterpart (Fig 6.6). We speculate that this could be attributed to the fact that we observe increased cell death in the knockout cell lines. Alternatively, this could be as a result of a greater number of virions produced by the cells that leads to lysis and death of the cell. Studies in other cell models showed contradictory findings where HeLa cells lacking DNA-PKcs showed more efficient HSV-1 replication (Lees-Miller *et al.*, 1996) and in Ku70 -/- mouse embryonic fibroblasts the viral yields were 50-fold higher (Taylor

and Knipe, 2004). Moreover, DNA-PK knockdown cancer cells produced higher titres of oncolytic alphavirus-M1 while interferon signalling was downregulated (Xiao *et al.*, 2018). The differences in virus titres we observe are not big enough to suggest an obvious phenotype and the outcomes from such an analysis can be sensitive to the method used for performing the growth curve assay.

Conclusions

In conclusion, we demonstrate that DNA-PKcs is required for the antiviral immune response to DNA in human fibroblasts. DNA-PKcs induces the production of IFN-I in STING/TBK1/IRF3-dependent manner in response to DNA and the DNA viruses, HSV ΔICP0 and MVA. We report that the kinase activity of the protein is not essential for its DNA sensing functions and define AZD7648 as a small molecule DNA-PKcs kinase inhibitor suitable for such assays. In the future, it will be important to validate these findings in a primary cell model by loss-of-function studies, as well as to gain more mechanistical insights on the early events of DNA-PK activation as to where the protein is localised and how it activates STING downstream. In addition, we have identified a role for DNA-PKcs beyond DNA sensing in HSV-induced cell death, which requires further work to understand the mechanisms behind this process.

Understanding how intracellular DNA is sensed by the innate immune system has implications not only for antiviral immunity, but can also be applied to autoimmunity, vaccine development and immunotherapy. Knowledge of the intricate interplay between viruses and hosts is pivotal in the development of vaccines, as well as the creation of viral vectors for gene therapy. Good expression systems, specific integration and preservation of host cell survival all depend on understanding the early events in host-pathogen interactions. Innate signalling components regulate the immunogenicity of DNA vaccines and gaining insights into DNA sensor functions can enable the development of more potent vaccines that generate a long-lasting adaptive immune response.

During sterile inflammation, self-DNA is recognised by innate nucleic acid sensors, which can cause aberrant activation of immune pathways and lead to the development of autoimmune disorders. Nucleic acids are structurally similar and therefore, there are many checkpoints in place to prevent the harmful activation of innate immunity. Others and we have shown that mutations in the DNA-PKcs DNA sensor are linked to an overactive immune response and the development of granuloma in patients (Sun *et al*, 2020) indicating the importance of DNA-PKcs activity in maintaining immune homeostasis. Therefore, gaining insights into the functions of DNA-PKcs in PRR sensing is important not only for antiviral immunity, but also for the inflammatory response to DNA in autoimmune disease conditions.

Moreover, nucleic acid sensing has been implicated in anti-tumour immune responses. Immune sensors activate the innate immunity and mediate the generation of adaptive immune responses that can counteract the immunosuppressive environments imposed by tumours. Small molecule drugs, such as agonists that target the STING signalling pathway can provide effective immunotherapy treatments. One type of immunotherapy are oncolytic viruses, such as Talimogene laherparepvec (T-vec), which is an oncolytic herpes virus. Understanding how oncolytic viruses are sensed by the host cancer cells to initiate lytic immune responses is pivotal in developing successful cancer treatment. Further mechanistic explorations of DNA-PKcs in sensing foreign and damaged DNA can impact all of these aspects of disease-related and translational science.

Bibliography

A., B. *et al.* (2015) 'Viruses transfer the antiviral second messenger cGAMP between cells', *Science*. American Association for the Advancement of Science, 349(6253), pp. 1228–1232. doi: 10.1126/science.aab3632.

Abe, T. *et al.* (2013) 'STING Recognition of Cytoplasmic DNA Instigates Cellular Defense', *Molecular Cell*. Elsevier, 50(1), pp. 5–15. doi: 10.1016/j.molcel.2013.01.039.

Abe, T. and Barber, G. N. (2014) 'Cytosolic-DNA-mediated, STING-dependent proinflammatory gene induction necessitates canonical NF-κB activation through TBK1', *Journal of virology*. 2014/03/05. American Society for Microbiology, 88(10), pp. 5328–5341. doi: 10.1128/JVI.00037-14.

Ablasser, A. *et al.* (2009) 'RIG-I-dependent sensing of poly(dA:dT) through the induction of an RNA polymerase III–transcribed RNA intermediate', *Nature Immunology*, 10(10), pp. 1065–1072. doi: 10.1038/ni.1779.

Ablasser, A. *et al.* (2013) 'Cell intrinsic immunity spreads to bystander cells via the intercellular transfer of cGAMP', *Nature*, 503(7477), pp. 530–534. doi: 10.1038/nature12640.

Agalioti, T. *et al.* (2000) 'Ordered Recruitment of Chromatin Modifying and General Transcription Factors to the IFN-β Promoter', *Cell*. Elsevier, 103(4), pp. 667–678. doi: 10.1016/S0092-8674(00)00169-0.

Akira, S., Uematsu, S. and Takeuchi, O. (2006) 'Pathogen Recognition and Innate Immunity', *Cell*. Elsevier, 124(4), pp. 783–801. doi: 10.1016/j.cell.2006.02.015.

Alandijany, T. (2019) 'Host Intrinsic and Innate Intracellular Immunity During Herpes Simplex Virus Type 1 (HSV-1) Infection', *Frontiers in Microbiology*, 10, p. 2611. doi: 10.3389/fmicb.2019.02611.

Almine, J. F. *et al.* (2017) 'IFI16 and cGAS cooperate in the activation of STING during DNA sensing in human keratinocytes', *Nature Communications*, 8(1), p. 14392. doi: 10.1038/ncomms14392.

Andrejeva, J. *et al.* (2004) 'The V proteins of paramyxoviruses bind the IFN-inducible RNA helicase, mda-5, and inhibit its activation of the IFN-β promoter', *Proceedings of the National Academy of Sciences of the United States of America*, 101(49), pp. 17264 LP – 17269. doi: 10.1073/pnas.0407639101.

Ansari, M. A. *et al.* (2015) 'Herpesvirus Genome Recognition Induced Acetylation of Nuclear IFI16 Is Essential for Its Cytoplasmic Translocation, Inflammasome and IFN-β Responses', *PLoS pathogens*. Public Library of Science, 11(7), pp. e1005019–e1005019. doi: 10.1371/journal.ppat.1005019.

Asselin-Paturel, C. *et al.* (2001) 'Mouse type I IFN-producing cells are immature APCs with plasmacytoid morphology', *Nature Immunology*, 2(12), pp. 1144–1150. doi: 10.1038/ni736.

Au, W.-C. *et al.* (1998) 'Characterization of the Interferon Regulatory Factor-7 and Its Potential Role in the Transcription Activation of Interferon A Genes *', *Journal of Biological Chemistry*. Elsevier, 273(44), pp. 29210–29217. doi: 10.1074/jbc.273.44.29210.

Aubert, M. and Blaho, J. A. (2003) 'Viral oncoapoptosis of human tumor cells', *Gene Therapy*, 10(17), pp. 1437–1445. doi: 10.1038/sj.gt.3302004.

Baeuerle, P. A. *et al.* (1988) *Phorbol-ester-induced activation of the NF-κB transcription factor involves dissociation of an apparently cytoplasmic NF-κB/inhibitor complex*. United States: The Cold Spring Harbor Laboratory. Available at: http://inis.iaea.org/search/search.aspx?orig_q=RN:22003652.

Balka, K. R. *et al.* (2020) 'TBK1 and IKKε Act Redundantly to Mediate STING-Induced NF-κB Responses in Myeloid Cells', *Cell Reports*, 31(1), p. 107492. doi: https://doi.org/10.1016/j.celrep.2020.03.056.

Barber, G. N. (2015) 'STING: infection, inflammation and cancer', *Nature Reviews Immunology*, 15(12), pp. 760–770. doi: 10.1038/nri3921.

Barnett, K. C. *et al.* (2019) 'Phosphoinositide Interactions Position cGAS at the Plasma Membrane to Ensure Efficient Distinction between Self- and Viral DNA', *Cell*. Elsevier, 176(6), pp. 1432-1446.e11. doi: 10.1016/j.cell.2019.01.049.

Bell, J. K. *et al.* (2003) 'Leucine-rich repeats and pathogen recognition in Toll-like receptors', *Trends in Immunology*. Elsevier, 24(10), pp. 528–533. doi: 10.1016/S1471-4906(03)00242-4.

Bharti, A. *et al.* (1998) 'Inactivation of DNA-dependent protein kinase by protein kinase Cdelta: implications for apoptosis', *Molecular and cellular biology*. American Society for Microbiology, 18(11), pp. 6719–6728. doi: 10.1128/MCB.18.11.6719.

Bosma, M. J. and Carroll, A. M. (1991) 'The SCID Mouse Mutant: Definition, Characterization, and Potential Uses', *Annual Review of Immunology*, 9(1), pp. 323–350. doi: 10.1146/annurev.iy.09.040191.001543.

Bosnjak, L. *et al.* (2005) 'Herpes Simplex Virus Infection of Human Dendritic Cells Induces Apoptosis and Allows Cross-Presentation via Uninfected Dendritic Cells', *The Journal of Immunology*, 174(4), pp. 2220 LP – 2227. doi: 10.4049/jimmunol.174.4.2220.

Boyd, D. F. *et al.* (2020) 'Exuberant fibroblast activity compromises lung function via ADAMTS4', *Nature*, 587(7834), pp. 466–471. doi: 10.1038/s41586-020-2877-5.

Boyer, J. A. *et al.* (2020) 'Structural basis of nucleosome-dependent cGAS inhibition', *Science (New York, N.Y.)*. 2020/09/10, 370(6515), pp. 450–454. doi: 10.1126/science.abd0609.

Brewerton, S. C. *et al.* (2004) 'Structural analysis of DNA–PKcs: modelling of the repeat units and insights into the detailed molecular architecture', *Journal of Structural Biology*, 145(3), pp. 295–306. doi: https://doi.org/10.1016/j.jsb.2003.11.024.

Brownell, J. *et al.* (2014) 'Direct, Interferon-Independent Activation of the CXCL10 Promoter by NF- B and Interferon Regulatory Factor 3 during Hepatitis C Virus Infection', *Journal of Virology*, 88(3), pp. 1582–1590. doi: 10.1128/JVI.02007-13.

Bürckstümmer, T. *et al.* (2009) 'An orthogonal proteomic-genomic screen identifies AIM2 as a cytoplasmic DNA sensor for the inflammasome', *Nature Immunology*, 10(3), pp. 266–272. doi: 10.1038/ni.1702.

Burdette, D. L. *et al.* (2011) 'STING is a direct innate immune sensor of cyclic di-GMP', *Nature*, 478(7370), pp. 515–518. doi: 10.1038/nature10429.

van der Burg, M. *et al.* (2009) 'A DNA-PKcs mutation in a radiosensitive T-B- SCID patient inhibits Artemis activation and nonhomologous end-joining', *The Journal of clinical investigation*. 2008/12/15. American Society for Clinical Investigation, 119(1), pp. 91–98. doi: 10.1172/JCI37141.

Burleigh, K. *et al.* (2020) 'Human DNA-PK activates a STING-independent DNA sensing pathway', *Science Immunology*. Science Immunology, 5(43). doi: 10.1126/sciimmunol.aba4219.

C., S. S. and Erik, F.-P. (2012) 'Sensing Adenovirus Infection: Activation of Interferon Regulatory Factor 3 in RAW 264.7 Cells', *Journal of Virology*. American Society for Microbiology, 86(8), pp. 4527–4537. doi: 10.1128/JVI.07071-11.

Chan, Y. K. and Gack, M. U. (2016) 'Viral evasion of intracellular DNA and RNA sensing', *Nature Reviews Microbiology*, 14(6), pp. 360–373. doi: 10.1038/nrmicro.2016.45.

Chen, Q., Sun, L. and Chen, Z. J. (2016) 'Regulation and function of the cGAS–STING pathway of cytosolic DNA sensing', *Nature Immunology*, 17(10), pp. 1142–1149. doi: 10.1038/ni.3558.

Chen, R. A.-J. *et al.* (2008) 'Inhibition of IkappaB kinase by vaccinia virus virulence factor B14', *PLoS pathogens*. Public Library of Science, 4(2), pp. e22–e22. doi: 10.1371/journal.ppat.0040022.

Chiliveru, S. *et al.* (2014) 'Inflammatory Cytokines Break Down Intrinsic Immunological Tolerance of Human Primary Keratinocytes to Cytosolic DNA', *The Journal of Immunology*, 192(5), pp. 2395 LP – 2404. doi: 10.4049/jimmunol.1302120.

Chiu, Y.-H., MacMillan, J. B. and Chen, Z. J. (2009) 'RNA Polymerase III Detects Cytosolic DNA and Induces Type I Interferons through the RIG-I Pathway', *Cell*. Elsevier, 138(3), pp. 576–591. doi: 10.1016/j.cell.2009.06.015.

Choubey, D. and Panchanathan, R. (2017) 'Absent in Melanoma 2 proteins in SLE', *Clinical Immunology*, 176, pp. 42–48. doi: https://doi.org/10.1016/j.clim.2016.12.011.

Christensen, M. H. *et al.* (2016) 'HSV-1 ICP27 targets the TBK1-activated STING signalsome to inhibit virus-induced type I IFN expression', *The EMBO Journal*. John Wiley & Sons, Ltd, 35(13), pp. 1385–1399. doi: https://doi.org/10.15252/embj.201593458.

Christensen, M. H. and Paludan, S. R. (2017) 'Viral evasion of DNA-stimulated innate immune responses', (January 2016), pp. 4–13. doi: 10.1038/cmi.2016.06.

Civril, F. *et al.* (2013) 'Structural mechanism of cytosolic DNA sensing by cGAS', *Nature*, 498(7454), pp. 332–337. doi: 10.1038/nature12305.

Clark, K. *et al.* (2011) 'Novel cross-talk within the IKK family controls innate immunity', *Biochemical Journal*, 434(1), pp. 93–104. doi: 10.1042/BJ20101701.

Condit, R. C., Moussatche, N. and Traktman, P. B. T.-A. in V. R. (2006) 'In A Nutshell: Structure and Assembly of the Vaccinia Virion', in. Academic Press, pp. 31–124. doi: https://doi.org/10.1016/S0065-3527(06)66002-8.

Conrady, C. D. *et al.* (2012) 'Resistance to HSV-1 infection in the epithelium resides with the novel innate sensor, IFI-16', *Mucosal Immunology*, 5(2), pp. 173–183. doi: 10.1038/mi.2011.63.

Crow, Y. J. (2013) 'Aicardi-Goutières syndrome', *Handbook of Clinical Neurology*,

113, pp. 1629–1635. doi: 10.1016/B978-0-444-59565-2.00031-9.

Cunha, C. W. *et al.* (2015) 'Widely Used Herpes Simplex Virus 1 ICP0 Deletion Mutant Strain dl1403 and Its Derivative Viruses Do Not Express Glycoprotein C Due to a Secondary Mutation in the gC Gene', *PloS one*. Public Library of Science, 10(7), pp. e0131129–e0131129. doi: 10.1371/journal.pone.0131129.

Dai-Ju, J. Q. *et al.* (2006) 'ICP27 Interacts with the C-Terminal Domain of RNA Polymerase II and Facilitates Its Recruitment to Herpes Simplex Virus 1 Transcription Sites, Where It Undergoes Proteasomal Degradation during Infection', *Journal of Virology*, 80(7), pp. 3567 LP – 3581. doi: 10.1128/JVI.80.7.3567-3581.2006.

Dai, P. *et al.* (2014) 'Modified vaccinia virus Ankara triggers type I IFN production in murine conventional dendritic cells via a cGAS/STING-mediated cytosolic DNA-sensing pathway', *PLoS pathogens*. Public Library of Science, 10(4), pp. e1003989–e1003989. doi: 10.1371/journal.ppat.1003989.

Danastas, K., Miranda-Saksena, M. and Cunningham, A. L. (2020) 'Herpes Simplex Virus Type 1 Interactions with the Interferon System', *International Journal of Molecular Sciences* . doi: 10.3390/ijms21145150.

Davis, A. J., Chen, B. P. C. and Chen, D. J. (2014) 'DNA-PK: a dynamic enzyme in a versatile DSB repair pathway', *DNA repair*. 2014/03/27, 17, pp. 21–29. doi: 10.1016/j.dnarep.2014.02.020.

Delaloye, J. *et al.* (2009) 'Innate immune sensing of modified vaccinia virus Ankara (MVA) is mediated by TLR2-TLR6, MDA-5 and the NALP3 inflammasome', *PLoS pathogens*. 2009/06/19. Public Library of Science, 5(6), pp. e1000480–e1000480. doi: 10.1371/journal.ppat.1000480.

Delphine, C.-L. *et al.* (2013) 'The Viral Ubiquitin Ligase ICP0 Is neither Sufficient nor Necessary for Degradation of the Cellular DNA Sensor IFI16 during Herpes Simplex Virus 1 Infection', *Journal of Virology*. American Society for Microbiology, 87(24), pp. 13422–13432. doi: 10.1128/JVI.02474-13.

Dhuriya, Y. K. and Sharma, D. (2018) 'Necroptosis: a regulated inflammatory mode of cell death', *Journal of Neuroinflammation*, 15(1), p. 199. doi: 10.1186/s12974-018-1235-0.

Diner, E. J. *et al.* (2013) 'The innate immune DNA sensor cGAS produces a noncanonical cyclic dinucleotide that activates human STING', *Cell reports*. 2013/05/23, 3(5), pp. 1355–1361. doi: 10.1016/j.celrep.2013.05.009.

Dobbs, N. *et al.* (2015) 'STING Activation by Translocation from the ER Is Associated with Infection and Autoinflammatory Disease', *Cell host & microbe*. 2015/07/30, 18(2), pp. 157–168. doi: 10.1016/j.chom.2015.07.001.

Doitsh, G. *et al.* (2014) 'Cell death by pyroptosis drives CD4 T-cell depletion in HIV-1 infection', *Nature*, 505(7484), pp. 509–514. doi: 10.1038/nature12940.

Durocher, D. and Jackson, S. P. (2001) 'DNA-PK, ATM and ATR as sensors of DNA damage: variations on a theme?', *Current Opinion in Cell Biology*, 13(2), pp. 225–231. doi: https://doi.org/10.1016/S0955-0674(00)00201-5.

E., J. K., Leela, C. and Bala, C. (2013) 'Herpes Simplex Virus 1 Infection Induces Activation and Subsequent Inhibition of the IFI16 and NLRP3 Inflammasomes', *Journal of Virology*. American Society for Microbiology, 87(9), pp. 5005–5018. doi: 10.1128/JVI.00082-13.

Eaglesham, J. B. *et al.* (2019) 'Viral and metazoan poxins are cGAMP-specific nucleases that restrict cGAS–STING signalling', *Nature*, 566(7743), pp. 259–263. doi: 10.1038/s41586-019-0928-6.

Eric, L., Saskia, S. and Erik, F.-P. (2014) 'Adenovirus Detection by the cGAS/STING/TBK1 DNA Sensing Cascade', *Journal of Virology*. American Society for Microbiology, 88(2), pp. 974–981. doi: 10.1128/JVI.02702-13.

Esenboga, S. *et al.* (2018) 'Two siblings with PRKDC defect who presented with cutaneous granulomas and review of the literature', *Clinical Immunology*, 197, pp. 1–5. doi: https://doi.org/10.1016/j.clim.2018.08.002.

Falck, J., Coates, J. and Jackson, S. P. (2005) 'Conserved modes of recruitment of ATM, ATR and DNA-PKcs to sites of DNA damage', *Nature*, 434(7033), pp. 605–611. doi: 10.1038/nature03442.

Ferguson, B. J. *et al.* (2012) 'DNA-PK is a DNA sensor for IRF-3-dependent innate immunity', *eLife*, 2012(1). doi: 10.7554/eLife.00047.

Fiola, S. *et al.* (2010) 'TLR9 Contributes to the Recognition of EBV by Primary Monocytes and Plasmacytoid Dendritic Cells', *The Journal of Immunology*, 185(6), pp. 3620 LP – 3631. doi: 10.4049/jimmunol.0903736.

Fitzgerald, K. A. *et al.* (2003) 'IKKε and TBK1 are essential components of the IRF3 signaling pathway', *Nature Immunology*, 4(5), pp. 491–496. doi: 10.1038/ni921.

Fitzgerald, K. A. and Kagan, J. C. (2020) 'Toll-like Receptors and the Control of Immunity', *Cell*. Elsevier, 180(6), pp. 1044–1066. doi: 10.1016/j.cell.2020.02.041.

FLECK, M. *et al.* (1999) 'Herpes Simplex Virus Type 2 Infection Induced Apoptosis in Peritoneal Macrophages Independent of Fas and Tumor Necrosis Factor-Receptor Signaling', *Viral Immunology*. Mary Ann Liebert, Inc., publishers, 12(3), pp. 263–275. doi: 10.1089/vim.1999.12.263.

Fok, J. H. L. *et al.* (2019) 'AZD7648 is a potent and selective DNA-PK inhibitor that enhances radiation, chemotherapy and olaparib activity', *Nature Communications*, 10(1), p. 5065. doi: 10.1038/s41467-019-12836-9.

Ford, E. and Thanos, D. (2010) 'The transcriptional code of human IFN-β gene expression', *Biochimica et Biophysica Acta (BBA) - Gene Regulatory Mechanisms*, 1799(3), pp. 328–336. doi: https://doi.org/10.1016/j.bbagrm.2010.01.010.

Fortier, M.-E. *et al.* (2004) 'The viral mimic, polyinosinic:polycytidylic acid, induces fever in rats via an interleukin-1-dependent mechanism', *American Journal of Physiology-Regulatory, Integrative and Comparative Physiology*. American Physiological Society, 287(4), pp. R759–R766. doi: 10.1152/ajpregu.00293.2004.

Franz, K. M. *et al.* (2018) 'STING-dependent translation inhibition restricts RNA virus replication', *Proceedings of the National Academy of Sciences*, 115(9), p. E2058 LP-E2067. doi: 10.1073/pnas.1716937115.

Fujii, Y. *et al.* (1999) 'Crystal structure of an IRF-DNA complex reveals novel DNA recognition and cooperative binding to a tandem repeat of core sequences', *EMBO Journal*, 18(18), pp. 5028–5041. doi: 10.1093/emboj/18.18.5028.

Fujimori, A. *et al.* (1997) 'The MurineDNA-PKcsGene Consists of 86 Exons Dispersed in More Than 250 kb', *Genomics*, 45(1), pp. 194–199. doi: https://doi.org/10.1006/geno.1997.4919.

Gaidt, M. M. *et al.* (2017) 'The DNA Inflammasome in Human Myeloid Cells Is Initiated by a STING-Cell Death Program Upstream of NLRP3', *Cell*. Elsevier, 171(5), pp. 1110-1124.e18. doi: 10.1016/j.cell.2017.09.039.

Galvan, V. and Roizman, B. (1998) 'Herpes simplex virus 1 induces and blocks apoptosis at multiple steps during infection and protects cells from exogenous inducers in a cell-type-dependent manner', *Proceedings of the National Academy of Sciences of the United States of America*. The National Academy of Sciences, 95(7), pp. 3931–3936. doi: 10.1073/pnas.95.7.3931.

Gao, D. *et al.* (2013) 'Cyclic GMP-AMP synthase is an innate immune sensor of HIV and other retroviruses', *Science*, 341(6148), pp. 903–906. doi: 10.1126/science.1240933.

Gao, P. *et al.* (2013) 'Cyclic [G(2′,5′)pA(3′,5′)p] Is the Metazoan Second Messenger Produced by DNA-Activated Cyclic GMP-AMP Synthase', *Cell*. Elsevier, 153(5), pp. 1094–1107. doi: 10.1016/j.cell.2013.04.046.

García-Arriaza, J. *et al.* (2013) 'Improving Adaptive and Memory Immune Responses of an HIV/AIDS Vaccine Candidate MVA-B by Deletion of Vaccinia Virus Genes (C6L and K7R) Blocking Interferon Signaling Pathways', *PloS one*. Public Library of Science, 8(6), pp. e66894–e66894. doi: 10.1371/journal.pone.0066894.

Georgana, I. *et al.* (2018) 'Virulent Poxviruses Inhibit DNA Sensing by Preventing STING Activation', *Journal of Virology*. Edited by J. U. Jung, 92(10), pp. e02145-17. doi: 10.1128/JVI.02145-17.

Giffin, W. *et al.* (1996) 'Sequence-specific DNA binding by Ku autoantigen and its effects on transcription', *Nature*, 380(6571), pp. 265–268. doi: 10.1038/380265a0.

Goebel, S. J. *et al.* (1990) 'The complete DNA sequence of vaccinia virus', *Virology*, 179(1), pp. 247–266. doi: https://doi.org/10.1016/0042-6822(90)90294-2.

Goubau, D., Deddouche, S. and Reis e Sousa, C. (2013) 'Cytosolic Sensing of Viruses', *Immunity*. Elsevier, 38(5), pp. 855–869. doi: 10.1016/j.immuni.2013.05.007.

Gui, X. *et al.* (2019) 'Autophagy induction via STING trafficking is a primordial function of the cGAS pathway', *Nature*, 567(7747), pp. 262–266. doi: 10.1038/s41586-019-1006-9.

Guo, H. *et al.* (2018) 'Species-independent contribution of ZBP1/DAI/DLM-1-triggered necroptosis in host defense against HSV1', *Cell death & disease*. Nature Publishing Group UK, 9(8), p. 816. doi: 10.1038/s41419-018-0868-3.

Gupta, S. and Meek, K. (2005) 'The leucine rich region of DNA-PKcs contributes to its innate DNA affinity', *Nucleic Acids Research*, 33(22), pp. 6972–6981. doi: 10.1093/nar/gki990.

Hamming, O. J. *et al.* (2013) 'Interferon lambda 4 signals via the IFNλ receptor to regulate antiviral activity against HCV and coronaviruses', *The EMBO Journal*. John Wiley & Sons, Ltd, 32(23), pp. 3055–3065. doi: https://doi.org/10.1038/emboj.2013.232.

Hansen, K. *et al.* (2014) 'Listeria monocytogenes induces IFNβ expression through an IFI16-, cGAS- and STING-dependent pathway', *The EMBO Journal*. John Wiley & Sons, Ltd, 33(15), pp. 1654–1666. doi: https://doi.org/10.15252/embj.201488029.

He, T. *et al.* (2020) 'Host shutoff activity of VHS and SOX-like proteins: role in viral

survival and immune evasion', *Virology Journal*, 17(1), p. 68. doi: 10.1186/s12985-020-01336-8.

Hemann, E. A., Gale Jr, M. and Savan, R. (2017) 'Interferon Lambda Genetics and Biology in Regulation of Viral Control', *Frontiers in immunology*. Frontiers Media S.A., 8, p. 1707. doi: 10.3389/fimmu.2017.01707.

Hemmi, H. *et al.* (2000) 'A Toll-like receptor recognizes bacterial DNA', *Nature*, 408(6813), pp. 740–745. doi: 10.1038/35047123.

Hew, K. *et al.* (2015) 'VP22 core domain from Herpes simplex virus 1 reveals a surprising structural conservation in both the Alpha- and Gammaherpesvirinae subfamilies', *Journal of General Virology*. Microbiology Society, 96(6), pp. 1436–1445. doi: https://doi.org/10.1099/vir.0.000078.

Hickman, H. D. *et al.* (2013) 'Anatomically Restricted Synergistic Antiviral Activities of Innate and Adaptive Immune Cells in the Skin', *Cell Host & Microbe*. Elsevier, 13(2), pp. 155–168. doi: 10.1016/j.chom.2013.01.004.

Hochrein, H. *et al.* (2004) 'Herpes simplex virus type-1 induces IFN-α production via Toll-like receptor 9-dependent and -independent pathways', *Proceedings of the National Academy of Sciences of the United States of America*, 101(31), pp. 11416 LP – 11421. doi: 10.1073/pnas.0403555101.

Hoffmann, H.-H., Schneider, W. M. and Rice, C. M. (2015) 'Interferons and viruses: an evolutionary arms race of molecular interactions', *Trends in immunology*. 2015/02/20, 36(3), pp. 124–138. doi: 10.1016/j.it.2015.01.004.

Honda, K. *et al.* (2005) 'IRF-7 is the master regulator of type-I interferon-dependent immune responses', *Nature*, 434(7034), pp. 772–777. doi: 10.1038/nature03464.

Honda, K., Takaoka, A. and Taniguchi, T. (2006) 'Type I Inteferon Gene Induction by the Interferon Regulatory Factor Family of Transcription Factors', *Immunity*. Cell Press, 25(3), pp. 349–360. doi: 10.1016/J.IMMUNI.2006.08.009.

Horan, K. A. *et al.* (2013) 'Proteasomal degradation of herpes simplex virus capsids in macrophages releases DNA to the cytosol for recognition by DNA sensors', *Journal of immunology (Baltimore, Md. : 1950)*. 2013/01/23, 190(5), pp. 2311–2319. doi: 10.4049/jimmunol.1202749.

Hornung, V. *et al.* (2009) 'AIM2 recognizes cytosolic dsDNA and forms a caspase-1-activating inflammasome with ASC', *Nature*, 458(7237), pp. 514–518. doi: 10.1038/nature07725.

Hristova, D. B., Lauer, K. B. and Ferguson, B. J. (2020) 'Viral interactions with non-homologous end-joining: a game of hide-and-seek', *Journal of General Virology*. Microbiology Society, 101(11), pp. 1133–1144. doi: https://doi.org/10.1099/jgv.0.001478.

Huang, Z. *et al.* (2015) 'RIP1/RIP3 Binding to HSV-1 ICP6 Initiates Necroptosis to Restrict Virus Propagation in Mice', *Cell Host & Microbe*. Elsevier, 17(2), pp. 229–242. doi: 10.1016/j.chom.2015.01.002.

Hultmark, D. (1994) 'Macrophage Differentiation Marker MyD88 Is a Member of the Toll/IL-1 Receptor Family', *Biochemical and Biophysical Research Communications*, 199(1), pp. 144–146. doi: https://doi.org/10.1006/bbrc.1994.1206.

Huxford, T. *et al.* (1998) 'The Crystal Structure of the IκBα/NF-κB Complex Reveals Mechanisms of NF-κB Inactivation', *Cell*. Elsevier, 95(6), pp. 759–770. doi: 10.1016/S0092-8674(00)81699-2.

Isaacs, A., Cox, R. A. and Rotem, Z. (1963) 'FOREIGN NUCLEIC ACIDS AS THE STIMULUS TO MAKE INTERFERON', *The Lancet*, 282(7299), pp. 113–116. doi: 10.1016/S0140-6736(63)92585-6.

Isaacs, A. and Lindenmann, J. (1957) 'Virus interference. I. The interferon', *Proceedings of the Royal Society of London. Series B-Biological Sciences*. The Royal Society London, 147(927), pp. 258–267.

Ishii, K. J. *et al.* (2006) 'A toll-like receptor-independent antiviral response induced by double-stranded B-form DNA', *Nature Immunology*, 7(1), pp. 40–48. doi: 10.1038/ni1282.

Ishii, K. J. *et al.* (2008) 'TANK-binding kinase-1 delineates innate and adaptive immune responses to DNA vaccines', *Nature*, 451(7179), pp. 725–729. doi: 10.1038/nature06537.

Ishikawa, H. and Barber, G. N. (2008) 'STING is an endoplasmic reticulum adaptor that facilitates innate immune signalling', *Nature*, 455(7213), pp. 674–678. doi: 10.1038/nature07317.

Ishikawa, H., Ma, Z. and Barber, G. N. (2009) 'STING regulates intracellular DNA-mediated, type i interferon-dependent innate immunity', *Nature*, 461(7265), pp. 788–792. doi: 10.1038/nature08476.

Jakobsen, M. R. *et al.* (2013) 'IFI16 senses DNA forms of the lentiviral replication cycle and controls HIV-1 replication', *Proceedings of the National Academy of Sciences*, 110(48), p. E4571 LP-E4580. doi: 10.1073/pnas.1311669110.

Janeway, C. A. and Medzhitov, R. (2002) 'Innate Immune Recognition', *Annual Review of Immunology*. Annual Reviews, 20(1), pp. 197–216. doi: 10.1146/annurev.immunol.20.083001.084359.

Jesper, M. *et al.* (2010) 'Early Innate Recognition of Herpes Simplex Virus in Human Primary Macrophages Is Mediated via the MDA5/MAVS-Dependent and MDA5/MAVS/RNA Polymerase III-Independent Pathways', *Journal of Virology*. American Society for Microbiology, 84(21), pp. 11350–11358. doi: 10.1128/JVI.01106-10.

Jiaxi, W. *et al.* (2013) 'Cyclic GMP-AMP Is an Endogenous Second Messenger in Innate Immune Signaling by Cytosolic DNA', *Science*. American Association for the Advancement of Science, 339(6121), pp. 826–830. doi: 10.1126/science.1229963.

Jin, L. *et al.* (2008) 'MPYS, a Novel Membrane Tetraspanner, Is Associated with Major Histocompatibility Complex Class II and Mediates Transduction of Apoptotic Signals', *Molecular and Cellular Biology*, 28(16), pp. 5014–5026. doi: 10.1128/MCB.00640-08.

Jin, T. *et al.* (2012) 'Structures of the HIN Domain:DNA Complexes Reveal Ligand Binding and Activation Mechanisms of the AIM2 Inflammasome and IFI16 Receptor', *Immunity*. Elsevier, 36(4), pp. 561–571. doi: 10.1016/j.immuni.2012.02.014.

Johnson, K. E. *et al.* (2014) 'IFI16 restricts HSV-1 replication by accumulating on the hsv-1 genome, repressing HSV-1 gene expression, and directly or indirectly modulating histone modifications', *PLoS pathogens*. Public Library of Science, 10(11), pp. e1004503–e1004503. doi: 10.1371/journal.ppat.1004503.

Jønsson, K. L. *et al.* (2017) 'IFI16 is required for DNA sensing in human macrophages by promoting production and function of cGAMP', *Nature Communications*, 8(1), p. 14391. doi: 10.1038/ncomms14391.

Justice, J. L. *et al.* (2021) 'Systematic profiling of protein complex dynamics reveals DNA-PK phosphorylation of IFI16 en route to herpesvirus immunity', *Science advances*. American Association for the Advancement of Science, 7(25), p. eabg6680. doi: 10.1126/sciadv.abg6680.

Kalamvoki, M. and Roizman, B. (2014) 'HSV-1 degrades, stabilizes, requires, or is stung by STING depending on ICP0, the US3 protein kinase, and cell derivation', *Proceedings of the National Academy of Sciences*, 111(5), p. E611 LP-E617. doi: 10.1073/pnas.1323414111.

Karpova, A. Y. *et al.* (2002) 'Interferon regulatory factor-3 is an in vivo target of

DNA-PK.', *Proc Natl Acad Sci U S A*, 99(5), pp. 2818–2823. doi: 10.1073/pnas.052713899.

Kato, H., Takahasi, K. and Fujita, T. (2011) 'RIG-I-like receptors: cytoplasmic sensors for non-self RNA', *Immunological Reviews*. John Wiley & Sons, Ltd, 243(1), pp. 91–98. doi: https://doi.org/10.1111/j.1600-065X.2011.01052.x.

Kawai, T. *et al.* (2005) 'IPS-1, an adaptor triggering RIG-I- and Mda5-mediated type I interferon induction', *Nature Immunology*, 6(10), pp. 981–988. doi: 10.1038/ni1243.

Kawai, T. and Akira, S. (2011) 'Toll-like Receptors and Their Crosstalk with Other Innate Receptors in Infection and Immunity', *Immunity*. Elsevier, 34(5), pp. 637–650. doi: 10.1016/j.immuni.2011.05.006.

Kerur, N. *et al.* (2011) 'IFI16 acts as a nuclear pathogen sensor to induce the inflammasome in response to Kaposi Sarcoma-associated herpesvirus infection', *Cell Host and Microbe*, 9(5), pp. 363–375. doi: 10.1016/j.chom.2011.04.008.

Kienker, L. J., Shin, E. K. and Meek, K. (2000) 'Both V(D)J recombination and radioresistance require DNA-PK kinase activity, though minimal levels suffice for V(D)J recombination.', *Nucleic acids research*. Oxford University Press, 28(14), pp. 2752–61. Available at: http://www.ncbi.nlm.nih.gov/pubmed/10908332 (Accessed: 11 June 2018).

Kim, T. *et al.* (2010) 'Aspartate-glutamate-alanine-histidine box motif (DEAH)/RNA helicase A helicases sense microbial DNA in human plasmacytoid dendritic cells', *Proceedings of the National Academy of Sciences*, 107(34), pp. 15181 LP – 15186. doi: 10.1073/pnas.1006539107.

Kim, T. K. and Maniatis, T. (1997) 'The Mechanism of Transcriptional Synergy of an In Vitro Assembled Interferon-β Enhanceosome', *Molecular Cell*. Elsevier, 1(1), pp. 119–129. doi: 10.1016/S1097-2765(00)80013-1.

Kinner, A. *et al.* (2008) 'Gamma-H2AX in recognition and signaling of DNA double-strand breaks in the context of chromatin', *Nucleic acids research*. 2008/09/04. Oxford University Press, 36(17), pp. 5678–5694. doi: 10.1093/nar/gkn550.

Klaus, S. *et al.* (1996) 'RAG Mutations in Human B Cell-Negative SCID', *Science*. American Association for the Advancement of Science, 274(5284), pp. 97–99. doi: 10.1126/science.274.5284.97.

Kondo, T. *et al.* (2013) 'DNA damage sensor MRE11 recognizes cytosolic double-stranded DNA and induces type I interferon by regulating STING trafficking', *Proceedings of the National Academy of Sciences*, 110(8), pp. 2969–2974. doi:

10.1073/pnas.1222694110.

Konno, H., Konno, K. and Barber, G. N. (2013) 'XCyclic dinucleotides trigger ULK1 (ATG1) phosphorylation of STING to prevent sustained innate immune signaling', *Cell*, 155(3). doi: 10.1016/j.cell.2013.09.049.

Kotenko, S. V *et al.* (2003) 'IFN-λs mediate antiviral protection through a distinct class II cytokine receptor complex', *Nature Immunology*, 4(1), pp. 69–77. doi: 10.1038/ni875.

Kotula, E. *et al.* (2013) 'DNA-PK target identification reveals novel links between DNA repair signaling and cytoskeletal regulation', *PloS one*. Public Library of Science, 8(11), pp. e80313–e80313. doi: 10.1371/journal.pone.0080313.

Koyama, A. H. and Adachi, A. (1997) 'Induction of apoptosis by herpes simplex virus type 1.', *Journal of General Virology*. Microbiology Society, 78(11), pp. 2909–2912. doi: https://doi.org/10.1099/0022-1317-78-11-2909.

Kranzusch, P. J. *et al.* (2013) 'Structure of Human cGAS Reveals a Conserved Family of Second-Messenger Enzymes in Innate Immunity', *Cell Reports*. Elsevier, 3(5), pp. 1362–1368. doi: 10.1016/j.celrep.2013.05.008.

Krausgruber, T. *et al.* (2020) 'Structural cells are key regulators of organ-specific immune responses', *Nature*, 583(7815), pp. 296–302. doi: 10.1038/s41586-020-2424-4.

Kruse, M. *et al.* (2000) 'Mature dendritic cells infected with herpes simplex virus type 1 exhibit inhibited T-cell stimulatory capacity', *Journal of virology*. American Society for Microbiology, 74(15), pp. 7127–7136. doi: 10.1128/jvi.74.15.7127-7136.2000.

Kujirai, T. *et al.* (2020) 'Structural basis for the inhibition of cGAS by nucleosomes', *Science (New York, N.Y.)*. 2020/09/10, 370(6515), pp. 455–458. doi: 10.1126/science.abd0237.

Kukhanova, M. K., Korovina, A. N. and Kochetkov, S. N. (2014) 'Human herpes simplex virus: Life cycle and development of inhibitors', *Biochemistry (Moscow)*, 79(13), pp. 1635–1652. doi: 10.1134/S0006297914130124.

Kulesza, P. and Lieber, M. R. (1998) 'DNA-PK is essential only for coding joint formation in V(D)J recombination', *Nucleic acids research*, 26(17), pp. 3944–3948. doi: 10.1093/nar/26.17.3944.

Kurimasa, A. *et al.* (1999) 'Requirement for the kinase activity of human DNA-

dependent protein kinase catalytic subunit in DNA strand break rejoining', *Molecular and cellular biology*. American Society for Microbiology, 19(5), pp. 3877–3884. doi: 10.1128/MCB.19.5.3877.

Lahaye, X. *et al.* (2018) 'NONO Detects the Nuclear HIV Capsid to Promote cGAS-Mediated Innate Immune Activation', *Cell*. Elsevier, 175(2), pp. 488-501.e22. doi: 10.1016/j.cell.2018.08.062.

Leahy, J. J. J. *et al.* (2004) 'Identification of a highly potent and selective DNA-dependent protein kinase (DNA-PK) inhibitor (NU7441) by screening of chromenone libraries', *Bioorganic & Medicinal Chemistry Letters*, 14(24), pp. 6083–6087. doi: https://doi.org/10.1016/j.bmcl.2004.09.060.

Lees-Miller, S. P. *et al.* (1996) 'Attenuation of DNA-dependent protein kinase activity and its catalytic subunit by the herpes simplex virus type 1 transactivator ICP0.', *Journal of Virology*, 70(11), pp. 7471 LP – 7477. Available at: http://jvi.asm.org/content/70/11/7471.abstract.

Lei, W., Mingyue, W. and Xuetao, C. (2019) 'Nuclear hnRNPA2B1 initiates and amplifies the innate immune response to DNA viruses', *Science*. American Association for the Advancement of Science, 365(6454), p. eaav0758. doi: 10.1126/science.aav0758.

Lemaitre, B. *et al.* (1996) 'The Dorsoventral Regulatory Gene Cassette spätzle/Toll/cactus Controls the Potent Antifungal Response in Drosophila Adults', *Cell*. Elsevier, 86(6), pp. 973–983. doi: 10.1016/S0092-8674(00)80172-5.

Leopardi, R. and Roizman, B. (1996) 'The herpes simplex virus major regulatory protein ICP4 blocks apoptosis induced by the virus or by hyperthermia', *Proceedings of the National Academy of Sciences of the United States of America*, 93(18), pp. 9583–9587. doi: 10.1073/pnas.93.18.9583.

Li, T. *et al.* (2012) 'Acetylation modulates cellular distribution and DNA sensing ability of interferon-inducible protein IFI16', *Proceedings of the National Academy of Sciences*, 109(26), pp. 10558–10563. doi: 10.1073/pnas.1203447109.

Li, X.-D. *et al.* (2013) 'Pivotal roles of cGAS-cGAMP signaling in antiviral defense and immune adjuvant effects', *Science (New York, N.Y.)*. 2013/08/29, 341(6152), pp. 1390–1394. doi: 10.1126/science.1244040.

Li, Y. *et al.* (2015) 'TLR3 ligand Poly IC Attenuates Reactive Astrogliosis and Improves Recovery of Rats after Focal Cerebral Ischemia', *CNS Neuroscience &*

Therapeutics. John Wiley & Sons, Ltd, 21(11), pp. 905–913. doi: https://doi.org/10.1111/cns.12469.

Li, Y. *et al.* (2016) 'Cytoplasm-Translocated Ku70/80 Complex Sensing of HBV DNA Induces Hepatitis-Associated Chemokine Secretion.', *Frontiers in immunology*. Frontiers Media SA, 7, p. 569. doi: 10.3389/fimmu.2016.00569.

Lijun, S. *et al.* (2013) 'Cyclic GMP-AMP Synthase Is a Cytosolic DNA Sensor That Activates the Type I Interferon Pathway', *Science*. American Association for the Advancement of Science, 339(6121), pp. 786–791. doi: 10.1126/science.1232458.

Lin, R. *et al.* (1998) 'Virus-dependent phosphorylation of the IRF-3 transcription factor regulates nuclear translocation, transactivation potential, and proteasome-mediated degradation', *Molecular and cellular biology*. American Society for Microbiology, 18(5), pp. 2986–2996. doi: 10.1128/MCB.18.5.2986.

Lin, R. *et al.* (2004) 'The Herpes Simplex Virus ICP0 RING Finger Domain Inhibits IRF3- and IRF7-Mediated Activation of Interferon-Stimulated Genes', *Journal of Virology*, 78(4), pp. 1675 LP – 1684. doi: 10.1128/JVI.78.4.1675-1684.2004.

Liu, H. *et al.* (2018) 'Nuclear cGAS suppresses DNA repair and promotes tumorigenesis', *Nature*, 563(7729), pp. 131–136. doi: 10.1038/s41586-018-0629-6.

Liu, S. *et al.* (2015) 'Phosphorylation of innate immune adaptor proteins MAVS, STING, and TRIF induces IRF3 activation', *Science*, 347(6227). doi: 10.1126/science.aaa2630.

Looker, K. J. *et al.* (2015) 'Global and Regional Estimates of Prevalent and Incident Herpes Simplex Virus Type 1 Infections in 2012', *PloS one*. Public Library of Science, 10(10), pp. e0140765–e0140765. doi: 10.1371/journal.pone.0140765.

Lopez-Pelaez, M. *et al.* (2014) 'Protein kinase IKKβ-catalyzed phosphorylation of IRF5 at Ser462 induces its dimerization and nuclear translocation in myeloid cells', *Proceedings of the National Academy of Sciences*, 111(49), pp. 17432 LP – 17437. doi: 10.1073/pnas.1418399111.

Luecke, S. and Paludan, S. R. (2015) 'Innate Recognition of Alphaherpesvirus DNA', *Advances in Virus Research*, 92, pp. 63–100. doi: 10.1016/bs.aivir.2014.11.003.

Lund, J. *et al.* (2003) 'Toll-like Receptor 9–mediated Recognition of Herpes Simplex Virus-2 by Plasmacytoid Dendritic Cells ', *Journal of Experimental Medicine*, 198(3), pp. 513–520. doi: 10.1084/jem.20030162.

M., D. C. *et al.* (2016) 'Nuclear envelope rupture and repair during cancer cell

migration', *Science*. American Association for the Advancement of Science, 352(6283), pp. 353–358. doi: 10.1126/science.aad7297.

Mahaney, B. L., Meek, K. and Lees-Miller, S. P. (2009) 'Repair of ionizing radiation-induced DNA double-strand breaks by non-homologous end-joining.', *The Biochemical journal*, 417(3), pp. 639–50. doi: 10.1042/BJ20080413.

Mamane, Y. *et al.* (1999) 'Interferon regulatory factors: the next generation', *Gene*, 237(1), pp. 1–14. doi: https://doi.org/10.1016/S0378-1119(99)00262-0.

Manzanillo, P. S. *et al.* (2012) 'Mycobacterium tuberculosis activates the DNA-dependent cytosolic surveillance pathway within macrophages', *Cell host & microbe*, 11(5), pp. 469–480. doi: 10.1016/j.chom.2012.03.007.

Mari, P.-O. *et al.* (2006) 'Dynamic assembly of end-joining complexes requires interaction between Ku70/80 and XRCC4', *Proceedings of the National Academy of Sciences*, 103(49), pp. 18597–18602. doi: 10.1073/pnas.0609061103.

Marié, I., Durbin, J. E. and Levy, D. E. (1998) 'Differential viral induction of distinct interferon-alpha genes by positive feedback through interferon regulatory factor-7', *The EMBO journal*, 17(22), pp. 6660–6669. doi: 10.1093/emboj/17.22.6660.

Martine, A. and A., B. J. (1999) 'The Herpes Simplex Virus Type 1 Regulatory Protein ICP27 Is Required for the Prevention of Apoptosis in Infected Human Cells', *Journal of Virology*. American Society for Microbiology, 73(4), pp. 2803–2813. doi: 10.1128/JVI.73.4.2803-2813.1999.

Martine, A., Jennifer, O. and A., B. J. (1999) 'Induction and Prevention of Apoptosis in Human HEp-2 Cells by Herpes Simplex Virus Type 1', *Journal of Virology*. American Society for Microbiology, 73(12), pp. 10359–10370. doi: 10.1128/JVI.73.12.10359-10370.1999.

Maruzuru, Y. *et al.* (2018) 'Herpes Simplex Virus 1 VP22 Inhibits AIM2-Dependent Inflammasome Activation to Enable Efficient Viral Replication', *Cell Host & Microbe*. Elsevier, 23(2), pp. 254-265.e7. doi: 10.1016/j.chom.2017.12.014.

Matsushima, N. *et al.* (2007) 'Comparative sequence analysis of leucine-rich repeats (LRRs) within vertebrate toll-like receptors', *BMC Genomics*, 8(1), p. 124. doi: 10.1186/1471-2164-8-124.

McGuire, T. C. and Poppie, M. J. (1973) 'Hypogammaglobulinemia and thymic hypoplasia in horses: a primary combined immunodeficiency disorder', *Infection and immunity*, 8(2), pp. 272–277. doi: 10.1128/iai.8.2.272-277.1973.

Meek, K. *et al.* (2001) 'SCID in Jack Russell Terriers: A New Animal Model of DNA-PKcs Deficiency', *The Journal of Immunology*, 167(4), pp. 2142 LP – 2150. doi: 10.4049/jimmunol.167.4.2142.

Meek, K., Dang, V. and Lees-Miller, S. P. (2008) 'Chapter 2 DNA-PK', in *Advances in immunology*, pp. 33–58. doi: 10.1016/S0065-2776(08)00602-0.

Meers, P. and Mealy, T. (1994) 'Phospholipid Determinants for Annexin V Binding Sites and the Role of Tryptophan 187', *Biochemistry*. American Chemical Society, 33(19), pp. 5829–5837. doi: 10.1021/bi00185a022.

Megjugorac, N. J. *et al.* (2004) 'Virally stimulated plasmacytoid dendritic cells produce chemokines and induce migration of T and NK cells', *Journal of Leukocyte Biology*. John Wiley & Sons, Ltd, 75(3), pp. 504–514. doi: https://doi.org/10.1189/jlb.0603291.

Megjugorac, N. J., Gallagher, G. E. and Gallagher, G. (2009) 'Modulation of human plasmacytoid DC function by IFN-λ1 (IL-29)', *Journal of Leukocyte Biology*. John Wiley & Sons, Ltd, 86(6), pp. 1359–1363. doi: https://doi.org/10.1189/jlb.0509347.

Meylan, E. *et al.* (2005) 'Cardif is an adaptor protein in the RIG-I antiviral pathway and is targeted by hepatitis C virus', *Nature*, 437(7062), pp. 1167–1172. doi: 10.1038/nature04193.

Di Micco, A. *et al.* (2016) 'AIM2 inflammasome is activated by pharmacological disruption of nuclear envelope integrity', *Proceedings of the National Academy of Sciences*, 113(32), p. E4671 LP-E4680. doi: 10.1073/pnas.1602419113.

Michalski, S. *et al.* (2020) 'Structural basis for sequestration and autoinhibition of cGAS by chromatin', *Nature*, 587(7835), pp. 678–682. doi: 10.1038/s41586-020-2748-0.

Mikloska, Z., Bosnjak, L. and Cunningham, A. L. (2001) 'Immature monocyte-derived dendritic cells are productively infected with herpes simplex virus type 1', *Journal of virology*. American Society for Microbiology, 75(13), pp. 5958–5964. doi: 10.1128/JVI.75.13.5958-5964.2001.

Mingjian, D. and J., C. Z. (2018) 'DNA-induced liquid phase condensation of cGAS activates innate immune signaling', *Science*. American Association for the Advancement of Science, 361(6403), pp. 704–709. doi: 10.1126/science.aat1022.

Moeko, M. *et al.* (2011) 'DDX60, a DEXD/H Box Helicase, Is a Novel Antiviral Factor Promoting RIG-I-Like Receptor-Mediated Signaling', *Molecular and Cellular Biology*. American Society for Microbiology, 31(18), pp. 3802–3819. doi:

10.1128/MCB.01368-10.

Morchikh, M. *et al.* (2017) 'HEXIM1 and NEAT1 Long Non-coding RNA Form a Multi-subunit Complex that Regulates DNA-Mediated Innate Immune Response', *Molecular Cell*, 67(3), pp. 387-399.e5. doi: 10.1016/j.molcel.2017.06.020.

Mori, M. *et al.* (2004) 'Identification of Ser-386 of Interferon Regulatory Factor 3 as Critical Target for Inducible Phosphorylation That Determines Activation *', *Journal of Biological Chemistry*. Elsevier, 279(11), pp. 9698–9702. doi: 10.1074/jbc.M310616200.

Moshous, D. *et al.* (2001) 'Artemis, a Novel DNA Double-Strand Break Repair/V(D)J Recombination Protein, Is Mutated in Human Severe Combined Immune Deficiency', *Cell*. Elsevier, 105(2), pp. 177–186. doi: 10.1016/S0092-8674(01)00309-9.

Moss, B. (2013) 'Poxvirus DNA replication', *Cold Spring Harbor perspectives in biology*. Cold Spring Harbor Laboratory Press, 5(9), p. a010199. doi: 10.1101/cshperspect.a010199.

Mukai, K. *et al.* (2016) 'Activation of STING requires palmitoylation at the Golgi', *Nature Communications*, 7(1), p. 11932. doi: 10.1038/ncomms11932.

Müller, D. B. *et al.* (2004) 'Frontline: Induction of apoptosis and modulation of c-FLIPL and p53 in immature dendritic cells infected with herpes simplex virus', *European Journal of Immunology*. John Wiley & Sons, Ltd, 34(4), pp. 941–951. doi: https://doi.org/10.1002/eji.200324509.

Murray, P. J. (2007) 'The JAK-STAT Signaling Pathway: Input and Output Integration', *The Journal of Immunology*, 178(5), pp. 2623 LP – 2629. doi: 10.4049/jimmunol.178.5.2623.

Muruve, D. A. *et al.* (2008) 'The inflammasome recognizes cytosolic microbial and host DNA and triggers an innate immune response', *Nature*, 452(7183), pp. 103–107. doi: 10.1038/nature06664.

Napetschnig, J. and Wu, H. (2013) 'Molecular basis of NF-κB signaling', *Annual review of biophysics*. 2013/03/11, 42, pp. 443–468. doi: 10.1146/annurev-biophys-083012-130338.

Nguyen, M. L., Kraft, R. M. and Blaho, J. A. (2005) 'African green monkey kidney Vero cells require de novo protein synthesis for efficient herpes simplex virus 1-dependent apoptosis', *Virology*, 336(2), pp. 274–290. doi: https://doi.org/10.1016/j.virol.2005.03.026.

Niewolik, D. *et al.* (2006) 'DNA-PKcs Dependence of Artemis Endonucleolytic Activity, Differences between Hairpins and 5′ or 3′ Overhangs *', *Journal of Biological Chemistry*. Elsevier, 281(45), pp. 33900–33909. doi: 10.1074/jbc.M606023200.

Nightingale, K. *et al.* (2018) 'High-Definition Analysis of Host Protein Stability during Human Cytomegalovirus Infection Reveals Antiviral Factors and Viral Evasion Mechanisms', *Cell Host & Microbe*. Elsevier, 24(3), pp. 447-460.e11. doi: 10.1016/j.chom.2018.07.011.

Ogunjimi, B. *et al.* (2017) 'Inborn errors in RNA polymerase III underlie severe varicella zoster virus infections', *The Journal of Clinical Investigation*. The American Society for Clinical Investigation, 127(9), pp. 3543–3556. doi: 10.1172/JCI92280.

Ohto, U. and Shimizu, T. (2016) 'Structural aspects of nucleic acid-sensing Toll-like receptors', *Biophysical Reviews*, 8(1), pp. 33–43. doi: 10.1007/s12551-015-0187-1.

Okabe, Y. *et al.* (2005) 'Toll-like receptor-independent gene induction program activated by mammalian DNA escaped from apoptotic DNA degradation.', *The Journal of experimental medicine*, 202(10), pp. 1333–9. doi: 10.1084/jem.20051654.

Okude, H., Ori, D. and Kawai, T. (2021) 'Signaling Through Nucleic Acid Sensors and Their Roles in Inflammatory Diseases ', *Frontiers in Immunology* . Available at: https://www.frontiersin.org/article/10.3389/fimmu.2020.625833.

Omura, H. *et al.* (2016) 'Structural and Functional Analysis of DDX41: a bispecific immune receptor for DNA and cyclic dinucleotide', *Scientific Reports*, 6(1), p. 34756. doi: 10.1038/srep34756.

Orzalli, M. H. *et al.* (2015) 'cGAS-mediated stabilization of IFI16 promotes innate signaling during herpes simplex virus infection', *Proceedings of the National Academy of Sciences*, 112(14), pp. E1773–E1781. doi: 10.1073/pnas.1424637112.

Orzalli, M. H., DeLuca, N. A. and Knipe, D. M. (2012) 'Nuclear IFI16 induction of IRF-3 signaling during herpesviral infection and degradation of IFI16 by the viral ICP0 protein', *Proceedings of the National Academy of Sciences*, 109(44), p. E3008 LP-E3017. doi: 10.1073/pnas.1211302109.

Paludan, S. and Bowie, A. (2013) 'Immune Sensing of DNA', *Immunity*, pp. 870–880. doi: 10.1016/j.immuni.2013.05.004.

Paludan, S. R. *et al.* (2011) 'Recognition of herpesviruses by the innate immune system', *Nature Reviews Immunology*, 11(2), pp. 143–154. doi: 10.1038/nri2937.

Parekh, N. J. *et al.* (2019) 'Type I interferon-dependent CCL4 is induced by a cGAS/STING pathway that bypasses viral inhibition and protects infected tissue, independent of viral burden', *PLoS pathogens*. Public Library of Science, 15(10), pp. e1007778–e1007778. doi: 10.1371/journal.ppat.1007778.

Pathare, G. R. *et al.* (2020) 'Structural mechanism of cGAS inhibition by the nucleosome', *Nature*, 587(7835), pp. 668–672. doi: 10.1038/s41586-020-2750-6.

Payne, L. G. (1980) 'Significance of Extracellular Enveloped Virus in the in vitro and in vivo Dissemination of Vaccinia', *Journal of General Virology*. Microbiology Society, 50(1), pp. 89–100. doi: https://doi.org/10.1099/0022-1317-50-1-89.

Pestka, S., Krause, C. D. and Walter, M. R. (2004) 'Interferons, interferon-like cytokines, and their receptors', *Immunological Reviews*. John Wiley & Sons, Ltd, 202(1), pp. 8–32. doi: https://doi.org/10.1111/j.0105-2896.2004.00204.x.

Peters, N. E. *et al.* (2013) 'A mechanism for the inhibition of DNA-PK-mediated DNA sensing by a virus', *PLoS pathogens*. Public Library of Science, 9(10), pp. e1003649–e1003649. doi: 10.1371/journal.ppat.1003649.

Peterson, S. R. *et al.* (1995) 'Loss of the catalytic subunit of the DNA-dependent protein kinase in DNA double-strand-break-repair mutant mammalian cells', *Proceedings of the National Academy of Sciences of the United States of America*, 92(8), pp. 3171–3174. doi: 10.1073/pnas.92.8.3171.

Pham, T. H. *et al.* (2013) 'DNA sensing-independent inhibition of herpes simplex virus 1 replication by DAI/ZBP1', *Journal of virology*. 2013/01/02. American Society for Microbiology, 87(6), pp. 3076–3086. doi: 10.1128/JVI.02860-12.

Philipp, P. *et al.* (2021) 'Entry Mechanisms of Herpes Simplex Virus 1 into Murine Epidermis: Involvement of Nectin-1 and Herpesvirus Entry Mediator as Cellular Receptors', *Journal of Virology*. American Society for Microbiology, 89(1), pp. 262–274. doi: 10.1128/JVI.02917-14.

Prokunina-Olsson, L. *et al.* (2013) 'A variant upstream of IFNL3 (IL28B) creating a new interferon gene IFNL4 is associated with impaired clearance of hepatitis C virus', *Nature genetics*. 2013/01/06, 45(2), pp. 164–171. doi: 10.1038/ng.2521.

Q. Marín, M. *et al.* (2018) 'Removal of the C6 Vaccinia Virus Interferon-β Inhibitor in the Hepatitis C Vaccine Candidate MVA-HCV Elicited in Mice High Immunogenicity in Spite of Reduced Host Gene Expression', *Viruses* . doi: 10.3390/v10080414.

Radtke, K. *et al.* (2010) 'Plus- and minus-end directed microtubule motors bind

simultaneously to herpes simplex virus capsids using different inner tegument structures', *PLoS pathogens*. Public Library of Science, 6(7), pp. e1000991–e1000991. doi: 10.1371/journal.ppat.1000991.

Rathinam, V. A. K. *et al.* (2010) 'The AIM2 inflammasome is essential for host defense against cytosolic bacteria and DNA viruses', *Nature Immunology*, 11(5), pp. 395–402. doi: 10.1038/ni.1864.

Rathinam, V. A. K. and Fitzgerald, K. A. (2011) 'Cytosolic surveillance and antiviral immunity', *Current Opinion in Virology*, 1(6), pp. 455–462. doi: https://doi.org/10.1016/j.coviro.2011.11.004.

Régnier, C. H. *et al.* (1997) 'Identification and Characterization of an IκB Kinase', *Cell*. Elsevier, 90(2), pp. 373–383. doi: 10.1016/S0092-8674(00)80344-X.

Reinert, L. S. *et al.* (2016) 'Sensing of HSV-1 by the cGAS–STING pathway in microglia orchestrates antiviral defence in the CNS', *Nature Communications*, 7(1), p. 13348. doi: 10.1038/ncomms13348.

Rice, G. *et al.* (2007) 'Heterozygous Mutations in TREX1 Cause Familial Chilblain Lupus and Dominant Aicardi-Goutières Syndrome', *The American Journal of Human Genetics*, 80(4), pp. 811–815. doi: 10.1086/513443.

Rivera-Calzada, A. *et al.* (2007) 'Structural model of full-length human Ku70-Ku80 heterodimer and its recognition of DNA and DNA-PKcs', *EMBO reports*. 2006/12/08, 8(1), pp. 56–62. doi: 10.1038/sj.embor.7400847.

Roberts, K. L. and Smith, G. L. (2008) 'Vaccinia virus morphogenesis and dissemination', *Trends in Microbiology*. Elsevier, 16(10), pp. 472–479. doi: 10.1016/j.tim.2008.07.009.

Rothenfusser, S. *et al.* (2005) 'The RNA Helicase Lgp2 Inhibits TLR-Independent Sensing of Viral Replication by Retinoic Acid-Inducible Gene-I', *The Journal of Immunology*, 175(8), pp. 5260 LP – 5268. doi: 10.4049/jimmunol.175.8.5260.

Roy, A. *et al.* (2019) 'IFI16, a nuclear innate immune DNA sensor, mediates epigenetic silencing of herpesvirus genomes by its association with H3K9 methyltransferases SUV39H1 and GLP', *eLife*. eLife Sciences Publications, Ltd, 8, p. e49500. doi: 10.7554/eLife.49500.

Saitoh, T. *et al.* (2009) 'Atg9a controls dsDNA-driven dynamic translocation of STING and the innate immune response', *Proceedings of the National Academy of Sciences*, 106(49), pp. 20842 LP – 20846. doi: 10.1073/pnas.0911267106.

Sakaguchi, S. *et al.* (2003) 'Essential role of IRF-3 in lipopolysaccharide-induced interferon-β gene expression and endotoxin shock', *Biochemical and Biophysical Research Communications*, 306(4), pp. 860–866. doi: https://doi.org/10.1016/S0006-291X(03)01049-0.

Sanfilippo, C. M. and Blaho, J. A. (2006) 'ICP0 gene expression is a herpes simplex virus type 1 apoptotic trigger', *Journal of virology*. American Society for Microbiology, 80(14), pp. 6810–6821. doi: 10.1128/JVI.00334-06.

Santilli, G. *et al.* (2008) 'Gene therapy of inherited immunodeficiencies', *Expert Opinion on Biological Therapy*. Taylor & Francis, 8(4), pp. 397–407. doi: 10.1517/14712598.8.4.397.

Sato, M. *et al.* (1998) 'Positive feedback regulation of type I IFN genes by the IFN-inducible transcription factor IRF-7', *FEBS Letters*. John Wiley & Sons, Ltd, 441(1), pp. 106–110. doi: https://doi.org/10.1016/S0014-5793(98)01514-2.

Sato, M. *et al.* (2000) 'Distinct and Essential Roles of Transcription Factors IRF-3 and IRF-7 in Response to Viruses for IFN-α/β Gene Induction', *Immunity*. Elsevier, 13(4), pp. 539–548. doi: 10.1016/S1074-7613(00)00053-4.

Satoh, T. *et al.* (2010) 'LGP2 is a positive regulator of RIG-I- and MDA5-mediated antiviral responses', *Proceedings of the National Academy of Sciences of the United States of America*. 2010/01/08. National Academy of Sciences, 107(4), pp. 1512–1517. doi: 10.1073/pnas.0912986107.

Schneider, W. M., Chevillotte, M. D. and Rice, C. M. (2014) 'Interferon-stimulated genes: a complex web of host defenses', *Annual review of immunology*. 2014/02/06, 32, pp. 513–545. doi: 10.1146/annurev-immunol-032713-120231.

Schoggins, J. W. *et al.* (2014) 'Pan-viral specificity of IFN-induced genes reveals new roles for cGAS in innate immunity', *Nature*, 505(7485), pp. 691–695. doi: 10.1038/nature12862.

Schroder, K. *et al.* (2004) 'Interferon-γ: an overview of signals, mechanisms and functions', *Journal of Leukocyte Biology*. John Wiley & Sons, Ltd, 75(2), pp. 163–189. doi: https://doi.org/10.1189/jlb.0603252.

Scutts, S. R. *et al.* (2018) 'DNA-PK Is Targeted by Multiple Vaccinia Virus Proteins to Inhibit DNA Sensing', *Cell reports*. Cell Press, 25(7), pp. 1953-1965.e4. doi: 10.1016/j.celrep.2018.10.034.

Seth, R. B. *et al.* (2005) 'Identification and Characterization of MAVS, a Mitochondrial

Antiviral Signaling Protein that Activates NF-κB and IRF3', *Cell*. Elsevier, 122(5), pp. 669–682. doi: 10.1016/j.cell.2005.08.012.

Shang, G. *et al.* (2012) 'Crystal structures of STING protein reveal basis for recognition of cyclic di-GMP', *Nature Structural & Molecular Biology*, 19(7), pp. 725–727. doi: 10.1038/nsmb.2332.

Shang, G. *et al.* (2019) 'Cryo-EM structures of STING reveal its mechanism of activation by cyclic GMP–AMP', *Nature*, 567(7748), pp. 389–393. doi: 10.1038/s41586-019-0998-5.

Sheppard, P. *et al.* (2003) 'IL-28, IL-29 and their class II cytokine receptor IL-28R', *Nature Immunology*, 4, p. 63+. Available at: https://link.gale.com/apps/doc/A188808394/AONE?u=anon~8b5c4be6&sid=googleScholar&xid=ce71b6f5.

Smith, G. and Jackson, S. (1999) 'The DNA-dependent protein kinase', *Genes & Development*, 13(8), pp. 916–934. doi: 10.1101/gad.13.8.916.

Smith, S. *et al.* (2014) 'Structure of the herpes simplex virus 1 genome: manipulation of nicks and gaps can abrogate infectivity and alter the cellular DNA damage response', *Journal of virology*. American Society for Microbiology, 88(17), pp. 10146–10156. doi: 10.1128/JVI.01723-14.

Smith, Z. D. and Meissner, A. (2013) 'DNA methylation: roles in mammalian development', *Nature Reviews Genetics*, 14(3), pp. 204–220. doi: 10.1038/nrg3354.

Sokolowska, O. and Nowis, D. (2018) 'STING Signaling in Cancer Cells: Important or Not?', *Archivum immunologiae et therapiae experimentalis*. 2017/07/26. Springer International Publishing, 66(2), pp. 125–132. doi: 10.1007/s00005-017-0481-7.

Sonia, S. *et al.* (2003) 'Triggering the Interferon Antiviral Response Through an IKK-Related Pathway', *Science*. American Association for the Advancement of Science, 300(5622), pp. 1148–1151. doi: 10.1126/science.1081315.

Steiner, I. and Benninger, F. (2013) 'Update on Herpes Virus Infections of the Nervous System', *Current Neurology and Neuroscience Reports*, 13(12), p. 414. doi: 10.1007/s11910-013-0414-8.

Stetson, Daniel B. and Medzhitov, R. (2006) 'Recognition of cytosolic DNA activates an IRF3-dependent innate immune response', *Immunity*, 24(1), pp. 93–103. doi: 10.1016/j.immuni.2005.12.003.

Stetson, Daniel B and Medzhitov, R. (2006) 'Type I Interferons in Host Defense',

Immunity. Elsevier, 25(3), pp. 373–381. doi: 10.1016/j.immuni.2006.08.007.

Stow, N. D. and Stow, E. C. (1986) 'Isolation and characterization of a herpes simplex virus type 1 mutant containing a deletion within the gene encoding the immediate early polypeptide Vmw110', *Journal of General Virology*, 67(12), pp. 2571–2585. doi: 10.1099/0022-1317-67-12-2571.

Stratmann, S. A. *et al.* (2015) 'The innate immune sensor IFI16 recognizes foreign DNA in the nucleus by scanning along the duplex', *eLife*. eLife Sciences Publications, Ltd, 4, pp. e11721–e11721. doi: 10.7554/eLife.11721.

Sui, H. *et al.* (2017) 'STING is an essential mediator of the Ku70-mediated production of IFN-λ1 in response to exogenous DNA', *Science Signaling*, 10(488), p. eaah5054. doi: 10.1126/scisignal.aah5054.

Sui, H., Chen, Q. and Imamichi, T. (2021) 'Cytoplasmic-translocated Ku70 senses intracellular DNA and mediates interferon-lambda1 induction', *Immunology*. John Wiley & Sons, Ltd, 163(3), pp. 323–337. doi: https://doi.org/10.1111/imm.13318.

Sumner, R. P., Ren, H. and Smith, G. L. (2013) 'Deletion of immunomodulator C6 from vaccinia virus strain Western Reserve enhances virus immunogenicity and vaccine efficacy', *Journal of General Virology*. Microbiology Society, 94(5), pp. 1121–1126. doi: https://doi.org/10.1099/vir.0.049700-0.

Sun, B. *et al.* (2017) 'Dengue virus activates cGAS through the release of mitochondrial DNA', *Scientific Reports*, 7(1), p. 3594. doi: 10.1038/s41598-017-03932-1.

Sun, C. *et al.* (2019) 'Cellular Requirements for Sensing and Elimination of Incoming HSV-1 DNA and Capsids', *Journal of Interferon & Cytokine Research*. Mary Ann Liebert, Inc., publishers, 39(4), pp. 191–204. doi: 10.1089/jir.2018.0141.

Sun, H. *et al.* (2021) 'A Nuclear Export Signal Is Required for cGAS to Sense Cytosolic DNA', *Cell Reports*. Elsevier, 34(1). doi: 10.1016/j.celrep.2020.108586.

Sun, L. *et al.* (2013) 'Cyclic GMP-AMP synthase is a cytosolic DNA sensor that activates the type I interferon pathway', *Science*, 339(6121), pp. 786–791. doi: 10.1126/science.1232458.

Sun, W. *et al.* (2009) 'ERIS, an endoplasmic reticulum IFN stimulator, activates innate immune signaling through dimerization', *Proc Natl Acad Sci U S A*, 106(21), pp. 8653–8658. doi: 0900850106 [pii]\r10.1073/pnas.0900850106.

Sun, X. *et al.* (2020) 'DNA-PK deficiency potentiates cGAS-mediated antiviral innate

immunity', *Nature communications*. Nature Publishing Group UK, 11(1), p. 6182. doi: 10.1038/s41467-020-19941-0.

Swider, A. *et al.* (2014) 'Regulation of interferon lambda-1 (IFNL1/IFN-λ1/IL-29) expression in human colon epithelial cells', *Cytokine*, 65(1), pp. 17–23. doi: https://doi.org/10.1016/j.cyto.2013.09.020.

Takahama, M. *et al.* (2017) 'The RAB2B-GARIL5 Complex Promotes Cytosolic DNA-Induced Innate Immune Responses', *Cell Reports*. Elsevier, 20(12), pp. 2944–2954. doi: 10.1016/j.celrep.2017.08.085.

Takeuchi, O. and Akira, S. (2010) 'Pattern Recognition Receptors and Inflammation', *Cell*, pp. 805–820. doi: 10.1016/j.cell.2010.01.022.

Tan, X. *et al.* (2015) 'Detection of Microbial Infections Through Innate Immune Sensing of Nucleic Acids', *Annual Review of Microbiology*. Annual Reviews, 72(1), pp. 447–478. doi: 10.1146/annurev-micro-102215-095605.

Tanaka, Y. and Chen, Z. J. (2012) 'STING specifies IRF3 phosphorylation by TBK1 in the cytosolic DNA signaling pathway', *Science signaling*, 5(214), pp. ra20–ra20. doi: 10.1126/scisignal.2002521.

Tang, Q., Chakraborty, S. and Xu, G. (2018) 'Mechanism of vaccinia viral protein B14–mediated inhibition of IκB kinase β activation', *Journal of Biological Chemistry*. Elsevier, 293(26), pp. 10344–10352. doi: 10.1074/jbc.RA118.002817.

Taniguchi, T. *et al.* (1980) 'Human leukocyte and fibroblast interferons are structurally related', *Nature*, 285(5766), pp. 547–549. doi: 10.1038/285547a0.

Taniguchi, T. *et al.* (2001) 'IRF Family of Transcription Factors as Regulators of Host Defense', *Annual Review of Immunology*. Annual Reviews, 19(1), pp. 623–655. doi: 10.1146/annurev.immunol.19.1.623.

Taylor, T. J. and Knipe, D. M. (2004) 'Proteomics of Herpes Simplex Virus Replication Compartments: Association of Cellular DNA Replication, Repair, Recombination, and Chromatin Remodeling Proteins with ICP8', *Journal of Virology*, 78(11), pp. 5856 LP – 5866. doi: 10.1128/JVI.78.11.5856-5866.2004.

Thibaut, D., Maria, K. and M., S.-G. R. (2021) 'Evasion of the STING DNA-Sensing Pathway by VP11/12 of Herpes Simplex Virus 1', *Journal of Virology*. American Society for Microbiology, 91(16), pp. e00535-17. doi: 10.1128/JVI.00535-17.

Tomoya, K. *et al.* (2020) 'Structural basis for the inhibition of cGAS by nucleosomes',

Science. American Association for the Advancement of Science, 370(6515), pp. 455–458. doi: 10.1126/science.abd0237.

Tsuchida, T. *et al.* (2010) 'The ubiquitin ligase TRIM56 regulates innate immune responses to intracellular double-stranded DNA', *Immunity*, 33(5), pp. 765–776. doi: 10.1016/j.immuni.2010.10.013.

Turnell, A. S. and Grand, R. J. (2012) 'DNA viruses and the cellular DNA-damage response', *Journal of General Virology*. Microbiology Society, 93(Pt_10), pp. 2076–2097. doi: 10.1099/vir.0.044412-0.

Unterholzner, L. *et al.* (2010) 'IFI16 is an innate immune sensor for intracellular DNA', *Nature Immunology*, 11(11), pp. 997–1004. doi: 10.1038/ni.1932.

Unterholzner, L. *et al.* (2011) 'Vaccinia virus protein C6 is a virulence factor that binds TBK-1 adaptor proteins and inhibits activation of IRF3 and IRF7', *PLoS pathogens*. 2011/09/08. Public Library of Science, 7(9), pp. e1002247–e1002247. doi: 10.1371/journal.ppat.1002247.

Volkman, H. E. *et al.* (2019) 'Tight nuclear tethering of cGAS is essential for preventing autoreactivity', *eLife*. eLife Sciences Publications, Ltd, 8, p. e47491. doi: 10.7554/eLife.47491.

Volz, A. and Sutter, G. (2017) 'Chapter Five - Modified Vaccinia Virus Ankara: History, Value in Basic Research, and Current Perspectives for Vaccine Development', in Kielian, M., Mettenleiter, T. C., and Roossinck, M. J. B. T.-A. in V. R. (eds). Academic Press, pp. 187–243. doi: https://doi.org/10.1016/bs.aivir.2016.07.001.

Walker, J. R., Corpina, R. A. and Goldberg, J. (2001) 'Structure of the Ku heterodimer bound to DNA and its implications for double-strand break repair', *Nature*, 412(6847), pp. 607–614. doi: 10.1038/35088000.

Wang, J. *et al.* (2010) 'NF- B RelA Subunit Is Crucial for Early IFN- Expression and Resistance to RNA Virus Replication', *The Journal of Immunology*, 185(3), pp. 1720–1729. doi: 10.4049/jimmunol.1000114.

Wang, J. *et al.* (2017) 'Ku70 Senses HTLV-1 DNA and Modulates HTLV-1 Replication', *The Journal of Immunology*, 199(7), pp. 2475–2482. doi: 10.4049/jimmunol.1700111.

Wang, X. *et al.* (2014) 'Direct activation of RIP3/MLKL-dependent necrosis by herpes simplex virus 1 (HSV-1) protein ICP6 triggers host antiviral defense', *Proceedings of the National Academy of Sciences of the United States of America*.

2014/10/14. National Academy of Sciences, 111(43), pp. 15438–15443. doi: 10.1073/pnas.1412767111.

Wassermann, R. *et al.* (2015) 'Mycobacterium tuberculosis Differentially Activates cGAS- and Inflammasome-Dependent Intracellular Immune Responses through ESX-1', *Cell Host & Microbe*, 17(6), pp. 799–810. doi: https://doi.org/10.1016/j.chom.2015.05.003.

Watson, R. O. *et al.* (2015) 'The Cytosolic Sensor cGAS Detects Mycobacterium tuberculosis DNA to Induce Type I Interferons and Activate Autophagy', *Cell host & microbe*. 2015/06/02, 17(6), pp. 811–819. doi: 10.1016/j.chom.2015.05.004.

de Weerd, N. A. and Nguyen, T. (2012) 'The interferons and their receptors--distribution and regulation', *Immunology and cell biology*. 2012/03/13. Nature Publishing Group, 90(5), pp. 483–491. doi: 10.1038/icb.2012.9.

Weissmann, C. and Weber, H. (1986) 'The Interferon Genes', in Cohn, W. E. and Moldave, K. B. T.-P. in N. A. R. and M. B. (eds). Academic Press, pp. 251–300. doi: https://doi.org/10.1016/S0079-6603(08)60026-4.

Wu, X. *et al.* (2014) 'Molecular evolutionary and structural analysis of the cytosolic DNA sensor cGAS and STING', *Nucleic acids research*. 2014/06/30. Oxford University Press, 42(13), pp. 8243–8257. doi: 10.1093/nar/gku569.

Xiao, X. *et al.* (2018) 'DNA-PK inhibition synergizes with oncolytic virus M1 by inhibiting antiviral response and potentiating DNA damage', *Nature Communications*, 9(1), p. 4342. doi: 10.1038/s41467-018-06771-4.

Xu, L.-G. *et al.* (2005) 'VISA Is an Adapter Protein Required for Virus-Triggered IFN-β Signaling', *Molecular Cell*. Elsevier, 19(6), pp. 727–740. doi: 10.1016/j.molcel.2005.08.014.

Xusha, Z. *et al.* (2021) 'hnRNPA2B1 Associated with Recruitment of RNA into Exosomes Plays a Key Role in Herpes Simplex Virus 1 Release from Infected Cells', *Journal of Virology*. American Society for Microbiology, 94(13), pp. e00367-20. doi: 10.1128/JVI.00367-20.

Yaneva, M., Kowalewski, T. and Lieber, M. R. (1997) 'Interaction of DNA-dependent protein kinase with DNA and with Ku: biochemical and atomic-force microscopy studies', *The EMBO journal*, 16(16), pp. 5098–5112. doi: 10.1093/emboj/16.16.5098.

Yang, Y. G., Lindahl, T. and Barnes, D. E. (2007) 'Trex1 Exonuclease Degrades ssDNA to Prevent Chronic Checkpoint Activation and Autoimmune Disease', *Cell*, 131(5),

pp. 873–886. doi: 10.1016/j.cell.2007.10.017.

Yasuda, K. *et al.* (2009) 'Requirement for DNA CpG Content in TLR9-Dependent Dendritic Cell Activation Induced by DNA-Containing Immune Complexes', *The Journal of Immunology*, 183(5), pp. 3109 LP – 3117. doi: 10.4049/jimmunol.0900399.

Yeow, W.-S. *et al.* (2000) 'Reconstitution of Virus-mediated Expression of Interferon α Genes in Human Fibroblast Cells by Ectopic Interferon Regulatory Factor-7 *', *Journal of Biological Chemistry*. Elsevier, 275(9), pp. 6313–6320. doi: 10.1074/jbc.275.9.6313.

Yoneyama, M. *et al.* (1998) 'Direct triggering of the type I interferon system by virus infection: activation of a transcription factor complex containing IRF-3 and CBP/p300', *The EMBO journal*, 17(4), pp. 1087–1095. doi: 10.1093/emboj/17.4.1087.

Yoneyama, M. *et al.* (2004) 'The RNA helicase RIG-I has an essential function in double-stranded RNA-induced innate antiviral responses', *Nature Immunology*, 5(7), pp. 730–737. doi: 10.1038/ni1087.

Yu, L. *et al.* (2016) 'Functional Roles of Pattern Recognition Receptors That Recognize Virus Nucleic Acids in Human Adipose-Derived Mesenchymal Stem Cells', *BioMed research international*. School of Basic Medical Sciences, Xinxiang Medical University, Xinxiang, Henan 453003, China; Henan Collaborative Innovation Center of Molecular Diagnosis and Laboratory Medicine, Xinxiang, Henan 453003, China., 2016, p. 9872138. doi: 10.1155/2016/9872138.

Yu, X. and He, S. (2016) 'The interplay between human herpes simplex virus infection and the apoptosis and necroptosis cell death pathways', *Virology journal*. BioMed Central, 13, p. 77. doi: 10.1186/s12985-016-0528-0.

Yuan, S.-S. F. *et al.* (2012) 'Role of MRE11 in Cell Proliferation, Tumor Invasion, and DNA Repair in Breast Cancer', *JNCI: Journal of the National Cancer Institute*, 104(19), pp. 1485–1502. doi: 10.1093/jnci/djs355.

Zandi, E. *et al.* (1997) 'The IκB Kinase Complex (IKK) Contains Two Kinase Subunits, IKKα and IKKβ, Necessary for IκB Phosphorylation and NF-κB Activation', *Cell*. Elsevier, 91(2), pp. 243–252. doi: 10.1016/S0092-8674(00)80406-7.

Zhang, J. *et al.* (2012) 'TRIM32 protein modulates type I interferon induction and cellular antiviral response by targeting MITA/STING protein for K63-linked

ubiquitination', *The Journal of biological chemistry*. 2012/06/28. American Society for Biochemistry and Molecular Biology, 287(34), pp. 28646–28655. doi: 10.1074/jbc.M112.362608.

Zhang, J. *et al.* (2018) 'Species-Specific Deamidation of cGAS by Herpes Simplex Virus UL37 Protein Facilitates Viral Replication', *Cell Host & Microbe*. Elsevier, 24(2), pp. 234-248.e5. doi: 10.1016/j.chom.2018.07.004.

Zhang, X. *et al.* (2011) 'Cutting Edge: Ku70 Is a Novel Cytosolic DNA Sensor That Induces Type III Rather Than Type I IFN', *The Journal of Immunology*, 186(8), pp. 4541–4545. doi: 10.4049/jimmunol.1003389.

Zhang, X., Flavell, R. A. and Li, H.-B. (2019) 'hnRNPA2B1: a nuclear DNA sensor in antiviral immunity', *Cell Research*, 29(11), pp. 879–880. doi: 10.1038/s41422-019-0226-8.

Zhang, Xu *et al.* (2013) 'Cyclic GMP-AMP Containing Mixed Phosphodiester Linkages Is An Endogenous High-Affinity Ligand for STING', *Molecular Cell*, 51(2), pp. 226–235. doi: https://doi.org/10.1016/j.molcel.2013.05.022.

Zhang, Z. *et al.* (2011) 'The helicase DDX41 senses intracellular DNA mediated by the adaptor STING in dendritic cells', *Nature immunology*, 12(10), pp. 959–965. doi: 10.1038/ni.2091.

Zhao, B. *et al.* (2020) 'The molecular basis of tight nuclear tethering and inactivation of cGAS', *Nature*, 587(7835), pp. 673–677. doi: 10.1038/s41586-020-2749-z.

Zhong, B. *et al.* (2008) 'The Adaptor Protein MITA Links Virus-Sensing Receptors to IRF3 Transcription Factor Activation', *Immunity*, 29(4), pp. 538–550. doi: 10.1016/j.immuni.2008.09.003.

Zhong, B. *et al.* (2009) 'The Ubiquitin Ligase RNF5 Regulates Antiviral Responses by Mediating Degradation of the Adaptor Protein MITA', *Immunity*. Elsevier, 30(3), pp. 397–407. doi: 10.1016/j.immuni.2009.01.008.

Zhong, L. *et al.* (2020) 'Phosphorylation of cGAS by CDK1 impairs self-DNA sensing in mitosis', *Cell Discovery*, 6(1), p. 26. doi: 10.1038/s41421-020-0162-2.